Protect neurons from ischemia-induced death by targeting BNIP3 gene family

By

JIEQUN WENG

A thesis submitted to the Faculty of Graduate Studies of

The University of Manitoba

in partial fulfilment of the requirements of the degree of

DOCTOR OF PHILOSOPHY

Department of Human Anatomy and Cell Science

University of Manitoba

Winnipeg

For my family

I could never make it this far without you!

Abstract

The BNIP3 family, a group of death-inducing mitochondrial proteins, includes BNIP3, NIX and BNIP3h. These proteins share structural and functional similarities. BNIP3 causes neuronal cell death in a necrosis-like, caspase-independent manner with mitochondrial dysfunction. We reported that BNIP3 plays a role in delayed neuronal death in stroke models. Over-expression of BNIP3 causes up to 70% neuronal death, while knockdown of BNIP3 only protects 23% neurons from hypoxia. Thus, we hypothesize that other members of the BNIP3 subfamily compensate for the loss of BNIP3.

BNIP3 and NIX were highly upregulated in the oxygen and glucose deprivation (OGD)/reoxygenation model, and knockdown of BNIP3 or NIX protected about 20% - 44% of neurons. Knockdown of BNIP3 family reduced neuronal death by 48%. Mitochondrial membrane potential loss, mitochondrial permeability transition pore (MPTP) opening and reactive oxygen species (ROS) production were all significantly attenuated by BNIP3 and/or NIX inhibition. AIF and EndoG were reported involving in caspase-independent cell death in ischemic stroke. We found that AIF was released from mitochondria and translocated into nuclei in neurons after OGD/reoxygenation, while inhibition of BNIP3 blocked AIF and EndoG translocation and prevented neuronal death. Over-expression of BNIP3 and NIX caused AIF translocation and subsequent neuronal death. These data reveal the effects of the BNIP3 family in neuronal death and indicate that AIF and EndoG are two downstream factors in the BNIP3-mediated cell death pathway.

Meanwhile, necrostatin-1 (Nec-1), an inhibitor for a caspase-independent necrotic cell death, is able to protect neurons from death in stroke, mechanism of which is unclear. Here, we confirmed that Nec-1 significantly increased survival of neurons in models of stroke *in vivo* and *in vitro*. It also attenuated hypoxia or BNIP3-induced mitochondrial dysfunction and prevented mitochondrial release of AIF. Nec-1 did not affect the expression levels of BNIP3 but prevented its integration into mitochondria. These results suggest that Nec-1 protects neurons against ischemia by targeting BNIP3.

In summary, this research indicates that the BNIP3 family is one of the regulators of caspase-independent neuronal death in stroke and that Nec-1 is an inhibitor for BNIP3 and a potential therapeutic agent for stroke.

Acknowledgements

This thesis would not have been possible without the support and guidance of some very special people. First, I wish to show deepest gratitude to my supervisor, Dr. Jiming Kong, for his mentorship during my six years as a graduate student. Under his guidance, I have learned a great deal about the trivialness and tribulations of academic research, including what it takes to persevere and succeed as an independent investigator.

I would also like to thank my advisory committee members, Dr. Judith Anderson, Dr. Maria Vrontakis-Lautatzis, Dr. Fiona Parkinson, Dr. Mike Namaka and Dr. Emma Frost, who provided crucial guidance as my project changed directions time and again. Especially, Dr. Anderson and Dr. Vrontakis-Lautatzis, not only have provided invaluable support and encouragement for the last six years, but also have been influential in my career development. I would also like to thank my external examiner, Dr. Yutian Wang, for his critical review of my thesis and for traveling to Winnipeg for my oral defense.

Dozens of people have helped and taught me immensely in the lab. It is an honor for me to work with Dr. Lin Zhao, who helped me finish all the *in vivo* surgery in my project. I am grateful to Dr. Surong Zhang and Mr. Xiuli Ma, who taught me the research techniques since I was an inexperienced student, and to Jacqueline Hogue, who spent a lot of time revise my thesis. I also received excellent guidance and technical assistance from Dr. Xinmin Li and his lab. I would like to acknowledge to my friends in the lab and outside of the lab for providing a fun and stimulating environment. Words cannot even describe how thankful I am for being around you for the enjoyable six years.

I would like to thank MICH/MHRC and CIHR for my studentship funding, as well as the University and the Province of Manitoba for their generous travel awards and annual top-up funds.

Finally, I want to thank my husband and my parents. Although we could not spend enough time together, you are always my spirit support, inspiring me to succeed and pushing me to explore new possibilities.

Contents

List of Figures

List of Tables

List of Abbreviation

(ce)BNIP3	Caenorhabditis elegans ortholog BNIP3
2-VO	two-vessel occlusion
3-MA	3-methyladenine
4-VO	four-vessel occlusion
aCSF	artificial cerebrospinal fluid
AIF	apoptosis inducing factor
AIP	Apaf-1-interacting protein
AMPA	2-amino-3-(5-methyl-3-oxo-1,2- oxazol-4-yl)propanoic acid
ANT	Adenine Nucleotide Translocase
Apaf-1	apoptosis interacting factor-1
ASICs	acid-sensing ion channels
BH	Bcl-2 homology
BHLH-PAS	basic helix-loop-helix PAS domain
BNIP3	BCL2/adenovirus E1B 19 kDa protein-interacting protein 3
BNIP3ΔTM	dominant-negative form of BNIP3
BSA	bovine serum albumin
BSS	balanced salt solution
CA1	cornu ammonis 1
CAD	caspase-activated deoxyribonuclease
CBF	cerebral blood flow
CCA	common carotid artery
CsA	cyclosporin A
CypA	cyclophilin A
Cyto c	cytochrome c
DBD	DNA binding domain
DISCs	intracellular death-inducing sigaling complexes
DNA	Deoxyribonucliei acid
DND	delayed neuronal death
Drp1	Dynamin-related protein-1
EndoG	Endonuclease g
ER	endoplasmic reticulum
FADD	Fas-associated death domain
GBM	glioblastoma multiforme
GST	glutathione S-transferase
GFP	green fluorescence protein
HGF	hepatocyte growth factor
HIF-1	hypoxia-inducible factor-1
HIFdn	dominant-negative form of HIF-1α
HQ	Harlequin
HRE	hypoxia responsive elements
HtrA2	High temperature requirement protein A2
Hsp70	heat-shock protein70

ICAD	inhibitor of caspase activated DNase
ISEL	in situ end libelling
KA	kainic acid
LDH	Lactate dehydrogenase
MAO-B	monoamine oxidase B
MBM	monobromobimane
MCA	middle cerebral artery
MCAO	middle cerebral artery occlusion
MMP	mitochondrial membrane potential
MNNG	N-methyl-N'-nitro-N'-nitrosoguanidine
MOM	mitochondrial outer membrane
MPTP	mitochondrial permeability transition pore
Nec-1	Necrostatin-1
NIX	BNIP3 like protein X
NMDA	N-methyl-D-aspartate
OGD	oxygen glucose deprivation
PARP-1	poly(ADP-ribose) polymerase-1
PBS	phosphate buffered saline
PHC	Penehyclidine hydrochloride
PI	propidium iodide
PMCA	plasma membrane calcium pump
PTD	protein transduction domain
RIP1	receptor interacting protein 1
RNAi	RNA interference
ROS	reactive oxygen species
Smac	second mitochondria derived activator
TAT	transactivator domain
TBS	Tris-buffered saline
tFCI	transient focal cerebral ischemia
TNF	tumor necrosis factor
TNF-α	tumour necrosis factor-α
TRAF2	tumor necrosis factor receptor-associated 2
TRAILR1	TNF-related apoptosis inducing ligand receptor 1
TUNEL	in situ terminal deoxytransferase-mediated dUTP nick end labeling
VDAC	voltage-dependent anion channel
XIAP	X chromosome-linked inhibitor of apoptosis
WT	wild-type

Chapter 1. Introduction

1.1 Stroke

Stroke, the interruption of the blood flow or the rupture of blood vessels in the brain, is the third leading cause of death in Canada. Each year, there are over 50,000 strokes in Canada and nearly 14,000 Canadians die from stroke (CANSIM Table 102-0529: Deaths, by cause 2010). Stroke costs the Canadian economy $3.6 billion a year in physician services, hospital costs, lost wages, and decreased productivity (Tracking Heart Disease and Stroke in Canada June 2009). Overall, about 87% of strokes are ischemic, which is caused by the interruption of blood flow to the brain due to a blood clot, while about 9% of strokes are hemorrhagic, which is caused by uncontrolled bleeding in the brain, and 4% are due to subarachnoid hemorrhage (Marsh and Keyrouz 2010). The common causes of ischemic stroke include thromboembolism, such as artherosclerosis, and heart disease, such as atrial fibrillation (Ay 2010). Depending on the affected area of the brain, patients will have different symptoms, including language, cognition, motor or sensory deficits. Treatment of acute ischemic stroke is aimed at removing the artery blockage by breaking the clot down (thrombolysis), or by removing it mechanically (thrombectomy) (Molina 2011). The more rapidly blood flow is restored to the brain, the fewer brain cells die. In the last decade, treatment has made considerable progress, however, a large percentage of stroke victims still do not benefit from these active therapeutic strategies, either due to the small window of opportunity for effective intervention or limitations of efficient therapeutic potential (Mink and Miller 2011). In the last 20 years, basic research has

revealed several cell death mechanisms and therapeutic strategies that provide a great hope for the alleviation of stroke.

Ischemic neuronal death may occur in two forms: acute and delayed (Graham and Chen 2001). In focal ischemia, acute neuronal death occurs mostly in the ischemic "core" region of a stroke, where most of the cells experience severe hypoxia and hypoglycemia that result in energy depletion, loss of calcium homeostasis and swelling of cellular organelles leading to rapid cell death (Ferrer and Planas 2003). There is a wealth of evidence to suggest that such acute neuronal damage is followed by a second round of neuronal injury, called delayed neuronal death, which occurs hours to days following brain ischemia, in the neighbouring areas called penumbra. There is evidence that even if cerebral blood flow (CBF) is re-established quickly enough to prevent immediate cell death, many of the initially surviving neuronal cells still die several days after reperfusion (Ferrer and Planas 2003; Graham and Chen 2001). In fact, the term delayed neuronal death was first coined by Kirino to describe the selective loss of the hippocampal cornu ammonis 1 (CA1) neurons that does not become morphologically obvious until two to three days following a transient episode of global ischemia (Kirino 2000).

Delayed neuronal death is considered a hallmark feature of brain ischemia and the primary target for neuroprotective strategies. There are several hypotheses proposed, such as glutamate excitotoxicity (An et al. 2002), prolonged inhibition of protein synthesis (Thilmann et al. 1986), disturbed heat shock protein expression (Fujiki et al. 2006), degradation of phospholipids, accumulation of cytotoxic breakdown products of lipids (Siesjo and Katsura 1992), accumulation of free radicals (Lang-Rollin et al. 2003),

perturbations in energy metabolism and cerebral circulation (Arai, Passonneau, and Lust 1986), damage of neurotrophic factor receptors (Wang et al. 2004) and disturbance of mitochondrial DNA expression (Abe et al. 1995). Nevertheless, the molecular mechanisms by which hypoxic-ischemic insults cause delayed cell death are unclear. In this chapter, I will focus on recent basic research on ischemic stroke, and describe ischemic stroke models, ischemia-induced cell death pathways, the regulation of ischemic neuronal death by Bcl-2 family and current therapeutic strategies.

1.2 Systems used to study cerebral ischemia

1.2.1 Ischemic stroke models: *in vivo*

In recent decades, several animal models have been designed specifically to mimic human stroke and serve as an indispensable tool in the stroke research field. Due to the cost and ethical concern, the majority of ischemic stroke models are carried out in rodents (Ginsberg and Busto 1989). Both *in vivo* and *in vitro* models have been used to better understand the mechanisms of ischemic injury and prevent post-stroke brain damage.

Human stroke can be caused by small vessel occlusion, large artery occlusive disease, artery-to-artery embolism or cardioembolism, so it is impossible to set up a single universally appropriate model for stroke. Many *in vivo* stroke models have been established in which blood flow disruption is focal or global, complete or incomplete, permanent or transient (Hossmann 2008; Ginsberg and Busto 1989). In this section, I will describe the major models of ischemic stroke divided into two subgroups: global ischemia and focal ischemia.

1.2.1.1 Global ischemia models

Global ischemia involves blocking the major blood vessels that supply the forebrain and results in ischemia over a large proportion of the brain. One of the easiest methods to produce global ischemia without recirculation is decapitation (Nemoto et al. 1982). However, there are complicating factors, such as venous congestion and vagus nerve compression, which can lead to variable ischemic outcomes in this model. In 1982, Pulsinelli and Brierley developed the four-vessel occlusion (4-VO) model to provide a method of reversible forebrain cerebral ischemia in rats (Pulsinelli, Brierley, and Plum 1982). This model provides a near-complete reduction of blood flow in the cortex, striatum, and hippocampus, and a rather extensive pathological change (Pulsinelli, Levy, and Duffy 1983). After 30 minutes of ischemia, striatal neurons are damaged, and hippocampal damage occurs 3 to 6 hours after reperfusion; neocortex damage occurs 1 to 3 days after ischemia (Pulsinelli, Brierley, and Plum 1982). This model is a useful tool to study the unusual pattern of delayed neuronal death observed after global ischemia. It has also been used to test the neuroprotective activity of drugs by many investigators (Kirino 2000). The two-vessel (2-VO) model of forebrain ischemia was initially used to characterize the cerebral energy state following ischemia (Haraldseth, Gronas, and Unsgard 1991). In this model, bilateral common carotid artery occlusion is coupled with systemic hypotension to produce a reversible forebrain ischemia (Haraldseth, Gronas, and Unsgard 1991). The 2-VO plus hypotension model produces brain damage similar to the 4-VO model, except there is less injury on the Purkinje fibers of the cerebellar brain stem, which explains why the animals recovering from 2-VO have fewer respiratory problems

(Sheng et al. 1999; McBean and Kelly 1998). The major advantages of the 2-VO plus hypotension model over the 4-VO model in producing forebrain ischemia are that the 2-VO model requires a more simple surgical preparation and reperfusion can be readily accomplished (McBean and Kelly 1998). A major problem with this 2-VO plus hypotension is that the exsanguination and reinfusion of blood (now heparinized) is not rapid enough to compensate for blood pressure fluctuations that occur in response to the lowered arterial blood pressure. Later, a modified rat 2-VO model, which controls blood pressure by simply using the alterations in the level of halothane anesthetic, was established. This procedure produced a high-grade forebrain ischemic insult, easily achievable recirculation, and the possibility of testing the animals post-insult with a variety of learning and memory tests (McBean et al. 1995). Although these global ischemia models have been well-validated and well-described, they are used much less now as compared to a few years ago because they are now generally considered to model the cerebral consequences of cardiac arrest rather than stroke.

1.2.1.2 Focal ischemia models

In focal ischemic models, a specific vessel to a very distinct, specific brain region is occluded and blood flow is reduced (McAuley 1995). The Middle Cerebral Artery Occlusion (MCAO) model is the most frequently used model of focal ischemia because around 80% of cerebral ischemia happens in the MCA territory in clinical situations (Howells et al. 2010; Chiang, Messing, and Chou 2011).

MCAO results in a reduction of CBF and produces cerebral infarction in the striatum and overlying frontal, parietal and temporal cortices as well as in a portion of the occipital cortex. MCAO also results in variable damage in the thalamus, substantia nigra and hypothalamus (Engel et al. 2011; Rickels 1993). Widespread damage affects functionally diverse regions in the brain and results in motor, sensory, autonomic, or cognitive deficits (Gupta, Sinha, and Chaudhary 2002; Stutzmann et al. 2002; Bederson et al. 1986). The degree of brain damage depends on the duration of MCAO (Chiang, Messing, and Chou 2011), the site of occlusion along the middle cerebral artery (MCA) (Kobayashi et al. 2007), and the amount of collateral blood flow into the MCA territory (Nagasawa and Kogure 1989). Several different types of MCAO models exist, among which the model using intraluminal suture is the most common (Ardehali and Rondouin 2003). It involves inserting a monofilament into the internal carotid artery and advancing until it blocks blood flow to the MCA. The most common duration of suture occlusion of the MCA in the rat is 60, 90, 120 min or permanent occlusion (Calloni et al. 2010). This model also avoids opening the skull and minimizes surgical injury to the brain, but lesion volume varies depending on the anatomy of the Circle of Willis and the degree of occlusion achieved. Modifications in the technique such as variations in suture diameter (Tureyen et al. 2005; Hata et al. 1998), coating of the suture (Belayev et al. 1996; Aspey et al. 1998) and insertion length of the thread (Calloni et al. 2010) along with application of advanced imaging techniques (Hata et al. 1998) have made this model more reproducible and reliable than it was originally. The major shortcomings of MCAO are that it does not model thromboembolism or thrombolysis and that the complication of subarachnoid hemorrhage is quite common (Gerriets et al. 2004).

There are two other distal occlusion models of the MCA: the transcranial surgical MCAO (Tamura et al. 1981) and the three-vessel occlusion model (Yanamoto et al. 1998). In the former model, MCAO is carried out after the MCA gives off lenticulostriate branches at the basal surface of the lateral part of the cerebral hemisphere (Tamura et al. 1981; Betz et al. 1994). The latter MCAO model functions by occluding the distal MCA on the surface of the brain and bilateral common carotid artery for more than one hour (Yonekura et al. 2004). Both of these distal MCAO models produce more restricted damage to the cerebral hemisphere (Yanamoto et al. 1998), but both involve highly skilled surgical operation and may be accompanied by significant surgical trauma. Most MCAO models are either permanent or temporary (after occlusion, the artery blockage is removed to allow reperfusion), allowing examination of the damage that results from both ischemia and reperfusion. These MCAO models have been used extensively for studying pharmacological neuroprotection and mechanisms of injury from ischemia, and for characterization of genes and proteins involved in stroke.

Other models of focal ischemia have been utilized, including embolic models (Zhang et al. 1997), photothrombotic models (Hilger et al. 2004), endothelin-1 (Frost et al. 2006) or balloon-catheter-induced stroke models and a pial vessel occlusion model. Embolic models are induced most commonly by the injection of autologous thrombi into the internal carotid artery to reach the more distal intracranial arteries throughout the brain (Zhang et al. 1997; Wang et al. 2001). These models not only closely mimic human stroke but also have the potential to test thrombolytic agents and to evaluate the progress of the ischemic lesion after thrombolysis (Dinapoli et al. 2006; Wang, Yang, and Shuaib

2001). However, the size and location of infarcts produced by thrombi are smaller and more variable than in suture-induced MCAO (Beech et al. 2001), which makes comparative analysis of neuroprotective treatments difficult. Photothrombosis induces a cortical infarct by the systemic injection of a photoactive dye in combination with irradiation by a light beam at a specific wavelength (Wood et al. 1996). The region of irradiation can be determined in any desired cortical area with minimal surgical manipulation (Zhang et al. 2008; Kuroiwa et al. 2009). A photothrombotic ischemic lesion has relatively little ischemic penumbra (Pevsner et al. 2001), but microvascular insult results in thrombosis generally distributed over all vessels illuminated (Hoff et al. 2005; Nakayama et al. 1988). Endothelin-1 acts as a potent vasoconstrictor and can be applied directly by stereotaxic intracerebral injection into the MCA area or cortex (Fuxe et al. 1997; Sharkey and Butcher 1995). The advantage of endothelin-1 application is that it is reproducible and less invasive (Sharkey and Butcher 1995), while the disadvantage is that extent and duration of blood flow are uncertain (Nikolova et al. 2009). Furthermore, endothelin-1 receptors are also found on astrocytes and neurons. Endothelin-1 receptors exert a direct, receptor-mediated signalling effect that may interfere with the production and interpretation of neural repair experiments (Carmichael 2005; Wang, Hsieh, and Yang 2011; Zhou, Strichartz, and Davar 2001). Since a great number of strokes are caused by the insult of small-vessel ischemia, which only affects the white matter and gray matter of the cerebral surface, the pial vessel occlusion model has been established to mimic this type of stroke (Sun et al. 2008). The conventional pial vessel disruption model involves the stripping of all vessels in an area of the cortex, and this procedure leads to a massive rectangular lesion that is more reminiscent of a traumatic rather than

an ischemic event. A modified pial vessel model that involves disruption of only the medium vessels within a 5-mm diameter area, better mimics the specific ischemia caused by smaller vessels than the original pial vessel model (Hua and Walz 2006).

Although the majority of strokes happen in elderly people, neonatal stroke is an increasingly recognized cause of neurological disability in children and is one of the top ten causes of death in children (Ramenghi et al. 2010; Hunt and Inder 2006). In order to investigate the pathophysiologic mechanisms and potential neuroprotective strategies for neonatal stroke, different models have been developed (Ashwal and Pearce 2001; Northington 2006). In the last two decades, the most commonly used model is the hypoxia-ischemia model, which is composed of the unilateral permanent ligation of the common carotid artery (CCA) of postnatal-day 7 (P7) rats and the subsequent exposure of the animals to systemic hypoxia (8% oxygen) for 1–3 h (Sola et al. 2008). This model was initially reported by Rice et al. It causes moderate to severe ischemic neuronal changes in the ipsilateral cerebral cortex, striatum, and hippocampus (Rice, Vannucci, and Brierley 1981). Like adult rodent stroke models, selective and delayed neuronal death is observed in the dentate gyrus (Tuor, Del Bigio, and Chumas 1996; Northington et al. 2001). This model has been widely used to study ischemic-hypoxia injury, but the question remains as to how closely this model reflects neonatal stroke. Similar to stroke in the elderly, more than 80% of neonatal stroke involves the vascular territory supplied by the MCA (Guzzetta, Deodato, and Rando 2000). Therefore, in spite of technical difficulties, several groups have used the filament technique to induce transient MCAO for the newborn (Ashwal et al. 1995; Derugin et al. 2000; Wen et al. 2004). The pups

used in the transient MCAO filament technique are usually P7, or P14 to P18-day old. Vannucci indicated that the P7 day old rat is histologically similar to a human fetus at 32- to 34-weeks gestation or to a newborn infant (Vannucci and Vannucci 1997). Other investigators concluded that P10 to P12 days is developmentally closer to that of the human newborn by examining parameters like synapse formation and electrocortical function (Romijn, Hofman, and Gramsbergen 1991). In fact, the age of the pups, which reflects the developmental stage of the brain, does affect the susceptibility of the brain to ischemia-hypoxia (Sheldon, Chuai, and Ferriero 1996). Furthermore, neurobehavioural and functional studies have been performed with these models to investigate long-term outcomes. Only limited behavioural tests can be used following the induction of stroke due to the developmental immaturity of the neonate; however, different learning and memory tasks, as well as motor responses have been modified or used as endpoints to study the effects of pharmacologic treatment (Borlongan et al. 2004; Balduini et al. 2001; Chang et al. 2005). Thus, these models give scientists a great opportunity to study the effects of neonatal stroke on brain development, behaviour and functional outcomes.

1.2.1.3 Limitation of *in vivo* stroke models

The ideal stroke model should be able to mimic the ischemic process and pathophysiologic response to human stroke, produce reproducible lesion size and location, use techniques that are easy to perform, and be reasonably cost-efficient. Although these animal models have provided us with most of our knowledge about the pathogenic mechanisms and potential treatment of ischemic stroke, many compounds showing neuroprotective effects in preclinical studies have failed to show efficacy in clinical

studies (Kaste 2005; Fisher and Tatlisumak 2005). This is mainly due to the level of relevance of animal stroke models to human stroke. A number of different parameters, if not stringently controlled, can confound the validity of the model (Wiebers, Adams, and Whisnant 1990; Lo 2008). The severity of ischemia and the size of infarction, which are both closely related to local CBF, are two major factors that affect to the failure of drugs in clinical trials. The main sources of variability in animal stroke modeling include: animal-related factors including age, strain and sex; physiological parameters including temperature, arterial blood pressure, arterial blood gases, and blood glucose; confounding factors associated with the invasiveness of the model procedure: skull trauma, external blood vessel injury, changes in intracranial pressure (Howells et al. 2010). All of these parameters need to be monitored and controlled during an animal experiment to produce stroke in an animal model that is comparable to human stroke.

1.2.2 Ischemia stroke models: *in vitro*

Although *in vivo* focal ischemia models are the most physiologically accurate of the stroke models, they have a very "low throughput" for identifying compounds that are capable of reducing the rate at which damage spreads after a focal ischemic insult. The technical demands and high costs of *in vivo* models also make it difficult for researchers to determine rapidly the efficacy and mechanism of action of the test compounds. *In vitro* models, on the other hand, enjoy some advantages over *in vivo* models, including greater control of variables, very controlled and quantitative drug delivery and comparably low cost. Therefore, *in vitro* models are amenable to a wide variety of pharmacological manipulations. Moreover, *in vitro* ischemia models are also commonly used the studies of

gene/protein functions. The most common *in vitro* models currently used in stroke research include: *in vitro* dissociated cell models and *in vitro* brain-slice models (Lipton 1999).

1.2.2.1 *In vitro* dissociated cell models

Primary neuronal culture is a powerful and highly versatile tool for dissecting molecular and cellular mechanisms in neuroscience. They have been established from different species, such as rat, mouse and chicken, and from different regions of the brain, such as cortex, hippocampus, striatum and septum. Cortical and hippocampal neurons have become the most widely used cultures and they have been instrumental in the analysis of dendritic spine morphology and synaptic plasticity (Lei et al. 2006; Piccini and Malinow 2001) and in dissecting mechanisms in stroke (Lewerenz et al. 2003; Culmsee et al. 2005). These neuronal cultures can be established from rat or mouse fetuses (gestational day 16 to 18), and can last up to four weeks in culture medium (Meberg and Miller 2003; Lesuisse and Martin 2002). Due to the development of selective culture medium, researchers can control the differentiation and proliferation of the cells. Using neurobasal medium with B-27 supplements has helped researchers to obtain a survival rate and purity up to 95% (Brewer 1995; Xie, Markesbery, and Lovell 2000).

In *in vitro* ischemic models, neurons are exposed to a combined deprivation of oxygen and glucose (OGD) or a prolonged hypoxic conditions to mimic the reduced intracellular energy state that occurs in neurons during and following cerebral ischemia (Jones, Novak, and Elliott 2011; Zhang, Yang, et al. 2007). Neurons are generally cultured with glucose-

free balanced-salt solution (BSS) or medium in an anaerobic or hypoxic incubator for several minutes or hours, and then neurons are placed in normal culture medium and normal oxygen condition for hours to days to mimic the reperfusion *in vivo* (Tanaka et al. 2005; Zhao et al. 2009). Recently, Meloni et al. established and characterized an OGD/reperfusion model that induce acute or delayed neuronal cell death by placing neurons into BSS and culture medium with different concentrations of glucose (Meloni et al. 2011). Prolonged hypoxia is commonly used for cancer research but it can also be used in neuronal cultures to investigate the single effect of low or no oxygen on neurons (Hong et al. 2007). Like *in vivo* models, the time course of neuronal death in response to *in vitro* ischemia also depends on the duration and severity of the insult (Li, Shao, et al. 2007; Zhu et al. 2010). By quantifying the responses on a morphological, biochemical or molecular basis, these models will provide valuable tools to further investigate ischemic neuronal death and neuronal survival mechanisms. Unfortunately, as *in vitro* models, they are the least physiologically accurate because the cells are not maintained in conditions that are similar to their normal environment, after they are enzymatically and mechanically dissociated (Choi 1990).

1.2.2.2 *In vitro* brain slice models

Another *in vitro* method to study ischemic damage is to use organotypic brain-slice cultures. The brain slices were initially used to assess the physiological significance, including synaptic connections and chemical signalling (Elliott, Malouf, and Catterall 1995; Thomas et al. 1998). Now this approach represents a widely accepted model in neurotoxicological screening and mechanistic studies (Noraberg 2004) and has been

increasingly used in molecular biology, electron microscopy, imaging, electrophysiology and immunohistochemical studies (Holopainen 2005; Opitz-Araya and Barria 2011). Different regions of brain can be cultured separately including the cerebellum, hippocampus, striatum, thalamus and other regions. The hippocampus slice is the most common one (Opitz-Araya and Barria 2011; Krassioukov et al. 2002). Most brain-slice cultures are derived from early postnatal (P0-P7) animals, although increasing evidence indicates that healthy organotypic slices can be obtained from adult animals (De Simoni and Yu 2006). Once the culture is established, the viable brain slices can reach up to 20 weeks, which offers the possibility of studying a variety of processes over time (De Simoni and Yu 2006). The most commonly used source of brain-slice preparation are rats and mice but, in recent years, rabbits, pigs and even human fetal brain tissue have been used (Savas et al. 2001; Walden et al. 1990; Merz et al. 2010). Due to the development of genetic engineering techniques, more and more transgenic mice are used in this brain-slice culture model (Duff et al. 2002; Brachmann and Tucker 2011). Within each slice, cytoarchitecture is maintained and thus many of the cell-to-cell interactions and neuronal networks remain intact (Gahwiler, Thompson, and Muller 2001). These models have similar throughput compared with the cell culture model, but slice preparations are far more representative of normal physiology. Hence, this model is well-suited for physiological experiments to assess the mechanism of action of drugs as well as to study brain damage, neuroprotection and neuro-repair in neurodegenerative diseases, including stroke (Noraberg et al. 2005).

Predominant *in vitro* ischemic models involve OGD media on brain-slice, to induce energy-failure conditions and mimic *in vivo* global ischemia (Reiner, Laycock, and Doll 1990). The commonly used culture media in the slice model is as artificial cerebrospinal fluid (aCSF), and the gas content of the bathing solution is changed from a mixture of oxygen/carbon dioxide to nitrogen/carbon dioxide in the absence or presence of glucose, modeling in ischemia or anoxia respectively (Bali, Nagy, and Kovacs 2007). Neuronal death is detected two hours after OGD and is extended to all subfields of the hippocampus by 24 hours post-injury (Bali, Nagy, and Kovacs 2007). Recently, Richard et al. developed an *in vitro* focal ischemia model by applying OGD medium to a small portion of a brain slice while bathing the remainder of the slice with normal oxygenated media (Richard et al. 2010). Based on the electrophysiological study, rapid depolarization in the "core" region was noted in the OGD medium, while progressive depolarization was observed in neurons in the surrounding area (Richard et al. 2010). Other ischemia studies have focused on excitotoxic models using glutamate and excitotoxins. In hippocampal slice cultures exposed to N-methyl-D-aspartate (NMDA), kainic acid (KA) and 2-amino-3-(5-methyl-3-oxo-1,2- oxazol-4-yl)propanoic acid (AMPA), ischemia-like damage is produced, and these preparations have been used for studies of excitotoxicity, glutamate receptor-induced neuronal cell death, receptor modulation and related neuroprotection (Kristensen, Noraberg, and Zimmer 2001; Zimmer et al. 2000). To check and qualify the cell death within the slice, nuclear marker propidium iodide (PI) (Laake et al. 1999), mitochondria-dependent tetrazolium (Krassioukov et al. 2002) and *in situ* terminal deoxytransferase-mediated dUTP nick-end labeling(TUNEL) (Krassioukov et al. 2002) are used. Like *in vivo* stroke models, apoptosis, necrosis and mixed types of cell death

have been reported. The high susceptibility of hippocampal CA1 neurons to OGD or NMDA of hippocampal slice cultures is similar to their selective vulnerability to ischemia *in vivo* (Laake et al. 1999; Piccini and Malinow 2001). The major drawback of these methods is that the reagents cannot diffuse freely through the tissue; therefore, assessment of slice viability is limited to the top layer of cells.

1.3 Ischemia-induced neuronal death

1.3.1 Morphological features of ischemic neuronal death

The response of brain tissue to ischemic insult is primarily determined by the severity and length of the ischemia and, to a lesser degree, the susceptibility of individual neurons (Lipton 1999; Dijkhuizen et al. 1998). A severe and long-lasting ischemia results in acute and massive neuronal death in the targeted areas. The brain tissue rapidly falls into infarction. Under moderate ischemia, the affected brain tissue undergoes a slower process to "mature" into infarction. A mild ischemia may not induce an obvious brain infarct, but may cause selective loss of susceptible neurons in certain brain areas such as the hippocampal CA1 region (Kirino 2000). Depending on the energy resources and other parameters such as availability of growth factors, cell maturity, and stress stimuli during the ischemia, the eventual death mode of neurons include apoptosis, necrosis, autophagic cell death and hybrid cell death. Although it is still debated, the general idea is that morphological changes of neurons are different by time and region: at the early stage of hypoxia-ischemia, most neurons die by necrosis, while in the later stage, neurons show apoptotic features; neuronal death in the central region or core is necrosis, while neurons

in the penumbra die by apoptosis. Similar to the adult rat, it has been reported that the early neurodegeneration after hypoxia-ischemia is necrosis while delayed neuronal death is apoptosis in neonatal rat. Another two types of cell death, autophagic and hybrid cell death were reported mostly in the later stage and in the penumbra area of ischemia similar to apoptosis.

1.3.1.1 Apoptosis

Apoptosis is a distinct form of cell death that is an active process of gene-directed cellular self-destruction. Typically, apoptosis is a regulated form of cell death that is the result of insults of minor severity and is associated with activation of a "genetic program" (Zhang, Yin, and Chen 2004). Apoptosis plays an important role in embryogenesis as well as in pathogenesis. Delayed neuronal death following brain ischemia shows morphological features of apoptosis, although the sequential morphological changes are still controversial. The most common morphological features of apoptosis observed in ischemic dying neurons by light and electronic microscopy include cell shrinkage, condensation of nuclear chromatin and membrane-bounded vacuoles (Padosch and Bottiger 2003). As the apoptosis progresses, the apoptotic bodies, which are characterized by dark brown staining under electrical microscope, increase gradually and form plasma-membrane blebs and protuberances on the cell surface. Deoxyribonucleic acid (DNA) fragmentation can be detected by TUNEL, in situ end labeling (ISEL) in the CA1 pyramidal neurons, and DNA laddering on gel electrophoresis of extracted nuclear DNA, during the processes of delayed neuronal death (Nitatori et al. 1995; Petito et al. 1997). Typically, apoptotic cells identified by plasma membrane binding of the tagged annexin-

V and exclusion of PI contribute to delayed infarct and cell death in the border zone, dorsolateral cortex and hippocampus after MCAO. Since apoptosis is an energy-consuming process, ATP-dependent migration of the fragmented DNA from the nucleus into the apical dendrite in CA1 pyramidal cells strongly supports the hypothesis that delayed neuronal death is indeed apoptotic (Hara, Mori, and Niwa 2000). At later stages of a brief period of brain ischemia, phagocytosis of fragmented DNA by microglial cells in the CA1 region is also evident (Nitatori et al. 1995). Furthermore, apoptosis-related caspases such as caspase-3 are activated in the CA1 region following transient brain ischemia (Cao et al. 2002). Typical apoptosis is mostly observed in the penumbra area of cerebral infarction but it is also found in the "necrotic core" in the early stage, indicated by a number of morphological, physiological and biochemical feature of apoptosis (Benchoua et al. 2001). Collectively, all of these observations suggest that apoptotic processes are involved in ischemic neuronal death.

1.3.1.2 Necrosis

In contrast to apoptosis, necrosis has been traditionally thought to be a passive form of cell death with more similarities to an accident than to a suicide (Yuan, Lipinski, and Degterev 2003). It is usually associated with alteration in calcium and sodium ion homeostasis. Necrosis is likely to be induced by severe ischemia at an earlier stage of ischemia but it is also involved in delayed neuronal death. After MCAO and reperfusion, electron microscopic changes of necrotic cells include aggregation of loosely textured chromatin, dilation of the endoplasmic reticulum, mild dispersal of ribosomes and degraded mitochondrial matrix densities (Li et al. 1995). At the later stage, cells exhibit

irregular, small dense clumps of chromatin (karyolysis), disruption of cellular organelles and deterioration of the membrane (Li et al. 1995). Necrotic cells can be detected with TUNEL staining in the striatum and cortex at 6h recirculation, showing the features of a large, diffuse, light brown colour in both the cell nucleus and cytoplasm, without apoptotic bodies (Fukuda et al. 1999). These changes suggest random DNA fragmentation and fragility of the nuclear membrane, and also indicate that TUNEL staining should be evaluated with morphological changes. Flow cytometric analysis of Annexin-V (marks apoptosis) and PI (marks necrosis) labeling cells shows that MCAO dominantly induces necrosis in the ischemic core (Carloni et al. 2007). Apoptotic cells are cleaned up by microglial cells, whereas necrotic cells are associated with neutrophils contiguous to neurons (Li et al. 1995). Necrosis-related proteins such as calpain and cathepsin B are up-regulated (Chaitanya and Babu 2008), while calpain inhibitors protect neuronal cells from ischemia-hypoxia in mice (Tsubokawa et al. 2006).

1.3.1.3 Autophagic cell death

Another mechanism participating in ischemic neuronal death is autophagic cell death, a type II programmed cell death (PCD) (Kroemer et al. 2009). Autophagy is a physiological intracellular bulk degradation process, whereby cytosolic proteins and organelle are sequestered and degraded (Smith et al. 2011). The level of autophagy is increased in cerebral ischemia. Different levels of autophagy have different consequences. A high level of autophagy can protect cells from apoptosis, while excessive autophagy can also kill cells. Recent results showing that autophagy inhibitors protect against ischemia-induced neuronal death suggest that autophagy plays a detrimental role (Wen et

al. 2008). Using electron microscopy, autophagosomes, C-shaped double-membrane structures, and engulfment of cytoplasmic materials by autophagosomes, were found in neurons in the model of permanent focal ischemia (Tian et al. 2010). In this model, the autophagy inhibitor 3-methyladenine (3-MA) significantly reduced infarct volume, brain edema and motor deficits (Wen et al. 2008). In a neonatal stroke model, post-ischemic intracerebroventricular injections of 3-MA strongly reduce lesion volume by 46% even when given more than 4 hours after the beginning of the ischemia. By comparison, pan-caspase inhibitors, carbobenzoxy-valyl-alanyl-aspartyl(OMe)-fluoromethylketone and quinoline-val-asp(OMe)-Ch2-O-phenoxy, provided no protection against stroke in this model (Puyal et al. 2009). Furthermore, numbers of lysosomes and the level of lysosomal cysteine proteinases increased, along with appearance of autophagic vacuole-like structures in the CA1 pyramidal neurons 3 days after ischemic insult (Nitatori et al. 1995). Lysosomal protease inhibitors also protected against neuronal death produced by global ischemia and reduced the lesion volume in rat neonatal stroke (Yamashima et al. 1998). The autophagy-related proteins Beclin1 and LC3II increased in both adult and neonatal brain ischemia/hypoxia. Down-regulation of Beclin1 by RNA interference (RNAi) improved outcomes after transient MCAO in rats (Zheng et al. 2009). A lack of autophagic-related protein Atg7 dramatically protected neurons from neonatal hypoxia-ischemia in mice (Uchiyama, Koike, and Shibata 2008).

1.3.1.4 Hybrid cell death

In addition to the three well-known forms of cell death, several atypical morphological changes have been reported. Fukuda et al. found a distinct form of cellular disintegration

in some hippocampal neurons (Fukuda et al. 1999): the nuclei of these neurons were TUNEL-positive without showing nuclear fragmentation; perikarya of degenerating neurons shrinked as apoptosis without apoptotic body; organelles other than mitochondria disappeared, but plasma and mitochondrial membrane were still not disrupted. The apoptosis-to-necrosis continuum is also demonstrated by a concurrent increase in caspase-3 and cathepsin-B activities. Kirino described delayed neuronal death as having distinct morphological features with atypical clumping of nuclear chromatin and non-membrane-bound dense structures (Kirino 2000). Deshpande et al. found that, ultrastructurally, delayed neuronal death is characterized by polysome disaggregation and electron-dense, fluffy, dark materials associated with tubular saccules at the early stage (Deshpande et al. 1992). The dark material may be the non-membrane dense structure mentioned by Kirino, although its nature is still unclear. It appears that there is a hybrid form of cell death that shares features of apoptosis, necrosis and autophagy (Wei et al. 2004). Recently, Yuan et al. described an atypical cell death, necroptosis or programmed necrosis, which manifests features of necrosis but differs from unregulated necrosis in that it can be regulated and inhibited like other forms of PCD (Rosenbaum et al.). The definition of programmed necrosis is descriptive (based on morphological features, such as partial stage nuclear chromatin condensation and absence of dilation of intracellular organelles) and negative (based on the elimination of other cell death mechanism or the lack of activation of some proteins, such as caspases). Programmed necrosis can be induced by the activation of a death receptor or certain other conditions such as heavy metal, DNA alkylating agents and shikonin (Han et al. 2009; Moubarak et al. 2007). It is corroborated by the activiation of the executors such as receptor-interacting protein 1

(RIP1) and apoptosis-inducing factor (AIF) (Galluzzi, Kepp, and Kroemer 2009; Boujrad et al. 2007). The small molecule inhibitor of necroptosis, necrostatin-1 (Nec-1), is identified as a potent inhibitor of receptor inactivating protein (RIP1) kinase activity (Degterev et al. 2005). Other proteins that have been reported to be involved in programmed necrosis include endonuclease G (EndoG) (Higgins, Beart, and Nagley 2009), Bcl-2/adenovirus E1B 19 kDa protein-interacting protein 3 (BNIP3) (Galluzzi and Kroemer 2009) and poly(ADP-ribose) polymerases-1 (PAPR-1) (Moubarak et al. 2007), which will be described below. Further morphological and biochemical studies suggest that programmed necrosis is also characterized by mixed features of apoptosis, necrosis and autophagy (Wei et al. 2004).

Currently, PCD pathways are subdivided into three types: PCD-type I (apoptosis), PCD-type II (autophagic cell death) and PCD-type III (programmed necrosis) (Yuan, Lipinski, and Degterev 2003). These cell death pathways may exist in a variety of relationships: in parallel and in series, with any one upstream of the other types. It is also possible for some or all of these relationships to exist simultaneously, since the continuums between apoptosis and necrosis, apoptosis and autophagic cell death have been implicated concomitantly in the same neuronal cells in the penumbra of infarction (Unal-Cevik et al. 2004; Wei et al. 2004). Neurons with TUNEL-positive nuclei show apoptotic changes and cytosolic vacuolization and membrane deterioration typical of necrotic alteration (Wei et al. 2004). A subpopulation of Beclin-1-upregulating cells also expresses the active form of caspase-3 and shows dense staining for LC3 (Rami 2008). The autophagy inhibitor 3-MA blocks the post-ischemic increases in both caspase activation and AIF

translocation to the nucleus in a neonatal stroke model (Wang, Xia, et al. 2011). Due to the overlap and shared signalling pathways between the different death programs, exclusive definitions are difficult to make and are probably artificial. It has been postulated that the dominant cell-death phenotype is determined by the relative speed of available death programs. Although characteristics of several death pathways can be displayed, only the fastest and most dominant death pathway is usually evident (Broker, Kruyt, and Giaccone 2005). The mechanism and regulation on how a cell death pattern is determined is still unknown. Those cell-death modes may not be independent phenomena but act synergistically. These mixed-type cell deaths may be classified as hybrid cell death, or they may be explained as a transition stage of a cross-talk process.

1.3.1.5 Cross-talk between cell death phenotypes

The cross-talks among different types of cell death were observed. Once the environment changes, or under a particular treatment, blocking one type of cell death may turn the neurons toward an alternative mode of cell death. For example, tumor necrosis factor-α (TNF-α) elicits necrotic cell death when caspases are blocked by the addition of synthetic caspase inhibitors or by over-expression of CrmA, a cowpox caspase-1 and caspase-8 specific inhibitor. The final morphological features of necrosis observed in the core area of a stroke may result from the aborted apoptotic process because of severe energy depletion (Liu, Siesjo, and Hu 2004). Activated caspases or calpain in apoptosis eventually cleave the ion pumps proteins, such as the plasma membrane calcium pump (PMCA) and the Na^+/Ca^{2+} exchanger. This may result in the disruption of calcium homeostasis and finally switch apoptotic signalling toward necrosis. This can also explain

why TUNEL-positive neurons in an ischemic cortex can end up being necrotic (Fukuda et al. 1999). These results indicate that necrotic cell death may function as a backup cell death pathway when caspases are blocked or when caspase-dependent pathways cannot be properly activated. In reverse, necrotic cell death can revert to apoptosis in the presence of Nec-1, a specific inhibitor of programmed necrosis, partially due to the change from permeability of the inner mitochondrial membrane to permeability of outer mitochondrial membrane. Should this scenario bear out, it would necessitate a more careful examination and review of the contribution of each type of cell death to disease pathogenesis. Although earlier experiments would still be valid in terms of effects on reduction of total cell death, a re-examination may provide a more complete understanding of the mechanisms of cell death.

1.3.2 Caspase-dependent neuronal-death pathways

After cerebral ischemia, cell-death programs are activated and result in neuronal death (Kuschinsky and Gillardon 2000; Choi 1996). Caspase activation is one of the key biochemical features for apoptosis (Gorman, Orrenius, and Ceccatelli 1998), and members of the Bcl-2 family are also involved. Caspases involved in apoptosis can be divided into the initiator caspases (-2, -8, -9, and -10) and the effector caspases (-3, -6 and -7). The initiator caspases have long prodomains that interact with the death domains (DDs) of other transmembrane and intracellular proteins involved in initiating apoptosis. By comparison, the effector caspases have short prodomains and are directly responsible for cleavage of cellular substrates that in turn is responsible for most of the morphological and biochemical features of apoptosis (Li and Yuan 2008). Existing as

inactive zymogens in living cells, caspases become activated during apoptosis either through the action of adaptor proteins or through cleavage by other caspases. The adaptor molecules link signalling events to caspase activation; they also define two basic pathways for apoptosis: the extrinsic pathway with death receptors and the intrinsic pathway with mitochondria (Kuschinsky and Gillardon 2000).

The death receptors are a family of type I transmembrane proteins characterized by the presence of multiple cysteine-rich repeats in the extracellular domain and a protein-protein interaction module known as the death domain in the cytoplasmic tail. The death receptor family includes tumor necrosis factor receptor 1, Fas, TNF-related apoptosis-inducing ligand receptor 1(TRAILR1), TRAILR2, Death receptor 6 (DR6), and nerve growth factor receptor (Guicciardi and Gores 2009). Upon interaction with their respective ligands, the death receptors form intracellular death-inducing signalling complexes (DISCs) that may include multiple adaptor molecules (Chen and Wang 2002). In the case of Fas, FasL binds to Fas and this leads to the formation of a homotrimeric ligand-receptor complex that recruits the adaptor protein, Fas-associated death domain (FADD). FADD then binds protein-interaction motifs in the prodomains of procaspase-8, resulting in its autocatalytic cleavage and activation (Thorburn 2004). Activated caspase-8 induces the activation of downstream caspases, such as caspase-3 and caspase-7 to complete the execution of apoptosis, or initiates the mitochondrial death pathway via cleavage of the BH3-only pro-apoptotic Bcl-2 family member, Bid (Kruidering and Evan 2000).

A number of stimuli such as oxidative stress or chemotherapeutic agents, mediates apoptosis via the mitochondrial pathway (Mohamad et al. 2005). The mitochondria-mediated apoptosis pathway is triggered by release of cytochrome c (Cyto c), certain procaspases, High temperature requirement protein A2 (HtrA2, also known as Omi), and the second mitochondria-derived activator (Smac, also known as DIABLO) from the intermembranous space of mitochondria (Jordan, de Groot, and Galindo 2011). Cytochrome c, an essential component of the respiratory chain, becomes an active cell killer once it is released from mitochondria and goes into the cytosol. It binds to apoptosis-interacting factor-1 (Apaf-1) to form apoptosomes that recruit and activate procaspase-9. Active caspase-9 then activates downstream effector caspases such as caspase-3, 6 and 7 (Plesnila 2004). Smac/DIABLO and HtrA2/Omi promote cytochrome c-dependent caspase activation by eliminating the inhibitory effect of apoptosis-inhibiting proteins and X-chromosome-linked inhibitor of apoptosis (XIAP) (Saelens et al. 2004). Activated effector caspases initiate apoptotic DNA fragmentation by triggering their target nuclease, the caspase-activated deoxyribonuclease (CAD, also known as DNA fragmentation factor 40, DFF 40), which is kept inactive by the binding of an inhibitor (ICAD, or DFF 45) (Enari et al. 1998). Activation of CAD occurs when its inhibitor, ICAD, is cleaved by effector caspases (Sakahira, Enari, and Nagata 1998).

Accumulating evidence indicates that the cell-killing machinery utilized in apoptosis, the caspase family, for instance, plays a significant role in delayed neuronal death. Genome-wide gene expression analysis shows caspase-2 and caspase-3 mRNA upregulation results from transient global ischemia (Kawahara et al. 2004). For example, caspase-3,

the executor of apoptotic cell death, was activated in CA1 neurons following ischemia (Rami et al. 2003); its inhibitor, zDEVD-FMK, has the ability to protect neurons against ischemia (Chen et al. 1998). Neurons of caspase-$3^{-/-}$ mice are also more resistant to ischemic stress both *in vivo* and *in vitro* (Le et al. 2002). Though caspase-1 is found in microglia, astrocytes and some non-pyramidal neurons, the delayed neuronal death of CA-1 pyramidal cells is significantly reduced by Ac-WEHD-CHO, a specific caspase-1 inhibitor (Hayashi, Jikihara, et al. 2001). Mice with caspase-1 mutation or deficiency show significantly reduced brain injury after MCAO (Friedlander et al. 1997; Schielke et al. 1998). Activation of caspase-8,-9 and -11 has also been demonstrated in both global and focal cerebral ischemia (Ferrer and Planas 2003). Pharmacological pre-treatment of mice with broad-spectrum caspase inhibitor or with a selective inhibitor of caspase reduced ischemia-induced neuronal death (Himi, Ishizaki, and Murota 1998) and prevented neurological outcomes of stroke (Mouw et al. 2002; Padosch, Vogel, and Bottiger 2001).

Molecular events of caspase-mediated apoptosis are also involved in neuronal death after transient cerebral ischemia: cytochrome c, which activates the precursor forms of caspases, is released from mitochondria to the cytosol 72 hours after transient ischemia (Antonawich 1999). Smac/DIABLO increases in neuronal death, which may be associated with alteration of the levels of XIAP and activation of caspase-3 (Siegelin et al. 2005). A negative correlation occurs between apoptosis and regulation of XIAP gene in the border zone (Xu, Zhang, et al. 2006). Overexpression of XIAP prevents activation of

procaspase-3 and degeneration of CA1 neurons reduces the infarct size and results in better neurological outcome after transient forebrain ischemia (Xu et al. 1999).

There are also some reports showing neuroprotection by indirect inhibition of caspase activities in experimental brain ischemia. Activation of NMDA receptor has been implicated in activation of caspase-3 in ischemic brain. NMDA receptor-antagonist MK-801 reduces brain injury, caspase-3 activation and DNA fragmentation in the cerebral cortex of immature rat brain after ischemia (Puka-Sundvall et al. 2000). More recently there was another report of indirect inhibition of caspase-3 activation in transient global cerebral ischemia in rats. Treating the ischemic animals with monobromobimane (MBM) protected hippocampal neurons from death through inhibition of mitochondrial swelling and thereafter inhibition of the caspase-3-dependent apoptotic pathway (Abe et al. 2004). Further, the neuroprotective effect of insulin, a PI3K agonist, on hippocampal CA1 neurons in ischemic brain injury in rats has been shown to be due to inhibition of the JNK signalling pathway and indirect attenuation of caspase-3 activation (Hui et al. 2005).

Caspase-dependent apoptosis is currently the best-known PCD modality. The caspase-dependent apoptotic pathway is regulated primarily by members of Bcl-2 family (Kuwana and Newmeyer 2003). Pro-apoptotic members of this family including Bad, Bax, Bid and Bim promote cytochrome c release. Anti-apoptotic members of the Bcl-2 family preserve mitochondrial integrity and prevent cytochrome c release. The details of these regulations will be described in the following section.

1.3.3 Caspase-independent neuronal-death pathways

In addition to caspase-dependent apoptosis, emerging evidence from a large proportion of experimental systems supports the notion that cell death can occur independently of caspases (Stefanis 2005; Cho and Toledo-Pereyra 2008; Kroemer and Martin 2005; Kim, Emi, and Tanabe 2005). It was reported that when caspase activation was inhibited, neurons may undergo a delayed, caspase-independent death after cerebral ischemia (Kim, Emi, and Tanabe 2005). Caspase inhibitors, such as the broad-spectrum caspase inhibitor zVAD-FMK, provided limited neuroprotection in brain ischemia but often caused a switch to caspase-independent apoptotic processes (Himi, Ishizaki, and Murota 1998). In addition, knockout of caspase-3 or 9, which play a central role in cell-death signalling, ultimately did not alter the number of cells that remain alive (Kroemer and Martin 2005). Under cerebral ischemia, neuronal death was also found in caspase-3 knockout mice as well as wild-type (WT) mice regardless of caspase activation (Le et al. 2002; Didenko et al. 2002). Furthermore, caspase-independent neuronal death was identified in neurons of Apaf-1 deficient mice (Cregan et al. 2002). Taken together, these experiments suggest that an alternative caspase-independent pathway is activated after ischemia and can be an important safeguard mechanism to dismantle dying neurons. This notion is further supported by the fact that, after cerebral ischemia, a small amount of caspase-activated DNase-related DNA fragments of 200-1000 bp was found, together with high molecular weight DNA fragments of 50 kbp, possibly independent of caspase activity in dying neurons (MacManus et al. 1997). In this scenario, two caspase-independent mitochondrial proteins, apoptosis inducing factor (AIF) and endonuclease G (EndoG),

and one nuclear protein, poly(ADP-ribose) polymerase-1 (PARP1), are implicated to date (Cho and Toledo-Pereyra 2008).

1.3.3.1 Apoptosis-inducing factor

AIF is a mitochondrial flavoprotein and normally resides in the intermembrane mitochondrial space where it performs an oxidoreductase function. The expression of AIF gradually increases with brain maturation and peaks in adulthood (Krantic et al. 2007). Brain tissue obtained from Harlequin (HQ) mice, which express about 20% lower levels of AIF than normal mouse neurons, revealed the increase of oxidative stress and cerebellar degeneration after 7 months of age (Klein et al. 2002). Similar to the role of cytochrome c, AIF also plays a pivotal role in PCD. This was shown by Joza et al., who reported that targeted disruption of the AIF gene inhibits the first wave of PCD during embryogenesis (Joza et al. 2001).

Upon conditions leading to apoptosis, the 62 kDa mitochondrial form AIF is cleaved at position G102/L103 to yield a soluble pro-apoptotic protein (truncated AIF, tAIF) with an apparent molecular weight of 57 kDa (Krantic et al. 2007). AIF becomes active when released from mitochondria to the cytosol and then goes to the nuclei, where it participates in chromatin condensation and is associated with large-scale DNA fragmentation at the size of 50 kbp (Zhang et al. 2002). However, evidence that the action of AIF could not be blocked by the broad spectrum caspase inhibitor zVAD-FMK (Daugas et al. 2000) or zDEVD-FMK (Cao et al. 2003), and that AIF translocation and cell death could still proceed in Apaf-$1^{-/-}$ and caspase $3^{-/-}$ cells (Joza et al. 2001), indicates

that AIF is involved in caspase-independent apoptosis. Moreover, caspase inhibition is equally protective against hypoxia-ischemia in HQ mice and WT mice; the Hq mutation did not inhibit hypoxia-ischemia-induced mitochondrial release of cytochrome c or activation of calpain and caspase-3 (Zhu, Wang, Huang, et al. 2007).

Although AIF is widely accepted as a pro-apoptotic mediator that functions independent of caspase, its functional role in caspase activation remains a subject of considerable debate. Several studies have provided compelling evidence demonstrating that AIF is a caspase-independent death effector that can function in parallel and independent of the mitochondrial activated-caspase cascade and that AIF release does not need caspase activation (Daugas et al. 2000; Yu et al. 2002). AIF release and subsequent cell death can be triggered by excessive calcium influx resulting from overactivation of PARP-1, independent of caspase (Yu et al. 2003). AIF translocation and condensation of nuclear chromatin occurred within 15 min of exposure to DNA-alkylating agent N-methyl-N'-nitro-N'-nitrosoguanidine (MNNG), while cytochrome c dissipation and caspase activation were not evident until 1-2 h after exposure. In mitochondria isolated from liver or HeLa cells, caspases activated by incubation with a low level of cytochrome c are unable to release AIF. However, more convincing data are needed to demonstrate that the release of AIF is independent of caspases. Arnoult et al. have demonstrated that AIF translocation is diminished in the presence of a caspase inhibitor after staurosporine or actinomycin D insult, and mitochondrial release of AIF occur downstream of cytochrome c in response to certain stimuli (Arnoult et al. 2002). In another study, it was reported that P53-induced caspase-2 activation may be involved in mitochondrial AIF release (Seth et

al. 2005). It is possible that AIF-mediated cell death is caspase-independent while the release or the function of AIF may need assistance from caspases, but this theory requires further scrutiny. These contradictory results seemingly account for several factors, such as cell type- and stimulus-specific responses. The possibility that the methods are not sufficiently sensitive to detect the earlier release of a subpool of mitochondrial proteins has to be excluded.

In the brain, the involvement of AIF in neuronal death has been reported after hypoglycemia (Imai et al. 2003), global cerebral ischemia (Plesnila et al. 2004), hypoxia-ischemia neonatal stroke (Zhu, Wang, Huang, et al. 2007) and traumatic brain injury (Slemmer et al. 2008). Death of hippocampal CA1 neurons following global cerebral ischemia is associated with nuclear translocation of AIF, nuclear pyknosis, and DNA fragmentation. Around 80% of all TUNEL-positive neurons had nuclear AIF staining in one study (Thal et al. 2011). Inhibition of AIF caused a 37-60% of reduction in neuronal death induced by glutamate toxicity and OGD-induced neuronal death, two major contributing factors in ischemic insult (Culmsee et al. 2005). HQ mice display smaller infarct volumes and less neuronal death after cerebral ischemia compare to normal mice (Culmsee et al. 2005). In a neonatal hypoxia-ischemia model, AIF translocation was observed and was not affected by a multi-caspase inhibitor boc-Asp-fmk. The combination of Hq mutation and caspase-inhibitor, Q-VD-OPh treatment showed an additive neuroprotective effect (Zhu et al. 2003). Thus, AIF seems to act as a lethal, caspase-independent effector of apoptosis in ischemic neuronal death.

Notwithstanding the role of AIF in caspase-independent death, the mechanisms responsible for AIF release from the mitochondria remain to be elucidated. Several elements that take part in AIF translocation have been established. First, two families of cysteine proteases, calpain and cathepsins, are involved. Calpain cleaves AIF into tAIF in a Ca^{2+}-dependent manner (Cao et al. 2007), and cathepsin D has been reported to trigger AIF release, independent of the caspase cascade (Bidere et al. 2003). Enzymatic inhibition of calpain by calpeptin precluded AIF release (Cao et al. 2007), demonstrating that proteolytic activity is required for AIF release from mitochondria. Calpeptin and cyclosporin A, the mitochondrial permeability transition pore (MPTP) antagonist, also inhibited calcium-induced AIF release from mouse-liver mitochondria, implicating the involvement of an endogenous mitochondrial calpain in release of AIF during permeability transition (Cao et al. 2007). Second, neuronally-derived nitric oxide (NO) is reported as a major factor contributing to nuclear AIF accumulation after stroke (Li, Nemoto, et al. 2007). The time course of the nuclear translocation of AIF after experimental stroke may vary with the severity of injury and may be accelerated by oxidant stress associated with reperfusion and NO production. Inhibition and gene deletion of neuronal NO synthase attenuated nuclear AIF accumulation (Li, Nemoto, et al. 2007). Third, translocation of AIF is positively regulated by cyclophilin A (CypA) (Zhu, Wang, Deinum, et al. 2007; Cande et al. 2004) and negatively regulated by the heat-shock protein (Hsp)70 (Cande et al. 2002). CypA possesses a latent, apoptosis-related DNase activity (Montague, Hughes, and Cidlowski 1997). After cerebral hypoxia-ischemia, nuclear translocation of AIF was reduced (by ~ 90%) in injured neurons in CypA $^{-/-}$ mice compared to injured neuron in WT mice. Conversely, CypA translocation

to the nuclei was reduced (by ~80%) in HQ mice (Zhu, Wang, Deinum, et al. 2007). Immunoprecipitation and surface-plasmon resonance revealed functional and physical interaction of CypA and AIF after hypoxia-ischemia in neurons (Zhu, Wang, Deinum, et al. 2007). These results suggest that CypA is required for the optimal nuclear translocation of AIF in damaged neurons and, vice versa, that AIF is needed for the nuclear translocation of CypA after hypoxia-ischemia. AIF was neutralized by Hsp70 (Cande et al. 2002), and transgenic mice with Hsp70 overexpression showed diminished brain injury following neonatal ischemia accompanied by reduced nuclear import AIF (Matsumori et al. 2005). Forth, AIF translocation is also regulated by permeabilization of the mitochondrial outer membrane (MOM), caused either by opening of the MPTP or by insertion of pro-apoptotic molecules from the Bcl-2 family, which will be described in the following section. The regulation of AIF by these proteins is not necessarily independent, and their interaction and ordering relationships need further investigation.

The AIF protein contains a strong, positive, electrostatic potential at the surface, which indicates that this domain might bind to DNA, and mutations in AIF are defective in DNA-binding activity and are unable to induce cell death (Cande et al. 2002). The mechanism of AIF-mediated chromatin condensation and DNA fragmentation in cell death is unclear, but AIF might bind to DNA and recruit the proteases and nuclease that cause chromatin condensation (Cregan, Dawson, and Slack 2004).

AIF is also one of the key regulators in the programmed necrosis (Delavallee et al.; Artus et al. 2010). In the model of programmed necrosis mediated by DNA damage from alkylating agent MNNG, following sequential activation of PARP1, calpain and Bax, AIF

was translocated into nuclei (Moubarak et al. 2007) and organized a DNA-degrading complex with histone H2AX and CypA (Artus et al. 2010). H2AX is a membrane of the histone H2A family and is associated primarily with DNA damage repair (Sedelnikova et al. 2003). In MNNG-induced programmed necrosis, H2AX is a key nuclear partner of AIF. AIF-DNA binding is nonspecific, which strongly suggests that other types of interaction might be involved. AIF can directly interact with endonuclease CypA (Cande et al. 2004) in AIF-mediated DNA and chromatin reconfiguration. TNFR1-induced programmed necrosis, another effector, RIP-1, is identified as playing a critical role (Galluzzi, Kepp, and Kroemer 2009). Recently, a relationship between AIF and RIP1 was suggested by using Nec-1 in retinal-detachment-induced photoreceptor necrosis (Trichonas et al. 2010) and glutamate-induced cell death in hippocampal HT-22 cells (Xu et al. 2007). However, whether or not these two proteins are responsible for ischemia-induced programmed necrosis in neurons and how they lead to this mixed cell death remain unknown.

1.3.3.2 Endonuclease G

Another protein that potentially contributes to caspase-independent cell death is EndoG, a mitochondrial specific nuclease (van et al. 2001). Mammalian EndoG is nuclear-encoded and synthesized as an zymogen about 33 kDa in size and is cleaved after translocation into mitochondria, to generate the 29 kDa mature form of the nuclease (Low 2003). EndoG was proposed to participate in mitochondrial replication through the generation of RNA primers required for the initiation of mitochondrial DNA synthesis (Prats et al. 1997). Normally, EndoG joins other mitochondrial proteins including cytochrome c,

Omi/HtrA2, Smac/DIABLO and AIF as cell-death effectors that are sequestered in the mitochondria, and released during cell-death process (Varecha et al. 2007).

There is genetic and biochemical evidence that EndoG is released from the intermembrane space of mitochondria and translocates to the nucleus to initiate caspase-independent apoptosis. EndoG was first demonstrated in DFF45/ CAD-deficient mice; although DNA fragmentation was significantly reduced in these transgenic mice, there was still show residual DNA fragmentation and are phenotypically normal (Li, Luo, and Wang 2001). EndoG cleaves chromatin DNA into nucleosomal fragments independent of CAD. Furthermore, DNA fragmentation can be blocked by an EndoG antibody, indicating that DNA fragmentation is at least partially attributable to EndoG. When the caspase-dependent machinery is silenced, ischemia causes caspase-independent cell death in cardiomyocytes that involves translocation and activation of EndoG (Bahi et al. 2006). Treatment with the caspase inhibitor z-VAD-FMK can inhibit DNA fragmentation caused by DFF, but cannot inhibit the release of EndoG from mitochondria following ultraviolet irradiation (Li, Luo, and Wang 2001). EndoG may act alone to degrade DNA or function with other endonucleases. EndoG can be stimulated by exonuclease and DNase I to facilitate DNA processing at physiological ionic strengths (Widlak et al. 2001). In contrast, Hsp70 protein can interact with EndoG in both vital and dying cells, and inhibit DNase activity in the presence of high concentrations of ATP (Kalinowska et al. 2005).

The involvement of EndoG translocation in cell death was reported during early embryogenesis (Zhang, Dong, et al. 2003) as well as in pathological conditions such as

cerebral ischemia (Lee et al. 2005). Mitochondrial EndoG showed a significant reduction as early as 4 h and a significant increase in the number of EndoG-positive nuclei at 12 and 24 h after transient focal cerebral ischemia(tFCI) (Lee et al. 2005) and permanent MCAO (Nielsen et al. 2009). The buildup of nuclear EndoG corresponds with depletion of mitochondrial EndoG. Double staining of EndoG and TUNEL suggests that DNA fragmentation is spatially correlated to nuclear EndoG-positive nuclei in dying cells (Lee et al. 2005). Interestingly, the translocation of EndoG was only observed in degenerating neurons, but not in astrocytes and microglia, which express caspase 3 activation in FCI (Nielsen et al. 2009). Furthermore, exposure of primary cortical neurons to prolonged hypoxia (Zhang, Yang, et al. 2007) and OGD (Zhao et al. 2009) causes a similar nuclear translocation of EndoG, which supports a role for activation of EndoG in ischemic neuronal death. CA3 and CA1 pyramidal neurons in EndoG $^{+/-}$ mice, which express low levels of EndoG, are more resistant to kainic acid-induced cell death than that in WT mice (Wu et al. 2004). This indicates that reduced expression of EndoG leads to resistance to excitotoxicity in neurons.

The mechanism of EndoG release is not clear. Contrary to AIF, EndoG translocation is not dependent on its cleavage, but most reports support that it has many similarities to AIF. The most popular theory of mitochondrial release of EndoG is through disruption of MOM (James et al. 2007). In the tBid-treated mitochondria, both EndoG and cytochrome c were released from mitochondria, but mitochondrial Hsp70 was not, indicating that the inner membrane of mitochondria remained intact (Li, Luo, and Wang 2001). Like AIF, EndoG translocation is regulated by Bcl-2 family, which I will discuss in the chapter

1.4.1.2. The caspase independent release of EndoG is also called into question, since it has been documented that the release of EndoG from mitochondrial intermembranous space is downstream of caspase activation (Arnoult et al. 2003). Another recently reported mechanism is that EndoG release can also be regulated by the mitochondrial fusion and fission machinery, which is necessary for the maintenance of organelle fidelity (James et al. 2007). Dynamin-related protein-1(Drp1), which triggers mitochondrial fission, was required for the release of EndoG from mitochondria. Knockdown of Drp1 can attenuate DNA fragmentation. Mitofusin 1 (Mfn 1), which is able to induce mitochondrial fusion, prevented EndoG release from mitochondria and the consequent DNA fragmentation (Li, Zhou, et al. 2010).

Similar to AIF, EndoG is also involved in programmed necrosis triggered by oxidative stress (Higgins, Beart, and Nagley 2009). H_2O_2, which causes severe oxidative stress, neither induces caspase-7 activity nor activates caspase-3. Knockdown of EndoG reduced both nuclear condensation and DNA fragmentation cause by H_2O_2, but not staurosporine, which is considered an apoptosis inducer in neurons (Higgins, Beart, and Nagley 2009). These reports might cause us to question whether AIF and EndoG are involved in the same pathway, even if both are involved in caspase-independent cell death pathway. It is suggested that EndoG promotes the production of double-stranded DNA cleavage products and that AIF, which has the DNA-binding ability but does not have the nuclease activities, may cooperate with EndoG to promote DNA degradation (Cregan, Dawson, and Slack 2004). This hypothesis is supported by the finding that the translocated EndoG nuclei are predominantly co-localized with AIF at 24 h after tFCI in mice (Lee et al.

2005). In C. *elegans*, the interaction between the homologues of AIF and EndoG, WAH1 and CPS6, has been identified (Wang et al. 2002). The translocation of both AIF and EndoG are also found in different types of cell deaths such as taxol-induced NIH3T3 fibroblast cell death (Hocsak et al. 2010) and sulindac-induced human colon cancer cell line HT-29 cell death (Park et al. 2005). However, little is known regarding their direct interaction in mammalian cells. Their interaction is also challenged by the findings that both AIF and EndoG can cleave chrome DNA in a cell-free system individually (Widlak et al. 2001; Zamzami et al. 1996). Thus, the specific nature of the relationship between EndoG and AIF in mammalian cells has yet to be identified.

Although a majority of reports support the cell death-inducing role of EndoG in cerebral ischemia, a total agreement has yet to be reached, due to controversial results with EndoG-null mice. EndoG-null mice have been generated by different labs; they show variable characteristics. Zhang et al. reported that embryos with EndoG homozygous mutation die between embryonic day 2.5 and 3.5, and that mice with EndoG heterozygous mutation appear normal and exhibit increased resistance to both TNF-α and staurosporine-induced cell death and reduced DNA fragmentation (Zhang, Dong, et al. 2003). On the other hand, EndoG-null mice from Liber and Dawson's lab showed no obvious difference compared to WT mice, which indicates that EndoG is dispensable in embryogenesis and normal apoptosis (Irvine et al. 2005; David et al. 2006). In additional, EndoG-null mice in Dawson's lab show no difference in infarct volume and neurologic deficit scores after tFCI compared to the WT mice (Xu, Zhang, et al. 2010). Thus, additional investigations are needed to determine the validity of EndoG-deficiency mice,

the pathways involved in activation of EndoG and to what extent EndoG is involved in ischemic neuronal cell death.

1.3.3.3 Poly(ADP-ribose) polymerase 1

Poly(ADP-ribosyl)ation is post-translational modifications of proteins and plays a crucial role in cell cycle, gene transcription, DNA integrity and repair, and cell death in eukaryotic cells (Bouchard, Rouleau, and Poirier 2003). PARP1, also known as poly(ADP-ribose) synthetase and poly(ADP-ribose) transferase, is a highly conserved, 113 kDa nuclear enzyme. It catalyzes the formation of $(ADP\text{-}ribose)_n$ chains by consuming nicotinamide adenine dinucleotide (NAD^+) (Bouchard, Rouleau, and Poirier 2003). PARP-1 activity rapidly increases up to 500-fold in response to DNA strand breaks and is known as "guardian of the genome" (Muiras and Burkle 2000). However, excessive DNA damage, which leads to over-activation of the PARP-1, would result in a rapid decline in cellular NAD^+. NAD^+ affects the activities of the enzymes involved in glycolysis, the pentose phosphate shunt, and the Krebs cycle. In an attempt to restore NAD^+ pools, the cell resynthesizes NAD^+ by combining nicotinamide with 2 ATP. As a consequence, cellular ATP levels become depleted, and a cellular energy crisis may arise, which may lead to cell death (Koh, Dawson, and Dawson 2005).

It has been proposed that the ATP intracellular level is crucial for the decision of activating the energy-dependent apoptotic pathway or the passive necrosis. Since PARP-1 over-activation depletes energy stores, PARP-1-mediated death should be necrotic (Yu et al. 2003). PARP inhibitors attenuated OGD-induced injury in cortical neurons, which

exhibit ultrastructural features of necrotic cell death and no caspase-3 activation (Moroni et al. 2001). These inhibitors were unable to reduce apoptotic CA1 pyramidal cell death in organotypic hippocampus culture after OGD (Moroni et al. 2001). However, the necrotic nature of PARP-1-mediated death has been challenged by Yu et al., who observed that cell death initiated from PARP-1 overactivation has features associated with traditional apoptotic death, including chromatin condensation and phosphatidylserine exposure on the outer membrane (Yu et al. 2003). Thus, cells undergoing PARP-1-induced cell death exhibit characteristics commonly associated with both apoptosis and necrosis. Under which circumstance PARP overactivation would result in rapid energy depletion and necrotic cell death or typical apoptosis is still not clear.

It is unknown how PARP-1 activation regulates cell death phenotypes, but PARP-1 cleavage is different in apoptosis and necrosis (Soldani and Scovassi 2002). PARP-1 has three distinct functional domains: the DNA binding domain (DBD, 46 kDa), which is located in the N-terminus; the automodification domain (22 kDa) at the central region of the protein; and the NAD^+-binding domain (55 kDa) at the C-terminus, which is essential for the conversion of NAD^+ into ADP-ribose (Virag 2005). During apoptosis, almost all caspases *in vitro* and only caspase-3 and caspase-7 *in vivo* can cleave and inactivate PARP-1 (Soldani and Scovassi 2002). Caspase 3 can recognize a specific site in the DBD, which leads to a 24-kDa N-terminal fragment and an 89-kDa C-terminus fragment (D'Amours et al. 1998). The 24kDa fragment is able to irreversibly bind DNA end and promote apoptosis by inhibiting DNA repair and ADP-ribose formation. The 89-kDa-

fragment retains the basal enzymatic activity, but it cannot be stimulated by strand breaks (Soldani and Scovassi 2002). The cleavage of PARP-1by caspase is responsible for the inactivation of the poly(ADP-ribosylation) process. It protects the pool of energetic substrates against the use of these substrates by PARP-1, leaving sufficient energy to finish the apoptotic process (Herceg and Wang 1999). During necrosis, PARP-1 is degraded differently from apoptosis. It can be cleaved by the lysosomal proteases such as cathepsin B, D and G into 55kDa and 62 kDa fragments (Gobeil et al. 2001). This may be due to the inactivation of caspases in necrotic cell death, but whether or not caspase is the key to decide cell death destiny has to be further investigated.

PARP-1-mediated caspase independent cell death is demonstrated by the findings that broad-spectrum caspase inhibitors can not prevent PARP-1-induced necrotic cell death (Gobeil et al. 2001). Hyperactivation of PARP-1 has been linked to two other mediators in programmed necrosis, AIF (Yu et al. 2002; Hong, Dawson, and Dawson 2004) and RIP1 (Xu, Huang, et al. 2006). Activation of PARP-1 initiates a nuclear signal that propagates to mitochondria and triggers AIF release in alkylating DNA damage, which induces necrotic cell death (Moubarak et al. 2007). Genetic suppression of PARP-1 (Yu et al. 2002) and administration of PARP-1 inhibitors (Culmsee et al. 2005) decreased AIF translocation. In reverse, microinjection of an antibody to AIF protects against PARP-1-dependent cytotoxicity (Yu et al. 2002). The mechanism of how the nuclear enzyme PARP-1causes mitochondrial AIF release is still not clear. It is reported that poly(ADP-ribose) binds to AIF and triggers AIF release from cytosolic side of the MOM. Mutation of the binding site in AIF does not affect the biological function of AIF but blocks AIF

release from mitochondria after PARP-1 activation (Wang, Kim, et al. 2011). Calpain and Bax are identified as two essential molecular links between PARP-1 and AIF. PARP-1 activation induced by alkylating DNA damage initiates AIF release and necrosis through a mechanism requiring calpain, but not cathepsins or caspases. In this model, ablation of Bax prevents AIF translocation and cell death (Moubarak et al. 2007). Overexpression of the endogenous calpain inhibitor calpastatin reduces AIF translocation in MNDA-induced neuronal excitotoxic stress (Vosler et al. 2009). Put together, these data suggest the molecular ordering of PARP-1, calpains, Bax and AIF activation in programmed necrosis (Moubarak et al. 2007). The key regulator RIP1 is indicated as the upstream of PARP-1 signalling to mitochondria in programmed necrosis. Knockouts of RIP1 and tumor necrosis factor receptor-associated 2 (TRAF2) causes a resistance to PARP-1 induced cell death (Xu, Huang, et al. 2006). Nec-1 inhibited RIP1 activity (Degterev et al. 2008) and reduced PARP-1 activity after glutamate treatment in HT-22 cells (Xu, Chua, et al. 2010).

PARP-1 activation has been linked to ischemic brain injury for many years. During ischemia, increased intracellular Ca^{2+} and reactive oxygen species (ROS) may cause neuronal death by inducing DNA strand breaks, which leads to over-activation of PARP-1 (van Wijk and Hageman 2005). PARP activation is responsible for neuronal cell death after glutamate toxicity (Duan, Gross, and Sheu 2007) and OGD (Tanaka et al. 2005) *in vitro* and after experimental stroke *in vivo* (van Wijk and Hageman 2005). Inhibition of PARP-1 by gene silence or administration of an appropriate dose of PARP-1 inhibitors within a reasonable time drastically reduced the infarct volume in *in vitro* and *in vivo*

models of cerebral ischemia (Moroni et al. 2001; Iwashita et al. 2004; Chiarugi et al. 2003). In addition, neurons obtained from PARP-deficient mice are resistant to NMDA toxicity and OGD injury (Pieper et al. 1999); and brain infarct volume after MCAO is significantly reduced in PARP-$1^{-/-}$ mice compared with WT mice (Li, Klaus, et al. 2010). The mechanism by which PARP-1 deficiency protects neurons against ischemia is still under investigation. Although there is a decrease of infarct size in PARP-1 deficient ischemic brain, the apoptosis markers such as oligonucleosomal DNA damage and TUNEL are not different from control (Sairanen et al. 2009). During OGD/reoxygenation, PARP-1 activation is accompanied by mitochondrial permeability transition, membrane depolarization, and mitochondrial release of cytochrome c, AIF and EndoG in cortical neurons (Tanaka et al. 2005).These changes are attenuated through inhibition of PARP-1 by its inhibitors 1,5-dihydroxyisoquinoline and benzamide, or by small interfering RNA (Tanaka et al. 2005). Hence, excessively activated PARP-1 in ischemic neurons may be associated with necrotic features of neuronal death and appears to be caspase-independent.

1.3.3.4 Questions about caspase-independent cell death

The caspase-independent cell death pathway could either be a default pathway that is activated only when caspases are inhibited or a parallel pathway that is activated by the original death stimulus. Cerebral ischemia can cause both caspase dependent and independent neuronal death. How neurons commit to a certain death pathway is still unknown. It has been proposed that energy depletion, free radical generation, and the MPTP remaining open are the underlying mechanisms that determine how neurons die.

Overexpression of a viral caspase inhibitor (crmA or p35) inhibited the release of AIF in mixed cortical cultures exposed to OGD, suggesting that there is cross-talk between the caspase-dependent and the caspase-independent pathway (Singh et al. 2010). However, more intensive research has to be done to identify the relationship between these two pathways under cerebral ischemia.

In the past decades, PCD was considered synonymous with apoptosis, which is actively executed by specific proteases, the caspases. So is caspase-independent PCD apoptosis? The presence of chromatin condensation and DNA fragmentation alone might lead us to think that caspase-independent PCD is classically apoptotic, but it is clear that the peripheral chromatin condensation and large-scale DNA fragmentation in AIF and EndoG-induced cell death is distinct from the global chromatin condensation and oligonucleosomal DNA fragmentation in caspase-dependent apoptosis (Park et al. 2005). These differences suggest that AIF and EndoG cause a unique type of cell death via a unique intracellular pathway. Different groups have characterized AIF-mediated cell death differently: some continue to refer to it as apoptosis, while others use the term programmed necrosis, since the proteins (AIF, EndoG and PARP-1) play critical roles in caspase-independent cell death pathway are all involved in the programmed necrosis. This raises the possibility that caspase-independent PCD and programmed necrosis might, in fact, be the same process.

1.4 Bcl-2 family regulates caspase-dependent/independent neuronal death pathway

1.4.1 Bcl-2 family

The Bcl-2 family play important roles in cellular homeostasis and PCD. To date, over 25 Bcl-2 family members have been identified. These proteins can be broadly divided into two classes: those that inhibit apoptosis and those that promote apoptosis. Homeostasis is maintained by controlling the balance of active pro- and anti-apoptotic family members along with tissue-specific patterns of expression (Festjens et al. 2004). Stimuli such as ischemia can lead to increased expression of pro-apoptotic family members, disrupt the balance between pro- and anti-apoptotic proteins and subsequently lead to PCD. On the other hand, if the balance tips towards increased anti-apoptotic protein levels, then unchecked cellular proliferation results in tumorigenesis (Youle and Strasser 2008). Indeed, emerging biochemical and genetic evidence also demonstrate that Bcl-2 family members are integral components of distinct homeostatic pathways and carry out "daily jobs" beyond regulating apoptosis. They are not only involved in the mitochondrial energy metabolism, including metabolite transfer across the mitochondrial membrane, ER-mitochondrial trafficking of calcium, mitochondrial dynamics and nutrient metabolism, but also play roles in cell cycle checkpoints and cellular quality control mechanism such as autophagy and unfolded protein response (Danial, Gimenez-Cassina, and Tondera 2010).

The Bcl-2 family shares sequence homology with α helical segments known as "Bcl-2 homology" (BH) domains. Four of these domains (BH1-4) have been identified, and each

Bcl-2 family member contains at least one BH3 domain. The anti-apoptotic proteins such as Bcl-2 and Bcl-x_L, possess all four BH domains. BH4 domain is sufficient for an anti-apoptotic effect. The pro-apoptotic class of Bcl-2 family members has been divided into two subclasses based on the presence of one or more BH domains: the "multi-domain" family pro-apoptotic proteins, such as Bax and Bak, possess sequence homology for the BH1, BH2, and BH3 regions; BH3-only pro-apoptotic proteins, such as Bid and BNIP3, have strong homology only in the BH3 region (Kelekar and Thompson 1998). Mutagenesis studies indicate that the BH1, BH2, and BH3 domains strongly influence homo- and hetero-dimerization of these proteins. For example, the BH3 region is responsible for mediating the interactions of Bax with anti-apoptotic proteins and promoting PCD (Zha et al. 1996). Peptides derived from the BH3 region of pro-apoptotic Bcl-2 family members can bind to anti-apoptotic family members such as Bcl-x_L and modulate apoptotic pathways in living cells (Moreau et al. 2003). According to their relative affinity, it has been proposed that the BH3-only proteins neutralize anti-apoptotic Bcl-2 proteins; free multi-domain pro-apoptotic family members execute cell death (Lindsay, Esposti, and Gilmore 2011). Besides the BH region, some of the Bcl-2 family members possess a carboxy-terminal hydrophobic domain, which is predicted to be responsible for membrane attachment and cellular localization (Yasuda et al. 1998). Patterns of membrane localization differ among these Bcl-2 family proteins. For example, Bcl-2 has been shown to reside on the cytoplasmic face of the mitochondrial outer membrane, which enables Bcl-2 to modulate mitochondrial membrane integrity (Gotow et al. 2000). In contrast to Bcl-2, pro-apoptotic family members, such as Bax, are found mainly in the cytosol and are only localized to the mitochondrial membrane upon

activation (Suzuki, Youle, and Tjandra 2000). In additional, in some BH3-only pro-apoptotic proteins like BNIP3, the C-terminal transmembrane domain is not only essential for membrane anchoring, but also critical for promoting apoptosis (Yasuda et al. 1998).

1.4.1.1 Bcl-2 family and caspase-dependent cell death pathway

The regulatory role of Bcl-2 family has been described in the intrinsic mitochondrial cell death pathway. It appears that the pro-apoptotic family members like Bax and Bak are crucial for inducing permeabilization of the MOM (Dewson and Kluck 2009) and the subsequent release of apoptotic molecules such as cytochrome c and DIABLO, which leads to caspase activation (Belizario et al. 2007). The exact mechanism by which Bcl-2 family proteins induce permeabilization of the MOM is controversial and still under intense investigation. So far, several models have been proposed. One of the mechanisms is via its interaction with pre-existing channels such as the MPTP. The MPTP is a non-specific large proteinaceous pore that spans the inner and outer mitochondrial membranes, allowing the passage of ions and substrates. It is a voltage-dependent channel that can be activated by Ca^{2+}, and inhibited by protons or ADP (Bernardi and Forte 2007). Bax is able to cause opening of MPTP by directly interacting with and the voltage-dependent anion channel (VDAC) and Adenine Nucleotide Translocase (ANT), two components of MPTP, and modulates their activities (Vyssokikh et al. 2004). A MPTP inhibitor cyclosporine A inhibits apoptosis induced by over-expression of Bax in Jurkat T cells (Pastorino et al. 1998). Bax/Bak-induced loss of membrane potential is found in WT mice but not VDAC1-deficient yeast mitochondria, and anti-VDAC antibody blocks Bax-

induced cytochrome c release (Shimizu, Narita, and Tsujimoto 1999). The second possible mechanism is forming channels themselves by Bcl-2 family proteins in mitochondrial membrane. Bax has the capability to form channels through inserting its oligomerization into outer membrane of mitochondria (Antonsson et al. 2000). These Bax channels play an important role in mediating neuronal death, as Bax channel inhibitors prevent cytochrome c release from mitochondria, inhibits the decrease in the mitochondrial membrane potential, and protects cells against apoptosis (Hetz et al. 2005). It was also proposed that Bax-VDAC interaction results in a large pore, VDAC-Bax channel, through which apoptogenic proteins were released (Banerjee and Ghosh 2004). Overall, these mechanisms may not be necessarily exclusive. They may occur in a sequential and parallel fashion depending on cell type, stimulus and level of stress. All of them lead to the same ending: loss of mitochondrial membrane potential, mitochondrial matrix swelling, and rupture of the MOM at the end stages of apoptosis. However, these models cannot explain the specific release of pro-apoptotic proteins residing in the intermembrane space. Some studies propose that, at this early stage of mitochondrial permeabilization, pore formation of the outer membrane leads to the release of small amounts of cytochrome c. This process is thought to be reversible, since previous studies have shown that mitochondria can undergo a reuptake of cytochrome c and thereby arrest the death process (Ripple, Abajian, and Springett 2010). If apoptosis continues, however, the loss of mitochondrial membrane potential may lead to the rupture of the outer membrane of mitochondria or the opening of specific channels responsible for the release of the greater portion of cytochrome c and other death-inducing proteins, and lead to irreversible cell death (Gogvadze, Orrenius, and Zhivotovsky 2006).

The anti-apoptotic family members such as Bcl-2 and Bcl-x_L prevent apoptosis either by preventing releasing of mitochondrial apoptogenic factors into the cytoplasm or by sequestering performance of caspases (Lindsay, Esposti, and Gilmore 2011). Anti-apoptotic proteins tend to preserve mitochondrial integrity, although the mechanism still remains to be determined. It is proposed that Bcl-x_L binds directly with VDAC and blocks Bax/Bak-induced cytochrome c release through VDAC (Shimizu, Narita, and Tsujimoto 1999). Like Bax, Bcl-2 and Bcl-x_L can also form ion channels in synthetic lipid membrane. Unlike Bax, which creates channels to unsettle homeostasis, Bcl-2 and Bcl-x_L form heterodimers with Bax and thereby antagonize Bax activity (Lang-Rollin et al. 2005). Furthermore, Bcl-x_L binds indirectly to both pro-caspase-8 and Apaf-1/pro-caspase-9 complex to sequester caspases to prevent their activation (Stegh et al. 2002; Hu et al. 1998). Thus, the Bcl-2 family acts as a critical life-death decision point within the common pathway of apoptosis.

1.4.1.2 Bcl-2 family and caspase-independent cell death pathway

It is widely accepted that mitochondrial proteins like AIF and EndoG translocation require permeabilization of the outer mitochondrial membrane, an event that is under tight control of Bcl-2 family. AIF translocation involves the activation of pro-apoptotic molecules from Bcl-2 family, such as Bid and Bax. Truncated Bid (tBid) is associated with AIF release, and cleavage of Bid has been demonstrated to occur simultaneously with AIF translocation from mitochondria into the nuclei (Landshamer et al. 2008). MOM permeabilization caused by tBid resulted in cytochrome c and AIF release from isolated liver or brain mitochondria (Polster et al. 2005). Bax expression also leads to an

increase of AIF efflux from mitochondria in neurons. Accordingly, a model of AIF release has been proposed: tBid and Bax interact with mitochondria to open MPTP or form a membrane pore where they cleave AIF and thereby disassociate AIF from the inner mitochondrial membrane. Such proteolytic cleavage is necessary for AIF before leaving the mitochondria to the nucleus to execute DNA degradation and cell death (Arnoult et al. 2003). The anti-apoptotic proteins Bcl-x_L and Bcl-2 can prevent AIF translocation in neuronal cultures challenged with transient OGD (Cao et al. 2003; Tsujimoto 1998). This may account for the acquisition of resistance to neuronal cell death following brief ischemia.

Similar to AIF, EndoG release is also under the control of Bcl-2 family. The release of EndoG from mitochondria was originally described following treatment of isolated mitochondria with tBid, a membrane-targeted death ligand, by caspase-8. In this study, mitochondrial efflux of EndoG could be induced by tBid in normal mice but not in Bcl-2 transgenic mice (van et al. 2001). EndoG release can also be blocked by Bcl-x_L (Kim, Emi, and Tanabe 2005). What is more, another pro-apoptotic protein Bim, which mediates cell death in a caspase-independent fashion, is able to induce EndoG release (Schneiders et al. 2009). This release can also be blocked by both Bcl-x_L and EndoG antibodies (Noda et al. 2009). These results indicate that the balance of pro-apoptotic and anti-apoptotic proteins decides the EndoG translocation. Recently, we found that another pro-apoptotic protein BNIP3 induced a caspase-independent neuronal death pathway is mediated by EndoG in hypoxia and stroke (Zhang, Yang, et al. 2007). The precise mechanism by which Bcl-2 family controls EndoG release from mitochondria remains

controversial. One proposed model involves rupture of MOM as a consequence of mitochondrial swelling after the opening of the MPTP. A Ca^{2+} induced MPTP induced complete EndoG release has been reported and EndoG release can be prevented by MPTP inhibitor cyclosporine A (Belizario et al. 2007). However, opening of MPTP induced mitochondrial proteins release is non-selective, and these proteins include cytochrome c, AIF, Smac/DIABLO and HtrA2/Omi (Uren et al. 2005). This does not agree with other reports on the selective release of EndoG and AIF. In the cells treated with pro-apoptotic drugs that result in the eventual loss of mitochondrial membrane potential, the caspase-inhibitor zVAD-fmk or Apaf-1 deficiency prevent EndoG and AIF diffusion into the cytosol, whereas cytochrome c, Smac/DIABLO and HtrA2/OMI release were unaffected (Arnoult et al. 2003). On the other hand, Bax/Bak induce a selective process of outer membrane permeabilization, allowing the selective release of proteins soluble in the inner-membrane space such as cytochrome c, but not EndoG and AIF (Arnoult et al. 2003). Although an agreement has yet to be reached, it has been suggested that release of cytochrome c would activate caspase 3, which in turn would be required for release of EndoG (Li, Zhou, et al. 2010). If this is the case, although the DNA fragmentation caused by EndoG is caspase-independent, the translocation of EndoG is caspase-dependent. However, one cannot exclude that differences in the sensitivities of proteins detection may explain the observation of differential release between EndoG and cytochrome c.

1.4.1.3 Bcl-2 family and ischemic neuronal death

Altered expression of Bcl-2 family members by hypoxic-ischemic injury has been reported, and the role of Bcl-2 family members in regulating neuron death has been extensively investigated in animal models *in vivo* and *in vitro*. For example, Bax was upregulated at both mRNA and protein levels in CA1 neurons with morphological features of apoptosis after transient global cerebral ischemia (Ferrer et al. 1998). Several studies demonstrate that Bax contributes to neuronal death in the infarcted thalamus and cortex and plays a role in determining cell survival in sub-lethally injured cells following focal cerebral ischemia (Gillardon et al. 1996). Translocation of Bax from cytosol to mitochondria has also been found in caudate neurons, with a temporal profile and regional distribution coinciding with the mitochondrial release of cytochrome c and activation of caspase-9. Bax forms a heterodimer with the MPTP. A MPTP inhibitor bonkrekic acid, which prevents Bax and MPTP interactions and inhibits Bax-triggered cytochrome c and caspase-9 release, offered significant neuroprotection against ischemia-induced neuronal death in the brain (Cao et al. 2001). Bax-deficient mice exhibit significantly decreased caspase-3 activation and infarct volume as compared with WT mice in a neonatal hypoxia-ischemia model (Gibson et al. 2001). Also involved is another pro-apoptotic member Bid, cleavage of which to tBid plays a role in mediating delayed neuronal death after stroke (Plesnila et al. 2001).

Elevated expression of anti-apoptotic Bcl-2 family members has been demonstrated in hypoxia model in cultured neurons *in vitro* and several ischemic models *in vivo*. Levels of Bcl-2 were found to be high in CA3, a region where neurons are less susceptible to

ischemic damage (Chen et al. 1996). Bcl-2-deficient mice show increased infarct size and more severe neurological deficits following transient MCAO as compared with heterozygous and WT littermates (Hata et al. 1999). A decline in the cell death repressor Bcl-2 is accompanied by an increase in cell death effectors, whereas over expression of anti-apoptotic Bcl-2, using a herpes simplex amplicon, inhibits cytosolic accumulation of cytochrome c and caspase-3 activation, and partially prevents neurons from ischemic cell death (Zhao et al. 2004). CNS injection of viral vectors drives over-expression of other anti-apoptotic Bcl-2 family members such as Bcl-x_L and Bcl-w and results in significant diminution in neuronal cell death and infarct size. Nonetheless, induction of Bcl-2 mRNA and protein was observed in CA1 pyramidal neurons in the gerbil hippocampus following transient forebrain ischemia, suggesting that expression of anti-apoptotic Bcl-2 is not sufficient to prevent delayed neuronal death (Chen et al. 1996). Another group demonstrated that Bcl-2 level increased at the early stage of ischemia but decreased during the ischemia progression, suggesting that Bcl-2 contributes to the neuronal survival against ischemia (Zhang and Wang 1999). It appears that Bcl-2 expression may be influenced by the degree of insult, time course of insult, and other factors, like species and gender (Alkayed et al. 2001). Overall, these studies suggest that the expression of pro- and anti-apoptotic Bcl-2 family members critically regulates responsiveness to hypoxic-ischemic injury and that inhibition of Bcl-2 family-dependent death pathways could offer significant protection from stroke.

1.4.2 BNIP3 subfamily

1.4.2.1 BNIP3

BNIP3 (formerly known as NIP3) is a 194 amino acid pro-apoptotic BH3-only member of the Bcl-2 protein family. Under physiological conditions, BNIP3 is expressed in skeletal muscle and the brain at a low level. It is normally located in the cytosol and loosely attached to the mitochondrial membrane, but during the induction of cell death, it can tightly integrate into the MOM and cause cell death in a variety of cells, including neurons (Lee and Paik 2006). Native BNIP3 is shown to be a 30 kDa protein that covalently dimerizes to 60 kDa in Western blot, as reducing conditions are not usually sufficient to resolve the dimer configuration (Vande et al. 2000). The BNIP3 protein has four domains: a PEST domain that targets for BNIP3 degradation, a BH3 domain that is homologous to other members of the Bcl-2 family, a CD domain that is conserved from C. elegans to humans and a C-terminal transmembrane domain (ΔTM) that is required for its mitochondrial localization as well as for its death-inducing activity (Yasuda et al. 1998). Many members of the Bcl-2 family require a BH3 domain to induce or prevent apoptosis. However, the BH3 domain of BNIP3 is not required for its heterodimerization with Bcl-2 family members or for its ability to stimulate cell death (Kim et al. 2002) - this suggests that BNIP3 induces cell death through a different mechanism. Cell transfection studies further showed that the BNIP3-induced cell death does not involve Apaf-1, caspase activation, or cytochrome c release (Vande et al. 2000; Zhang, Yang, et al. 2007). Integration of BNIP3 into mitochondrial membranes causes MPTP opening, mitochondrial membrane potential suppression and ROS production (Vande et al. 2000).

There is considerable debate in the literature regarding what type of cell death is induced by BNIP3. Although BNIP3 is identified as an apoptogenic protein, it is also involved in necrotic cell death and autophagic cell death. Vande et al. first showed that the morphology of cell with BNIP3 transfection is necrotic-like (Vande et al. 2000): cells exhibit early plasma membrane permeability, mitochondrial damage, extensive cytoplasmic vacuolation, and mitochondrial autophagy. Webster et al. found that BNIP3 activates an atypical programmed cell death pathway with features of both apoptosis and necrosis in cardiac myocytes (Webster, Graham, and Bishopric 2005). Recently, BNIP3 is identified as being required for mitochondrial membrane permeabilization in Shiegella-induced programmed necrosis (Galluzzi and Kroemer 2009). Furthermore, TNF upregulated BNIP3 expression, which leads to increased sensitivity to the programmed necrosis (Kim et al. 2011). Finally, BNIP3 is also considered as the upstream regulator of AIF (Walls et al. 2009) and EndoG(Zhang, Yang, et al. 2007), two proteins that have previously been implicated in programmed necrosis. It has been observed that BNIP3 can also cause autophagy. Loss of BNIP3 is protective against hypoxia-induced autophagic cell death (Azad and Gibson 2010), and ectopic expression of BNIP3 triggers autophagy in normoxia (Azad et al. 2008). So BNIP3 may play dual roles in these cell death phenotypes. Further studies are required to establish the nature of cell death regulated by BNIP3.

BNIP3 has been prominently implicated in cell elimination in a variety of cells including myocytes and neurons under ischemic conditions. Under hypoxic condition, BNIP3 mRNA increased 12-fold, and BNIP3 protein increased 6-fold in cardiac myocytes. It

was one of the most strongly up-regulated genes in a microarray analysis of cardiac myocytes exposed to hypoxia (Webster, Graham, and Bishopric 2005). This is highlighted by studies with transgenic mice in which forced cardiac overexpression of BNIP3 increased myocyte cell death, while BNIP3 deficiency inhibits the myocyte death and diminishes myocardial dysfunction following ischemia/reperfusion (Diwan, Krenz, et al. 2007).Using the dominant-negative form of BNIP3 (BNIP3ΔTM) suggests BNIP3 homodimerization and mitochondrial insertion are required for BNIP3-mediated myocyte death in ischemia (Regula, Ens, and Kirshenbaum 2002). Further, transduction of a cell-permeable version of BNIP3ΔTM into whole heart confers protection against ischemia/reperfusion injury and improves cardiac function (Kubli et al. 2008). BNIP3 is not detectable in normal brain neurons, but it has been shown to play a role in neuronal cell death during stroke. BNIP3 is induced in a rat MCAO model: levels of BNIP3 were low for up to 24 hours but started to accumulate 48 hours post-MCAO (Zhang, Yang, et al. 2007). The expressed BNIP3 was in its active form because it was membrane-bound and localized to mitochondria. BNIP3 expression was also induced in cultured primary neurons by hypoxia (Zhang, Yang, et al. 2007) and OGD/reoxygenation (Zhao et al. 2009). The level BNIP3 started to accumulate after hypoxic exposure for 36 hours and increased up to 10-fold after 72 hours of hypoxia exposure. Inhibition of BNIP3 by RNAi protects neurons from hypoxia-induced cell death (Zhang, Yang, et al. 2007). Besides hypoxia and ischemia, BNIP3 has also been implicated in cancer (Leo, Horn, and Hockel 2006), macrophage cell death induced by anthrax lethal toxin (Ha et al. 2007) and synovial hyperplasia in rheumatoid arthritis (Kammouni et al. 2007).

Ischemia is associated with both hypoxia and acidosis due to increased glycolysis and lactic acid production. Prolonged hypoxia induces the expression of BNIP3 mRNA and protein in cardiac myocytes, but acidosis is required to activate the death pathway. The accumulation of BNIP3 is more rapid under acid environment and peaks at more than 3-fold higher than in the pH neutral sample, and acidic pH promotes a stronger alkali-resistant association of BNIP3 with mitochondrial membrane (Kubasiak et al. 2002). These indicate that BNIP3 protein may be stabilized by acidosis. Furthermore, acidic pH mediates increased half-lives of BNIP3 dimers and monomers , while neutralization of the extracellular medium of cardiac myocyte cultures under hypoxia-acidosis results in rapid degradation of accumulated BNIP3 (Frazier et al. 2006). BNIP3 accumulates under hypoxia at neutral and acidic pH, but cell death occurs only with coincident acidosis, which explains why hypoxia does not induce cardiac myocyte apoptosis in the absence of acidosis (Graham et al. 2004). The characteristics of hypoxia-acidosis induced cardiac myocytes death include extensive DNA fragmentation and opening of MPTP. This cell death can be blocked by exposure to MPTP inhibitors or BNIP3 antisense oligonucleotides, but not by caspase inhibitors (Webster, Graham, and Bishopric 2005). These findings are consistent with BNIP3-induced caspase-independent cell death pathway. Fourteen years ago, acid-sensing ion channels (ASICs) were first cloned and shown to be widely distributed in the nervous system, and it is now well accepted that ASIC1a channels mediate ischemic neuronal death (Wang and Xu 2011). Thus, it would be interesting to find out whether or not ASIC contributes to the BNIP3 mediated neuronal death.

The expression of BNIP3 is primarily, if not solely, regulated by the transcriptional factor hypoxia-inducible factor (HIF-1) (Althaus et al. 2006). HIF-1 is a basic helix-loop-helix PAS domain (BHLH-PAS) transcription factor that normally regulates the adaptive response to hypoxia in cells (Greijer and van der 2004). This heterodimeric transcription factor is composed of two subunits: HIF-1α and HIF-1β. Although HIF-1β protein is expressed constitutively, the expression of HIF-1α is tightly regulated by cellular oxygen levels. HIF-1α undergoes proline hydroxylation and is ultimately broken down after ubiquitination under normoxia, but it becomes stabilized under hypoxic conditions by binding to HIF-1β subunit to form the active HIF-1 complex. HIF-1 then translocates to the nucleus and binds to hypoxia responsive elements (HRE) present in the promoter region of its target genes to initiate gene transcription (Wang and Semenza 1993). In most cases, HIF-1-activated gene expression is an adaptive response of the body to regain cellular homeostasis. However, HIF-1 has also been shown to initiate the expression of several death genes (Greijer et al. 2005). Characterization of the BNIP3 gene revealed that the BNIP3 promoter contains a functional HIF-1-responsive element and that expression of BNIP3 could be potently activated by both hypoxia and forced expression of HIF-1α (Sowter et al. 2001). Results from our laboratory showed that both BNIP3 and HIF-1α increase under hypoxia in neurons. Inhibition of HIF-1 activity by knocking down HIF-1α, abolishes BNIP3 expression and rescues neurons from hypoxia. This observation is also supported by Halterman and his colleagues, who found that a dominant-negative form of HIF-1α (HIFdn) was able to reduce delayed neuronal death following hypoxic stress once delivered to the cortical neuronal cultures by herpes amplicon (Halterman, Miller, and Federoff 1999). Additionally, we also obtained data

that the increase of delayed apoptotic death highly corresponds to p53 expression and that the knockdown of p53 significantly protects neurons from hypoxia. The involvement of p53 in delayed neuronal death is also supported by reduced ischemic damage in p53 knockout mice (Crumrine, Thomas, and Morgan 1994). Enhanced resistance of p53-null cortical culture to hypoxia (Halterman, Miller, and Federoff 1999) re-established hypoxia-induced cell death after restoration of p53 to p53-null background (Ludwig, Bates, and Vousden 1996). Halterman and his colleagues proposed that hypoxic activation of HIF-1 signaling depends on p53 for its apoptotic readout. This came about when they found that HIFdn did not promote survival in p53-null neurons exposed to lethal levels of hypoxia in contrast to its ability to protect WT neurons (Halterman, Miller, and Federoff 1999). Recently, we reported that oxidative stress functioned as a redox signal to induce HIF-1α accumulation and subsequent activation of BNIP3 (Zhang, Zhang, et al. 2007). The transcription of BNIP3 can be suppressed by the activation of the NF-κB signalling pathway through NF-κB response elements within the BNIP3 promoter (Baetz et al. 2005). It has been suggested that the tight regulation of BNIP3 expression is a prerequisite for maintaining the mitochondrial intentity and for cell survival.

1.4.2.2 NIX

Several human homologues of BNIP3 have been reported: NIX (BNIP3 like protein X, also called BNIP3L or BNIP3a), BNIP3h and Caenorhabditis elegans ortholog(ce)BNIP3(Zhang, Cheung, et al. 2003). All aforementioned proteins in combination with BNIP3 form a unique subfamily of death-inducing mitochondrial proteins. NIX is not an alternatively spliced product of BNIP3, but it has about 56%

amino acid sequence homology to BNIP3 and induces apoptosis at comparable rates in cell culture (Chen et al. 1999). BNIP3h shares the identical cDNA with NIX, but it has different nucleotide sequences at both 5' and 3' untranslated regions (Farooq et al. 2001). Homology researches have found that ceBNIP3 has 21% amino acid homology to BNIP3. The homology between ceBNIP3 and the mammalian members includes a highly conserved 19-amino-acid sequence encompassing the BH3 domain and the TM domain. However, the BH3 domain of ceBNIP3 is somewhat divergent from those of the mammalian BNIP3 and NIX (Cizeau et al. 2000).

NIX not only shares structure similarity with BNIP3, but also functions like BNIP3: (1) NIX is also characterized by the presence of PEST sequences at the N-terminal region, and its degradation is dependent on the same active proteasome. (2) NIX encodes a 23.8 kDa protein but it is expressed as a 48 kDa protein in Western blot, suggesting that it homodimerizes similarly to BNIP3. (3) NIX induces cell death (Chen et al. 1999). Mice with NIX overexpression in conditional cardiac expression system died after about one week of life, and pathological and histological studies revealed left ventricular dilation and poor contractility as well as striking increases of cardiomycytes apoptosis (Dorn and Kirshenbaum 2008). (4) Pro-apoptotic activity of NIX is controlled by the ΔTM domain. NIX localizes to mitochondria via C-terminal transmembrane domain by altering mitochondrial membrane permeability (Chen et al. 1999). (5) NIX binds to the anti-apoptotic proteins, such as Bcl-2 and Bcl-x_L (Imazu et al. 1999). (6) BNIP3 and NIX are strongly activated by hypoxia in specific cell types, such as cardiomyocytes and neurons, and constitute important mitochondrial sensors for various stress stimuli (Dorn and

Kirshenbaum 2008). In addition, although it was reported that NIX promotes cell death involving cytochrome c release and caspases activation (Yussman et al. 2002), recent research in cardiomyopathy indicate that mitochondrial NIX activates Bax/Bak and caspase-independent apoptosis, whereas ER-NIX activates MPTP-dependent necrosis (Chen et al. 2010). Thus, it seems that both BNIP3 and NIX stimulate cell death with features of both apoptosis and programmed necrosis. In the context of recent studies, a role for NIX as well as BNIP3 in mitochondrial autophagy has been identified, which positions BNIP3 and NIX at the apex of multiple parallel pathways leading to PCD. Although a clear relationship between BNIP3 and NIX awaits further investigation, they may have very similar cellular effects.

Endogenous NIX is upregulated by ischemia injury. Transgenic mice that overexpress NIX in the heart die as neonates (6–7 days after birth) and show features of cardiac hypertrophy and apoptosis. Cardiac-specific deletion of NIX provided a high degree of protection against cardiomyopathies induced by Gq overexpression or by pressure overload (Dorn 2010). These studies suggest that NIX is not only an initiator and effector of cell death pathway but also a sensor of cardiac stress that helps to coordinate transcriptional and physiological cues for programmed cardiomyocyte death. In neurons, NIX upregulation and mitochondrial translocation are observed in ipsilateral cortex and striatum 6 hrs after MCAO. However, these changes of NIX are not preceded by Bax activation or caspase cleavage, which is opposite to the *in vitro* finding in hypoxia/serum-deprived CHO-K1 cells (Birse-Archbold et al. 2005). Moreover, NIX is highly induced in wild-type p53 expressing cells during hypoxia, and cell death induced by hypoxia

exposure is reduced by NIX knockdown (Fei et al. 2004). Therefore, NIX also plays a role in p53-dependent apoptosis during hypoxia. In summary, these results suggest that NIX is a critical determinant in cell death, and BNIP3 and NIX may be important therapeutic targets.

1.4.2.3 BNIP3 mediated caspase-independent cell death pathway

Although BNIP3 is identified as one of the direct transcriptional targets for HIF-1 and NF-κB, the downstream proteins of BNIP3 have hardly been investigated. Previously, we established a BNIP3-induced and EndoG-mediated neuronal death pathway in stroke: BNIP3 upregulation and EndoG translocation were observed in neurons after focal brain ischemia in a rat model of stroke and in cultured primary neurons exposed to hypoxia and OGD/reoxygenation (Zhang, Yang, et al. 2007). Both forced expression of BNIP3 by plasmid transfection and induced expression of BNIP3 by hypoxia in primary neurons increased the opening probability of MPTP and resulted in mitochondrial release and nuclear translocation of EndoG (Zhao et al. 2009). We also found that incubation of BNIP3- glutathione S-transferase (GST) protein with isolated mitochondria revealed integration of BNIP3 into MOM and release of EndoG from mitochondria as determined by Western blot (Data unpublished). Importantly, the released EndoG was able to cleave chromatin DNA. In cardiomyocytes, expression of EndoG and BNIP3 increases in the heart throughout development, while the caspase-dependent machinery is silenced. Ischemia-induced high and low molecular weight DNA fragmentation is blocked by repressing EndoG expression. Ischemia-induced EndoG translocation and DNA degradation are prevented by silencing the expression of BNIP3 (Bahi et al. 2006; Zhang

et al. 2011). These findings show that BNIP3 induces translocation of EndoG, which also explains why BNIP3-mediated cell death does not involve caspases activation.

EndoG is a mediator of BNIP3-induced cell death. The time course of mitochondrial release and nuclear translocation of EndoG correlates well with that of BNIP3 expression in neurons exposed to hypoxia. Forced expression of BNIP3 resulted in EndoG translocation and 65% neuronal death within 24 hours. Knockdown of BNIP3 by RNAi inhibited EndoG translocation and protects neurons against hypoxia (Zhang, Yang, et al. 2007). We have also obtained evidence that BNIP3 may interact with VDAC, a component of MPTP. In these experiments, we incubated freshly isolated mitochondria with a recombinant BNIP3 protein and performed co-immunoprecipitation using a purified monoclonal BNIP3 antibody to detect BNIP3-interacting proteins. By mass spectrometry, we identified a tryptic peptide that matched the amino acids 257 to 266 of VDAC. The presence of VDAC in the BNIP3-interacting proteins was further confirmed by Western blotting using a specific VDAC antibody (data unpublished). From these data we have proposed a BNIP3-activated and EndoG-mediated neuronal cell death pathway. In this pathway, BNIP3 is transcriptionally upregulated by HIF-1 in hypoxia and stroke, causes mitochondrial dysfunction and results in mitochondrial release of EndoG, which translocates to the nucleus and cleaves chromatin DNA, leading to a form of caspase-independent neuronal cell death. The BNIP3 pathway explains why brain-specific knock-out of HIF-1α reduces rather than increases hypoxic-ischemic damage to the brain (Helton et al. 2005). From the time-course of BNIP3 expression, it is likely that the BNIP3 pathway is primarily responsible for the delayed neuron death in stroke.

The role of BNIP3 in AIF-mediated neuronal death has also been implicated in tumor cells. In the glioblastoma multiforme (GBM) tumours, BNIP3 is translocated to the nuclei and binds to the promoter of the AIF gene and represses its expression. This BNIP3-mediated reduction in AIF expression leads to decreased temozolomide-induced apoptosis in glioma cells (Burton, Eisenstat, and Gibson 2009). So BNIP3 may also function as a novel transcriptional repressor causing reduced AIF expression and increased resistance to apoptosis. However, the translocation of BNIP3 into nuclei is not observed in neuron *in vitro* and *in vivo* in our system, so this conclusion may not apply to all cells. In the neuronal precursor cells, BNIP3 expression was increased after OGD or hypoxia-mimetic exposure, and knockdown BNIP3 inhibited AIF nuclear translocation and cell death (Walls et al. 2009). BNIP3-induced AIF release is also supported by the small molecule Nec-1, which blocks glutamate-induced BNIP3 integration and AIF release in HT-22 cells (Xu et al. 2007). As the key regulators in caspase-independent cell death pathway, AIF shares similar functions with EndoG, so we suspect that BNIP3 may also cause AIF translocation in neurons.

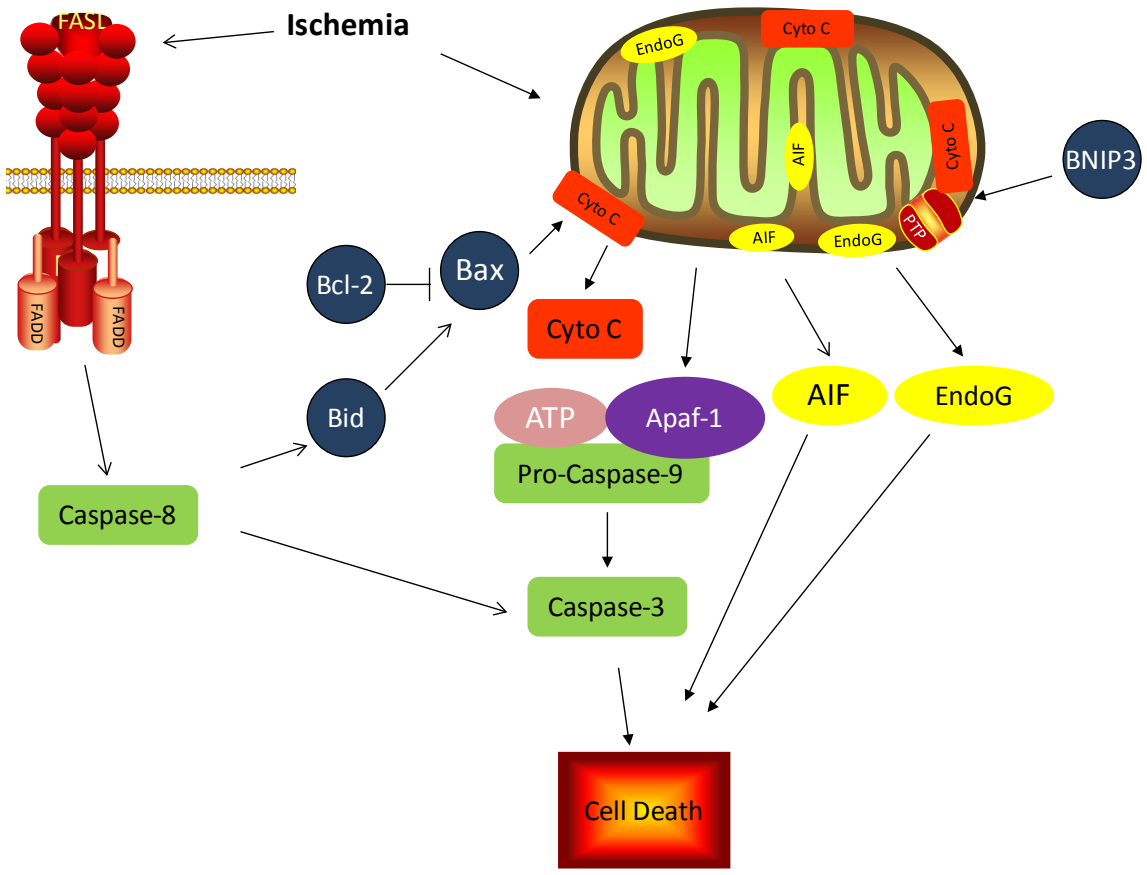

Figure 1.1 A simplified schematic diagram of the caspase-dependent and -independent pathways for cell death.

Two major pathways for caspase-dependent apoptosis have been identified: the extrinsic pathway, which involves death receptor family, and the intrinsic pathway, which is initiated by mitochondria. In the extrinsic pathway, death ligands bind and activate their receptors. Activated receptors, such as FADD, and pro-caspase 8 then form a DISC in which caspase 8 is activated. Caspase 8 can activate caspase 3 and can cleave the Bid, forming truncated Bid (tBid), which can activate the intrinsic apoptotic pathway. In intrinsic pathway, pro-apoptotic mitochondrial factors, such as cytochrome *c,* are released into the cytosol. Released cytochrome c binds to Apaf-1 to form apoptosomes that activate caspase 9. Activated caspase 9 then activates downstream effector caspases such as caspas-3. A range of Bcl-2 family proteins play important roles in regulating the intrinsic pathway. They initiate cell death by activating existed channels such as mitochondrial permeability transition pore (PTP) or forming channels themselves, permitting the escape of multiple proteins from the mitochondrial intermembrane space. Some of the mitochondrial proteins released (apoptosis inducing factor and endonuclease G) can promote caspase-independent death through mechanisms that are relatively poorly defined.

1.5 Therapy

Neurons are post-mitotic cells and cannot be easily replaced by cell renewal, so the damage caused by the death of neurons is more severe than in other tissues. Cerebral ischemia causes significant and progressive functional impairment, but there are no successful clinical trials for stroke with a neuroprotective drug, thus it is imperative that we develop effective therapeutics for stroke.

The ischemic core area in stroke is characterized by a core of necrotic cell death, which leads to rapidly and irreversibly neuronal loss. The penumbra is a moderately hypo-perfused meta-stable region that retains structural integrity but has lost or impaired function (Memezawa et al. 1992). Since this delayed neuronal death in penumbra matures over the course of days to weeks, there exists a time window to protect neurons from degeneration after stroke. The penumbra is believed to be the battle ground for stroke therapy. Basic research studies in the last decades have provided insight into the mechanisms by which neurons die under ischemic conditions, while treatments that interfere with a specific event in the death-signalling pathway have been reported to produce certain neuroprotection against neuronal death. However, none of them are successful for salvaging ischemic tissue and improving functional outcomes. Seeing as the pathology of ischemic stroke is complex, any approach targeting a single mechanism may not provide an effective therapy for stroke patients. Treatment strategies should optimally be directed at multiple targets and mechanisms.

1.5.1 Neuroprotection against caspase-dependent cell death

The caspase family plays critical roles in the activation, signal transduction and execution of ischemia induced neuronal death (Prunell, Arboleda, and Troy 2005). Previous studies have demonstrated protective effects of inhibiting caspase activities by various caspase inhibitors or genetic inactivation of distinct caspases in animal models of focal, global cerebral ischemia and neonatal hypoxic ischemic brain injury. Firstly, treatment with specific caspase-1 inhibitor (Ac-WEHD-CHO) or broad caspase family inhibitor (zVAD-fmk) is protective against delayed neuronal death of CA1 pyramidal cells (Hayashi, Jikihara, et al. 2001). Secondly, administration of zVAD-fmk and zDEVD-fmk not only attenuates delayed apoptotic cell death but also preserves neurological functions (Enari et al. 1998). Thirdly, intra-hippocampal injection of benzyloxycarbonyl-Asp-CH2 dichlorobenzene(zD), an irreversible inhibitor of caspases, saves hippocampal CA1 neurons from chromatin condensation and DNA fragmentation till post-ischemia days 4 and 8, respectively (Himi, Ishizaki, and Murota 1998). Lastly, transgenic mice expressing a dominant negative caspase-1 mutation or with knockout of caspase-1, as well as caspase-3 deficient mice were all more resistant to ischemic stress comparing with WT mice *in vivo* and *in vitro* (Le et al. 2002).

Besides the peptide-based caspase inhibitors described above, several endogenous inhibitors of caspases has been identified (Kanthasamy et al. 2006; Nyormoi, Wang, and Bar-Eli 2003). These inhibitory proteins that function in caspase dependent neuronal death can also be strategic targets. Virally mediated overexpression of the anti-apoptotic gene XIAP prevents both the production of catalytically active caspase-3 and the

degeneration of CA1 neurons after transient forebrain ischemia (Xu et al. 1999). Overproduction of the Apaf-1-interacting protein (AIP), a splice variant of caspase-9 endogenously expressed in the brain, has been shown to promote the survival of hippocampal neurons after transient global ischemia (Cao et al. 2004). Overall, these experiments provide evidence for the pharmaceutical industry to target caspase-dependent pathway as a neuroprotective strategy to prevent stroke-induced neuronal death.

Nevertheless, the therapeutic potential of currently available specific caspase inhibitors is still unclear. Compensatory activation of caspase-8-mediated PARP cleavage was shown in caspase-$3^{-/-}$ neurons *in vivo* and *in vitro* (Le et al. 2002). Administration of N-benzyloxycarbonyl-Asp(OMe)-Glu(OMe)-Val-Asp(OMe)-fluoromethyl ketone significantly attenuates caspase-3-like enzymatic activity and blocks delayed neuron loss in CA1 of hippocampus after ischemia but did not prevent impairment of induction of long-term potentiation after ischemia (Gillardon et al. 1999). zVAD-fk and zDEVE-fmk can reduce ischemic neuronal injury after transient cerebral ischemic insult; they are not effective in blocking injury following complete cessation of blood flow such as during global ischemia (Li et al. 2000). The inability of caspase inhibitors to reduce infarct size after permanent ischemia suggests that residual blood flow or reperfusion might be required for the activation of caspase, and persistent perfusion deficits appear to favour caspase-independent injury. These data suggest that caspase inhibition alone cannot preserve functional plasticity of neurons. In fact, inhibiting caspase-dependent apoptosis might shift the cell death mode to caspase-independent PCD (Vandenabeele, Vanden

Berghe, and Festjens 2006). Effective treatment of ischemic stroke will require a combination of pharmacological agents for inhibition of multiple pathways and factors in stroke.

1.5.2 Neuroprotection against caspase-independent cell death

More recently, therapeutic strategies have been directed to the prevention of the mitochondrial release of AIF and EndoG due to discoveries in caspase-independent cell death signalling in delayed neuronal death after cerebral ischemia. This can be directly or indirectly achieved by RNAi (Culmsee et al. 2005), inhibition of PARP using 3-aminobenzamide (Strosznajder and Gajkowska 2006), expression of hepatocyte growth factor (Niimura et al. 2006), inhibition of neuronal NO synthase (Li, Nemoto, et al. 2007) or inhibition of pro-apoptotic protein Bid (Culmsee et al. 2005). In HQ mice, which carry low levels of AIF, loss of neuronal cells was reduced by 60% after transient global cerebral ischemia, and reduction of mitochondrial AIF protein levels has led to a significant decline in neuronal cell death after ischemia (Thal et al. 2011).

Like AIF, down-regulation of EndoG appears to be another promising method that offers neuroprotection in delayed neuronal death. A delay in DNA degradation due to the EndoG deficiency may provide an opportunity for cells to repair protein and organelle damage generated by the initial apoptotic stimulation and to ultimately resist death. Data from our laboratory show that knockdown of BNIP3 by RNAi inhibited EndoG translocation and protected neurons against hypoxia and OGD/reperfusion-induced neuronal death (Zhao et al. 2009). Reduction in activity of cps-6, which encodes a

homologue of human mitochondrial EndoG, by a genetic mutation or RNAi, delays appearance of cell corpses (Parrish et al. 2001). Transgenic mice with mutant EndoG heterozygous gene are more resistant to neuronal death induced by TNF-α or staurosporine, and has less DNA fragments compared to the WT mice (Zhang, Dong, et al. 2003).

The role of PARP-1 in stroke has also been shown by utilizing PAPR-$1^{-/-}$ mice: primary neuronal cultures with PARP-1 deficient are resistant to the toxicity induced by OGD or NMDA treatment; PARP-1 null mice are more resistant to MCAO injury, and transfection of PARP-1 with recombinant virus into the brain of PARP-$1^{-/-}$ mice restores the post-ischemic brain damage (Li, Klaus, et al. 2010). Although PARP-1 can be activated by caspase, ischemia-induced apoptosis marker changes, such as oligonucleosomal DNA damage, total DNA fragmentation and the density of TUNEL positive cells, were not found in PARP-1-deficient mice and WT mice (Endres et al. 1997). Several PARP-1 inhibitors, such as 4-AN (4-amino-1,8-napthalimide) (Choudhury et al. 2011) and FR247304 (5-Chloro-2-[3-(4-phenyl-3,6-dihydro-1(2H)-pyridinyl)propyl]-4(3H)-quinazolinone (Iwashita et al. 2004), demonstrate significant protective effects in experimental models of cerebral ischemia *in vitro* and *in vivo*. Indeed, PARP-1 is proposed to promote AIF release in caspase-independent necrotic cell death (Moubarak et al. 2007). Thus, PARP-1 might be another potential intervention target to reduce ischemia-induced neuronal death.

Recently, more and more attention is being paid to programmed necrosis or necroptosis, and several molecules have been identified as programmed necrosis inhibitors. Nec-1 was

the first potent therapeutic agent identified after the concept of programmed necrosis is raised (Degterev et al. 2005). To date, it was reported that Nec-1 reduced neuronal damage in ischemic brain (Degterev et al. 2005) and retina injury (Trichonas et al. 2010), myocardial infarction (Smith et al. 2007), glutamate excitotoxicity (Xu et al. 2007) and ameliorates symptoms in R6/2 transgenic mouse model of Huntington's disease (Zhu et al. 2011). *In vitro*, Nec-1 inhibits TNF, FasL and Shikonin-induced necrotic cell death in L929 cells (Degterev et al. 2005), Jurkat cells deficient in FADD or pretreated with zVAD-fmk (Degterev et al. 2005) and HL60 cells (Han et al. 2009), respectively. Nec-1 only protects caspase-independent cell death but has no effect on caspase-dependent cell death. The exact mechanism by which Nec-1 protects neurons against cerebral ischemia is still unclear. It is generally accepted that Nec-1 blocks death-receptor-mediated necrotic cell death via targeting receptor-associated adaptor kinase RIP1 specifically (Degterev et al. 2008). Nec-1 reduces brain neutrophil influx and microglial activation against controlled cortical impact, which indicates its anti-inflammatory effect (You et al. 2008). Nec-1 may counteract the reduction in mitochondrial membrane potential in a cadmium-induced necrotic model (Hsu et al. 2009), and block BNIP3 mitochondrial integration and AIF release in glutamate-induced oxytosis in HT-22 cells (Xu et al. 2007), suggesting that mitochondria are the major acting site for Nec-1. Moreover, 3-methyladenine, a widely used autophagy inhibitor, has provided time-dependent protection of CA1 neurons against necrotic death after global cerebral ischemia (Wang, Xia, et al. 2011).

1.5.3 Neuroprotection by regulating Bcl-2 family

As Bcl-2 family regulates the cell death cascade of delayed neuronal death, targeted gene disruptions of Bcl-2 family members also represent a strategic target for neuroprotection. The protective effect of Bcl-2 protein has been discussed above. A single injection of a DNA plasmid encoding the protective Bcl-2 gene provided neuroprotection for injured neurons *in vivo* (Saavedra et al. 2000). Gene therapy with anti-apoptotic Bcl-2 protein has a potential to protect neurons against both apoptotic and necrotic death induced by several cerebral insults (Zhao et al. 2004). Over-expression of Bcl-2 protected against damage to the infarct margin induced by ischemia with and without reperfusion. Bcl-2 over-expression using gene therapy down-regulates apoptosis-related proteins, including caspase-3 (Zhao et al. 2003). A recent study suggests that transactivator domain (TAT)-mediated delivery of Bcl-x_L provided neuroprotection in neonatal rat brain ischemia by inhibiting the activities of caspases-9 and caspase-3 and also by preventing nuclear translocation of AIF (Yin et al. 2006).

Contrarily, the main strategies for neuroprotection of the pro-apoptotic members may lie in down-regulation of death gene expression. Plesnila and co-workers have developed low-molecular mass 4-phenylsulfanyl-phenylamine derivatives targeting Bid and have shown that they have the ability to inhibit tBid-induced Smac release, caspase-3 activation and cell death in isolated mitochondria and in cancer cell lines (Culmsee and Plesnila 2006). The Bid inhibitors preserve mitochondrial integrity and activation of caspase-3 as well as nuclear translocation of AIF and DNA condensation (Culmsee et al. 2005). Infarct volumes and cytochrome c release are also less in Bid knockout mice than

WT mice after mild focal ischemia. Neurons from Bid-null mice are resistant to cell death stimuli after OGD and maintain a significantly reduced caspase 3 cleavage (Plesnila et al. 2001). Likewise, mice deficient in Bax, Bad or Bim exhibit significantly reduced parenchymal loss along with decreased activated caspase-3 after neonatal hypoxia-ischemia injury (Ness et al. 2006; Gibson et al. 2001). In addition, several agents have been reported being able to protect neurons against ischemia by increasing the ratio of Bcl-2/Bax, such as KR-31378 (Hong et al. 2002) and Penehyclidine hydrochloride (PHC) (Wang, Ma, et al. 2011).

1.5.4 Other therapeutic strategies

In addition to therapeutic strategies discussed above, new techniques have emerged as well. Protein therapeutics combining the super anti-apoptotic factor FNK, generated from the anti-apoptotic Bcl-x gene, and the protein transduction domain (PTD) of the HIV-Tat protein have been found to be effective in preventing delayed neuronal death in the hippocampus caused by transient global ischemia (Asoh et al. 2002). Delivery of hepatocyte growth factor (HGF) gene to subarachnoid space prevented delayed neuronal death in gerbil hippocampal CA1 neurons after brain ischemia (Hayashi, Morishita, et al. 2001). Furthermore, other approaches that have been found to reduce delayed neuronal death of hippocampal pyramidal cells include (-)deprenyl, a selective irreversible inhibitor of monoamine oxidase B (MAO-B) (Paterson et al. 1997), K252a, a potent Trk inhibitor (Pan, Zhang, and Zhang 2005) , and 17β-estradiol (Fujita et al. 2006), a caspase inhibitor, in combination with isoflurane (Inoue et al. 2004) or systemic hypothermia (Adachi et al. 2001).

1.6 Summary

Ischemic stroke is a heterogeneous disorder; even a brief ischemic insult to the brain may trigger complex cellular events that lead to apoptotic, necrotic and atypical cell death in a progressive manner. Experimental ischemic stroke models have contributed to our understanding of the mechanisms occurring during ischemic brain injury. Intense research has investigated the role of caspases in the neuronal cell death. Recently, extensive evidence that a caspase-independent pathway plays significant role in delayed neuronal death in response to ischemic stroke. This pathway appears to occur in parallel with caspase-dependent programmed death or might serve as an alternative death pathway in the face of cellular energy depletion that precludes caspase activation. However, a better understanding of how cells can switch between two pathways is required in future studies. Currently identified mediators in caspase-independent PCD pathway include AIF, EndoG and PARP-1. Several Bcl-2 family proteins, such as BNIP3, have been identified as being able to regulate this caspase-independent cell death. Yet, the exact relationships between AIF, EndoG, PARP-1 and the Bcl-2 family await further investigation. Since multiple cell death pathways exist, and inhibition of one such pathway may enhance alternative ones, treatment strategies should optimally be directed at multiple targets and mechanisms. The continued study of caspase-independent cell death in ischemic stroke will be important for devising drug therapies that can comprehensively suppress delayed neuronal death.

1.7 Thesis Hypothesis and Objectives

1.7.1 Hypothesis

1) Knockdown of BNIP3 subfamily protects against OGD/Reoxygenation or ischemia-induced neuron death.
2) Nec-1 reduces hypoxia or ischemia-induced neuronal death by targeting BNIP3.

1.7.2 Objectives

The specific objectives of this project were to:

1) Determine the effects of inhibiting BNIP3 and NIX expression by RNAi on neuronal survival in OGD/reoxygenation and neonatal stroke.

2) Test the translocation of AIF in OGD/reoxygenation and neonatal stroke in neurons, and determine its role in BNIP3 or NIX induced neuronal death.

3) Determine the role of Nec-1 in hypoxia and ischemia induced neuronal death.

4) Determine the mechanism of Nec-1 on neuronal protection.

The methods used to accomplish these objectives are described in:

Chapter 2: Materials & Methods.

Results are presented in the following chapters:

Chapter 3: Knockdown of BNIP3 death gene family protected neurons against OGD/Reoxygenation.

Chapter 4: AIF is a mediator in BNIP3 and NIX induced neuronal death.

Chapter 5: Nec-1 protected against *in vitro* hypoxia and *in vivo* ischemia induced neuronal death.

Chapter 6: Nec-1 blocked BNIP3 integration into mitochondria and AIF release from mitochondria.

Finally, these results and their significance are discussed with respect to the relevant scientific literature in:

Chapter 7: Discussion.

Chapter 2. Materials and Methods

2.1 Reagents and Chemicals:

All chemicals and solvents were of reagent or analytical grade and were obtained from one of the following sources: Sigma-Aldrich (Oakville ON), GIBCO-BRL (Burlington ON), Fisher Scientific (Ottawa ON), Invitrogen (Burlington ON), Calbiochem (San Diego, CA), BIORAD (Mississauga ON), Alexis Biochemicals (San Diego CA), Roche (Mississauga ON), BD Biosciences (Oakville ON), or GE Lifesciences, (Baie d'Urfe QC).

Necrostatin-1(Nec-1) was purchased from Biomol International L.P. An inactive form of Necrostatin-1 (Nec-1i) was purchased from CALBIOCHEM. zVAD-fmk was purchased from BioVision.

2.2 Antibodies

Antibodies that were used for Western blot (WB) and immunofluorescence (IF) are listed in Table 2.1 (primary antibodies) and Table 2.2 (secondary antibodies).

Table 2.1. Primary antibodies

antibody	Host Species	Application (dilution)	Source	Cat
BNIP3 [mono]	Mouse	WB (1:1000) IF (1:500)	Dr. A. Greenberg	n/a
BNIP3(poly)	Rabbit	WB (1:1000) IF (1:250)	Santa Cruz	sc-1715
NIX (poly)	Rabbit	WB (1:1000) IF (1:250)	Novus	NB600-1155
NIX (mono)	Mouse	WB (1:1000) IF (1:250)	Santa Cruz	sc-166114

AIF	Goat	WB (1:1000) IF (1:250)	Santa Cruz	sc-5586
EndoG	Rabbit	WB (1:1000) IF (1:250)	Prosci Inc.	3035
Cytochrome c	Mouse	IF (1:250)	Santa Cruz	Sc-7148
Caspase-3		IF (1:250)		
Cathepsin-B	Rabbit	IF (1:250)	Millipore	06-480
Bcl-2	Mouse	IF (1:250)	Sigma	B3107
Bax	Mouse	IF (1:250)	Santa Cruz	sc-23959
Cox IV	Mouse	WB (1:5000)	Abcam	ab14744
Histone H10/H5	Mouse	WB (1:800)	Millipore	05-629
β-actin	Mouse	WB (1:5000)	Santa Cruz	sc-69879
GST	Rabbit	WB (1:1000)	Millipore	5782

Table 2.2 Secondary antibodies

Antigen	Host Species	Conjugate	Dilution	Source
mouse IgG	Sheep	horse radish peroxidise	WB(1:5000)	Amersham Pharmacia Biotech
rabbit IgG	Donkey	horse radish peroxidise	WB(1:5000)	Amersham Pharmacia Biotech
rabbit or mouse IgG	Goat	Alexa Fluor® 488	IF(1:1000)	Invitrogen
rabbit or mouse IgG	Goat	Alexa Fluor® 594	IF(1:1000)	invitrogen

2.3 Cell culture

Unless otherwise indicated, all cell lines were maintained in a humidified 5% CO_2 environment at 37°C. All the culture plates were purchased from Nunc and Costar. Cells were cultured in 6-well plates for protein detection, 24-well plates and culture glass for immunohistochemistry, and 96-well plates for cell death and mitochondrial parameters measurement.

2.3.1 Cell line

Due to the high transfection efficiency achievable in this cell line, we used the human embryonic kidney cell line, HEK293T and HEK293, to test the inhibition effect of short hairpin RNAs (shRNAs). HEK293 were cultured in Dulbecco's Modified Eagle's Medium (DMEM; Invitrogen, Burlington ON) with 100 units/mL penicillin and 100 μg/mL streptomycin (Invitrogen). Both cells were supplemented with 10% fetal bovine serum (FBS; Fisher Scientific) and were maintained in a humidified 5% CO_2 environment at 37°C. Cells were passaged at a 1/5 dilution after reaching 80% confluency, and were preserved for long-term storage in liquid nitrogen.

2.3.2 Primary Culture of Cortical Neurons

All primary cultures were performed with day-18 rat fetuses from pregnant female Sprague-Dawley (SD) rats and day-16 mouse fetuses from timed pregnant C57 mice. These plates were coated with poly D-lysine in 0.1 M borate buffer prior to use. All chemicals mentioned here were purchased from GIBCO (Invitrogen) unless otherwise specified. After isoflurane anesthesia, rat fetuses were removed from the womb, and their cerebral cortexes were then dissected out. They were submerged in dissection buffer [Hank's Balanced Salt Solution (HBSS) plus HEPES, and glucose at pH 7.4, osmolarity 310-320 mOsm/ L]. Cortices were triturated gently with a glass pipette until cloudy, settled for a few minutes, and cloudy supernatant was transferred to a second tube. Then 3-5 ml HBSS buffer was added and trituration was repeated. After mechanical trituration, neurons were centrifuged and plating medium (Neurobasal medium with 2% B27, 10%

fetal bovine serum, 1.2 mmol/L glutamine, 5 mmol/L HEPES and 25 μg/mL gentamicin) was added into the cortical neurons suspension. The number of cells was counted with a haemocytometer, and the neurons were then seeded on the culture plates or cover slips coated with poly-D-lysine and kept in the 5% CO_2-37°C incubator. Cell densities used is $1x10^4$ cells/cm^2.The media was switched to a maintenance medium (Neurobasal medium with 2% B27, 1.2 mmol/L glutamine, 5 mmol/L HEPES and 25 μg/mL gentamicin) one days after seeding, and, subsequently, media was changed every four days. On the seventh day, culture medium was replaced with maintenance medium but without glutamine. Matured neurons (7-10 days *in vitro*) were used.

2.4 Plasmid and expression constructs

Mouse NIX and NIX ΔTM in pGEMT vector were gifts from Dr. Zhengfeng Zhang. NIX and NIX ΔTM sequences were cut from the vector and ligated into pEGFP-C2 vector (Clontech). Plasmid pEGFP-C2-Mouse BNIP3 and BNIP3ΔTM were gifts from Dr. H.Y. Lee. BNIP3 and BNIP3 ΔTM sequences were cut from the vector and ligated into pcDNA vector. After sequencing, plasmids were transfected into HEK293 cells to test the transfection and expression efficiency.

2.4.1 Transient plasmid transfection

For transient transfection experiments, HEK293 cells were seeded in 6-well dishes 24 to 48 hours prior to transfection in order to achieve approximately 90% confluence. Prior to transfection, cultures were rinsed twice with serum-free medium. Cells were transfected using Lipofectamine 2000 (Invitrogen, Burlington ON) as per the manufacturer's

instructions. For each transfection, 4 g DNA diluted in 250 μL Opti-MEM reduced serum media was added drop-wise to 5 μL of Lipofectamine reagent diluted in 250 μL Opti-MEM reduced serum media, and the mixture was incubated for 20 min at room temperature in a microfuge tube. Then, the DNA/Lipofectamine mixture was added to each well in a drop-wise manner. The transfection reagent was incubated with the cells for 6 hrs before being replaced with fresh complete media. Transfection efficiency (determined by immunofluorescence) was approximately 90% in HEK293 cells.

2.4.2 shRNA Lentiviral Vectors

The shRNA sequences targeting NIX were designed using Invitrogen's BLOCK-iT RNAi Designer. The oligonucleotides were synthesized, annealed to generate double-stranded oligos, and cloned to pENTR/U6 vectors (Invitrogen). After cotransfection with pEGFP-C2-Mouse NIX plasmids into HEK293 cells, the inhibition efficiencies of the shRNAs were determined by immunofluorescence microscopy and quantitative Western blot analysis. Selected shRNA sequence was inserted into the BLOCK-IT Lentiviral RNAi Expression system (Invitrogen). Lentiviral stocks were produced using Trans-Lentiviral™ Packaging System (Fisher Scientific) and will be described in following section. Scrambled shRNA was generated by switching two pairs of nucleotides to be used as a negative control. shRNA targeting NIX and control shRNA were co-transfected individually with pEGFP-C2-NIX into HEK293 cell using Lipofectamine 2000 (Invitrogen, Burlington ON) to test the inhibition efficiency.

Custom shRNA targeted against BNIP3 and shRNA control were obtained from Thermo Fisher Scientific. These shRNA sequence had already been cloned into the GIPZ miRNA-adapted shRNA(shRNAmir) lentiviral vector with green fluorescence protein (GFP) as a marker. Inhibition efficiency was tested by co-transfection of shRNA targeting BNIP3 and control with BNIP3 plasmid to HEK293 cells.

Table 2.3 shRNA sequences

ShRNA target	Sequence
NIX	5'-CACCGCAGATCATGTTTGATGTTGACGAATCAACATCAAACATGATCTGC-3'
NIX control	5'-CACCGCCTAGAATTTGTTATGAGGTCGAAACCTCATAACAAATTCTAGGC-3'
BNIP3	5'-CCAGCCTCCGTCTCTATTTATTTAGTGAAGCCACACATGATATAAATAGAGACGGAGGCTGG-3'
BNIP3 control	5'-CUGUAAACAUCCUCGACUGGAAGCUGGAAGCCCAGAAUGCUUUCAGUCGAGGAUGUUUGCAG-3'

2.4.3 Constructs for inducible expression system

Mouse BNIP3 and BNIP3ΔTM, mouse NIX and NIXΔTM sequences were cloned into a pENTR2B vector individually. After the expression efficiency on HEK293 cells was tested, the vectors were sent to University of British Columbia Brain Research Centre for packaging. The plentif-lentiviral vectors containing sequences mentioned above were sent back along with lentiviral particles and were used for experiments.

2.4.4 Trans-Lentiviral™ Packaging and Lentivial particle concentration

All the shRNAs were packed into highly efficient lentiviral particles with trans-Lentiviral™ Packaging system from Thermo Fisher Scientific Open Biosystems. On Day 1, HEK293T cells were seeded in 10-cm dishes ($3x10^6$ cells/dish) with 9 ml DMEM culture medium. The cells grew to confluency around 30-40%. Chloroquine with final concentration of 25μM was added to the culture medium. For each dish, a lentiviral vector containing shRNA (8.4 g) was co-transfected into HEK293T with packaging plasmids psPAX2 (8.4g) and pMD2.G (4.2g) using the calcium phosphate transfection method. Three plasmids were mixed with 60 μL 2M $CaCl_2$ to make 1 ml DNA/Ca^{2+} mixture with ddH_2O. After the same amount of 2×HBS (50mM HEPES, 1.5mM Na_2HP0_4, 280mM NaCl, 10mM KCl, 12mM sucrose) was added, aliquot was added to each dish in a drop-wise manner. The transfection reagent was incubated with the cells for 6 hrs before being replaced with fresh complete media. Twenty to thirty dishes were used for each packaging. Transfection efficiency (determined by immunofluorescence) was approximately 80%. After five days, the lentiviral supernatant was harvested and filtered with 0.2 μm pore size filter for concentration. Lentiviral vector containing mouse BNIP3 and BNIP3ΔTM sequences, mouse NIX and NIXΔTM sequences were packed into active lentiviral particles using the same method.

Viruses were concentrated by incubation with 50% polyethylene glycol (PEG) 6000. Filtered culture medium (100mL) was incubated with 25.5mL 50% PEG6000, 10.85 mL 4M NaCl, 11.65 mL phosphate buffered saline (PBS) for 90 min at 4°C, and centrifuged at 7000g for 10 min. Virus pellet was suspended with 0.5mL 50mM Tris-HCl(PH 7.4)

and stored at -80°C. The titration of all these lentiviruses was tested on HEK293 cells and neurons before use.

2.5 Production of recombinant proteins

Mouse BNIP3 and BNIP3ΔTM sequences were cut from pEGFP-C2-Mouse BNIP3 and BNIP3ΔTM and cloned into pGEM-T vector (Promega) following the manufacturer's protocol. After the recombinant plasmid was digested with BamHI and NotI, the resulting fragments were purified and inserted into BamHI-NotI-digested expression vector pGEX-4T to generate the recombinant BNIP3 and BNIP3ΔTM plasmid. All constructs were confirmed by DNA sequencing. Then, 100 ml fresh LB culture medium was inoculated with 1.0 ml of overnight culture (BL21DE3) of each bacterial transfectant and vigorously shaken (220 rpm) at 37°C until the culture reached the exponential phase (OD 0.5-0.8). To induce the production of the fusion proteins, isopropylb-D-thiogalactopyranoside (IPTG, 0.1 mM final concentration) was added to the BL21DE3. After being vigorously shaken for 2 hrs at 25°C, the bacterial cultures were pelleted and lysed with Bacterial Protein Extraction Reagent (B-PER, Pierce, Rockford, 1L). The expressed proteins were recovered in the soluble bacterial fraction and purified by Glutathione Sepharose 4B (Amersham Biosciences) according to the manufacturer's protocol.

2.6 Experimental Stroke Models *In vitro* and *In vivo*

2.6.1 Hypoxia and Nec-1 treatment

On the seventh day, neurons were exposed to less than 1%-oxygen hypoxia for different time periods in a hypoxia chamber (Billups-Rothenberg Inc) flushed with a pre-analyzed

gas mixture of 5% CO_2 and 95% N_2. Neurons were collected and measured at the time points of 0, 12, 24, 36, 48, 60 and72 hrs of hypoxia exposure. Control manipulations were performed in parallel sister culture in an incubator with an atmosphere of 5% CO_2 balanced with air.

Twenty-four hours before hypoxia or OGD exposure, primary neurons were treated with Nec-1at the concentrations of 6.25μM, 12.5μM, 25μM or 50μM or with an inactive form of Nec-1 (Nec-1i). The same amount of dissolvent (DMSO) was added as control.

2.6.2 OGD/Reoxygenation and Lentivirus Multi-Transduction

On the seventh day, neurons were subjected to OGD with Earl's Balanced Salt Solution (EBSS) medium (in mg/L: 6800 NaCl, 400 KCl, 264 $CaCl_2 \cdot 2H_2O$, 200 $MgCl_2 \cdot 7H_2O$, 2200 $NaHCO_3$, and 140 $NaH_2PO_4 \cdot H_2O$, pH 7.2) and incubated in a hypoxia incubator filled with 1.5% O_2 and 5% CO_2 balanced with 93.5% nitrogen for 6 hrs. Then neurons were proceeded to normal oxygen and maintenance medium without glutamate to mimic *in vivo* reperfusion for up to 72 hrs.

Transduction of neurons was performed by adding the lentiviral particles to medium once a day from the second day till the fourth day of the culture. On each transduction, 2/3 of maintenance medium was removed (around 1 ml medium left), and 60 μL of the concentrated lentivirus was added to the medium. The lentivirus and neurons were incubated in normal culture condition for 1 hour, and then the medium was replaced with fresh medium. Knockdown and overexpression for target gene products was verified by

Western Blot as described in section 2.12. The repeated transduction increases the transduction efficiency from 40% to up to 90%.

2.6.3 Focal Brain Ischemia/Reperfusion and Nec-1 treatment

All animal protocols were approved by the University of Manitoba Animal Care Ethics Committee. Male SD rats weighing 250 to 300 g (University of Manitoba Central Animal Care Breeding Facility, Winnipeg, Canada) were used to perform the MCAO. The rats were anaesthetized by inhaling anesthetic isoflurane. A longitudinal incision was made on the dorsal surface of the neck, exposing the right common carotid, external carotid and internal carotid arteries. A 4–0 nylon suture with silicon-coated tip (Doccol Co) was inserted through the left external carotid artery to occlude the left MCA. Proper placement of the suture was determined by two indicators: 1) the length of suture inserted, which was the distance between the bifurcation of the carotid artery and the origin of the MCA (20 mm ± 0.5 mm for animals weighing 290-310 g), and 2) a small resistance that could be felt when the suture reached the origin of the MCA. MCAO partially blocked the supply of blood to the right hemisphere. The suture was withdrawn 90 minutes after MCAO to allow reperfusion. The right external carotid artery was tied off and the incisions were closed with sutures. Thereafter, the animal was returned to its home cage to recover from the surgical procedure. Sham surgery without the suture insertion was done on rats in the control condition. Overall mortality from the procedure was approximately 20%. Ischemic injury was confirmed by 2,3,5-triphenyltetrazolium chloride (TTC, Sigma) staining on fresh brain tissues 4 hours after surgery, as shown in figure 2.1.

Nec-1, Nec-1i or saline were dissolved in 4% methyl-β-cyclodextrin solution in PBS to make 4 mM stock solutions. Right after the onset of MCAO, animals received an intraperitoneal injection of Nec-1, Nec-1i or saline at 0.5 μl/g body weight. The injections were repeated once 2 hours after the onset of reperfusion and twice on the second day.

The rats were sacrificed two days after ischemia/reperfusion under anesthesia in a small jar containing cotton soaked with isoflurane. For histological analysis and immunohistochemistry staining, pups were perfused with buffered 10% formalin and embedded in paraffin, which will be described in the section 2.13. Macroscopically, ischemic brains consistently showed evidence of infarction, whereas those of control animals did not. For Western blot analysis, cortical tissues were dissected out (approximately 2 x 2 x 1 cm) from each of the brain hemispheres and were frozen with dry ice right away. These fresh tissues were kept in labelled cryovials stored in -80°C freezer for future experiments.

Figure 2.1 TTC staining on fresh brain tissue after MCAO surgery

Fresh brain tissues were cut into five 2-mm coronal sections, and each section was stained with 1% TTC for 30 min. All the sections were put into 4% PFA, and pictures of them were taken. The red region shows intact areas while the white colour indicates brain injury areas.

2.6.4 Neonatal hypoxic-ischemia model and lentivirus transduction through intrastriatal injection

SD rat pups were purchased from University of Manitoba Central Animal Care Breeding Facility. All the animals were caged with the dam and kept on a 12-hour light/dark schedule. Seven-day-old rat pups were anaesthetized with 4% isoflurane, and deep anesthesia was maintained with 2% isoflurane throughout the surgery. The neck was incised in the midline, and the right common carotid artery (CCA) was isolated from surrounding tissue. A silk thread was passed below the CCA, Then,CCA was doubly ligated with a 4-0 silk suture and severed between sutures bilaterally. Sham-operated rats underwent only the dissection of the left carotid tree. Total time of surgery never exceeded 10 minutes. Approximately 4 to 6 hours after surgery, the animals were exposed to a 90-min period of hypoxia (92% N_2, 8% O_2); this was achieved by placing them in an airtight chamber partially submerged in a 37°C water bath. The temperature inside the chamber was kept at 33°C. After a 30-min recovery period in a temperature-controlled incubator, the rat pups were returned to their dams and kept in a standard environment. Animals that underwent hypoxia-ischemia generally showed global neurological impairment that included severe motor and feeding dysfunction as compared to control animals. Overall mortality from the procedure was approximately 10%.

Animals were sacrificed seven days after the operation; isoflurane was used to achieve pre-euthanasia anesthesia as described above. For histological analysis and immunohistochemistry staining, pups were perfused with buffered 10% formalin and

cryoprotected with 30% sucrose before being frozen for cryostat sectioning. Macroscopically, ischemic brains consistently showed evidence of infarction, whereas those of control animals did not. For Western blot analysis, striatum were dissected out from each of the brain hemispheres and were frozen with dry ice right away. These fresh tissues were stored in -80°C freezer.

shRNAmir or control shRNAmir was injected into left and right sides of the striatum on post-natal day 3. During the surgery, pups were placed in a stereotaxic frame after isoflurane-inhalation-induced anesthesia. A 30-gauge needle was inserted through a burr hole on the skull into the striatum in both hemispheres. The injection site (stereotaxic coordinates; 1.8 mm lateral to the midline, 0.2 mm anterior to the bregma and 2.7 mm depth below the skull) was adjusted according the size difference between adult mice and newborn mice. 5 μL shRNAmir targeting BNIP3 were injected at a constant rate of 0.20 μL/min with a microinfusion pump. Control groups received an injection of the same volume of scrambled shRNA. Body temperature was maintained at 37 °C during surgery.

2.7 Cell death and viability assays

All the cell death or viability assays were performed in the 96-well plates (5×10^4 cells/well). Each test group had six duplicates, and each experiment was repeated at least three times.

2.7.1 Trypan blue exclusion assay

Cell death is typically assayed by quantifying plasma membrane damage. Many standard methods are based on the uptake or exclusion of vital dyes. Live cells possess intact cell membranes that exclude trypan blue, whereas dead cells do not. For each test, the culture medium was replaced with 50 μL PBS and 50 μL 0.4% trypan blue for 5 min at 37 °C. Dead neurons are stained as blue colour, while viable cells can exclude the dye, and both live and dead cells were counted under light microscope. Cell viability was calculated as the number of viable cells divided by the total number of cells.

2.7.2 LDH cytotoxicity assay

Lactate dehydrogenase (LDH) is a stable cytoplasmic enzyme that is present in all cells. When the plasma membrane is damaged, LDH is rapidly released into the culture supernatant. LDH activity can be determined by a coupled enzymatic reaction: LDH oxidizes lactate to pyruvate, which then reacts with tetrazolium salt to form formazan. 50 μL cell-free supernatant was collected into an optically clear 96-well plate, and neurons were lysis 100 μL by 1% triton X100 diluted in PBS. Cell membrane breakdown by triton x100 was observed under a light microscope. LDH activity was measured with LDH-cytotoxicity assay kit (Biovision). 50 μL supernatant and 10 μL cell lysate were mixed individually with LDH Reaction Mix and incubated for 30 min at room temperature. Fresh culture medium and 1% triton lysis buffer were also incubated with LDH reaction buffer and used as background control. The absorbance of all controls and samples was measured with a Wallac VICTOR3 multilabel microplate reader (Perkin Elmer Life

Sciences) equipped with 450 nm (440 nm to 490 nm) filter. The ratio of LDH in the supernatant to total LDH (supernatant and cell lysate) was used to represent the cytotoxicity.

2.7.3 MTT assay

The MTT colorimetric assay was performed to measure the neuronal cell viability. 50 μL of MTT reagent (3-[4,5-dimethylthiazol-2-yl]-2,5-diphenyl tetrasodium bromide, 1 mg/mL) was added directly to each well, and plates were incubated for 4 hour at 37°C in normoxia. In viable (metabolically active) cells, the yellow MTT reagent is reduced to insoluble purple formazan by mitochondrial enzymes. After incubation, 150 μL of DMSO was added to each well to dissolve the purple formazan crystals and the absorbance was read at 540 nm on a microplate reader.

2.7.4 PI and Hoechst 33342 double staining

Hoechst 33342 and PI can bind with DNA causing a blue or red fluorescence, respectively. As PI can only permeate through the membrane of dead cells while Hoechst 33342 can permeate through the membranes of both living and dead cells, the Hoechst-PI double-staining method was used for differentiating the live and dead cells. PI (red) and Hoechst 33342(blue) were added to the culture medium at the final concentration of 1μg/μL for 20 min. Cell nuclei were observed under fluorescence microscope, and fluorescence pictures were taken right away. The number of red and blue labeled nuclei

was counted by WCIF-Image J software. Cell death rate was calculated as the number of red nuclei divided by the number of blue nuclei.

2.8 Reactive oxygen species measurement

ROS production was detected using H_2DCF-DA (2′,7′-dichlorodihydrofluorescein diacetate; invitrogen). H_2DCF-DA is a cell-permeant indicator for ROS that is nonfluorescent until the acetate groups are removed by intracellular esterases and oxidation occurs within the cell. The dye reacts with ROS to form fluorescent DCF and cannot pass out of the cell. Culture medium were removed and replaced with warm PBS (37°C). H_2DCF-DA was added to the neuronal culture at the final concentration of 2μmol/L. After incubation for 15 min at 37°C, neurons were washed with PBS buffer three times. Fluorescence data were collected with a VICTOR3 multilabel microplate reader with an excitation wavelength of 485 nm and an emission wavelength of 525 nm.

2.9 Assessment of mitochondrial parameters

2.9.1 Mitochondrial membrane potential

To measure the mitochondrial membrane potential, neurons were incubated with JC-1(5,5’,6,6’-tetrachloro-1,1’,3,3’- tetraethylbenzimidazolylcarbocyanine iodide). JC-1 is a unique dye that signals the loss of mitochondrial membrane potential. In healthy cells, JC-1 aggregates form and stain the mitochondria with bright fluorescent red. In apoptotic cells, the mitochondrial membrane potential collapses, and the JC-1 cannot accumulate within the mitochondria. In these cells JC-1 remains in the cytoplasm in a green fluorescent monomeric form. Thus, apoptotic cells are easily differentiated from healthy

cells, which show green and red fluorescence, respectively. The aggregate red form and monomeric green form JC-1 dyes have absorption/emission maxima of 585/590 nm and 510/527 nm, respectively. JC-1 with the final concentration of 1μg/μL was placed in the culture medium in 37°C in the dark for 30 min, and neurons were washed with PBS three times. The fluorescence intensities were measured on a VICTOR3 1420 multilabel microplate reader. The ratio of red to green fluorescence was used to indicate the total mitochondrial membrane potential. Higher mitochondrial membrane potential has relatively higher red fluorescence and lower green fluorescence.

2.9.2 Mitochondrial permeability transition pore

MPTP opening was measured by calcein-AM. In live cells, the nonfluorescent calcein-AM is converted to a green-fluorescent calcein after acetoxymethyl ester hydrolysis by intracellular esterases. The calcein is a membrane-permeating fluorescent probe that freely enters mitochondria but cannot exit except through MPTP. Calcein fluorescence in the cytosol can be quenched by 1 mM $CoCl_2$. The more MPTP opens, the more fluorescence dye leaves in the mitochondria. Calcein-AM was incubated with neurons for 30 min. The concentration of Calcein-AM was determined at the wavelength pair excitation and emission at 488/529 nm. To test whether Nec-1 functions through MPTP, a specific MPTP inhibitor cyclosporine A was used as a positive control.

2.10 Isolation of mitochondria, incubation with recombinant proteins and Nec-1 treatment

2.10.1 Liver mitochondrial isolation

Liver tissue from C57 mouse was weighed and washed with ice-cold PBS twice. Then tissue was placed in ice-cold isolation buffer (225 mM mannitol, 75 mM sucrose, 5 mM HEPES and 1 mg/ml bovine serum albumin, pH 7.4) and minced in pre-chilled dounce homogenizer. After being centrifuged at 600g for 10 min at 4°C to remove intact cells and nuclei, crude mitochondria were pelleted from the supernatant by centrifugation at 10,000g for 15 min at 4°C. The mitochondria were washed by being centrifuged at 8,000g for 10 min. The mitochondria were suspended in respiratory buffer (10 mM HEPES-KOH, 0.3 M Mannitol, 5 mM KH_2PO_4, 10 mM sodium succinate, 1 mM EGTA, pH 7.4). The whole procedure was performed on ice, and the mitochondria were used within 4 hr after preparation. Mitochondria protein concentration was determined with the Quick Start™ Bradford Protein Assay (BIO-RAD), using bovine serum albumin (BSA) as a standard according to the manufacturer's instructions.

2.10.2 Nec-1 treatment

The mitochondria equivalent of 100μg proteins dissolved in 100μl respiratory buffer were incubated with Nec-1 at different concentrations (0, 12.5,25,50 or 100 μM) at room temperature for 1 hr. Then, BNIP3-GST or BNIP3ΔTM-GST proteins were incubated with each group of mitochondria for 1 hr. To test Nec-1's effect on mitochondria-BNIP3

interaction, Nec-1 and Nec-1i were pre-incubated with BNIP3-GST protein for one hour and then incubated with isolated mitochondria.

2.10.3 Assessment of mitochondrial membrane import of recombinant proteins

After mitochondria and BNIP3-GST or BNIP3ΔTM-GST were incubated together, mitochondria were washed three times by repeated spinning down (10000g, 5 min) and suspending, and the supernatant containing GST proteins were discarded. For the alkaline extraction, the mitochondrial pellets were resuspended (1 mg of protein/ml) in freshly prepared 100 mM Na_2CO_3 (pH 11.5), and incubated for 20 min on ice. The membranes were then pelleted by centrifugation at 100,000 g for 30 min at 4°C. Mitochondrial membrane pellets (the alkali-resistant fractions) and the corresponding volumes of supernatants (the alkali-sensitive fractions) were subjected to Western blot analysis to detect the BNIP3 or BNIP3ΔTM proteins that inserted into the mitochondrial membrane.

2.10.4 Mitochondrial membrane potential measurement

After incubating with recombinant proteins, mitochondria were washed with respiratory buffer for three times on ice. Then, assessment of the mitochondrial membrane potential with JC-1 occurred. Isolated mitochondria (1 mg/ml) were incubated with 80 nM JC-1 in respiration buffer for 15 mins at 37°C. After mitochondria were washed three times, two forms of JC-1 uptake were determined at the excitation and emission at 488/529 nm and

488/590 nm. The mitochondrial membrane potential was assessed by ratio of red to green fluorescence.

2.10.5 Mitochondrial permeability transition opening measurement

To assess the opening of MPTP, isolated mitochondria were washed and re-suspended in 100 μl incubation buffer (2 mM HEPES, 0.25 M sucrose, 10 mM succinate, and 1 mM potassium phosphate). Then, calcein-AM (Molecular Probes, final concentration at 5 μM) was added and incubated for another 30 min. After being washed, the fluorescence intensities of calcein were measured at an excitation wavelength of 485 nm and an emission wavelength of 525 nm. Cyclosporine A was used as positive control.

2.11 Cell lysis and subcellular fractionation isolation

2.11.1 Lysis for total protein from culture neurons

Neurons were scraped from 6-well plates with ice-cold PBS and washed by spinning down at 600g for 5 min. Then neurons were lysed by lysis buffer (1% triton, 50 mM Tris-Cl, 300mM NaCl, 5mM EDTA, 0.02% sodium azide, PH 7.4) and same amount of 2×loading buffer (125 mM Tris base, 20% glycerol, 2% SDS, 2% 2-mercaptoethenol, 400mg/100mL bromphenol blue). All samples were finally degraded by being boiled in water for 5 min and stored at -20°C (short term) or -80°C (long term).

2.11.2 Subcellular fractionation isolation from culture neurons

Mitochondrial, cytosolic and nuclear fractions of cultured neurons were isolated using Pierce's mitochondrial isolation kit (Pierce Biotechnology). Neurons (6×10^6) were scraped from the culture plates with ice-cold PBS. After being centrifuged at 600g for 5 min, neurons were re-suspended with 600 µl reagent A and vortex for 5 sec and incubated for 2 min. Reagent B and C were added to the neurons according to the instructions. Nuclear fraction was pelleted after the first centrifugation with 800g for 10 min, while mitochondrial fraction was pelleted for the second centrifugation with 12,000g for 15 min, and the remaining supernatant was collected as cytosolic fraction. Mitochondrial fraction was washed with reagent C before use. Mitochondrial and nuclear fractions were suspended with lysis buffer. All the fractions were degraded and stored as whole cell lysate samples.

2.11.3 Subcellular fractionation isolation from brain tissue

Cryo-preserved brain tissue from -80°C storage was warmed up on ice and and immediately placed into ice-cold isolation buffer (225 mM mannitol, 75 mM sucrose, 1 mM EGTA, 5 mM HEPES-KOH (pH 7.2) and 1 mg/ml of BSA). Protein samples were homogenized by a dounce glass tissue grinder and the homogenate was centrifuged at 1,300 *g* for 5 min in a refrigerated centrifuge as previously described (Sims and Anderson 2008). The supernatants were centrifuged in a tube at 21,000g at 4 °C for 10 min. During this centrifugation period, the lower layers of the density gradient, which consist of 23% Percoll above 40% Percoll in centrifuge tubes were prepared. Then the pellets were

suspended in cold 15% Percoll solution and slowly layered above the 23% Percoll in the centrifuge tube. The tubes were centrifuged in a fixed-angle rotor at 30,000g at 4 °C for 5 min. The mitochondria-enriched fraction was collected and the protein concentrations were determined by the BCA Protein Assay (Pierce, Thermo Scientific) using BSA as a standard control.

2.12 Sample Preparation, SDS-PAGE and Immunoblotting

Protein samples were separated on 10% polyacrylamide gels by SDS-PAGE at 45 volts (V) for 50 min and 90V for about 1 hour. After the electrophoresis, proteins were transferred to polyvinylidene flouride membranes (Amersham) at 90V for 3 hours. Membranes were blocked with 5% non-fat dry milk powder in Tris-buffered saline (TBS) with 0.05% Tween-20 detergent (TBS-T) and incubated with primary antibody overnight as indicated in Table 2.1. The Western blots were visualized on autoradiography film (Kodak) with enhanced chemiluminescence (ECL) solution (GE Healthcare). Western blot bands were imaged on a FluorChem 8900 imager (Alpha Innotech) and band densitometries were quantified using the QuantityOne software (BioRad). Each Western blot is representative of at least three independent experiments.

2.13 Brain tissue preparation

2.13.1 Trans-cardiac perfusion

Adult rats or pups were anesthetized with isoflurane and closely monitored to ensure complete anesthesia. After surgically retracting the rib cage to expose the beating heart, the right atrium was cut open with fine surgical scissors to allow for drainage of blood

and perfusion fluid. An 18-gauge cannula was immediately inserted through the left ventricle to the aorta, and the rats were slowly perfused with 50 mL of phosphate buffer (0.1 M, pH 7.4) to remove all traces of blood. Next, the rats were perfused with approximately 50 mL of fresh paraformaldehyde fixative (4% in 0.1M phosphate buffer, pH 7.4) until the tissues were adequately fixed and the rats became generally stiff. At this point, the cannula was removed from the heart and the brain was carefully removed and immersed in fixative for post-fixation at 4°C overnight. The next day, the fixed brain was processed for paraffin-embedding or cryopreservation, as described below.

2.13.2 Paraffin-embedding and sectioning

Paraffin-embedding and sectioning of perfusion-fixed whole brains was performed in the Histological Lab (Department of Human Anatomy and Cell Science, University of Manitoba). Whole brain was embedded in paraffin with Shandon Embedding center. Paraffin-embedded brains were cut into 8μm thick section and stored at room temperature for histological and immunohistochemical analysis.

2.13.3 Cryopreservation and sectioning

Fixed whole brains were cytoprotected in a sucrose gradient: brains were carefully transferred to 13 mL round-bottom snap-cap tubes and submerged in 10 mL of a 20% sucrose solution (20% v/v in 0.1 M phosphate buffer), and incubated on a rocking platform at 4°C until the tissue sank to the base of the tube (usually overnight). This procedure was repeated in 30% sucrose solution. Then, the sucrose solution was replaced

with optimal cutting temperature compound (OCT compound, Tissue-Tek) and the tissue was incubated for a further 60 min. Next, the brains were embedded in OCT over dry ice. Labeled plastic OCT molds (1 inch) were filled half-way with OCT and placed in a 100 mm plastic culture. As the OCT began to freeze from the bottom-up, the brain was carefully placed into the mold. Forceps were used to maneuver the brain into the desired orientation. Additional OCT was added to completely cover the tissue. Once the entire tissue-containing-OCT-filled mold was frozen (about 10 min), it was placed in an airtight bag and stored at -80°C until it was sectioned.

Cryosectioning was performed on a Leica SM2400 sliding microtone equipped with a freezing plate set to -30°C. The tissue-containing OCT block was transferred from -80°C storage to the cryostat. The orientation of the tissue was marked with ink prior to the plastic mold being discarded. The frozen OCT/tissue block was then allowed to equilibrate to -20°C in the cryostat for 1 hour prior to it being sectioned. At this point, the block was mounted onto the chuck with fresh OCT, and the "cryobar boost" setting was used. The top layer of OCT was cut away in 50 μm sections. Coronal sections were cut at 30 μm and were mounted on pre-labeled Superfrost PLUS glass slides (Fisherbrand) and kept inside the cryostat at -20°C. Slides were ultimately transferred to plastic storage boxes and kept at -80°C.

2.14 Histochemistry

2.14.1 Cresyl Violet staining

Cresyl violet is a stain used for highlighting acidic components of tissue, and is commonly used for nerve tissue sections. Staining with cresyl violet highlights areas called Nissl bodies in the neuronal cell; this highlighting is useful for determining neuronal structure. Every sixth slide was removed and allowed to dry at room temperature to be stained by cresyl violet for morphological analysis. After air-drying at room temperature, sections were stained in 1% cresyl violet acetate (Sigma-Aldrich) for 30 sec, washed in ddH_20 (2 x 2 min), and then dehydrated in increasingly pure ethanol: 75%, 85%, 95% and 100% (2 x 2 min each). Next, the sections were cleared with xylene (2 x 2 min) in a fume hood, and, finally, coverslips were applied with mounting medium (Richard-Allen Scientific). After drying for at least two hours, images of the stained sections were obtained using an Olympus BH2 equipped with an Olympus Qcolour5 digital camera (Diagnostic Instruments Inc.) and quantified by image ProPlus (Image and Computer, Milan, Italy). Anatomical regions were identified based on comparison with the online High Resolution Mouse Brain Atlas. The lesion area of the brain was detected as a pale zone lacking the acetate cresyl violet staining mainly reflecting the extent of necrotic neurons (Tureyen et al. 2004) (See figure 2.2). Cellular morphology analysis and cell counting were performed in the cortex at the ischemic core and penumbra area at 400× magnification.

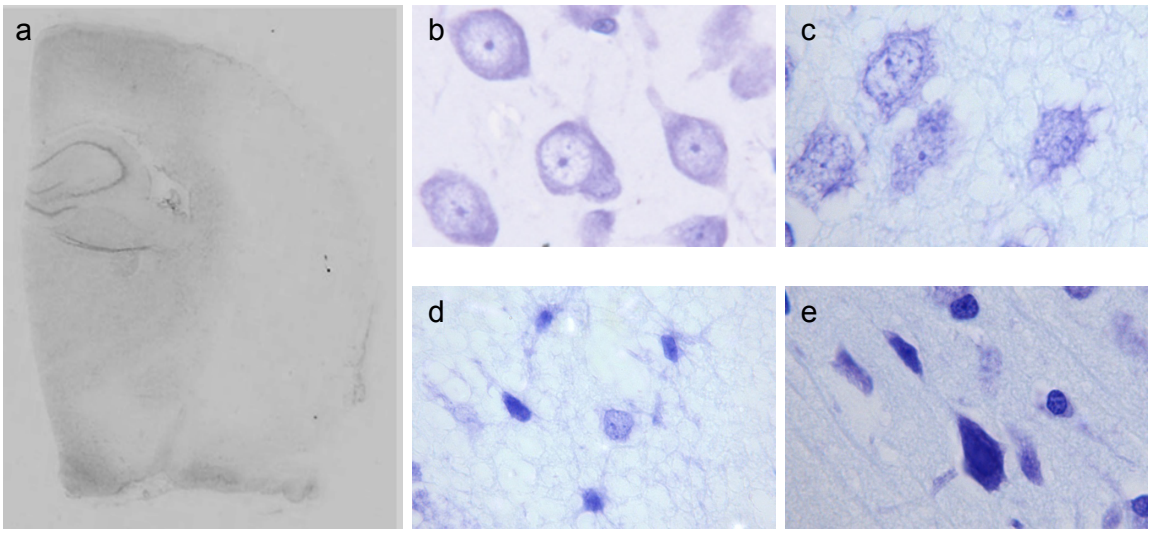

Figure 2.2 Morphological changes detected by cresyl violet staining in MCAO model

Ischemic tissue damage was found in the sensorimotor cortex and striatum after MCAO (a). Ischemic cellular morphological changes (c-e) including cell lysis, shrinkage of nucleus and cytoplasm, hyperchromia were compared with normal neurons (b).

2.14.2 Immunohistochemistry and Fluorescence Microscopy

2.14.2.1 Immunofluorescence on cultured cells

Cultured neurons were grown on coverslips or glass slides. Cells were fixed in 3.7% formaldehyde in PBS for 15 minutes at room temperature and then were washed three times with PBS. These slides could be kept in a fridge at 4°C for up to one week. Slides/slips were blocked in 1% BSA with 0.1%triton in PBS for 1 hour and then incubated with primary antibody in 1% BSA dilation in PBS overnight at 4°C as indicated in Table 2.1. Following three additional washes, slides/slips were incubated with secondary antibody for 1 hour at room temperature in darkness, as indicated in Table 2.2. After being washed three final times, neurons were incubated with Hoechst

33342 (Calbiochem) to counter-stain for nuclei, and then slides/slips were mounted with anti-fade reagent (Bio-Rad). Fluorescence pictures were taken on a Nikon TE2000-E microscope equipped with a RETIGA camera (QImaging).

2.14.2.2 Immunofluorescence on cryopreserved brain tissue

Brain cryosections (described in section 2.13) were removed from -80°C storage and air-dried at room temperature for 15 min. Slides were incubated with 150 µL blocking buffer (PBS with 5% goat serum, 0.2% TritonX 100, 1mg/mL BSA) for two hours at room temperature in a humid chamber. After being blocked, slides were incubated with 100 µL primary antibody diluted in blocking buffer (as indicated in Table 2.1) overnight at 4°C. The next day, after three 5-min washes (PBS with 0.1% NP40), slides were incubated with 100 uL fluorescent-conjugated secondary antibody (as indicated in Table 2.2) diluted in blocking buffer for 1.5 hours at room temperature in the dark. After three final washes, coverslips were counterstained with Hoechst 33342 for 3 min and mounted fluoromount. Fluorescence was visualized and captured as described above in section 2.14.1.

2.14.2.3 Immunofluorescence on paraffin-embedded brain tissue

Paraffin-embedded brain sections (described in section 2.15.5) were baked in a slide warmer (Fisher Scientific) at 60°C for 20 min. The slides were deparaffinized in coplin jars filled with xylene for 10 min and rehydrated by sequential incubation in 100, 95, 85, 75, and 50 % ethanol for 2 min each. After two 5-min washes in ddH_2O, antigen presentation was performed by microwaving the slides in a pressure cooker filled with

citrate buffer (10 mM citric acid monohydrate, pH 6.0) for 20 min on high power. The slides were removed, cooled to room temperature, and then washed three times for 5 min in PBS-T (0.5 % Triton X100). Blocking solution (PBS, 0.2 % Triton X100, 5 % goat serum and 0.1 % BSA) was added to each slide and incubated in a humidity chamber for 2 hrs at room temperature. Primary antibodies (Table 2.1) were diluted in blocking solution and added to the slides for overnight incubation at 4 °C. The next day, slides were washed three times with PBS-T, and the appropriate secondary antibody (Table 2.2) was prepared in blocking solution and added to the slides for 2 hrs at room temperature in the dark. After three final washes in PBS-T, slides were counterstained with Hoechst 33342 for 3 min and mounted with fluoromount. Fluorescence was visualized and captured using an Olympus BX51 fluorescent microscope with a Photometrics Cool Snap CF camera.

2.15 Statistical Analysis

One-way ANOVA and post-hoc unpaired t-tests was used to test for overall statistical significance. A difference was considered significant at $p<0.05$.

Chapter 3. Knockdown of BNIP3 death gene family protected neurons against OGD/Reoxygenation.

3.1 Rationale

BNIP3, a pro-apoptotic BH3-only member of the Bcl-2 family, was reported being upregulated in hypoxia and stroke, and caused neuronal cell death in a caspase-independent manner (Zhang, Yang, et al. 2007). BNIP3 as well as its homologues NIX and BNIP3h are mitochondrial-located members of the Bcl-2 family and have virtually identical structures and functions (Chen et al. 1999). Previous research in our lab showed that inhibition of the BNIP3 expression by RNAi protects 23% neurons from hypoxia, while over-expression of BNIP3 causes 70% neuronal death. Herein, we propose that NIX may partly cause the limited protection of BNIP3 inhibition; inhibiting BNIP3 and NIX expression together may improve the survival rate of neurons under hypoxia. We have identified a shRNAmir and a shRNA which are able to efficiently knockdown BNIP3 and NIX, respectively. Because NIX and BNIP3h express the same mRNA, it is likely that a NIX shRNA vector would inhibit both NIX and BNIP3h. Thus, transfection of these two shRNA vectors into the neurons will result in inhibition of the whole BNIP3 gene family. This will allow us to determine the role of the BNIP3 gene family in ischemia-induced neuronal death. Here, we first investigate the role of BNIP3 gene family *in* an *in vitro* model, in OGD/reoxygenation-induced neuronal death.

3.2 OGD induces BNIP3 and NIX up-regulation and mitochondrial localization in primary cortex neurons.

Previously, we reported that dimerized BNIP3 is up-regulated after 36 hours of hypoxia and gradually increases during the prolonged 72-hour hypoxia. Here, we used another *in vitro* model, an OGD/reoxygenation model, to mimic the *in vivo* ischemia. This model is more accurate than the prolonged hypoxia model, because it withdraws two major nutritional factors, glucose and oxygen, simultaneously. Another advantage of this model is that it allows reoxygenation after OGD injury, which can be used to mimic the clinical reperfusion process. The secondary cell death caused by reperfusion can be more severe than ischemia itself (Ning, Wang, and Lo 2009).

Primary rat cortical neurons were subjected to OGD for 6 hours and were reoxygenated for 0, 12, 24, 36, 48, 60, or 72 hrs. Level of BNIP3 and NIX expression were determined by Western blot analysis. Normally cultured neurons under normoxic conditions were set as controls. We found that, after the neurons were exposed to OGD, the level of dimerized BNIP3 protein remained low until reoxygenation 24 hours after OGD and reached the maximal level at 48 hours of reoxygenation. The activation of NIX in neurons is relatively earlier: the level of dimerized NIX increased right after 6 hours of OGD injury and continued increasing till 48 hours of reoxygenation. In addition, the increased level of NIX (16-fold) was much higher than BNIP3's (10-fold). The decreased expression of BNIP3 and NIX were found at 60 hours and 72 hours of reoxygenation, which may be due to the decrease in cell numbers or severe cellular damage. Thus, NIX responds faster and more dramatically to OGD injury than BNIP3 in neurons, which

suggested that BNIP3 plays roles in delayed neuronal death, while NIX may play roles in both immediate and delayed neuronal death.

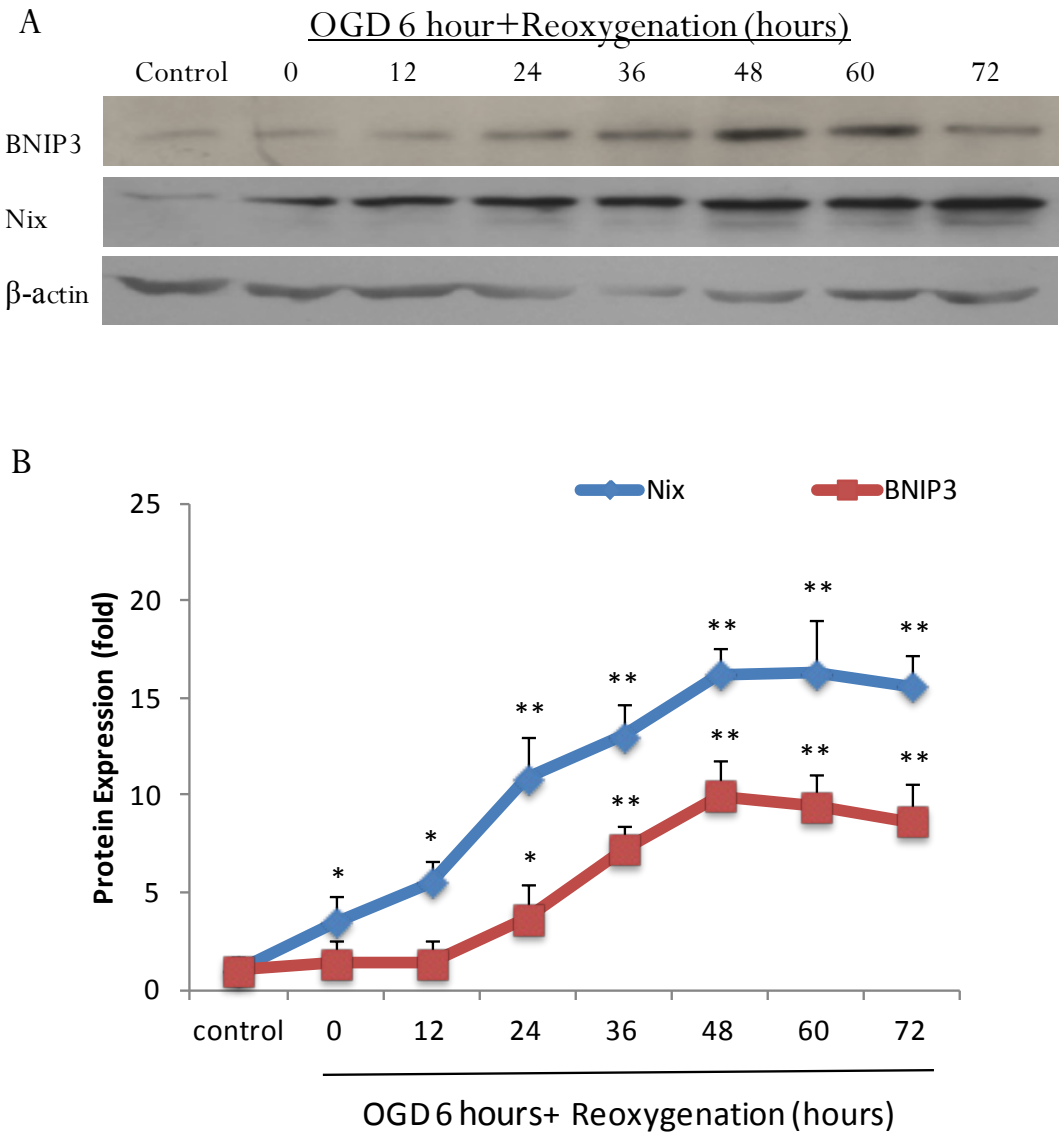

Figure 3.1 OGD/reoxygenation induced BNIP3 and NIX up-regulation in neurons.

Neurons were exposed to OGD for 6 hours and then were reoxygenated by being cultured in a normal medium and oxygenation condition. Different time points of reoxygenation, up to 72 hrs, were chosen. (A) BNIP3 and NIX were detected by Western blot. β-action was used as a internal

control. (B) Quantification of protein expression in neuronal cells at different time course groups and control group. Values are mean± SE and were analyzed by one-way ANOVA. (n=4) * $p<0.05$ vs. control group, ** $p<0.01$ vs. control.

Since mitochondrion is the major target for BNIP3 and NIX to cause cell death, we isolated mitochondrial and nuclear fractions from cortical neurons. The BNIP3 level in the mitochondrial fraction began to increase after 24 hours of reoxygenation and increased up to 8.5 folds at 48 hours of reoxygenation compared to the control group. Like the expression pattern in the whole cell, NIX localization in mitochondria is also faster. NIX level was already one time higher than control after 6 hours of OGD and increased an additional two times higher 48 hours after OGD. Probably due to the dilution of cellular content, protein detection in mitochondrial fractions seems higher than the same protein detected in the whole cell lysate, but the trend of the proteins upregulation is consistent.

To investigate the role of BNIP3 family in caspase-independent cell death, we measured the AIF expression in neurons. A great amount of AIF was detected in mitochondrial fraction in the control and OGD groups at the beginning, but it dramatically decreased after 24 hours of reoxygenation (Fig 3.2). Meanwhile, the level of nuclear AIF started to increase the same time as mitochondrial AIF decreased, and accumulated 24-fold till the end of experiment (72 hours of reoxygenation). The time course of AIF correlates with the BNIP3 upregulation and mitochondrial localization and is later than NIX, suggesting that BNIP3 and NIX may be the triggers leading to the AIF translocation.

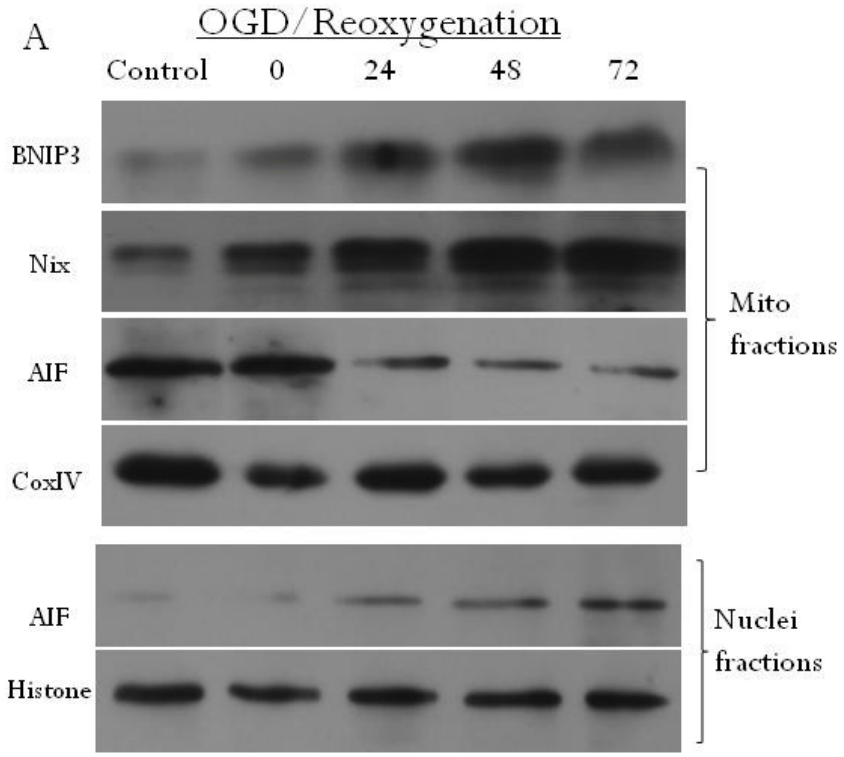
A
OGD/Reoxygenation
Control
0
24
48
72
BNIP3
Nix
AIF
CoxIV
Mito fractions
AIF
Histone
Nuclei fractions

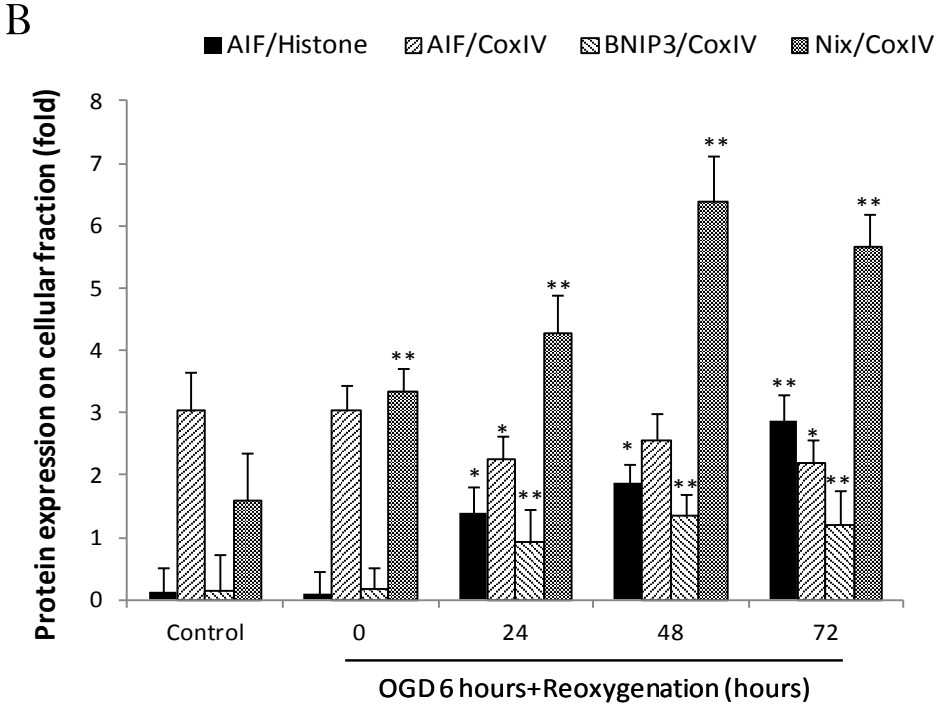
B
AIF/Histone
AIF/CoxIV
BNIP3/CoxIV
Nix/CoxIV
Protein expression on cellular fraction (fold)
0
1
2
3
4
5
6
7
8
Control
0
24
48
72
OGD 6 hours+Reoxygenation (hours)

Figure 3.2 OGD/reoxygenation induced BNIP3 and NIX localization in mitochondria, AIF translocation in neurons.

Neurons were exposed to OGD for 6 hours and then were reoxygenated by being cultured in a normal medium and oxygenation condition. Different time points of reoxygenation, up to 72 hrs, were chosen. At each time point, mitochondrial and nuclear fractions were isolated, and BNIP3, NIX and AIF level were evaluated in mitochondrial fraction, and AIF level were measured in nuclear fractions. (A) Representative Western blot images showing increased BNIP3 and NIX detection in mitochondria, released AIF from mitochondria to nuclei. CoxIV and HistoneH3 were used as mitochondria and nuclei marker for loading control (B) Quantification of proteins expression described above in cellular fractions at different time points. Values are mean± SE and were analyzed by one-way ANOVA. (n=3) * $p<0.05$ vs. control group, ** $p<0.01$ vs. control.

3.3 BNIP3 family gene silencing attenuates OGD-induced neuronal death.

Due to the high sensitivity to any micro-environmental change, the transfection of post-mitotic cells, including primary cortical neurons, has proven, for the most part, to be inefficient. Therefore, to determine the role of BNIP3 and NIX in ischemic neuronal death, we designed a shRNA to inhibit NIX using the method described previously. The shRNA was inserted into the lentiviral vector and transduced into neurons. Silencing of NIX mRNA caused 70% reduction of NIX protein expression within 72 hours, as demonstrated in primary cultured neurons by Western blot analysis (Fig 3.3C and E). GIPZ lentiviral shRNAmir targeting BNIP3 was purchased from Open Biosystems GIPZ lentiviral shRNAmir library and reduced to 90% BNIP3 protein expression measured by Western blot. In addition, by immunostaining the neurons with BNIP3 antibody, we observed that neurons that have a green fluorescence label have dramatically decreased BNIP3 staining. Seeing as the GIPZ lentiviral vectors contains EGPF tag, the inhibition efficiency can also be observed by counting the GFP positive cells and comparing this number to the total number cells. Both shRNA controls did not seem to interfere with the

protein expression. The combination of the two shRNA did not interfere with each other's inhibition efficiency.

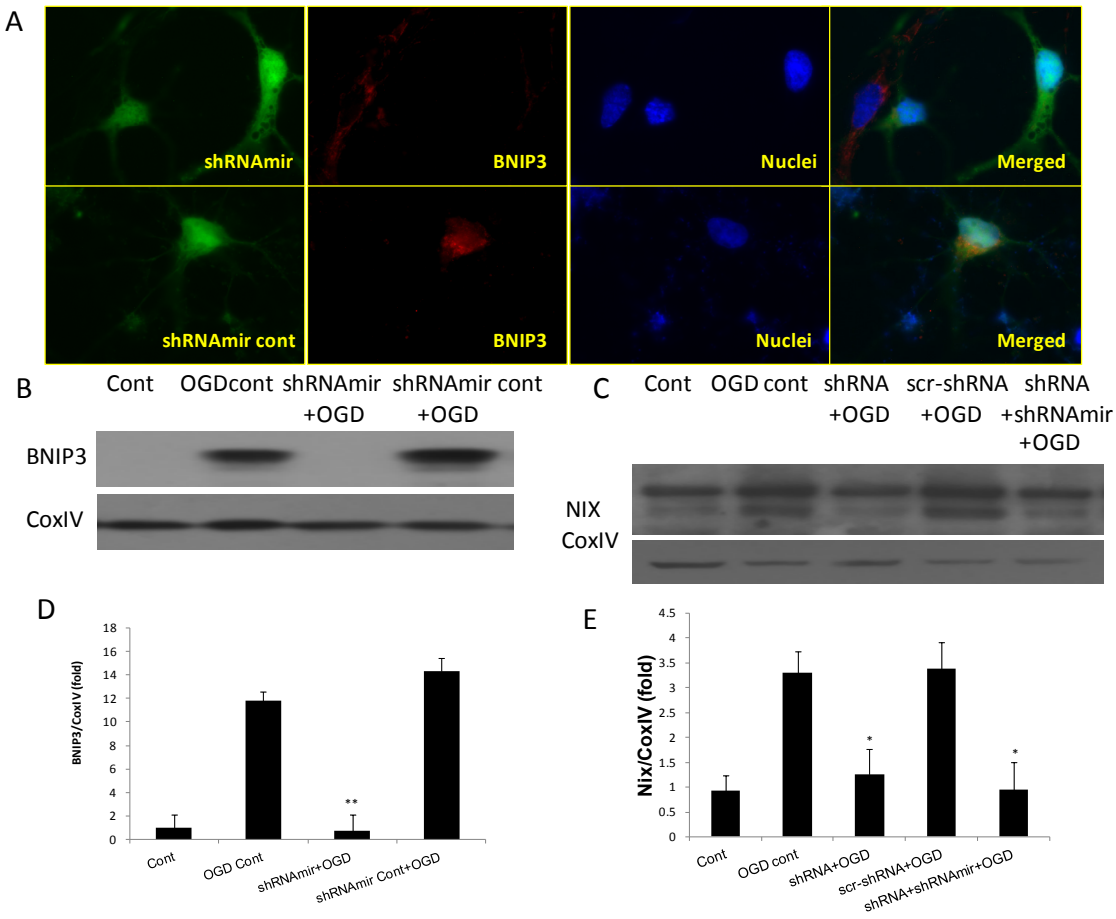

Figure 3.3 shRNAs efficiently inhibited BNIP3 and NIX induced by OGD/reoxygenation.

Small RNAs targeting BNIP3 and NIX were repeatedly transduced into neurons two days before OGD injury, and control shRNAs were used as control. (A) Neurons transduced with shRNAmir were observed with GFP under microscope. In these GFP positive cells, significant low level of BNIP3 were detected compared to GFP negative cells. The BNIP3 reduction was observed in more than 95% shRNAmir positive neurons. No difference of BNIP3 levels was observed between cells transduced with shRNAmir control and GFP negative cells. (B) and (C) After 6 hrs OGD and 48 hrs reoxygenation, mitochondrial fractions were isolated, in which BNIP3 and NIX were detected by Western blot. (D) and (E), Quantification of proteins expression of BNIP3 and NIX in each group to confirm the significant inhibition by shRNA. Values are mean± SE and

were analyzed by one-way ANOVA. (n=3) * $p<0.05$ vs. OGD control group, ** $p<0.01$ vs. OGD control.

We then tested the combined protective effect of both shRNAs and also tested the unique contribution of each shRNA against OGD-induced neuronal death using PI and Hoechst blue staining. PI staining picks up dead neurons, while Hoechst staining represents all neurons. Inhibition of single BNIP3 reduced 20% to 35% OGD/reoxygenation-induced neuronal death from 36 hours to 72 hours reoxygenation. While single knockdown of NIX also protected up to 44% neurons against OGD/reoxygenation from 24 hours to 72 hours reoxygenation. Both shRNAs obtained maximal protection at the time point of 48 hours of reoxygenation. In the same period as NIX (24hour ~72 hour), double knockdown of BNIP3 and NIX provides additional protection against OGD/reoxygenation compared to BNIP3 single knockdown, and reduces up to 48% of neuronal death after 60 hours of reoxygenation. At each time point, although not all significant, knockdown of NIX had the tendency to increase neuronal survival rate more than the knockdown of BNIP3 did. Neither protective nor toxic effects of shRNA controls were observed.

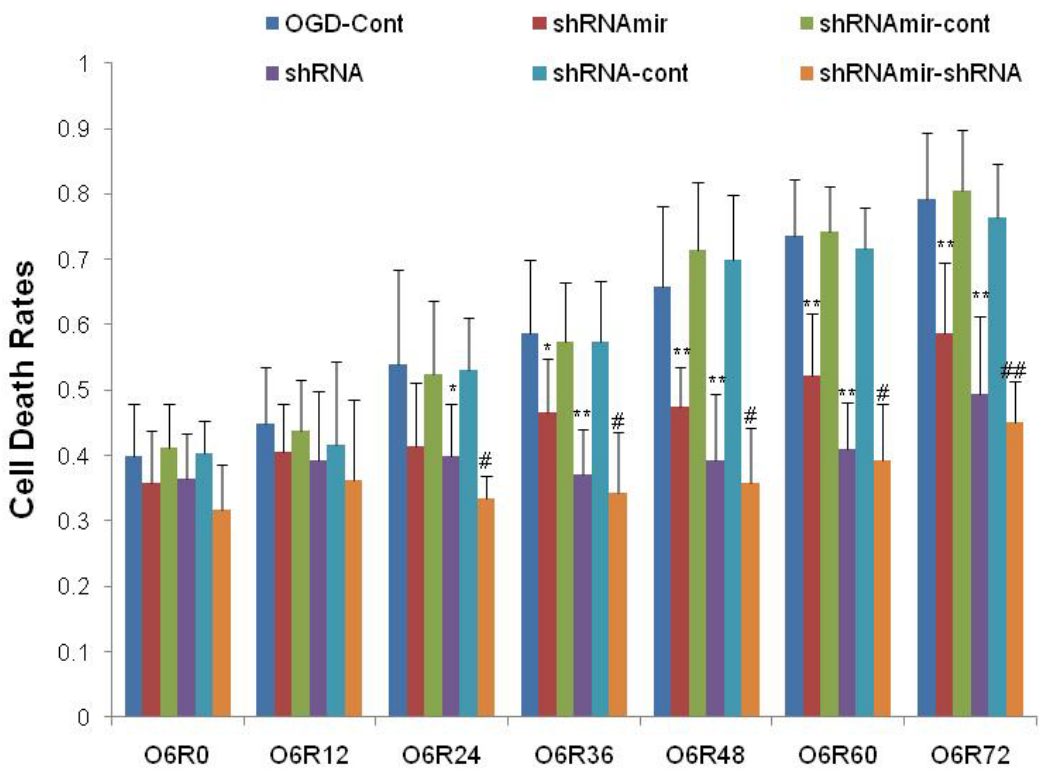

Figure 3.4 Knockdown of BNIP3 death gene family reduced OGD/reoxygenation induced neuronal death.

Small RNAs targeting BNIP3 and NIX were repeatedly transduced into neurons two days before OGD injury, and control shRNAs were used as control. After 6 hours OGD and reoxygenation for up to 72 hour, neurons were stained with PI and Hoechst to identified total number of dead cell and remaining cells, and the difference were considered as the number of live cells. The total number of dead cell was calculated by subtracting the number of neurons before OGD to live cells. Cell death rates were gotten by dividing dead cell to cell number before injury. Values are mean± SE and were analyzed by one-way ANOVA. (n=3) * $p<0.05$ vs. control group, ** $p<0.01$ vs. control, # $p<0.05$ vs. shRNAmir group, ## $p<0.01$ vs. shRNAmir group.

Since PI staining only picks up the dead cells or cells undergoing at the end stage of cell death, it may not represent the overall cell toxicity and viability after OGD and reoxygenation. To confirm the protective effect of BNIP3 and NIX knockdown, we used LDH cytotoxicity assay and MTT assay to test cell viability after 6 hours of OGD and 48

hours of reoxygenation. OGD and reoxygenation caused significant increase of LDH activity in the culture medium, while knockdown BNIP3 and NIX reduced LDH release by 14% and 20%, respectively. Double knockdown reduced LDH release by 29%, and this decrease is only significant compared to the BNIP3 knockdown group. Due to the cell death, OGD/reoxygenation caused a dramatic decrease of MTT activity, while interfering with the expression of BNIP3 and NIX increased MTT activity by 12% and 22%, and double knockdown increase MTT activity by 28% compared to control groups. These cell toxicity and viability results may not equal to the number of cell death, but both of them support the hypothesis that knockdown BNIP3 subfamily protects neurons against OGD/reoxygenation-induced cell death. All these data suggest that BNIP3 subfamily plays a role in ischemia-induced neuronal death, while knockdown of BNIP3 provides limited protection, which may be due to the cell death initiated by NIX. NIX may be more potent than BNIP3 once activated by ischemia.

A

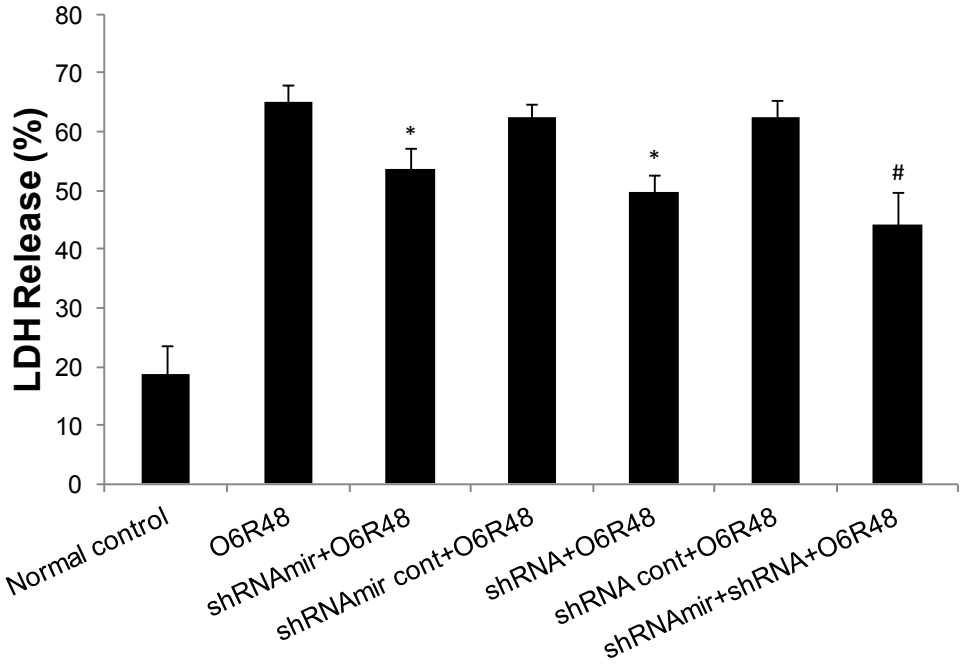
LDH Release (%)
80
70
60
50
40
30
20
10
0
*
*
#
Normal control
O6R48
shRNAmir+O6R48
shRNAmir cont+O6R48
shRNA+O6R48
shRNA cont+O6R48
shRNAmir+shRNA+O6R48

B

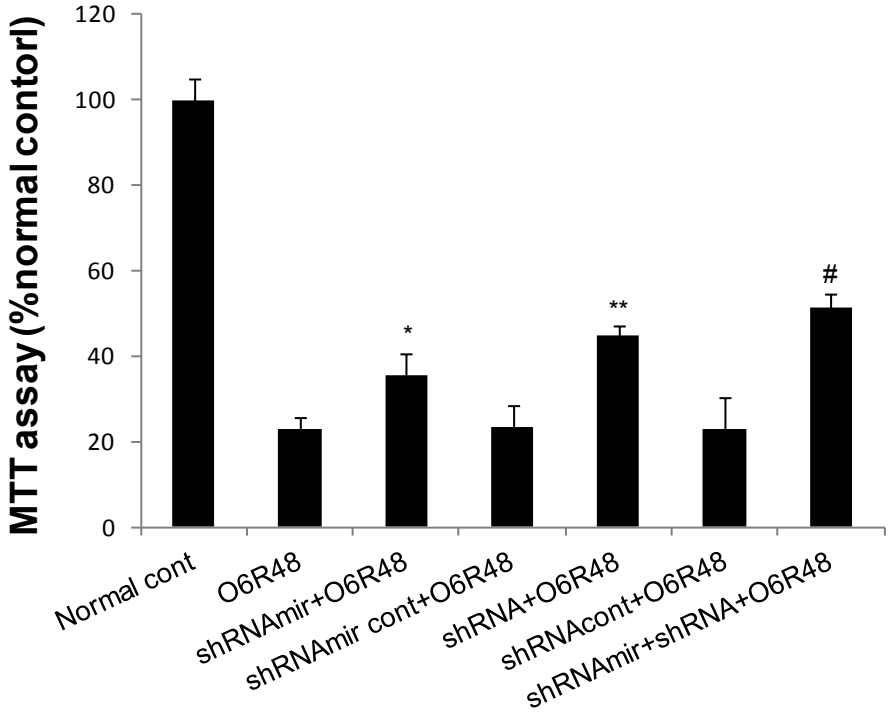
MTT assay (%normal contorl)
120
100
80
60
40
20
0
*
**
#
Normal cont
O6R48
shRNAmir+O6R48
shRNAmir cont+O6R48
shRNA+O6R48
shRNAcont+O6R48
shRNAmir+shRNA+O6R48

Figure 3.5 Knockdown of BNIP3 death gene family protected against OGD/reoxygenation induced neuronal injury.

Small RNAs targeting BNIP3 and NIX were repeatedly transduced into neurons two days before OGD injury, and control shRNAs were used as control. After 6 hrs of OGD and 48 hrs of reoxygenation (O6R48), LDH release (A) and MTT activity (B) were measured in each group to assess the protective effects of these shRNA and shRNAmir group. Values are mean± SE and were analyzed by one-way ANOVA. (n=4) * $p<0.05$ vs. control group, ** $p<0.01$ vs. control, # $p<0.05$ vs. shRNAmir group.

3.4 BNIP3 family gene silencing attenuates OGD-induced mitochondrial dysfunction.

To determine the role of BNIP3 in OGD/reoxygenation-induced neuronal death, we tested the mitochondrial function parameters with shRNA treatment. Because both BNIP3 and NIX were upregulated or peaked at 24 hours and 48 hours of reoxygenation after OGD, these two time points were chosen for each measurement. ROS production increased four and eight times higher than the basal ROS production at these two time periods, whereas inhibition of BNIP3 and NIX reduced ROS production by 27% and 65% after 24 hours of reoxygenation, and by 48% and 56% after 48 hours of reoxygenation, respectively. Double knockdown reduced ROS production by 75% and 67% at 24 hours and 48 hours of reoxygenation, respectively. Similar to the cell death rate, knockdown of NIX reduced more ROS production than knockdown of BNIP3, and double knockdown only showed a significant difference comparing with the BNIP3 knockdown group during the 24 and 48-hour reoxygenation period.

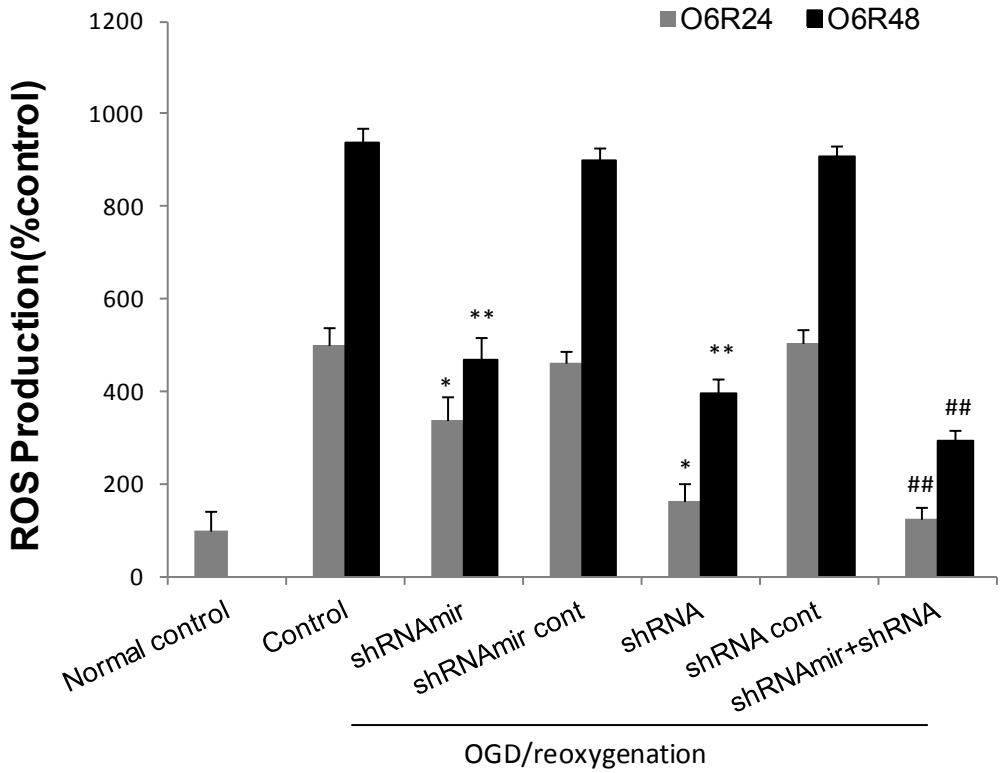

Figure 3.6 Knockdown of BNIP3 death gene family reduced OGD/reoxygenation induced ROS production in neurons.

Small RNAs targeting BNIP3 and NIX were repeatedly transduced into neurons two days before OGD injury, and control shRNAs were used as control After 6 hrs of OGD and 24 or 48 hrs of reoxygenation (O6R24 or O6R48), H2DCF-DA was incubated with neurons in each group to assess the ROS production. Values are mean± SE and were analyzed by one-way ANOVA. (n=4) * $p<0.05$ vs. control group, ** $p<0.01$ vs. control, ## $p<0.01$ vs. shRNAmir group.

Following the same protocol as described previously, mitochondrial membrane potentials were compared using JC-1. Mitochondrial membrane potential was dramatically decreased after OGD/reoxygenation injury, and knockdown of BNIP3 or NIX preserved around 30% membrane potential in neurons against OGD exposure and 24 hour reoxygenation. Prolongation of reoxygenation to 48 hours and knockdown of BNIP3 and

NIX reduced mitochondrial membrane potential loss by 43% and 70%. Double knockdown of BNIP3 and NIX increased the percentages to 47% and 78%. No specific effect of shRNA controls on mitochondrial membrane potential was observed. The MPTP is a high conductance channel of the inner membrane whose opening leads to an increase in permeability to solutes of apoptogenic factors and induces depolarization of the trans-membrane potential (Crompton 1999). MPTP opening evaluated by calcein release revealed that knockdown of BNIP3 or NIX significantly reversed OGD/reoxygenation-induced MPTP opening by 16% and 13% after 24 hour reoxygenation and by 26% and 17% after 48 hour reoxygenation. Double knockdown increased the protection to 28% and 21% at each time point described above. Taken together, these data suggest that neuronal protection against OGD/reoxygenation by knocking down BNIP3 and/or NIX may work through prereserving mitochondrial function.

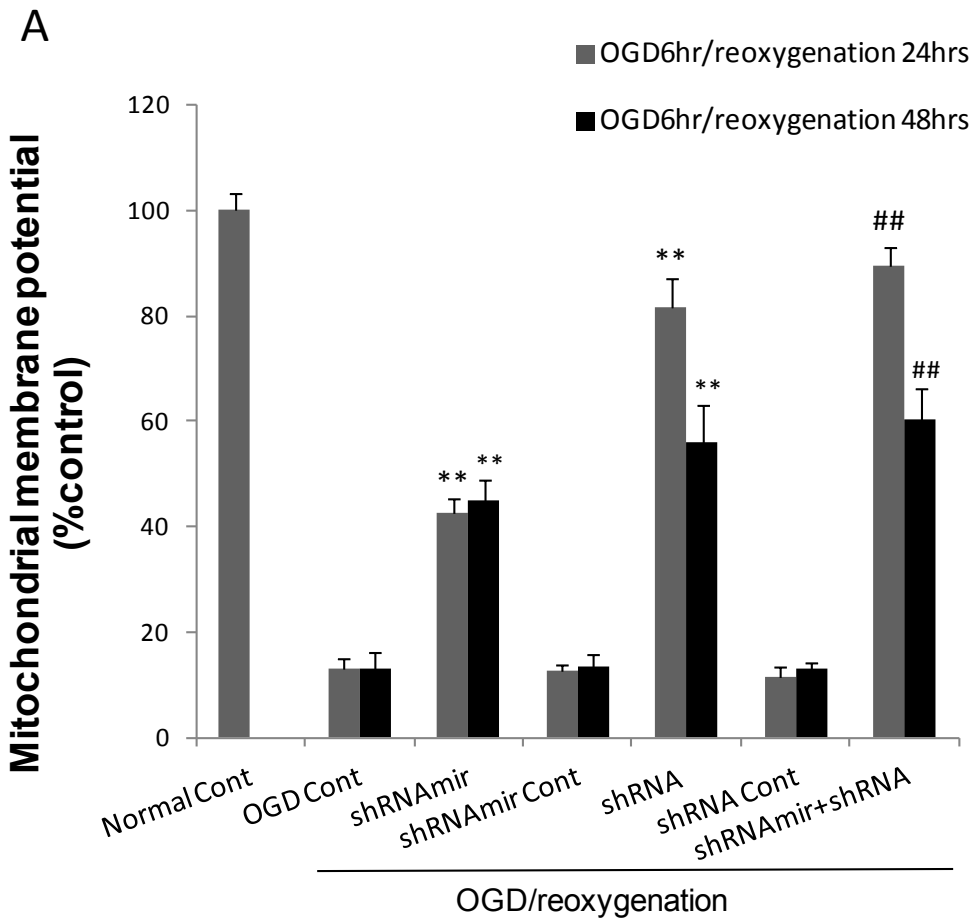
A
OGD6hr/reoxygenation 24hrs
OGD6hr/reoxygenation 48hrs
Mitochondrial membrane potential (%control)
120
100
80
60
40
20
0
**
**
**
**
##
##
Normal Cont
OGD Cont
shRNAmir
shRNAmir Cont
shRNA
shRNA Cont
shRNAmir+shRNA
OGD/reoxygenation

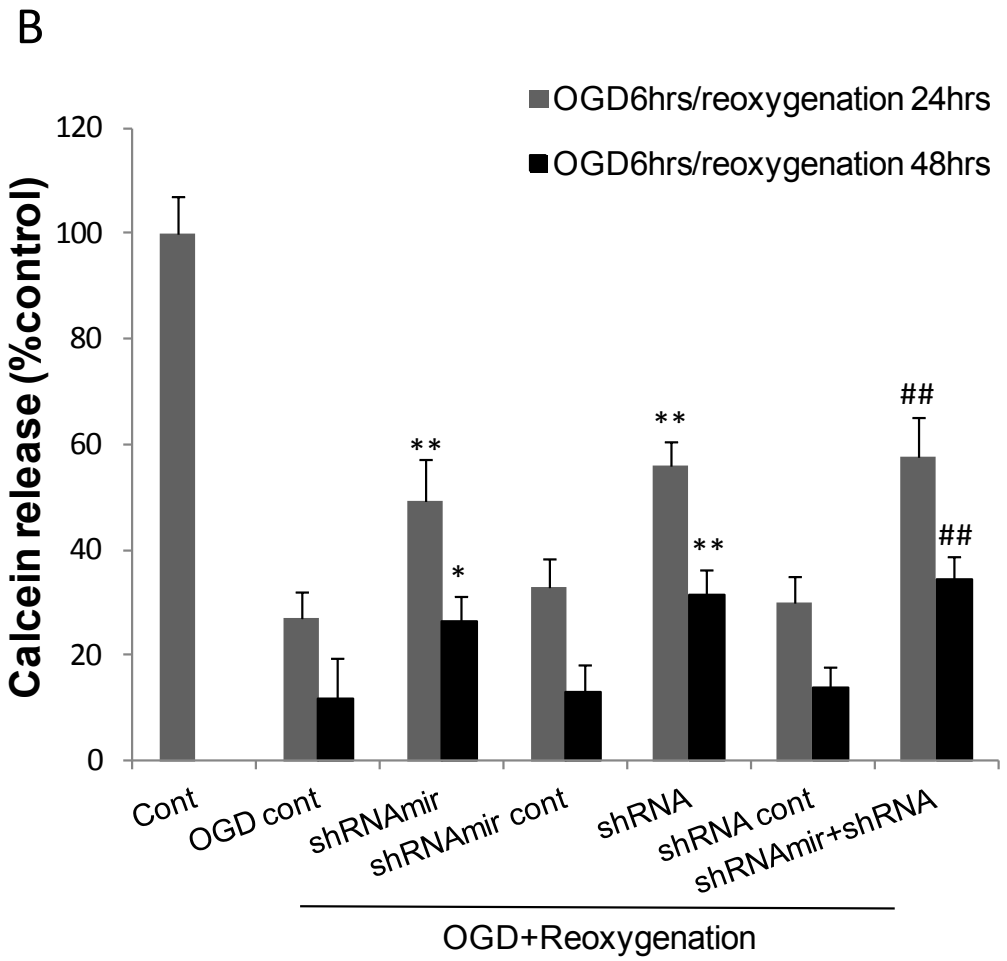

Figure 3.7 Knockdown of BNIP3 death gene family reduced OGD/reoxygenation induced mitochondrial dysfunction.

Small RNAs targeting BNIP3 and NIX were repeatedly transduced into neurons two days before OGD injury, and control shRNAs were used as control. After 6 hour OGD and 24hours or 48 hours reoxygenation (O6R24 or O6R48), (A) JC-1 and (B) Calcein-AM were incubated with neurons in each group to assess the mitochondrial membrane potential and MPTP opening. Values are mean± SE and were analyzed by one-way ANOVA. (n=5) * $p<0.05$ vs. control group, ** $p<0.01$ vs. control, ## $p<0.01$ vs. shRNAmir group.

3.5 Knockdown of BNIP3 upgraded NIX expression.

To investigate the underlying changes that occur after BNIP3 inhibition and to explain the mechanisms by which NIX knockdown adds protection in addition to the protection

provided by BNIP3 knockdown, we tested NIX expression as well as other proteins in neurons where BNIP3 was inhibited. Using immunohistochemical staining, we found that NIX was slightly upregulated when BNIP3 is down-regulated. This change was observed in 72% of EGFP positive cells (GIPZ lentiviral vector has the EGFP tag). In contrast, BNIP3 inhibition did not change the expression level of other proteins that regulated the caspase-dependent cell death pathway, such as Bax, Bcl-2 and cytochrome C. These phenomena were observed in 83.3%, 94.4% and 87% of EGFP positive cells, respectively. These results suggest that NIX also plays a role in OGD/reoxygenation-induced neuronal death, while traditional caspase-dependent cell death pathway may not play the major role. The NIX-mediated cell death pathway may work as an alternate once BNIP3 is inhibited. The expression level of caspase 3 and cathepsin B, two proteins that involved typical apoptosis and necrosis, were not changed in 93.3% and 90% of EGFP positive cells. However, their enzymatic activities have to be further tested to exclude the possibility that knockdown of BNIP3 alone did not turn cell death into traditional apoptosis and necrosis.

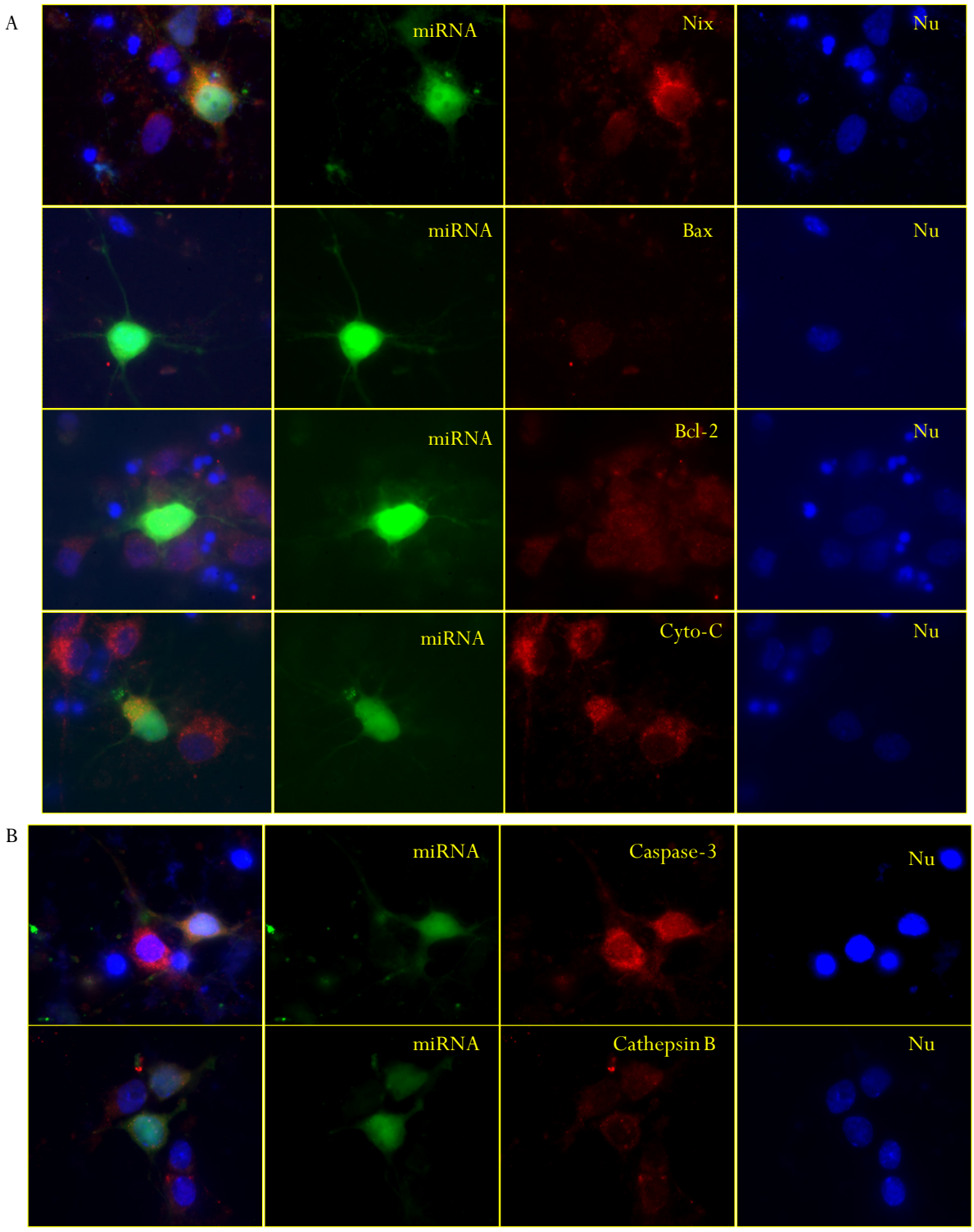

Figure 3.8 Knockdown of BNIP3 upregulated the expression of NIX after OGD/reoxygenation in neurons.

shRNAmir targeting BNIP3 was repeatedly transduced into neurons two days before OGD injury. After 6 hrs OGD and 48 hrs reoxygenation, neurons were immunostained with different antibodies, including NIX, Bax, Bcl-2 and cytochrome C, as well as one apoptosis marker, caspase-3 and one necrosis marker, cathepsin B. The expression level and pattern of these proteins were compared between EGFP-positive and -negative neurons.

3.6 Chapter Summary

In summary, the results in this chapter demonstrated the following:

1. BNIP3 and NIX are gradually upregulated during six hours OGD followed by up to 72 hours reoxygenation.
2. Knockdown of BNIP3 or NIX protect against neuronal death caused by OGD/reoxygenation, while double knockdown of these two proteins reduce further cell death compared to single BNIP3 knockdown.
3. Knockdown of BNIP3 or NIX reduces ROS production, mitochondrial membrane potential loss and MPTP opening against OGD/reoxygenation, while double knockdown of BNIP3 and NIX provides further reduction on these parameters compared to single BNIP3 knockdown.
4. Knockdown of BNIP3 upregulates NIX expression, but does not affect other proteins involved in the caspase-dependent cell death pathway.

Significance

The pro-apoptotic protein BNIP3 plays an important role in ischemia-induced neuronal death, but knockdown of BNIP3 protects limited number of neurons after hypoxia. Here, we found that additional inhibition of NIX to BNIP3 increases survival rate after OGD/reoxygenation, suggesting that NIX may compensate for the loss of BNIP3. In

addition, ROS production, mitochondrial membrane potential loss and MPTP opening are also inhibited in double knockdown groups compared to the BNIP3-alone group, indicating that NIX leads to the neuronal death in a similar way as BNIP3. However, further research has to be done to identify why and how BNIP3 inhibition turns the cell into a NIX-mediated pathway.

Chapter 4. AIF is a mediator in BNIP3 and NIX induced neuronal death.

4.1 Rationale

We have reported that EndoG is involved in BNIP3-induced neuronal cell death; expression of BNIP3 results in mitochondrial release and nuclear translocation of EndoG, and knockdown of BNIP3 prevents hypoxia-induced EndoG translocation. Like EndoG, AIF also causes neuronal cell death in experimental stroke both *in vitro* and *in vivo* (Thal et al. 2011; Cao et al. 2003). Normally, AIF is localized in the intermembranous space of mitochondria. In response to ischemic injury, it translocates to the nucleus and induces chromatin condensation and DNA fragmentation. AIF has been widely accepted as a pro-apoptotic mediator whose main function is independent of caspases (Cande et al. 2002). Recently, it was reported that AIF is involved in the alkylating DNA damage (MNNG) programmed necrosis (Moubarak et al. 2007). Therefore, we propose that AIF may also act as a downstream mediator in the BNIP3-induced cell death pathway. Due to the similarities between NIX and BNIP3, we suspect that NIX may also cause AIF translocation. To investigate the role of AIF in BNIP3- or NIX-induced cell death, we will knockdown BNIP3 and/or NIX to test whether it will interfere with AIF translocation after OGD injury *in vitro* and neonatal stroke *in vivo*. We will over-express BNIP3 and NIX to see whether AIF release is induced.

4.2 Knockdown BNIP3 or NIX blocked AIF translocation.

Cell death mediated by BNIP3 and NIX via mitochondrial dysfunction has been indicated in chapter 3. However, in this cell death pathway, does the mitochondrial function change directly or indirectly lead to cell death? How do these changes result in cell death? We explored the involvement of a mitochondrial protein, AIF, as the potential downstream protein of BNIP3 and NIX, in response to OGD/reoxygenation. In normal neurons, AIF was localized in mitochondria surrounding nuclei observed under a microscope. AIF localization changes were observed in neurons with BNIP3 inhibition. We found that neurons with shRNAmir (BNIP3 knockdown) showed decreased nuclear localization of AIF compared to the non-transduced neurons, whereas the shRNAmir control did not change the localization of AIF (Fig 4.1). The results were also confirmed by the Western blot analysis using mitochondrial fractions. Groups with BNIP3 reduction had higher levels of AIF in the mitochondria compared to the shRNAmir control group. Cox IV and histone H3 antibodies were used as mitochondria and nuclei fractions for sample loading controls. To confirm this data, we also used EndoG as a "positive" control. EGFP labelled neurons evenly distributed EndoG staining compared to non-labelled neurons. These results suggest that, like EndoG, BNIP3 inhibition blockes AIF translocation after OGD/reoxygenation in neurons and AIF may function as a downstream protein in the BNIP3-mediated cell death pathway.

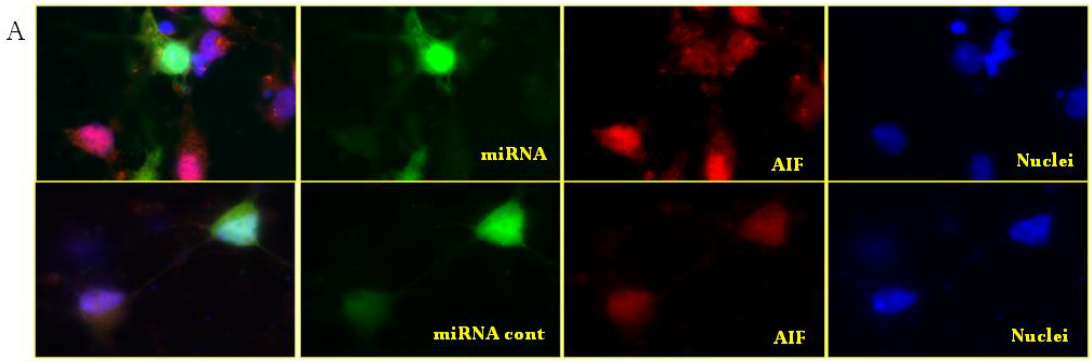
A
miRNA
AIF
Nuclei
miRNA cont
AIF
Nuclei

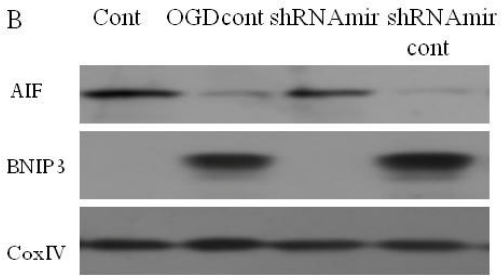
B
Cont
OGD cont
shRNAmir
shRNAmir cont
AIF
BNIP3
CoxIV

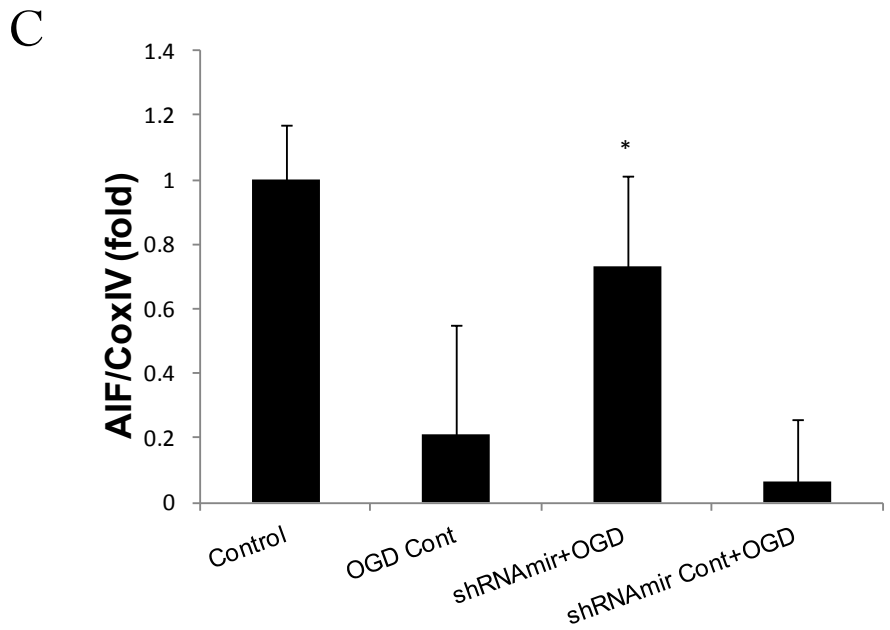
C
AIF/CoxIV (fold)
1.4
1.2
1
0.8
0.6
0.4
0.2
0
*
Control
OGD Cont
shRNAmir+OGD
shRNAmir Cont+OGD

D

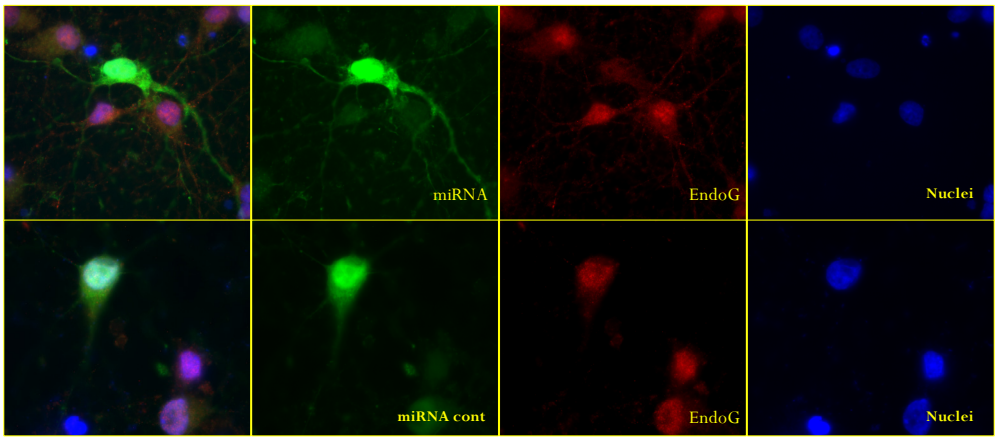

Figure 4.1 Cellular localization of AIF with BNIP3 knockdown in response to OGD/reoxygenation in neurons.

Cultured cortical neurons were transduced with shRNAmir to knockdown BNIP3, and then stained with AIF (A) or EndoG (D) antibody. (A) After OGD/reoxygenation, neurons showed accumulation of AIF in the nuclei. Neurons with BNIP3 knockdown (indicated by EGFP) showed reduced AIF release from mitochondria into nuclei, while shRNA control had no impact on the AIF translocation. (B) and (C) Quantification of proteins expression of BNIP3 and AIF in each group to confirm the significant inhibition of shRNA and AIF translocation. The CoxIV was included as a mitochondrial loading control. The ratio of BNIP3 and AIF to CoxIV were compared between each groups. (D) OGD/reoxygenation also caused significant release of EndoG in neurons, while BNIP3 knockdown diminished central AIF localization. shRNA control did not seem to change the EndoG expression pattern. Values are mean± SE and were analyzed by one-way ANOVA. (n=3) * $p<0.05$ vs. OGD control group.

To test whether AIF is involved in the neuronal protection by double knockdown of BNIP3 and NIX in OGD/reoxygenation-induced in neurons, we measured AIF release in neurons after two shRNAs were transduced. BLOCKIT lentiviral vectors do not have EGFP label, so we only used Western blot to detect AIF release. Neurons with 63% NIX knockdown showed 70% reduction of AIF release from mitochondria after OGD/reoxygenation (Fig 4.2). The quantity of AIF in the mitochondrial fractions was almost the same between the shRNA control group and the OGD control group. Thus, inhibition either BNIP3 or NIX would block AIF translocation in neurons against OGD,

while inhibiting both BNIP3 and NIX did not further increase the blockage of AIF release compared to single knockdown. The control shRNA showed no effect on NIX expression and AIF translocation. These results suggeste that NIX mediates ischemia-induced neuronal death in a similar way as BNIP3 did — through AIF translocation.

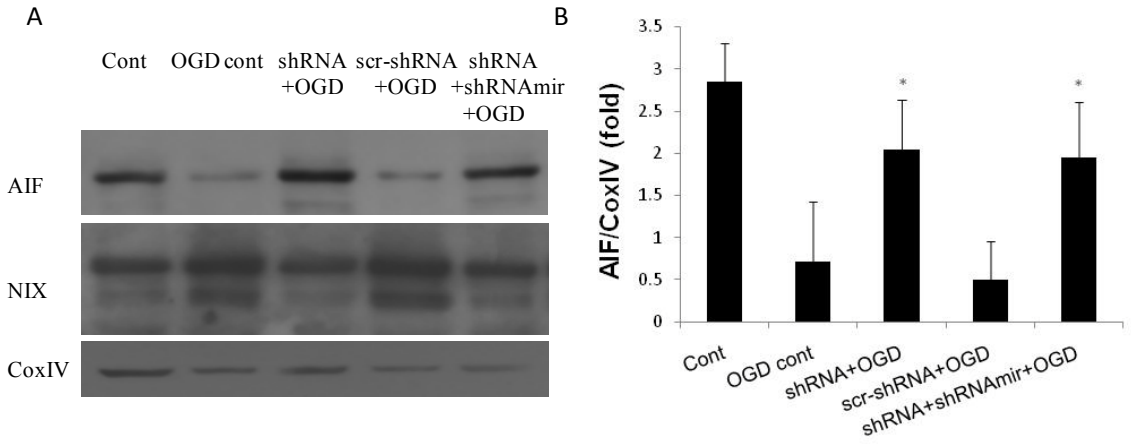

Figure 4.2 Cellular localization of AIF with NIX knockdown in response to OGD/reoxygenation in neurons.

Cultured cortical neurons were transduced with shRNA to knockdown NIX. (A) Quantification of protein expression of NIX and AIF in each group were detected by Western blot to confirm the inhibition efficiency of shRNA and AIF translocation. The CoxIV was included as a mitochondrial loading control. shRNAmir in combination with shRNA was added as another group to compare the AIF translocation between single NIX knockdown and double BNIP3 and NIX knockdown. (B) The ratio of BNIP3 and AIF to CoxIV were compared among groups. Values are mean± SE and were analyzed by one-way ANOVA. (n=3) * $p<0.05$ vs. OGD control group.

4.3 Knockdown BNIP3 *in vivo* reduced hypoxia-ischemia induced brain damage and blocked AIF translocation.

Furthermore, we tested the role of BNIP3 in ischemic neuronal death in neonatal stroke model *in vivo*. Neonatal stroke triggered by right common carotid artery ligation and hypoxia causes global ischemia on the ipsilateral hemisphere. Twenty-four mouse pups

were underwent neonatal ischemia, and all survived. Each group consisted of eight animals for further analysis. Mouse brains were dissected seven days after surgery, and morphological analysis with cresyl violet staining showed that hypoxia-ischemia damaged the majority of cerebral cortex and striatum. However, unlike the MCAO model, the border of damaged brain is not so clear. It is difficult to measure and compare the infarct area or count the number of delayed cell death as in the MCAO model. Interestingly, hypoxia-ischemia injury causes a severe enlargement of ipsilateral lateral ventricle. In the normal rat pup, the two lateral ventricles are identical; 7 days after hypoxia-ischemia injury, the ratio between ipsilateral to contralateral ventricles increased more than eight times. shRNAmir which targeting BNIP3 into striatum provided significant protection against ischemia and reduced the ratio to 2.8 times. The volumes of striatum in the ipsilateral hemisphere were measured and compared with the contralateral side, according to the method described by Oorschot (Oorschot 1996). However, no significant changes of volume were observed after hypoxia-ischemia with or without shRNAmir treatment. Thus, we calculated the cell numbers in the cortex and hippocampus areas indicated as figure 4.3. We found that neonatal stroke cause significant neuronal loss in the central ischemic area. In the penumbra area and hippocampus, about 56% and 43% neurons survived, respectively, including cells with minor damage. Knockdown of BNIP3 through the shRNA treatment increased the survival rates to 85% and 70% in these two areas. However, in spite of the increased cell number, most of the surviving neurons lost the normal morphological characteristics: cells were diffusely swollen and the axons were shrunken or disappeared. In hippocampal CA1 subfields, pyramidal neurons were scattered and shrunken.

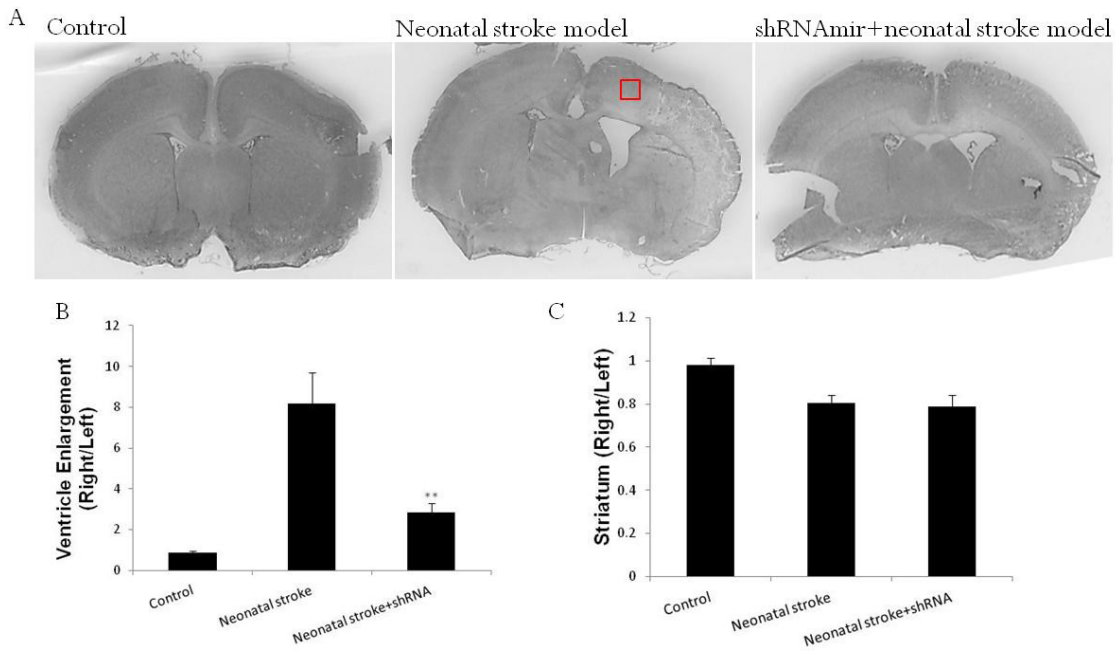

Figure 4.3 BNIP3 knockdown reduced cerebral ischemic damage against neonatal stroke.

Seven-day-old pups were exposed to hypoxia-ischemia, and their brain tissues were fixed 7 days after surgery. Brain slices were stained with cresyl violet to measure brain tissue and cellular damage. (A) Representative photographs of normal, neonatal stroke and neonatal stroke accompanied by shRNA treatment are shown. Hypoxia-ischemia not only caused lesionneonatal stroke in cortex and striatum in ipsilateral hemisphere, but also caused ipsilateral ventricle enlargement. (B) and (C) shRNA which knocked down around 62% BNIP3 expression did not change the volume of striatum, but significant decreased the enlarged lateral ventricle. Values are mean± SE and were analyzed by one-way ANOVA. (n=4) **p<0.01 vs. OGD control group.

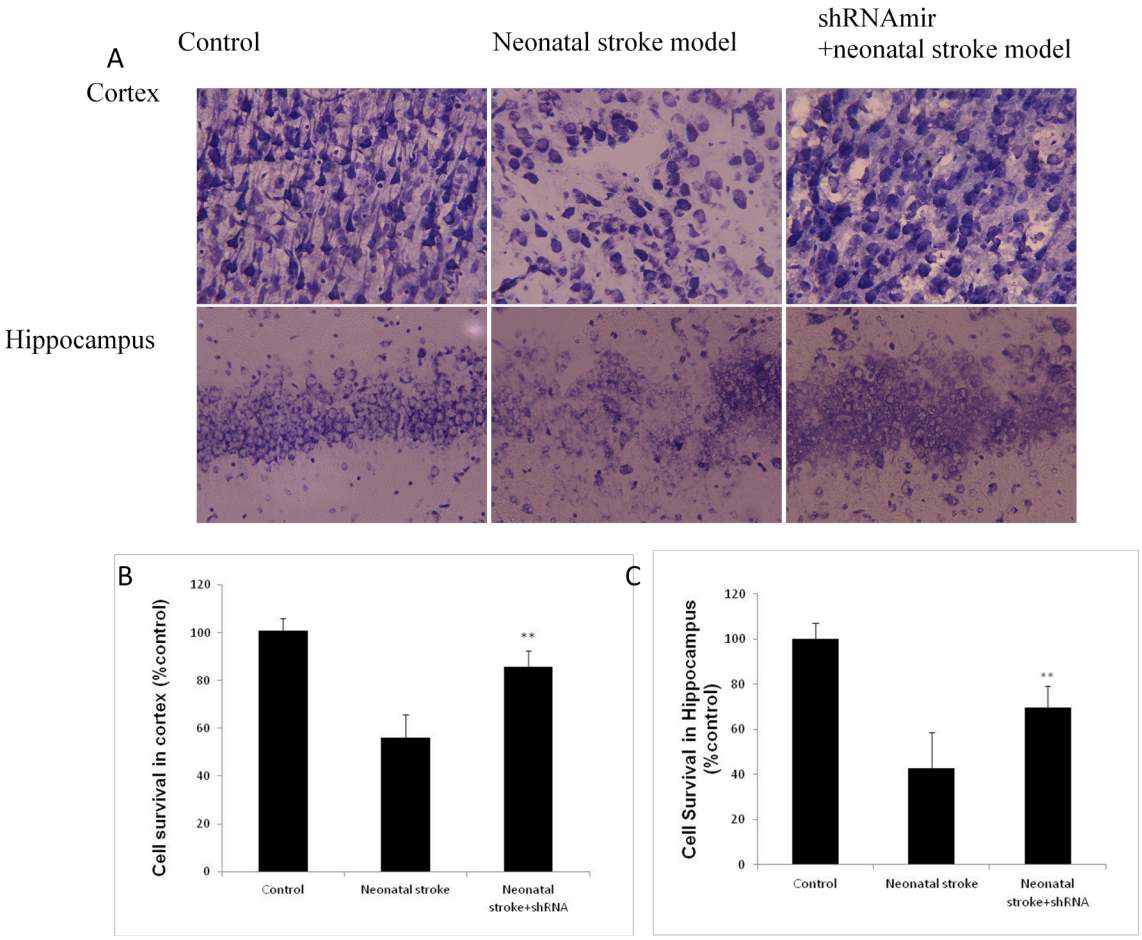

Figure 4.4 BNIP3 knockdown increased neuronal survival against neonatal stroke.

Brain slices stained with cresyl violet were used to measure neuronal cell death and cellular damage. (A) Representative photographs of normal, neonatal stroke and neonatal stroke accompanied by shRNA treatment in cortex and hippocampus are shown. (B) and (C) Neonatal stroke induced neuronal loss, in both cortex and hippocampus. Neurons were shown cellular swollen and nuclei condensation. shRNA treatment significantly increased neuronal survival rate against hypoxia-ischemia. Values are mean± SE and were analyzed by one-way ANOVA. (n=4) **$p<0.01$ vs. OGD control group.

Depending on the morphological changes and injection site of shRNA, striatum were isolated from the whole brain. To investigate the impact of BNIP3 knockdown on AIF and EndoG translocation, mitochondrial and nuclear fractions were further isolated from both sides of hemispheres, and BNIP3, AIF and EndoG were detected by Western blot.

We found that hypoxia-ischemia upregulated BNIP3 expression in ischemic striatum, while shRNA administration inhibited 62% of BNIP3 expression. On the contralateral striatum, which can be considered as an internal control, BNIP3 remained low and shRNA did not change the BNIP3 level. In the same mitochondrial fractions, AIF was released from mitochondria and translocated into the nuclei by ischemia in the ipsilateral striatum, while it was blocked up to 72% by shRNA. This result supports our *in vitro* data that BNIP3 inhibition blocks AIF release and suggests that BNIP3 is an upstream regulator in AIF-mediated cell death. Like AIF, EndoG was also translocated from mitochondria to the nuclei, although the release of EndoG was moderate compared with AIF. On the contralateral side, where the brain did not have ischemic injury, no noticeable changes were found on the level of AIF and EndoG. These results suggest that BNIP3 induced neuronal cell death through AIF and EndoG translocation in hypoxia-ischemia.

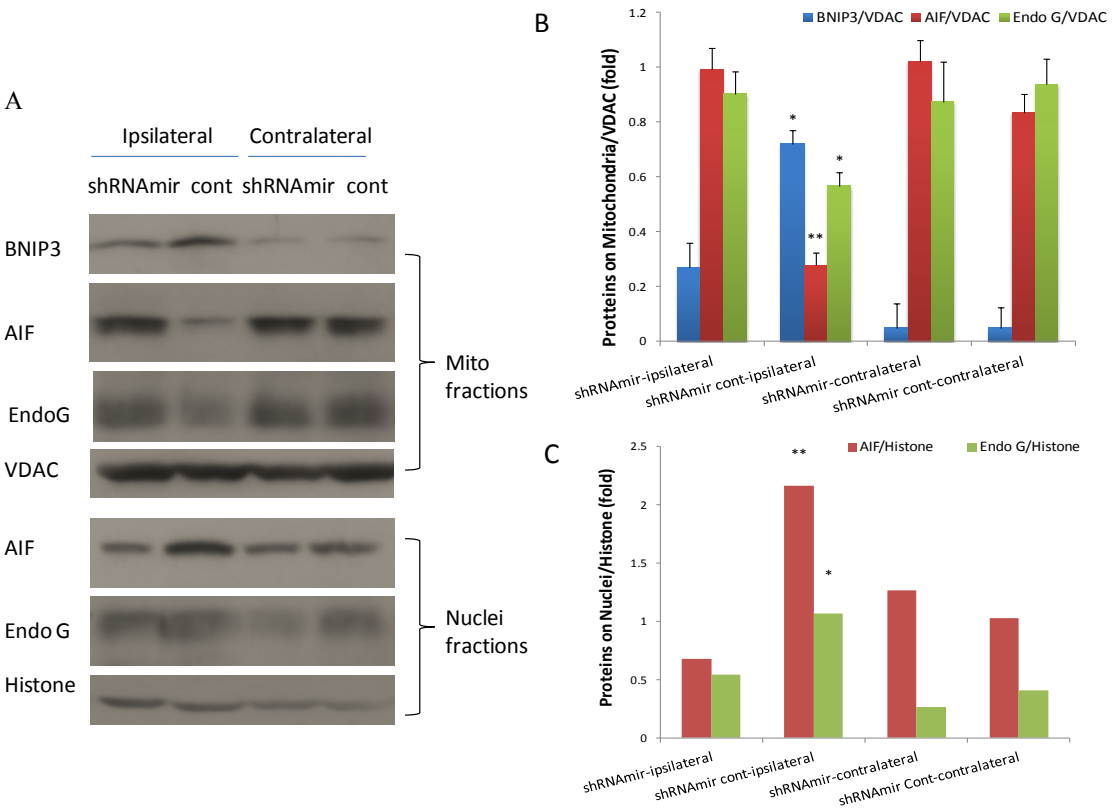

Figure 4.5 Cellular localization of AIF and EndoG with BNIP3 knockdown in response to neonatal stroke.

Seven-day-old pups were exposed to a hypoxia-ischemia model, and fresh brain tissue were separated 7 days after surgery. Striatum where shRNA was injected into was isolated from each hemisphere. Mitochondrial and nuclear fractions were further isolated from each striatum. (A) Hypoxia-ischemia caused significant upregulation of BNIP3 and translocation of AIF and EndoG in ipsilateral striatum. shRNA significantly blocked AIF and EndoG release. shRNA control did not impact on the AIF or EndoG translocation. On the contralateral side, no noticeable BNIP3 upregulation and AIF or EndoG release was observed. shRNA did not interfere with the protein expression or localization. (B) and (C) The CoxIV was included as a mitochondrial loading control. The ratio of BNIP3 and AIF to CoxIV were compared between each groups. Values are mean± SE and were analyzed by one-way ANOVA. (n=4) * $p<0.05$ vs. OGD shRNAmir control-ipsilateral group; ** $p<0.01$ vs. shRNAmir control-ipsilateral group.

4.4 Overexpression of BNIP3 or NIX caused AIF translocation and mitochondrial dysfunction.

To further explore the role of BNIP3 and NIX in neuronal cell death, we constructed lentiviral vectors containing full-length BNIP3 or NIX. The same vector containing BNIP3-ΔTM or NIX-ΔTM was used as control. LDH release was used to measure cytotoxicity of these proteins to the neurons. BNIP3 and NIX increased 50% and 41% LDH release, while, surprisingly, BNIP3-ΔTM and NIX-ΔTM also increased 25% and 24% of LDH release, respectively. This suggests that, even without the transmembrane domain, these truncated BNIP3 and NIX are not harmless for neurons. According to a recent report, in addition to interacting with mitochondria through the transmembrane domain, BNIP3 and NIX may interact with ER, causing ER stress and cell death. This may explain the increased LDH release by BNIP3-ΔTM and NIX-ΔTM. To further investigate the mechanism of BNIP3 and NIX on neuronal cell death, mitochondrial function parameters were measured.

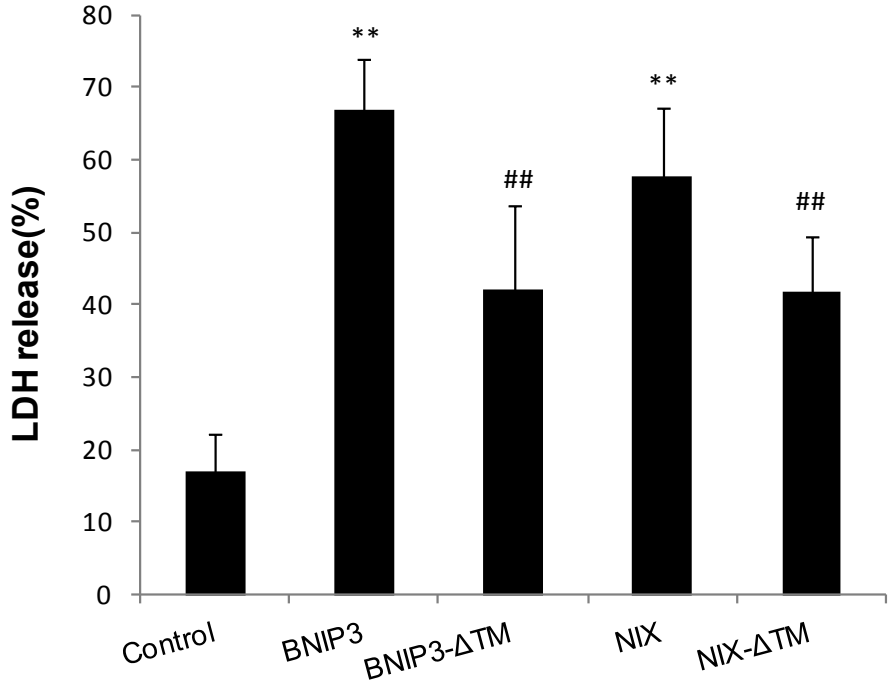

Figure 4.6 LDH release induced by BNIP3 or NIX over-expression in neurons.

Cultured cortical neurons were transduced with full-length BNIP3 or NIX sequence, as well as BNIP3ΔTM and NIX ΔTM with the help from lentiviral vector. Forty-eight hours after transduction, LDH cytotoxicity was measured in each group. BNIP3 and NIX caused significant release of LDH enzyme, while BNIP3ΔTM and NIX ΔTM also caused LDH release, although total mount of released LDH was much less than full-length proteins. Values are mean± SE and were analyzed by one-way ANOVA. (n=5) ** $p<0.01$ vs. BNIP3ΔTM group or NIXΔTM; ## $p<0.01$ vs. control group.

Mitochondrial membrane potential was measured after BNIP3 and NIX expression were enforced by JC-1 staining. BNIP3 and NIX upregulation caused 18% and 23% of mitochondrial membrane potential loss, respectively, while BNIP3-ΔTM and NIX-ΔTM did not cause any change on membrane potential. BNIP3 and NIX caused 27% and 28% of calcein release in neurons, respectively, while BNIP3-ΔTM and NIX-ΔTM slightly decreased calcein in mitochondria but not significantly. These results suggest that

transmembrane domain is required for BNIP3 and NIX to interfere with mitochondrial function, and cellular damage caused by BNIP3-ΔTM and NIX-ΔTM may not have major impact on mitochondrial dysfunction.

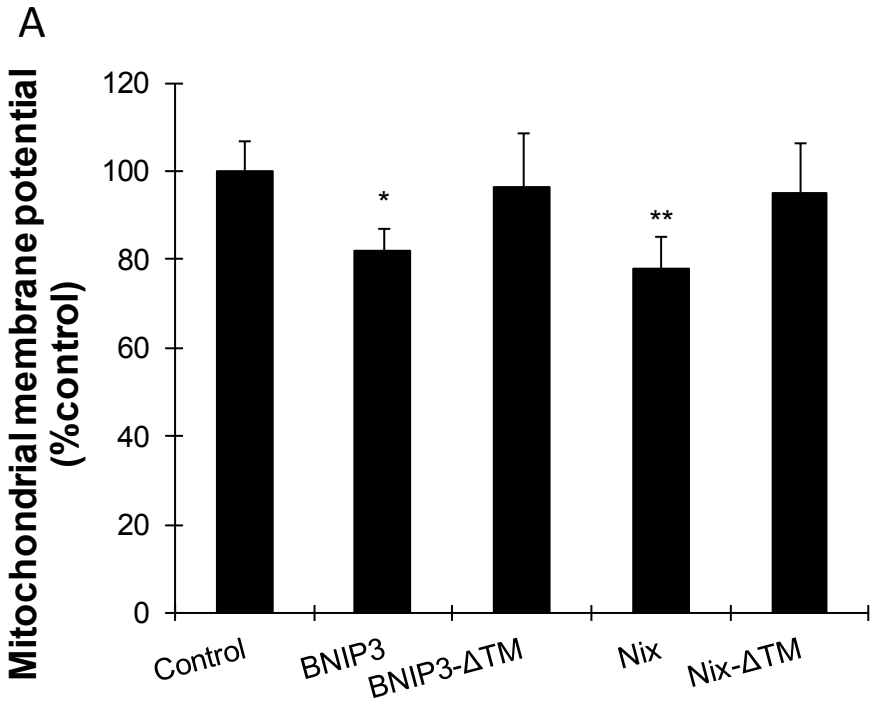

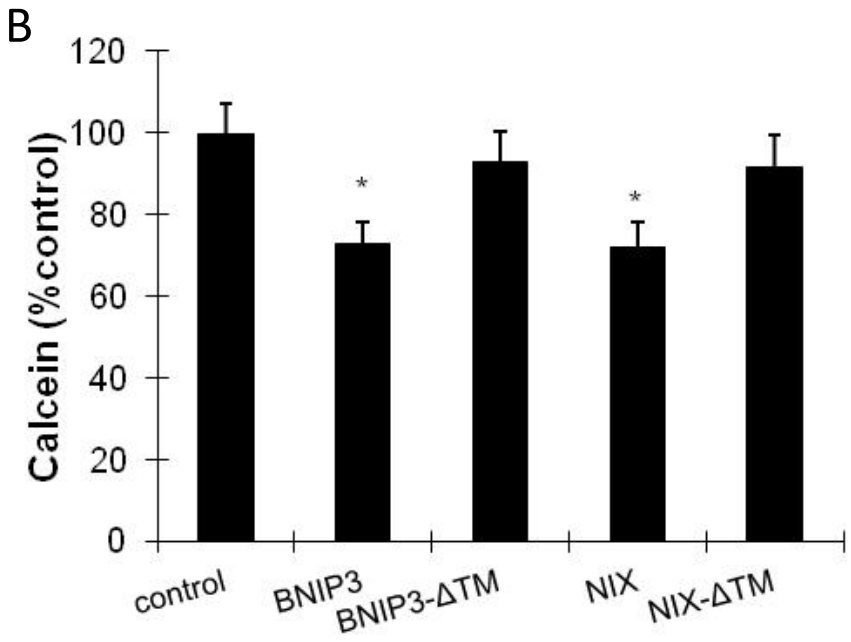

Figure 4.7 Mitochondrial dysfunction induced by BNIP3 or NIX over-expression in neurons.

Cultured cortical neurons were transduced with full-length BNIP3 or NIX sequence, as well as BNIP3ΔTM and NIX ΔTM using lentiviral vector. Forty-eight hours after transduction, fluorescence probes JC-1(A) and Calcein-AM (B) were used to measure the mitochondrial membrane potential loss and MPTP opening in each group. BNIP3 and NIX caused significant decrease mitochondrial membrane potential and MPTP opening. BNIP3ΔTM and NIX ΔTM did not change these two parameters of mitochondrial function. Values are mean± SE and were analyzed by one-way ANOVA. (n=5) * $p<0.05$ vs. BNIP3-ΔTM group or NIX-ΔTM group; ** $p<0.01$ vs. NIX-ΔTM group

Our data suggested that AIF is the downstream mediator in the BNIP3- and NIX-induced cell death pathway, so we tested the cellular localization of AIF in BNIP3-and-NIX-overexpressed neuronal culture. Immunohistochemical analysis showed that the BNIP3 and NIX over-expressing neurons had increased nuclear presence of AIF compared to the neurons that are transduced with BNIP3-ΔTM and NIX-ΔTM. Nuclei condensation and

fragmentation were observed in BNIP3- or NIX-positive cells. Western blot data further confirmed our finding and demonstrated the translocation of 65% and 59% of AIF in neurons with full-length BNIP3 and NIX transduced. These data suggest AIF translocation in BNIP3 and NIX induced neuronal death.

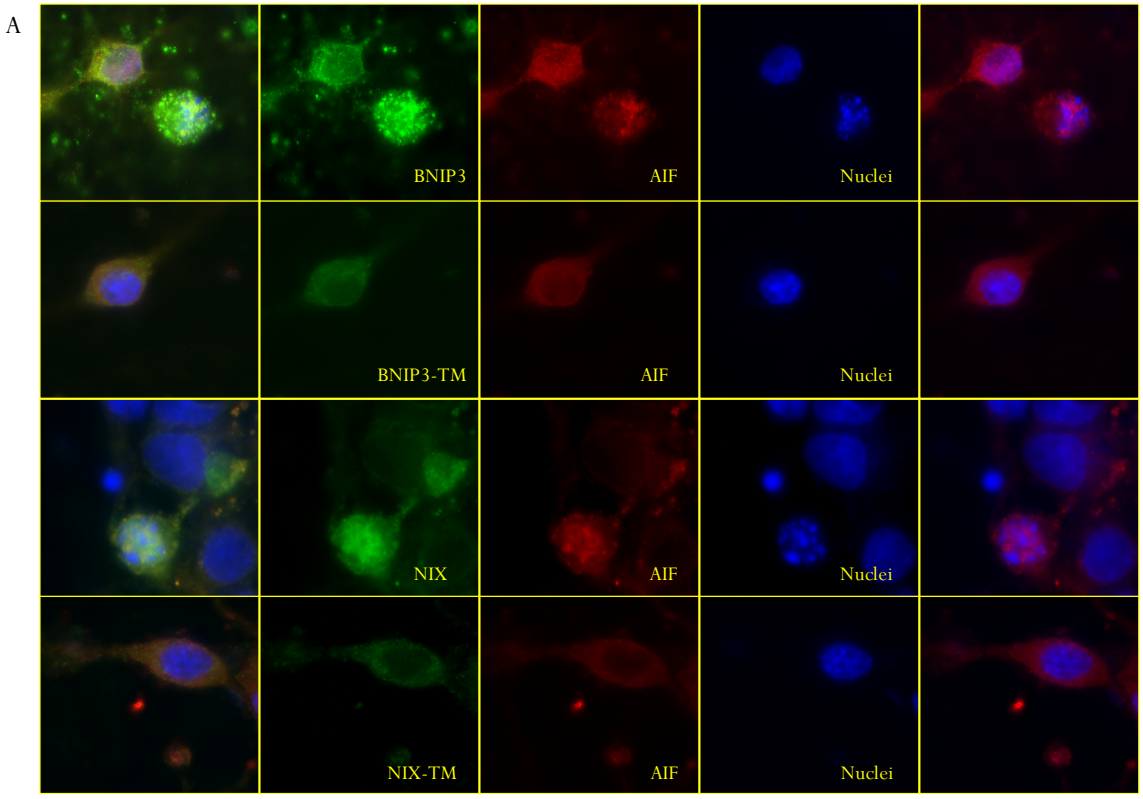

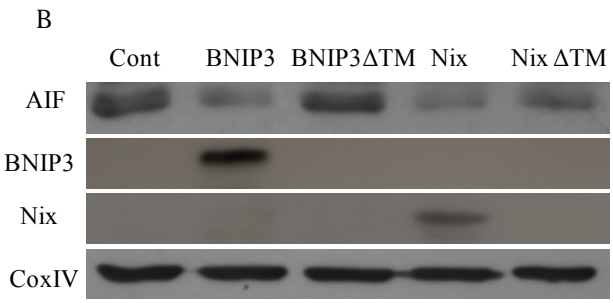

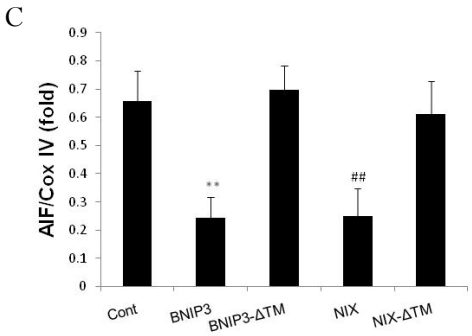

Figure 4.8 Cellular localization of AIF with BNIP3 or NIX over-expression in neurons.

Cultured cortical neurons were transduced with full-length BNIP3 or NIX sequence with the help from lentiviral vector. (A) Forty-eight hours after transduction, neurons were double stained with AIF as well as BNIP3or NIX. BNIP3- or NIX-positive cells significantly increase AIF nuclear localization and nuclear fragmentation, while BNIP3ΔTM- and NIX ΔTM-positive neurons did not show any changes compared to the normal cells. (B) After 48 hrs of incubation, mitochondrial fractions were isolated from the neurons. Quantification of proteins expression of BNIP3, NIX and AIF in each group was measured by Western blot to confirm the inhibition efficiency of shRNA and AIF translocation. Full-length BNIP3 or NIX was detected in the mitochondrial fraction while BNIP3-ΔTM and NIX-ΔTM failed to attach to the mitochondria. BNIP3 or NIX expression resulted in release of AIF from mitochondria, while BNIP3ΔTM and NIX ΔTM did not change the localization of AIF. The CoxIV was included as a mitochondrial loading control. (C) The ratio of BNIP3 and AIF to CoxIV were compared between each groups. Values are mean± SE and were analyzed by one-way ANOVA. (n=3) ** $p<0.01$ vs. BNIP3ΔTM group; ## $p<0.01$ vs. NIXΔTM group.

4.5 Chapter Summary

In summary, the results in this chapter demonstrated the following:

1. Both BNIP3 and NIX cause AIF translocation, and knockdown of them significantly blocks AIF release.
2. shRNA, which inhibits BNIP3, protects neurons against hypoxia-ischemia induced brain damage neonatal mice.
3. Knockdown of BNIP3 blocks AIF and EndoG in ipsilateral striatum in hypoxia-ischemia injury.
4. BNIP3 or NIX over-expression causes neuronal death, mitochondrial potential loss and MPTP opening, while BNIP3-ΔTM and NIX-ΔTM cause cell death but not mitochondrial dysfunction.

Significance

A wealth of evidence shows that the caspase-independent pathway plays very important role in neuronal death. BNIP3 induces cell death through a caspase-independent mechanism in a variety of cells. Results from our laboratory describe that BNIP3-induced EndoG-mediated cell death pathway in hypoxia and ischemia conditions. Here, we suggest that AIF is another mediator in BNIP3 mediated neuronal death in experimental stroke. In addition, the homogenous of BNIP3, NIX, also resulted in AIF translocation in neurons. The truncated form of both proteins lost the ability to cause AIF release, suggesting that the transmembrane domains of BNIP3 and NIX are required to induce AIF translocation. In summary, with mitochondrial function data, we propose that forced or induced expression of BNIP3 and NIX can cause mitochondrial dysfunction, which further results in the AIF or EndoG release, and cell death. Defining this novel cell death pathway would provide a new strategy for neuroprotection.

Chapter 5. Nec-1 protected against *in vitro* hypoxia and *in vivo* ischemia induced neuronal death.

5.1 Rationale

It is well known that hypoxia-ischemia causes sudden, irreversible acute neuronal death and slow progressive, reversible, delayed neuronal death. The phenotypes of delayed neuronal death include apoptosis, necrosis, autophagic cell death, and programmed necrosis. Due to failure of therapeutic targeting for necrosis and unsatisfactory protection against apoptosis and autophagical cell death, recently, more and more attention has been paid to programmed necrosis. Several molecules have been identified as programmed necrosis inhibitors, and Nec-1 is the first potent therapeutic agent. Nec-1 only protects caspase-independent cell death but has no effect on caspase-dependent cell death (Degterev et al. 2005). To date, it is reported that Nec-1 reduced ischemic brain injury (Degterev et al. 2005), ischemia/reoxygenation injury in retina (Trichonas et al. 2010), myocardial infarct size (Smith et al. 2007) and glutamate excitotoxic cell death (Xu et al. 2007), et cetera. Although Nec-1 can significantly prevent MCAO-induced neuronal death, its protective effect on *in vitro* hypoxic neuronal death and its post-stroke therapeutic effect on *in vivo* ischemia had not yet been tested. Thus, we sought to test the protection of Nec-1 on hypoxia- and ischemia-induced neuronal death *in vitro* and *in vivo*. Nec-1 counteracts the reduction in mitochondrial membrane potential in cadmium-induced necrotic model (Hsu et al. 2009) and blocks BNIP3 mitochondrial integration and AIF release in glutamate-induced oxytosis in HT-22 cells (Xu et al. 2007),

suggesting that mitochondria are the major site of action for Nec-1. Therefore, we also tested the role of hypoxia-induced mitochondrial dysfunction.

5.2 Nec-1 protected neurons from hypoxia induced cell death

Hypoxia is an energy-limiting cellular stress that decreases ATP production and promotes neuronal death. Although prolonged hypoxia shows less advantages mimicking *in vivo* stroke compared with OGD model, this model provides more consistent results and provides an intense insult to the neurons. To test the protective role of Nec-1 on hypoxia-induced neuronal death, we first treated neurons with different doses of Nec-1 one day before hypoxia (O_2<1%, for 24 or 48 hour) according to the previous report. Since Nec-1 cannot directly dissolve in the distil H_2O, it was dissolved in DMSO first and then added to the culture medium. Due to the toxic effect of dissolvent (DMSO), another control group was set up adding the same amount of DMSO (0.001%). Equivalent DMSO was also added to low-dose Nec-1 groups to eliminate contradictive effects of DMSO on cell death. The Nec-1 doses of 0, 6.25μM, 12.5μM, 25μM or 50μM were chosen because 100μM Nec-1 pre-treatment accompanied by 0.002% DMSO did not show protective effects and the DMSO group showed significant toxic effects in neurons. Cell death was detected by trypan blue staining, crystal violet staining and MTT assay. We found that hypoxia (24 hour) alone caused about 40% of cell death, and DMSO itself, although not significant, slightly increased the hypoxia-induced cell death. Thus, the DMSO treatment group was used as internal control to compare the cell death rate in the following experiments. In the lower dose groups, using crystal violet and trypan blue staining failed to reveal the protection of Nec-1 on neurons against hypoxia, while Nec-1 reached its

maximal protection at the doses of 25 μM and 50 μM, by reducing neuronal death by 26%~31% (Fig 5.1 A and B). Interestingly, using MTT assay, we detected a dose-dependent protective effect of Nec-1 against 24-hour hypoxia, and MTT activity was increased up to 40% compared to the DMSO group. To test the dose-dependent protection of Nec-1 on chronic hypoxia, neurons were also exposed to 48 hours of hypoxia followed by MTT assay. During this prolonged injury, Nec-1 increased MTT activity by 31%~42%, but the protective effect was only detected in high-dose groups. Furthermore, although primary neuronal cultures were initially tested and had >96% neurons, we stained neuronal culture with a neuronal-specific nuclear (NeuN) antibody to confirm that the protected cells by Nec-1 were neurons. Neuronal survival was analyzed by calculating-NeuN positive cells with normal morphology, which indicated that Nec-1, at the doses of 12.5 μM and 25 μM, reduced neuronal death by 34%~36%. Given this data, the high dose group (25 μM) was used to test Nec-1's further effect and protective mechanism. Nec-1 at this dose showed neither protective nor toxic effects on neurons in normoxia. Unfortunately, all the *in vitro* protective effects were detected from the Nec-1 pre-treatment, while there was no significant protection when Nec-1 was added during hypoxia or after hypoxia (data not shown).

A

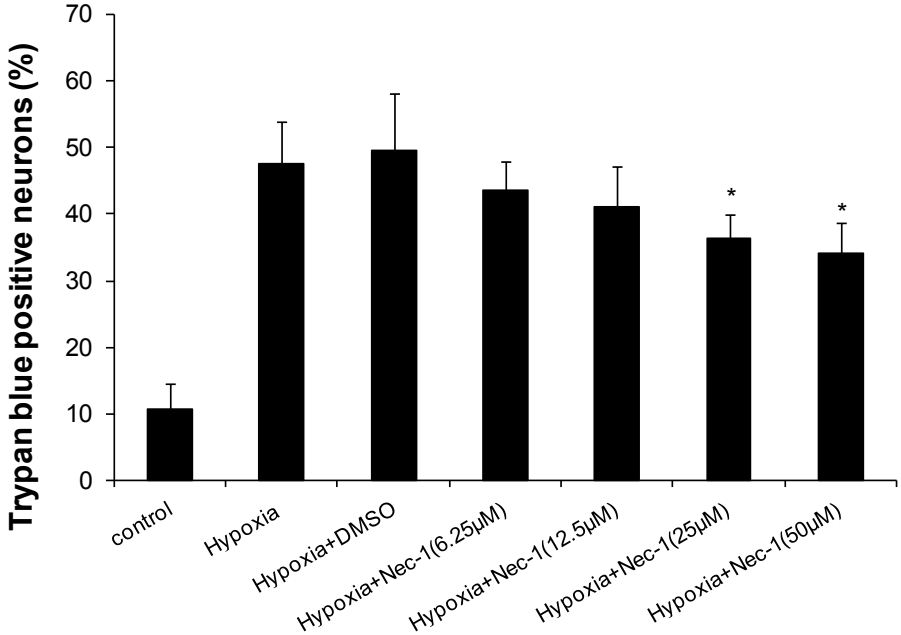
Trypan blue positive neurons (%)
70
60
50
40
30
20
10
0
*
*
control
Hypoxia
Hypoxia+DMSO
Hypoxia+Nec-1(6.25μM)
Hypoxia+Nec-1(12.5μM)
Hypoxia+Nec-1(25μM)
Hypoxia+Nec-1(50μM)

B

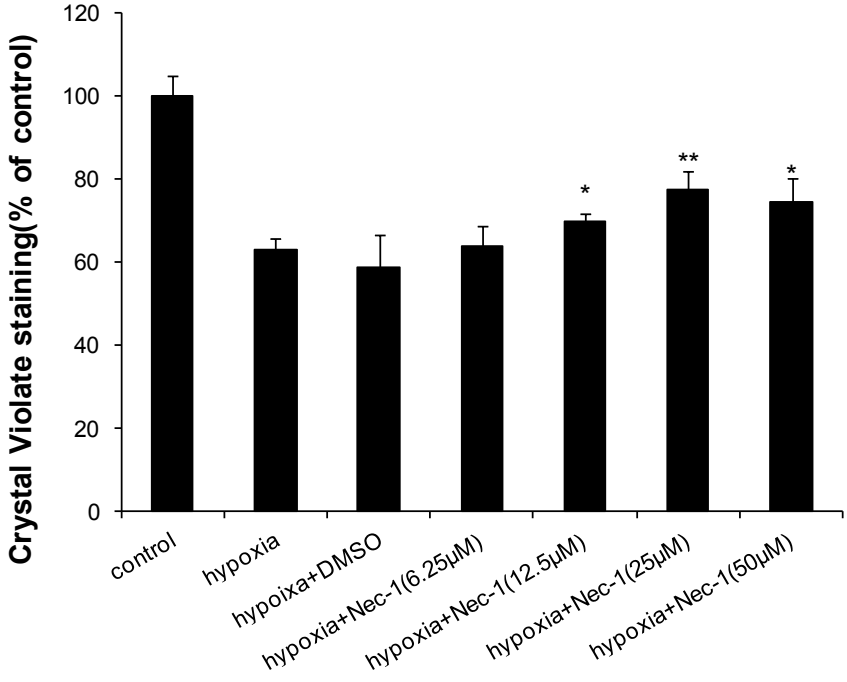
Crystal Violate staining(% of control)
120
100
80
60
40
20
0
*
**
*
control
hypoxia
hypoixa+DMSO
hypoxia+Nec-1(6.25μM)
hypoxia+Nec-1(12.5μM)
hypoxia+Nec-1(25μM)
hypoxia+Nec-1(50μM)

C

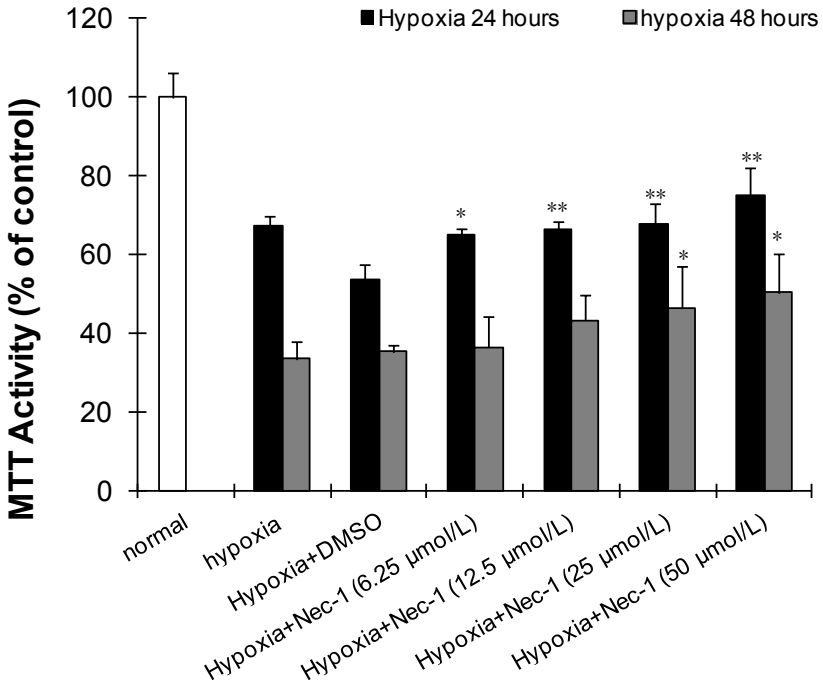
Hypoxia 24 hours
hypoxia 48 hours
MTT Activity (% of control)
120
100
80
60
40
20
0
normal
hypoxia
Hypoxia+DMSO
Hypoxia+Nec-1 (6.25 μmol/L)
Hypoxia+Nec-1 (12.5 μmol/L)
Hypoxia+Nec-1 (25 μmol/L)
Hypoxia+Nec-1 (50 μmol/L)

D

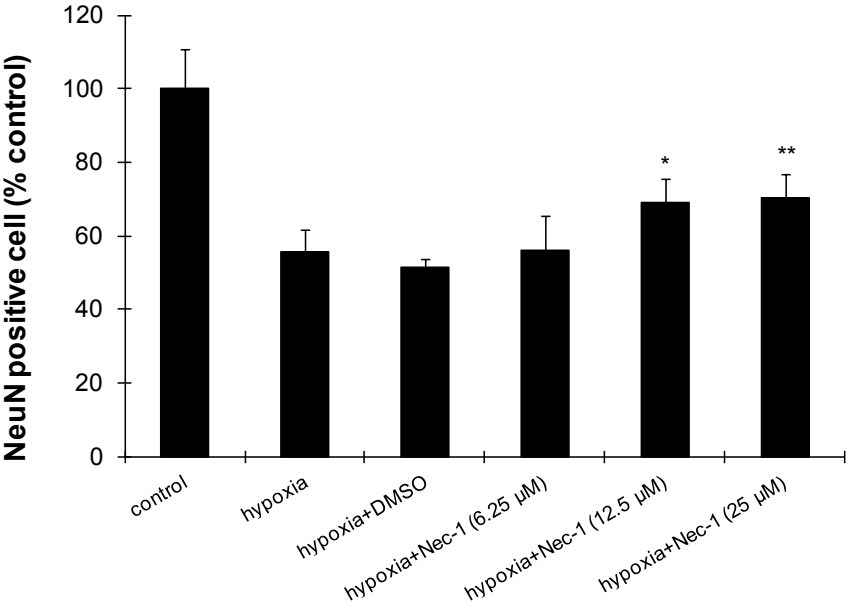
NeuN positive cell (% control)
120
100
80
60
40
20
0
control
hypoxia
hypoxia+DMSO
hypoxia+Nec-1 (6.25 μM)
hypoxia+Nec-1 (12.5 μM)
hypoxia+Nec-1 (25 μM)

Figure 5.1 Nec-1 protected against hypoxia induced neuronal death in dose dependent manner.

Primary neurons were treated with different doses of Nec-1 (0 μM, 6.25 μM, 12.5 μM, 25 μM or 50 μM) on Day 7 *in vitro*, and were exposed to hypoxia for 24 hours on Day 8. Trypan blue (A), Crystal Violet (B) and MTT assay (C) were used to measure cell death or the cell viability. With the same Nec-1 pre-treatment, neuronal viability was also evaluated by MTT assay after 48 hour hypoxia exposure (C). After Nec-1 treatment and hypoxia, neurons were immunostained with NeuN antibody. Neuronal loss was also calculated by NeuN staining with different dose of Nec-1 treatment (D). The control groups were treated with the same amount of medium or DMSO or without hypoxia. Values are mean± SE and were analyzed by one-way ANOVA. (n=6) *$p<0.05$ vs. hypoxia with DMSO, **$p<0.01$ vs hypoxia with DMSO.

Thanks to the commercial availability of the inactive form of Nec-1(Nec-1i), we tested the specificity of Nec-1on neuronal protection. Nec-1i is a cell-permeable N-demethylated thiohydantoin analog of Nec-1 devoid of anti-necroptotic properties (Degterev et al. 2005). The effect of Nec-1 and Nec-1i at the dose of 25μmol/L was compared against hypoxia, and our data confirmed that only Nec-1 has the ability to ameliorate MTT activity decrease and reduce LDH release after hypoxia, while Nec-1i served as a suitable inactive control. In the time course experiments, Nec-1 and Nec-1i (25μmol/L) were added to the neurons, which were subjected to 0, 12, 24, 36, 48 or 72 hours of hypoxia. My results indicate that Nec-1 treatment significantly protects neurons against 24 hrs, 36 hrs and 48 hrs of hypoxia, which corresponds to the time course of BNIP3 expression indicated by our previous data. However, since more than 60% of neurons died after 72 hrs of hypoxia and the standard deviation increased, Nec-1 failed to protect the neurons significantly.

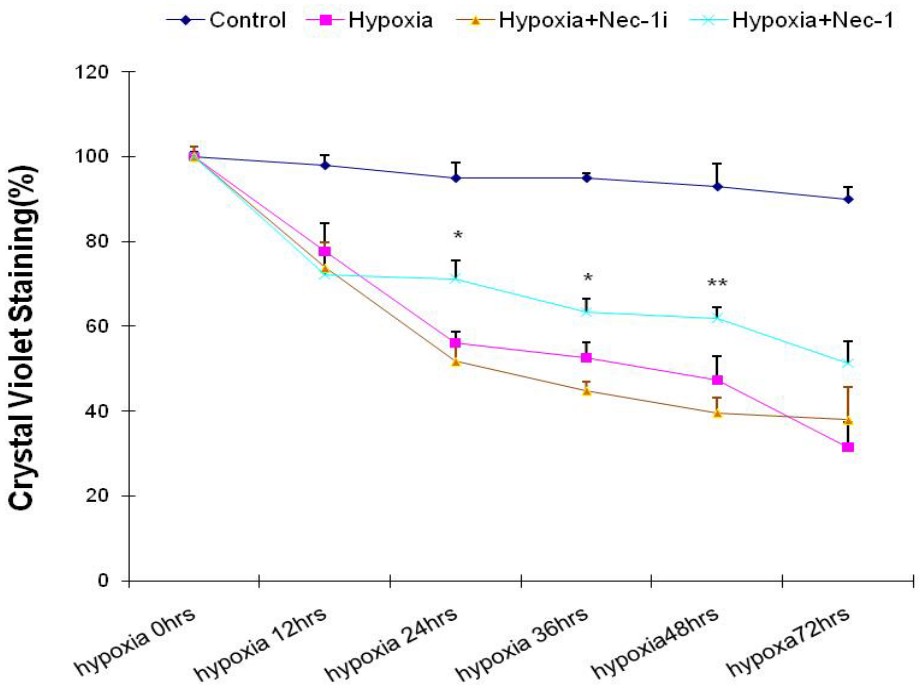

Figure 5.2 Nec-1 protected against hypoxia induced neuronal death in time dependent manner.

Neurons were treated with Nec-1 or Nec-1i (25 μM/L) on Day 7 *in vitro*, 24 hours before hypoxia (0, 12hrs, 24hrs, 36hrs, 48hrs or 72 hrs of hypoxia). Crystal violet was used to measure cell death. The control groups were treated with the same amount of medium or DMSO or without hypoxia. Values are mean± SE and were analyzed by one-way ANOVA. (n=3) *$p<0.05$ vs. hypoxia with DMSO treatment group.

Since all the reports indicated that Nec-1 only protected caspase-independent cell death, we want to test whether caspases were involved in Nec-1's protection against neuronal cell death in this prolonged hypoxia. Here, I included additional groups, adding a pan-caspase inhibitor zVAD-fmk to Nec-1, Nec-1i and hypoxia-alone groups. As shown in figure 5.3, the administration of Nec-1 reduced LDH release, while zVAD-fmk alone did not interfere with 24-hour or 48-hour hypoxia injury. Additional administration of zVAD-fmk with Nec-1 or Nec-1i failed to provide further protection of neurons. These

results suggest that zVAD-fmk offers no protection on neurons against prolonged-hypoxia-induced cell death and that caspases may not play a major role in this prolonged hypoxia model.

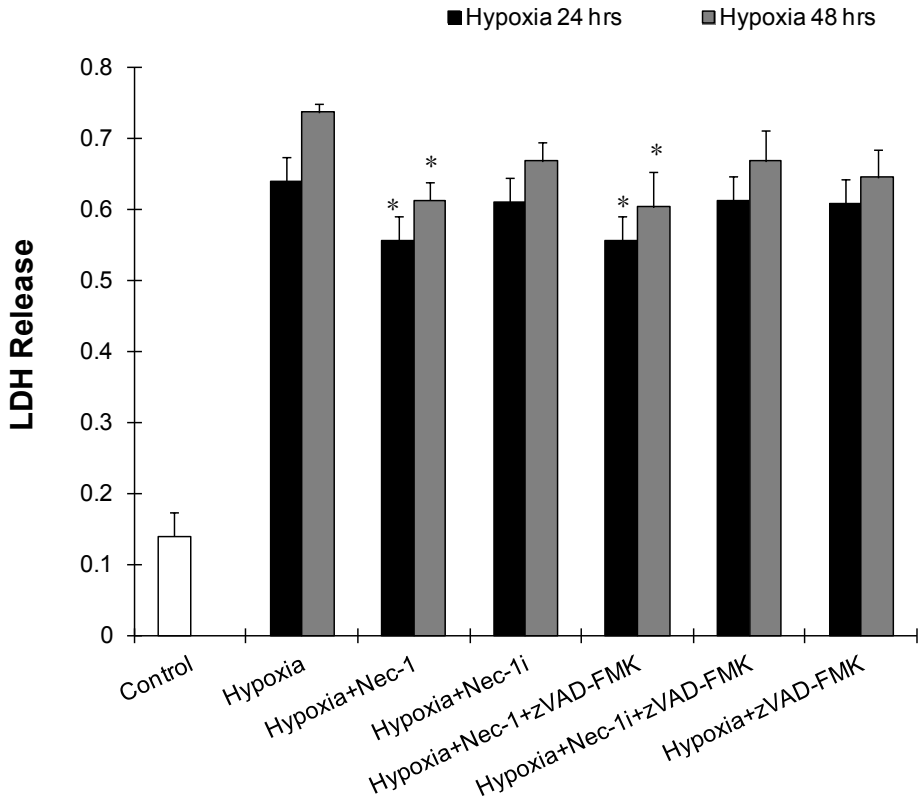

Figure 5.3 Nec-1 protected against hypoxia induced neuronal death in caspase-independent pattern.

Neurons were treated with Nec-1 or Nec-1i (25 μM), with or without caspase inhitibor zVAD-fmk on Day 7 *in vitro*, 24 hours before hypoxia (24 hours or 48 hours). LDH cytotoxicity assay was used to measure cell death. The control groups were treated with the same amount of medium or DMSO or without hypoxia. Values are mean± SE and were analyzed by one-way ANOVA. (n=4) *$p<0.05$ vs. hypoxia with DMSO, **$p<0.01$ vs hypoxia with DMSO.

To further test the protection of Nec-1 in prolonged hypoxia neuronal death, we also checked the effect of Nec-1 in another commonly used *in vitro* ischemia model, the

OGD/reoxygenation model. Through assessing MTT activity, we found that pre-treatment of Nec-1 increased MTT activity by 40% and 45% after 24 hour of hypoxia and 3 hrs OGD followed by 24 hrs reoxygenation, respectively. Similar to the effect in the hypoxia-only condition, Nec-1i did not protect neurons against OGD/reoxygenation injury.

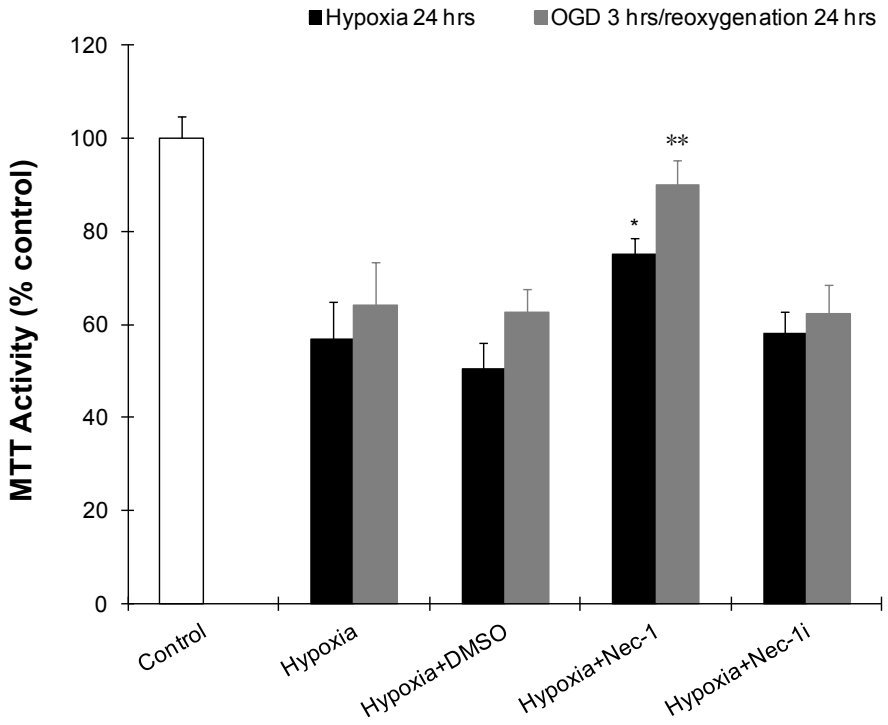

Figure 5.4 Nec-1 protected against both hypoxia and OGD/reoxygenation induced cell death.

Neurons were treated with Nec-1, Nec-1i (25 μM) or DMSO after 24 hrs hypoxia or 3 hrs OGD followed by 24 hrs reoxygenation with fresh medium. MTT assay was also used to evaluate the cell viability. The control groups were treated with the same amount of medium or DMSO or without hypoxia. Values are mean± SE and were analyzed by one-way ANOVA. (n=4) *$p<0.05$ vs. hypoxia with DMSO, **$p<0.01$ vs hypoxia with DMSO.

5.3 Nec-1 protects against hypoxia-induced mitochondrial dysfunction in neurons

It is believed that the ischemic injury *in vivo* and *in vitro* causes the release of oxygen-derived free radicals, dysregulation of intracellular calcium concentration, opening of the MPTP, loss of mitochondrial membrane potential and, finally, cell death. To clarify the mechanism of Nec-1's protective effect, neurons were incubated with H_2DCF-DA, an ROS-sensitive fluorescence indicator. After hypoxia for 24 hours, intracellular ROS increased up to 2.5-fold compared to the normoxia group. Nec-1 reduced about 5% of ROS production, which is much less than the reduced cell death by Nec-1, indicating that Nec-1 attenuates ROS production induced by oxidative toxicity resulting from hypoxia, but this may not be the only mechanism.

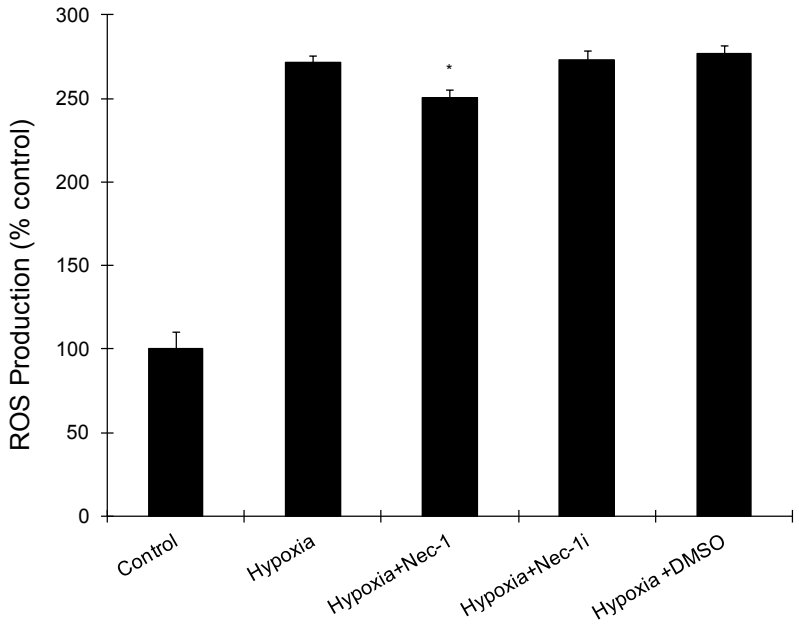

Figure 5.5 Nec-1 reduced hypoxia induced ROS production.

Neurons were treated with Nec-1, Nec-1i (25 μM/L) and same amount of DMSO on Day 7. Neurons were then exposed to hypoxia for 24 hours on Day 8. H_2DCF-DA was used to measure the ROS production. The control groups were treated with the same amount of medium or DMSO or without hypoxia. Values are mean± SE and were analyzed by one-way ANOVA. (n=6) * $p<0.05$ vs. hypoxia with DMSO.

To further explore the functional mechanism of Nec-1, we measured mitochondrial membrane potential by using JC-1. JC-1 changes its colour from green to red as membrane potential increases due to the reversible formation of JC-1 aggregates upon membrane polarization. Normally, the ratio of red to green fluorescence remains at around 4.8 in neurons, while, after 24 hrs and 48 hrs of hypoxia, it went down to around 1.5 and 0.9, respectively. Nec-1 preserved mitochondrial membrane potential by 21% and 27% against 24 hours and 48 hours of hypoxia, respectively. The control Nec-1i and DMSO did not show any effect on mitochondria function. This result indicates that Nec-1 rescuing neuron against hypoxia may partially be through attenuating mitochondrial membrane potential loss.

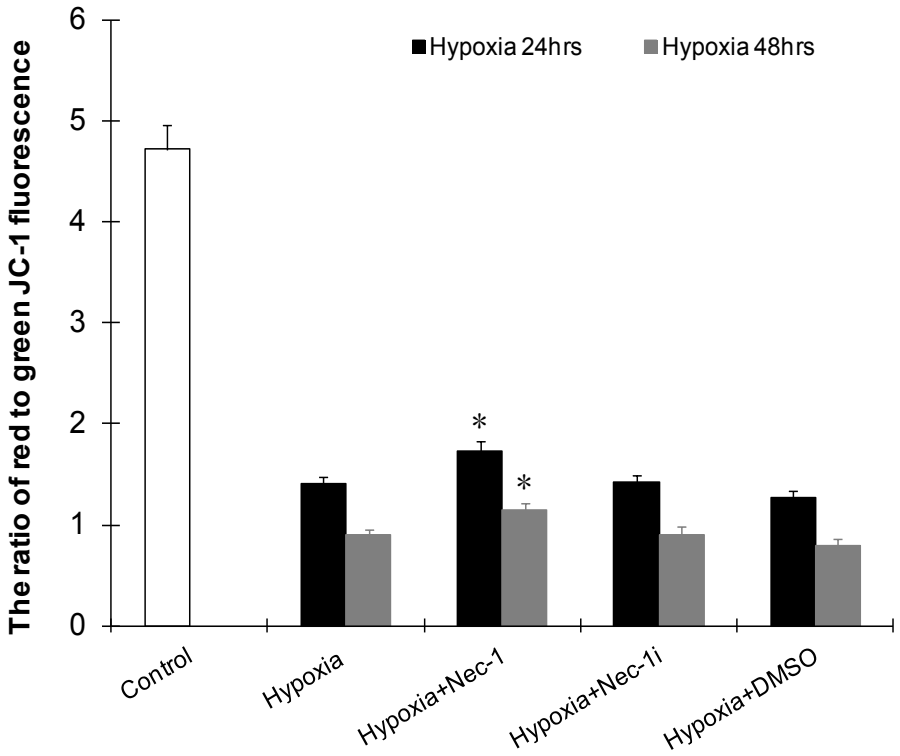

Figure 5.6 Nec-1 reserved mitochondrial function in hypoxia-challenged neuronal cells.

Neurons were treated with Nec-1, Nec-1i (25 μM/L) and same amount of DMSO on Day 7. Then neurons were exposed to hypoxia for 24 hours on Day 8. JC-1 was used to measure the mitochondrial membrane potential in neurons against hypoxia. The control groups were treated with the same amount of medium or DMSO or without hypoxia. Values are mean± SE and were analyzed by one-way ANOVA. (n=6) * $p<0.05$ vs. hypoxia with DMSO.

The MPTP, a large non-specific channel that spans mitochondrial membrane, is known to mediate the lethal permeability changes that initiate mitochondrial-driven neuronal death during ischemia. Since we found that Nec-1 was able to reduce mitochondrial membrane potential loss, we tested whether Nec-1 has an effect on MPTP opening, by measuring mitochondrial release of calcein. Our data shows that hypoxia alone caused around 77%

calcein release from mitochondria, while Nec-1 treatment (at the concentration of 25 μM) resulted in 59% calcein release. This means that Nec-1 reduced hypoxia-induced MPTP opening by 18%, and this may be responsible for the preserved mitochondrial membrane potential and reduced cell death by Nec-1.

To further validate whether or not Nec-1 inhibits MPTP opening by direct interaction, I included a MPTP inhibitor cyclosporin A (CsA). CsA was proposed to interact with cyclophilin D and inhibit ischemia-induced MPTP opening. Our results showed that CsA significantly blocked hypoxia-induced MPTP opening, while in the groups combining CsA with Nec-1, Nec-1i or DMSO, no significant difference of calcein release was found, indicating that CsA diminished Nec-1's effect on MPTP and Nec-1may compete to interact with MPTP.

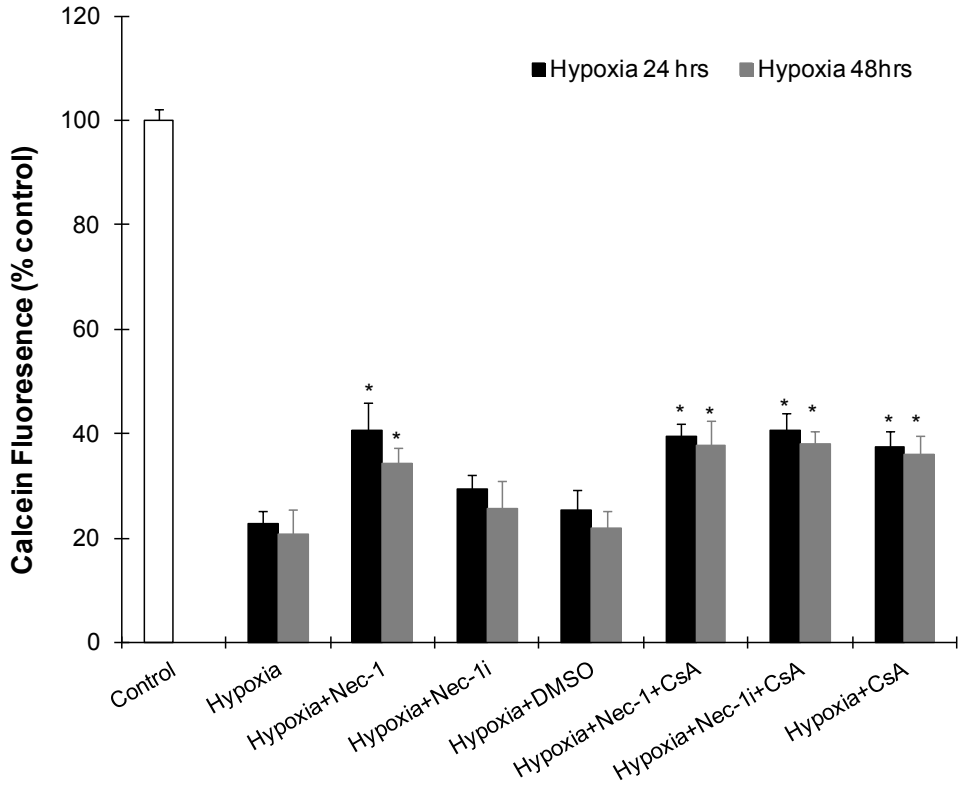

Figure 5.7 Nec-1 blocks MPTP opening in hypoxia-challenged neuronal cells.

Neurons were treated with Nec-1, Nec-1i (25 μM/L) and same amount of DMSO on Day 7, Then neurons were exposed to hypoxia for 24 or 48 hours on Day 8. Calcein-AM was used to measure the MPTP opening after hypoxia, in presence or absence of MPTP inhibitor cyclosporin A (CsA). The control groups were treated with the same amount of medium or DMSO or without hypoxia. Values are mean± SE and were analyzed by one-way ANOVA. (n=6) * $p<0.05$ vs. hypoxia with DMSO.

5.4 Nec-1 protects against MCAO-induced neuronal death

The protective effect of Nec-1 adminstration by intraventricular injection (Degterev et al. 2005) has been reported in a mouse MCAO model; this effect was further confirmed in our rat MCAO model. Thirty rats underwent MCAO; 16 of them survived. Each group consisted of four animals for further analysis. By analyzing infarct size with cresyl violet

staining, unilateral MCAO induced around 38% brain areas damage in the right hemisphere. The rats were administered with Nec-1 during or after surgery. Lesion size was significantly reduced by 77% compared to the groups treated with the vehicle or inactive analog. We chose to administer Nec-1 through the intra-peritoneal path rather than the intra-ventricular route because it is more practical and feasible for further clinical research. The ability of Nec-1 to protect neurons against ischemia/reperfusion insult indicates that Nec-1, no matter whether it is modified or not before entering the central nerve system, itself or its metabolite can pass through blood brain barrier during or after ischemia.

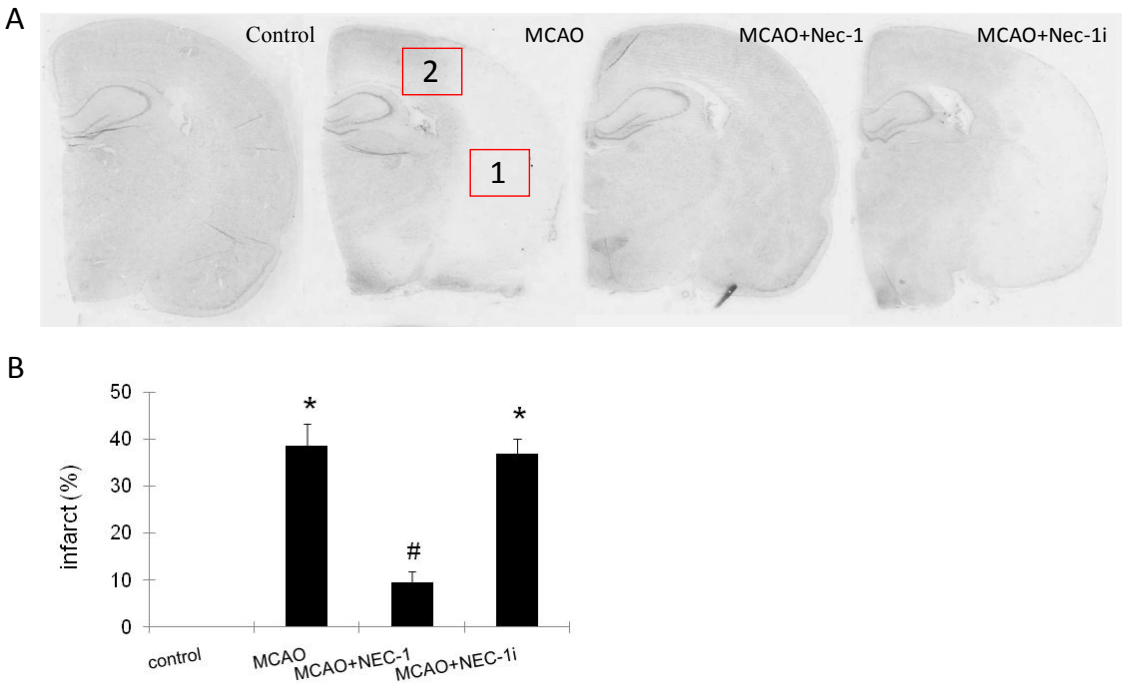

Figure 5.8 Nec-1 reduces the secondary neuronal injury in the ipsilateral cortex.

(A) Representative brain sections (bregma−3.3 mm) of different groups show the location of cerebral cortical infarction (white) and the normal region (grey) using cresyl violet staining. Administration of Nec-1 clearly ameliorates ischemia-induced neuronal damage secondary to

distal MCAO. Administration of Nec-1i does not clearly reduce ischemia size. (B) Quantification of the infarct area in Nec-1, Nec-1i, MCAO alone and control groups. Values are mean± SE and were analyzed by one-way ANOVA. (n=4) *$p<0.05$ vs. control group; # $p<0.05$ vs. MCAO group.

Focal cerebral ischemia causes most of the ischemic "core," which is characterized by the sudden reduction of cellular energy and rapid necrotic neuronal death, and ischemic "penumbra," where brain tissues are hypoperfused surrounding the core and neurons may undergo delayed neuronal death. To investigate these two types of cell death, we calculated the neuronal changes in these two areas (1 and 2) as indicated in figure 5.8. Under high magnification, cresyl violet staining identified ischemic cellular changes including cell lysis, nucleus and cytoplasm shrinkage and hyperchromia. In the core area, Nec-1 ameliorated 61% of ischemia-induced neuronal damage as described above, while Nec-1i was not able to reverse these changes against ischemia/reperfusion insult. In the penumbra area, Nec-1 rescued around 50% of neurons from damage compared to Nec-1i group. Put together, these results suggest that Nec-1 is not only able to protect the delayed neuronal death, but is also able to prevent neurons from acute death. This protection may come from its ability to inhibit the programmed necrosis. However, the specific markers are needed to indentify the phenotypes of cell death Nec-1 protected.

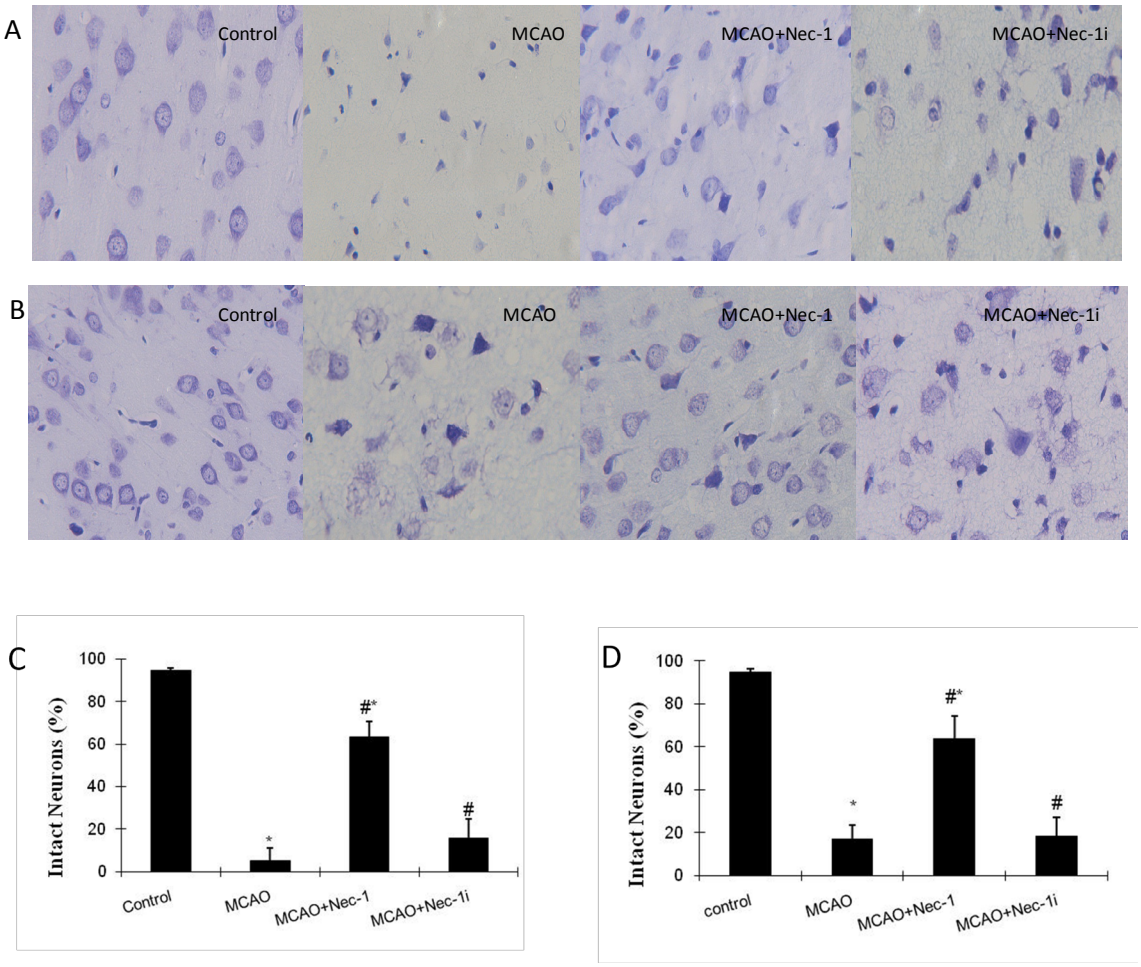

Figure 5.9 Nec-1 reduces the secondary neuronal injury in the ipsilateral cortex.

A, Representative brain sections (bregma−3.3 mm) using cresyl violet staining shows the neuronal alteration in the ipsilateral cortex at 48 hours after MCAO. Characteristic features of hyperchromia, shrinkage of nucleus and cytoplasm in neurons presents in the model group. Administration of Nec-1 clearly ameliorates ischemia-induced neuronal damage secondary to distal MCAO. Administration of Nec-1i does not noticeably impact neuronal injury. (C) and (D) Quantification of the number of neuronal cells in Nec-1, Nec-1i, MCAO alone and control groups. Scale bar: 50 μm. Values are mean± SE and were analyzed by one-way ANOVA. (n=4) *$p<0.05$ vs. control group; # $p<0.05$ vs. MCAO group.

5.5 Chapter summary

In summary, the results in this chapter demonstrated the following:

1. Nec-1 protects neurons against prolonged hypoxia in a dose- and time-dependent way.
2. Nec-1 protecting against neuronal death does not involve caspase activation.
3. Nec-1 also protects against OGD/reoxygenation induced neuronal death at the similar dose as in hypoxia model.
4. Nec-1 is able to reduce ROS production, maintain mitochondrial membrane potential and block MPTP opening.
5. By being administered through the intra-peritoneal route, Nec-1 can significantly reduce ischemia/reperfusion-induced neuronal damage *in vivo*.

Significance

Delayed neuronal death is a hallmark feature of cerebral ischemia and the primary target for neuroprotective strategies. The pro-apoptotic protein BNIP3 plays a role in the delayed neuronal death. Inhibition of BNIP3 expression would be a new strategy for rescuing neurons from delayed neuronal death and improving recovery of neurological functions in stroke. However, up to date, there is no identified BNIP3 inhibitor available. Here, we found that Nec-1, which is able to significantly protect neurons against cerebral ischemia, is a potential inhibitor of functional BNIP3.

Chapter 6. Nec-1 blocked BNIP3 integration into mitochondria and AIF release from mitochondria.

6.1 Rationale

Nec-1 is able to protect neurons against cerebral ischemia, but the exact mechanism by which this is accomplished is still unclear. Nec-1 also efficiently blocks a necrotic-like caspase-independent cell death (necroptosis) but has no effect on typical caspase-dependent apoptosis (Degterev et al. 2005). To date, receptor-associated adaptor kinase RIP1 has been identified as a potential target of Nec-1(Degterev et al. 2008); anti-inflammatory effect of Nec-1 was raised in traumatic brain injury (You et al. 2008), but this does not explain why Nec-1 only protects neurons from the caspase-independent cell death with specific features. The features of Nec-1 protecting neurons from cell death are similar to the profiles in BNIP3-mediated cell death. Recently, Nec-1 was also found to be able to block the glutamate-induced BNIP3 integration into mitochondria and AIF release from mitochondria in HT-22 cells (Xu et al. 2007). Overall, we speculate that BNIP3 may be a potential target for Nec-1, and Nec-1 may be an excellent candidate for inhibiting BNIP3 and protecting neurons from hypoxia/ischemia-induced neuronal cell death. We have also found that AIF and EndoG are two downstream mediators in BNIP3-induced neuronal death during ischemia. Therefore, we will use Nec-1 as an alternative BNIP3 inhibitor and test the AIF release in ischemia.

6.2 Nec-1 blocks the integration of BNIP3 into mitochondria *in vitro*

In the previous experiments, we found that Nec-1 protected against hypoxia-ischemia-induced neuronal death. Nec-1 was found to efficiently block a necrosis-like caspase-independent cell death, which is similar to BNIP3-mediated cell death. Therefore, I tested whether Nec-1's function is related to BNIP3. Nec-1 of different concentrations (0 μM, 6.25 μM, 12.5 μM, 25 μM, or 50 μM) were added into the neuronal culture medium before hypoxia, but we did not find changed expression of BNIP3 in neurons after 24 hours of hypoxia. Previous data in our lab have demonstrated that, after prolonged hypoxia, BNIP3 integrates into mitochondrial in a time-dependent manner. In the isolated mitochondria from neurons, dimerized BNIP3 was detected, while Nec-1treatment significantly reduced BNIP3 detection. This reduction corresponded to the increasing doses of Nec-1. The same blockage was found in prolonged hypoxia for 48 hrs.

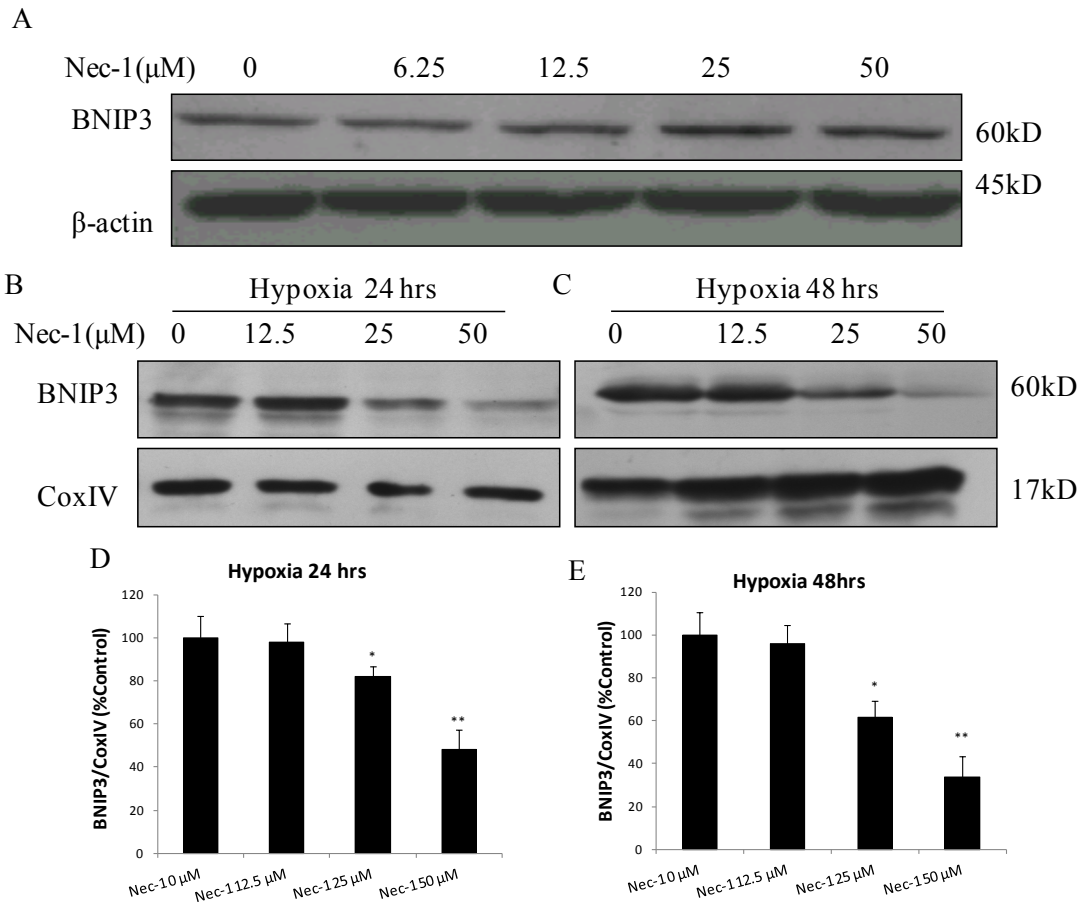

Figure 6.1 Nec-1 prevents hypoxia-induced BNIP3 translocation in neurons.

Neurons were treated with Nec-1 with different concentrations on Day 7, 24 hours before hypoxia (24 hours). (A) Western blot analysis of BNIP3 in cortical neuronal cultures exposed to hypoxia. β-actin (45kD) was included as a loading control. (B) Mitochondrial fractions were isolated, and BNIP3 was detected by Western blot analysis. CoxIV (16kD) was included as a mitochondrial protein loading control. (A) and (B) Representative Western blot of BNIP3 and CoxIV. (C) and (D) The quantitative analysis of BNIP3 and CoxIV. n=6 for each group. Values are mean± SE and were analyzed by one-way ANOVA. (n=3) *p<0.05, **<0.01 vs. control group

To further explore the connection between Nec-1 and BNIP3, mitochondria were isolated from mouse liver and incubated with Nec-1 in different doses for 1 hr. Then BNIP3 or BNIP3ΔTM was added into each group and incubated for another hour at room temperature. Proteins that loosely attached to the mitochondria were washed away by

Na_2CO_3, while mitochondria membranes and tightly attached proteins were pelleted by ultra-speed centrifugation. Western blot data showed that, similar to the effect of Nec-1 in neurons, Nec-1 blocked BNIP3 integration into isolated mitochondria and the decrease of mitochondrial BNIP3 depended on the dose of Nec-1. BNIP3 antibody could not detect bands in the BNIP3-ΔTM treatment group, probably because, without the transmembrane domain, BNIP3-ΔTM has lost the ability to integrate into mitochondria. These data confirmed that Nec-1 blocks the integration of BNIP3 into mitochondria.

Knowing that Nec-1 interrupts the interaction between BNIP3 and mitochondria, I sought to determine whether Nec-1 acts on BNIP3 or on mitochondria. Following the previous protocol, Nec-1 and Nec-1i (50 μM) were separately pre-incubated with mitochondria for 1 hr and then BNIP3 was added to each. In the other groups, Nec-1 and Nec-1i were separately incubated with BNIP3-GST protein for 1 hr and then incubated with mitochondria for another hour. Mitochondrial membranes with associated BNIP3 were collected after alkaline extraction and ultra-speed centrifugation. I found that Nec-1 failed to block the interaction between BNIP3 and mitochondria if it was incubated with BNIP3 first, while Nec-1-pretreated mitochondria had difficulty interacting with BNIP3 (shown by figure 6.2D and 6.3F). These results indicate that Nec-1 modifies mitochondria but does not directly modify BNIP3.

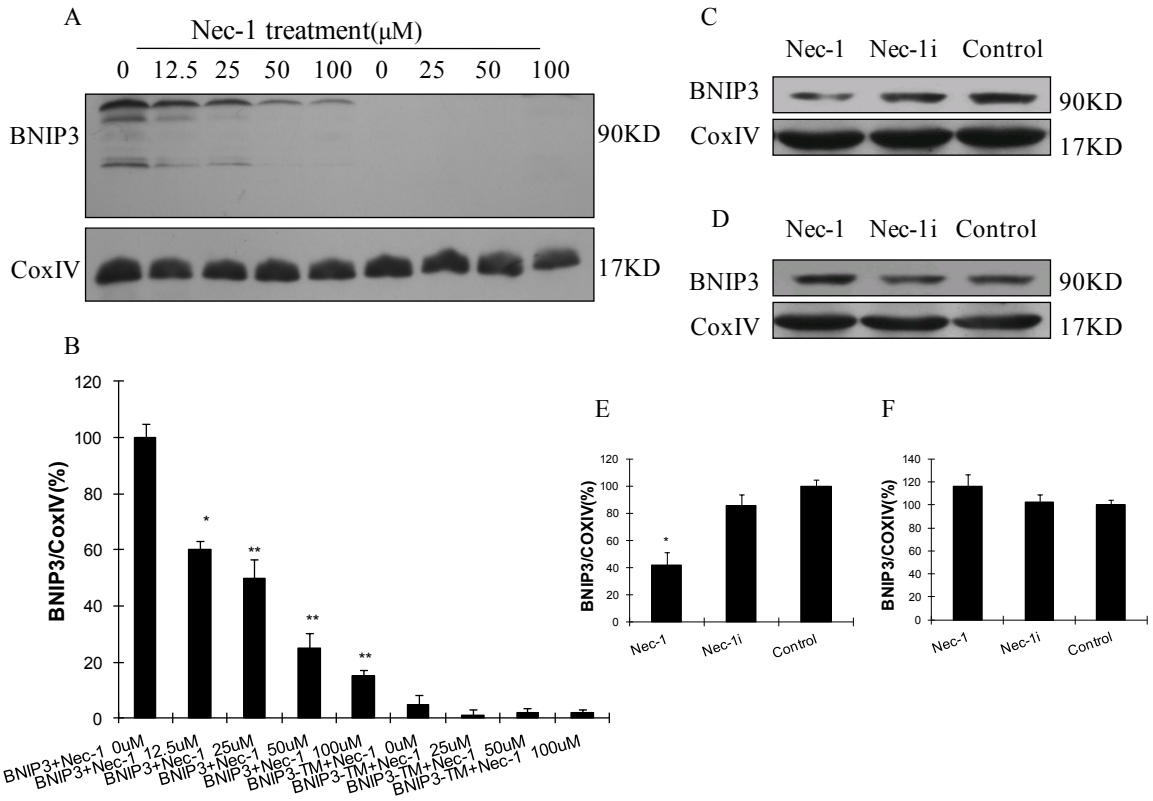

Figure 6.2 Nec-1 blocks the integration of BNIP3 into mitochondria by modifying mitochondria.

(A) and (B) Fresh mitochondria were isolated from mouse liver, purified by gradient density, and incubated with GST-BNIP3 or GST-BNIP3-ΔTM for 60 mins, after being treated with different concentrations of Nec-1(60 mins). (C) and (E) Isolated mitochondria were incubated with Nec-1, and Nec-1i pre-treatment for 60 mins, and then GST-BNIP3 was added(60 mins). (D) and (F) GST-BNIP3 was incubated with Nec-1 or Nec-1i for 60 mins, and then mitochondria was added for another 60 mins. BNIP3 were detected by Western blot analysis. CoxIV (16kD) was included as a mitochondrial protein loading control. Values are mean± SE and were analyzed by one-way ANOVA. (n=4) *p<0.05 vs. hypoxia with DMSO, **p<0.01 vs hypoxia with DMSO.

6.3 Nec-1 prevents BNIP3-induced mitochondrial dysfunction

To demonstrate that blocking BNIP3 integration into mitochondria by Nec-1 has a functional impact on cell death, mitochondrial parameters that are related to cell death were measured. In the presence of Nec-1 or Nec-1i, mitochondrial membrane potential

and MPTP were measured after isolated mitochondria were incubated with BNIP3-GST proteins. Mitochondrial membrane potential was demonstrated by JC-1. My data showed that the BNIP3 treatment alone led to up to 72% mitochondrial membrane potential loss, while Nec-1-treated mitochondria had a 12% higher ratio. The Nec-1i and DMSO groups had an equal amount of mitochondrial membrane potential loss as the H_2O group, which suggests that both Nec-1i and DMSO at the concentration tested have no effect on mitochondrial function. This result suggests that BNIP3 caused mitochondrial membrane potential loss and that Nec-1 has the ability to rescue this loss, which may be partially responsible for its cellular protection.

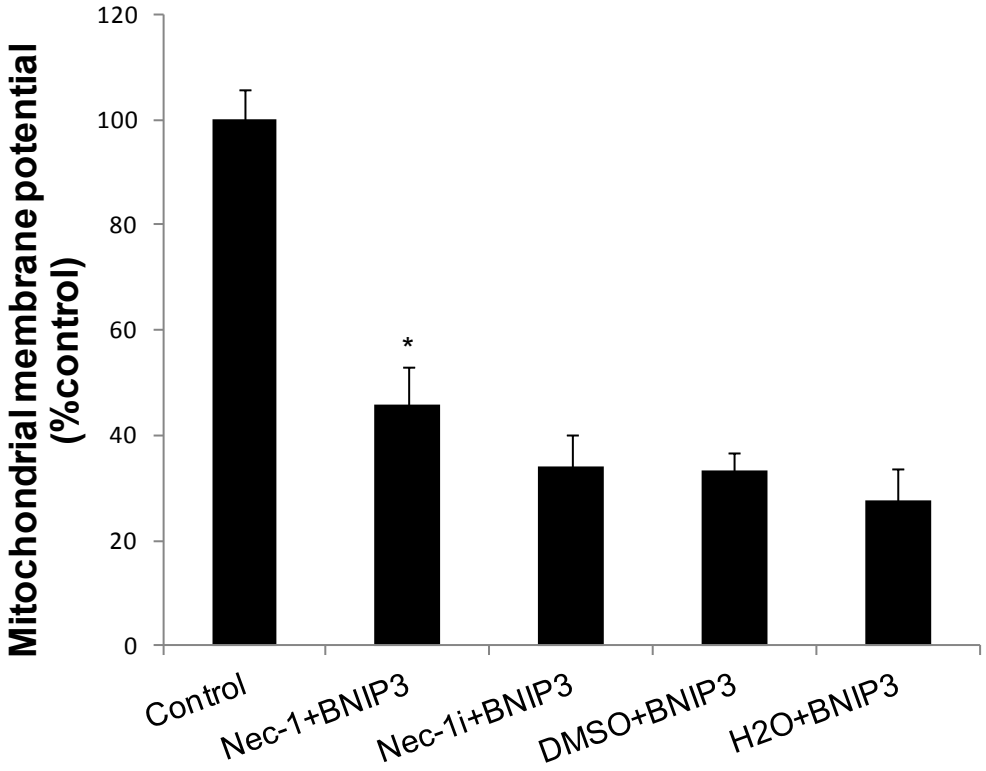

Figure 6.3 Nec-1 prevents BNIP3-induced mitochondrial membrane potential loss.

Fresh mitochondria were isolated from mouse liver and incubated with GST-BNIP3 for 60 mins, with or without Nec-1 pre-incubation (50 μM) for 60 mins. Mitochondrial membrane potential was measured by JC-1. Values are mean± SE and were analyzed by one-way ANOVA. (n=6) *p<0.05 vs. Nec-1i+BNIP3 group.

Studies showed that over-expression of BNIP3 increased the probability of MPTP opening in intact cells and isolated mitochondria (Vande et al. 2000). Studies also showed that BNIP3 induced cell death through opening of MPTP. Therefore, here we further evaluated the effect of BNIP3 and Nec-1 on MPTP opening by measuring calcein release. My data shows that BNIP3-GST proteins caused 60% of calcein release from isolated mitochondria and that the Nec-1 pre-treatment decreased around 25% of calcein release compared to the Nec-1i, DMSO or H_2O groups. Similar to the mitochondrial membrane potential results, Nec-1i and DMSO by themselves did not change MPTP opening. These data as well as the evidence from Chapter 5 suggest that BNIP3 mitochondrial integration may cause MPTP opening, which may result in mitochondrial membrane potential loss and cell death. Alternatively, Nec-1 may block BNIP3-mitochondria interaction and reduce MPTP opening, probably through interacting with a component of MPTP.

To further test the specific interaction between Nec-1 and MPTP, we included a MPTP inhibitor, CsA. We found that either CsA alone or CsA combined with Nec-1or Nec-1i caused significant decrease of calcein release in isolated mitochondria. CsA treatment slightly enhanced Nec-1's blockage on BNIP3-induced MPTP opening, but the effect is not significant. In addition, there was no significant difference among Nec-1+CsA, Nec-1i+CsA and CsA groups. These results indicate that CsA dampened Nec-1's effect on MPTP opening, and CsA and Nec-1 may block MPTP opening in the similar way. Thus,

MPTP may be one of the major modifying sites of Nec-1, and Nec-1 may also interact with cyclophin D like CsA did.

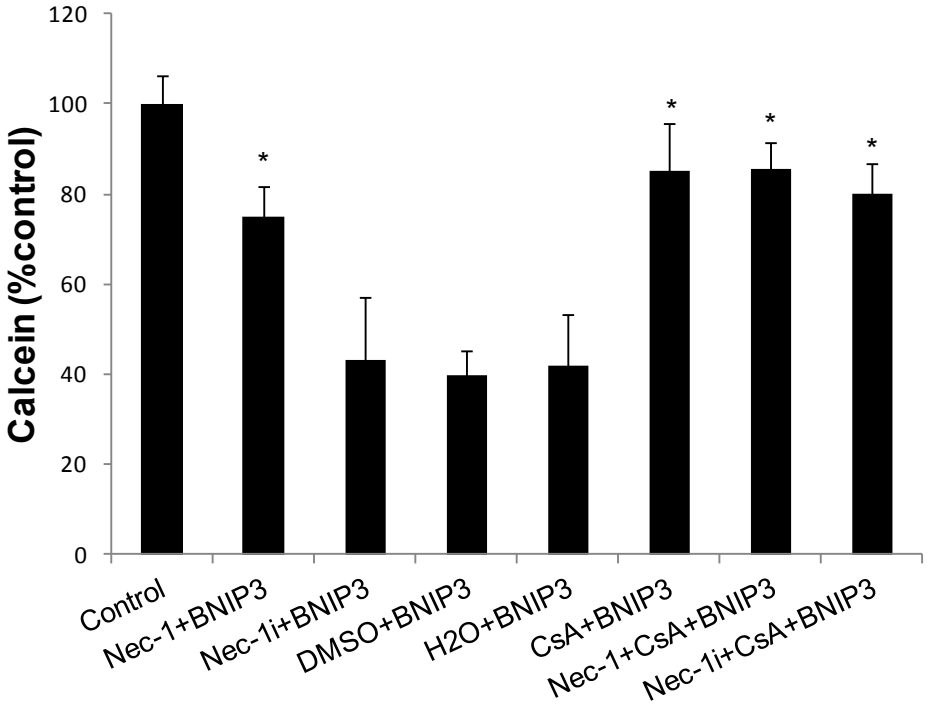

Figure 6.4 Nec-1 prevents BNIP3-induced MPTP opening.

Fresh mitochondria were isolated from mouse liver and incubated with GST-BNIP3 for 60 mins, with or without Nec-1 pre-incubation for 60 mins. Mitochondrial permeability transition pore opening was measured by Calcein-AM, and CsA was included to explore the mechanism of Nec-1's function. Values are mean± SE and were analyzed by one-way ANOVA. (n=6) *$p<0.05$ vs. Nec-1i+BNIP3 group.

6.4 Nec-1 inhibits the nuclear translocation of AIF, but not EndoG, in ischemia models *in vivo* and *in vitro*

Our previous data showed that zVAD-fmk did not protect neurons against prolonged hypoxia *in vitro,* so caspase-independent pathway plays the major role in this model.

Currently, two mitochondrial proteins, AIF and EndoG, are identified as mediating the caspase-independent cell death pathway. Thus, we tested whether AIF and EndoG are involved in Nec-1-protected neuronal death pathway. Using immunohistochemistry and Western blot, we found that hypoxia caused dramatic release of AIF from mitochondria and a corresponding increase of AIF in nuclei. Administration of Nec-1 markedly reduced the nuclear translocation of AIF-induced by hypoxia, while the control Nec-1i had no effect on its translocation. Although the translocation of EndoG was also observed in both models, Nec-1 failed to block EndoG release from mitochondria.

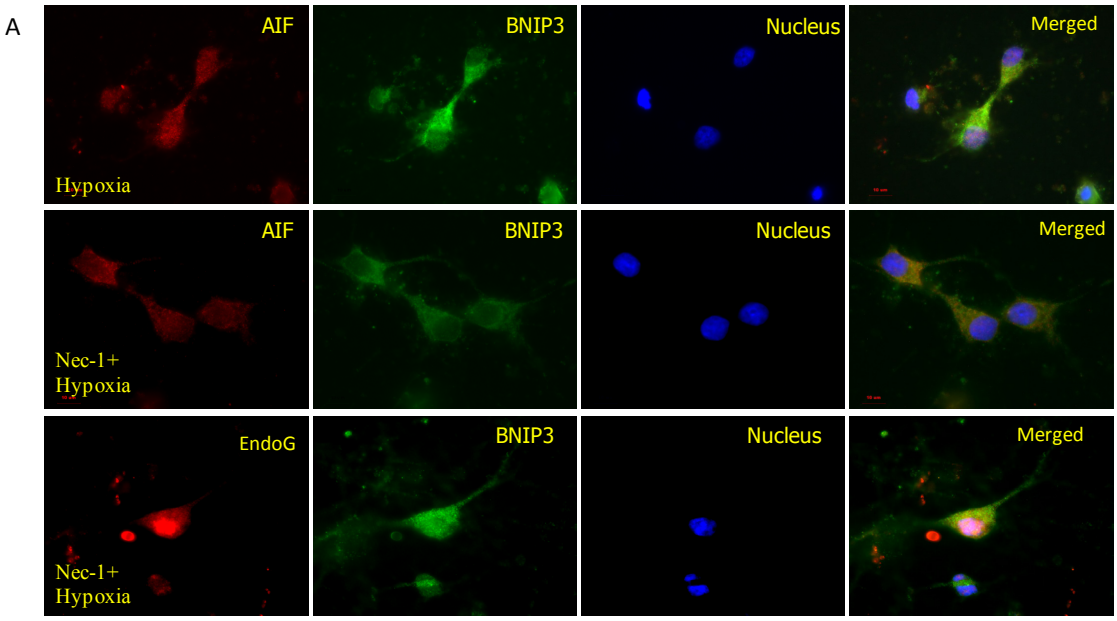

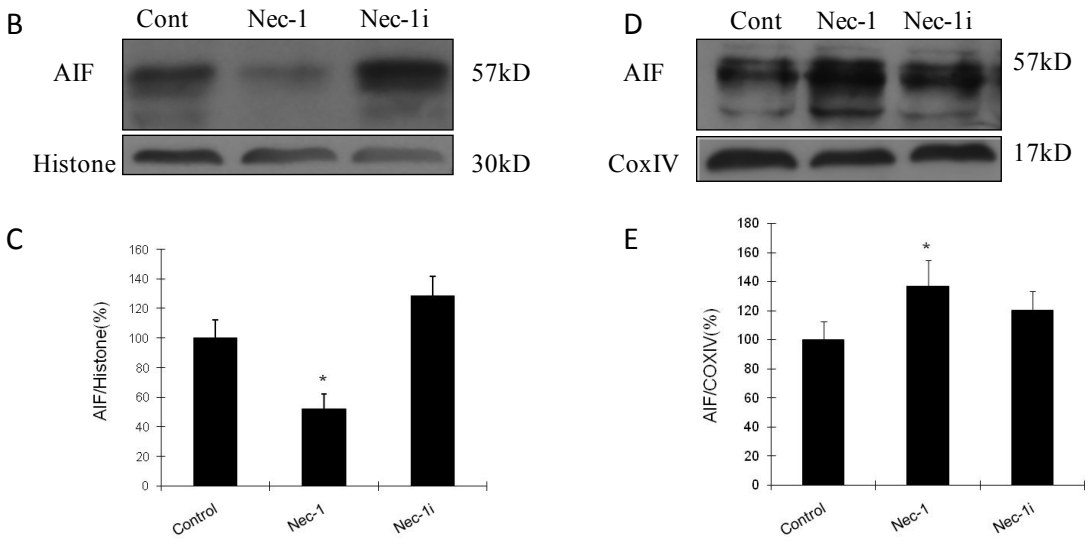

Figure 6.5 Nec-1 prevents hypoxia-induced AIF translocation in neurons.

(A) Representative immunohistochemical image of neurons treated with or without Nec-1 and then exposed to hypoxia for 24 hours. (B)-(E) Quantity analysis of expression of AIF in mitochondrial and nuclear fractions obtained from neurons treated with Nec-1 or Nec-1i before being subjected to hypoxia. CoxIV and Histone H3 were included as mitochondrial and nuclei loading controls. Values are mean± SE and were analyzed by one-way ANOVA. (n=3) *$p<0.05$ vs. Nec-1i group.

In addition to the *in vitro* data, the blockage of AIF translocation was also observed in cerebral ischemia model *in vivo*. MCAO caused AIF translocation in neurons, while Nec-1 significantly decreased AIF release from mitochondria. These results suggest that Nec-1 can specifically block AIF translocation during hypoxia *in vitro* and ischemia *in vivo*. The role of AIF in BNIP3-induced cell death was demonstrated by our previous data and by other researchers in the neuronal precursor cells. Knockdown of OGD induced BNIP3 inhibited AIF nuclear translocation and neuronal cell death, while over-expression of BNIP3 caused AIF translocation. We propose that Nec-1 may block AIF translocation through inhibiting BNIP3-mitochondria interaction.

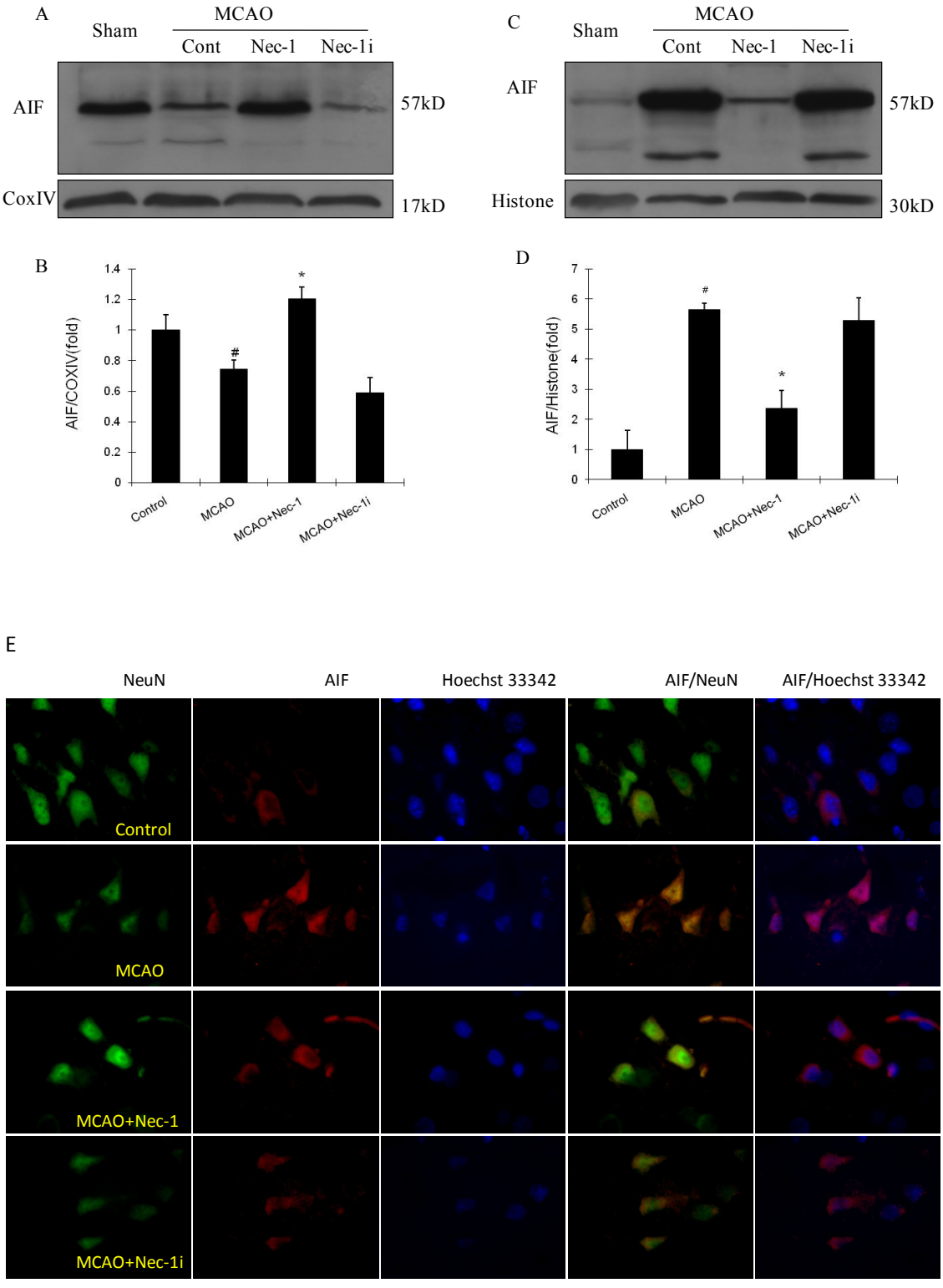

Figure 6.6 Nec-1 prevents ischemia-induced AIF translocation *in vitro* and *in vivo*.

(A) - (D) Expression of AIF in mitochondrial and nuclear fractions obtained from rats treated with Nec-1 and Nec-1i before having an MCAO operation. CoxIV and Histone H3 were included as a mitochondrial and nuclei loading control. (E), Representative images of neurons exposed to sham surgery and ischemia for 48 hours with treated with Nec-1, Nec-1i or saline control. Values are mean± SE and were analyzed by one-way ANOVA. Values are mean± SE and were analyzed by one-way ANOVA. (n=4) *$p<0.05$ vs. Nec-1i group, #$p<0.05$ vs. control group.

6.5 Chapter summary

In summary, the results in this chapter demonstrated the following:

1. Nec-1 blocks hypoxia-induced BNIP3 integration into mitochondria.
2. Nec-1 blocks BNIP3-GST integration into isolated mitochondria.
3. Nec-1 alleviates BNIP3-induced mitochondrial dysfunction.
4. Nec-1 may block BNIP3-mitochondrial interaction through MPTP.
5. Nec-1 blocks hypoxia- or ischemia-induced AIF translocation from mitochondria into nuclei *in vitro* and *in vivo*.

Significance

Previously, evidence from our laboratory showed that BNIP3 induces cell death through a caspase-independent mechanism and that members of the BNIP3 family genes are activated and AIF is translocated from mitochondria to nuclei in hypoxic and ischemic conditions. A BNIP3-activated and AIF-mediated caspase-independent cell death pathway in hypoxia-ischemia is strongly suggested. Here we found that Nec-1, a specific programmed necrosis inhibitor, is able to block the integration of BNIP3 into mitochondria and inhibit AIF translocation. The outcome of the project suggests what the

roles of BNIP3 and AIF in programmed necrosis are and that Nec-1 is a potential inhibitor targeting BNIP3.

Chapter 7. Discussion

Ischemia causes delayed neuronal death by up-regulating or activating various genes in neurons. Basic research studies in the last decade have provided rich insights into the mechanisms by which neurons die under ischemic condition, and treatments that interfere with specific events in the death-signalling pathway have been reported to produce certain neuroprotection against neuronal death. But none of them are successful for salvaging ischemic tissue and improving functional outcome. Previous results in our lab suggested that BNIP3 is a new target for neuronal rescue strategies. However, even that BNIP3 is almost completely knocked down, it provides limited protection to the neurons comparing with cell death caused by BNIP3 overexpression. The present study suggests that other member in BNIP3 subfamily, NIX, compensates for the loss of BNIP3 in ischemic neuronal death. Furthermore, for the first time, the study implies the essential role of AIF in BNIP3 and/or NIX mediated neuronal death *in vitro* and *in vivo*. To date, Nec-1 is well-accepted as an inhibitor of programmed necrosis or necroptosis. The protective effect of Nec-1 on ischemia-induced cellular damage has been reported, but the mechanism of Nec-1's protection on neurons remains elusive. Here, we showed that Nec-1 blocked BNIP3 integration into mitochondria and AIF translocation from mitochondria into the nuclei after hypoxia or ischemia in primary neurons. This blockage may be responsible for the mitochondrial dysfunction and neuronal death. Thus, BNIP3 and/or NIX define a novel pathway for ischemia-induced neuronal death.

7.1 BNIP3 and NIX expression in cerebral ischemia

Previous results in our lab suggested that BNIP3 is one of the delayed-cell-death genes. BNIP3 can only be detected 36 hours after hypoxia. In current experiments, BNIP3 was found to be increased 24 hours after OGD and dramatically upregulated until 48 hours after OGD, suggesting that BNIP3 may not be able to respond to OGD immediately. Our result is consistent with our previous report (Zhang, Yang, et al. 2007) and Althaus's report (Althaus et al. 2006), who found that BNIP3 accumulates in cells at late times after ischemia. However, these results seem not consistent with our colleague's, who found that BNIP3 was induced 2 hours after OGD (Zhao et al. 2009). One possible explanation is the difference of the OGD microenvironments. Another reason may be due to the sensitivity of different antibodies used to detect BNIP3. The expression pattern of BNIP3 itself is quite different in different cells (Kothari et al. 2003; Bruick 2000), suggesting that BNIP3-mediated cell death may be different in different cell types. In the primary cells, including neurons and myocardiocytes, BNIP3 was found upregulated late and activate an atypical programmed death pathway. Furthermore, our study has revealed that NIX expression is increased as BNIP3 upregulation in the same OGD condition. Although NIX up-regulation was reported in several cell lines and cardiomycytes following ischemic and non-ischemic injury (Yussman et al. 2002; Sowter et al. 2001), it has not been reported in neurons against OGD or cerebral ischemia, and the role of NIX in ischemic neuronal death needs to be clarified. The current researches have focused on the function of BNIP3 and NIX in cell death and suggest that they have great similarities on structure and functions, so we propose that NIX is functionally similar to BNIP3 in leading neuronal cell death in ischemia.

According to previous reports, BNIP3 is expressed at a low level in glial cells, but is not normally expressed in neurons (Zhang, Yang, et al. 2007; Burton et al. 2006). However, in some of my experiments, BNIP3 was clearly observed in the cultured neurons, even at very low levels. This observation may be due to experimental error, in the steps of culture condition control, cell lysis process or Western blot sample loading contamination, et cetera. The possibility that this BNIP3 protein is derived from glial cells or aging neurons has to be ruled out, although the number of these cells is quite small in normal neuronal culture. Walls reported a very low level of BNIP3 expression in neuronal precursor cells (Walls et al. 2009). If this is the case, these BNIP3 may pass by to the mature neurons, but it is not sufficient to cause cell death for certain reasons. Furthermore, although there is no protein level detected, Sandau and Handa detected BNIP3 mRNA in neonatal cortex, hippocampus, habenula and thalamus (Sandau and Handa 2006). This suggests that the production and degradation of BNIP3 is kept in a dynamic balance and that BNIP3 may be a mediator of cell death pathway in rat brain development. Unlike BNIP3, NIX is normally expressed in most tissues, including neurons, at a low level (Zhang and Ney 2009), but the exact role of NIX in normal neurons is still unknown. Research with NIX knockout mice suggests that maturational expression of NIX during erythropoiesis regulates erythroblast quantity and quality (Diwan, Koesters, et al. 2007). NIX-deficient reticulocytes have a significant defect of mitochondrial clearance (Diwan, Koesters, et al. 2007). With more and more evidence on the roles of NIX in autophagic cell death (Ding et al.), we suspect that NIX may also contribute to autophagy in physiological conditions in neurons and other tissues. On the other hand, we observed that BNIP3 or NIX

knockdown did not influence the normal survival of neurons before OGD *in vitro*, so the function of two proteins in normal cellular environment is limited.

7.2 The role of BNIP3 and NIX in ischemia induced neuronal death

BNIP3 and NIX share a lot of structural and functional similarities: human and murine NIX proteins have a 56% and 53% amino acid homology to human and murine BNIP3 (Chen et al. 1999); over-expression of either protein would lead to mitochondrial dysfunction and cell death (Zhang and Ney 2009); both proteins are upregulated by hypoxia/ischemia and play roles in ischemic cell death (Chinnadurai, Vijayalingam, and Gibson 2008). But most comparative research on these two proteins has only been done on certain cells, such as cancer cells (Bellot et al. 2009; Chinnadurai, Vijayalingam, and Gibson 2008) and cardiomyocytes (Dorn and Kirshenbaum 2008). In cancer cell lines, BNIP3 and NIX are upregulated by hypoxia through HIF-1α (Sowter et al. 2001), although the expression of NIX appears to be more constitutive than that of BNIP3 in several cellular contexts. In the cardiomyocytes, Dorn et al found that BNIP3 and NIX both play critical roles in responses to different cellular stress signals under distinct transcriptional control (Dorn and Kirshenbaum 2008). BNIP3 is uniquely induced in the heart by hypoxia, in contrast to other pro-apoptotic factors such as Bad, NIX, Bak and Bax. BNIP3 gene expression is initiated by a classical HIF-1 element and consensus sequences for the transcription factor nuclear factor-ƙB and an E2F-1 (Yurkova et al. 2008). NIX expression is not induced by hypoxia/ischemia in the heart, but induced by cardiac-specific overexpression of the heterotrimeric G protein (Gq), and Dom et al.'s

results suggest that NIX is a critical determinant in hypertrophic heart failure (Dorn and Kirshenbaum 2008). In addition, BNIP3 activates a caspase-independent atypical programmed death pathway with features of both apoptosis and necrosis (Webster, Graham, and Bishopric 2005), while mitochondria-NIX activates Bax/Bak and caspase-dependent apoptosis and ER-NIX activates Bax/Bak-independent MPTP-dependent necrosis (Chen et al.). The role of NIX in cardiomypathy suggests that the localization of NIX to mitochondria and ER determines whether NIX activates apoptosis or necrosis (Chen et al.; Diwan et al. 2009). Our current study demonstrates that NIX can also lead a caspase-independent cell death pathway followed by AIF translocation and DNA fragmentation. Therefore, this dual localization and roles of NIX and its regulation on cell death pathway may also be applied to neurons. Moreover, both BNIP3 and NIX have been implicated as being able to induce mitochondrial autophagy (mitophagy) as well as "mitochondrial pruning" that restrains mitochondrial proliferation in cardiomyocytes (Dorn 2010). To confirm the role of BNIP3 and NIX in neuronal death pathway, more experiments are required to identify their cellular location, interaction and regulation in neurons.

Here we explored the roles of BNIP3 and NIX in ischemia-induced neuronal death. Our data showed that ischemic stress was able to induce both BNIP3 and NIX expression in neurons, but it is still unclear whether they were upregulated by the same promoter or not. Knockdown of BNIP3 slightly increased NIX expression, suggesting that these two proteins may compete for the same promoter. According to our previous data and current reports, HIF-1 may be the one that turns on both BNIP3 and NIX in neurons. Our result

that knockdown of both BNIP3 and NIX reduces more neuronal death compared to single knockdown of each protein also supports this hypothesis. Thus, this implies that BNIP3 and NIX may share a similar upstream pathway, and knockdown of BNIP3 may switch the cell death to the NIX-initiated cell death pathway.

It is generally agreed that cell death mediated by BNIP3 and NIX is through their dimerization and mitochondrial integration (Chen et al. 1999). Therefore, we compared the BNIP3 and NIX expression on mitochondria and whole cell lysate. The expression tendencies of these two proteins in cell lysate and mitochondrial fraction are the same, but the increased level of BNIP3 and NIX in the whole cells is always more than in the mitochondrial fractions. This suggests that the increased BNIP3 or NIX may have other functions aside from mitochondria-related cell death, such as autophagy or autophagic cell death. (Zhang and Ney 2009; Tracy and Macleod 2007). However, specific markers are required to double stain with BNIP3 or NIX to determine the percentage of apoptosis, autophagical cell death and other types of cell death.

Although NIX shares many similarities with BNIP3 and even plays a similar role in the cell death pathway, according to our data, NIX seems more potent than BNIP3 in inducing cell death: (1) NIX upregulation is earlier and more than BNIP3; (2) Knockdown of NIX reduces more cell death than knockdown of BNIP3; (3) Mitochondrial dysfunction attenuation through knockdown of NIX is more significant than knockdown of BNIP3; (4) BNIP3 knockdown slightly turns on NIX expression, but NIX knockdown does not change the expression level of BNIP3. The early upregulation of NIX also suggests that NIX play roles in both acute and delayed neuronal death, while

BNIP3 mostly mediated the delayed neuronal death. In the later stage of the cell-death process, BNIP3 may assist NIX with causing cell death. We also found that knockdown of BNIP3 cannot change the expression level of other pro-apoptotic proteins such as Bax, cytochrome c, caspase-3 and cathepsin B as well as anti-apoptotic protein Bcl-2. The mechanism of how BNIP3 knockdown exclusively promotes NIX activation rather than other proteins remains unknown. Extensive research is needed to find out whether other genes are turned on by knocking down BNIP3 and its gene family.

Several researchers have reported that the C-terminal transmembrane domain is crucial in inducing mitochondrial permeability transition and cell death in isolated mitochondria (Vande et al. 2000; Kim et al. 2002) and cancer cell lines (Ray et al. 2000). My pilot experiments also confirmed that BNIP3 without transmembrane is not toxic to the HEK 293 cells. However, cellular toxicities and mitochondrial damage were observed in neurons that were transduced with BNIP3ΔTM and NIXΔTM sequence. There are several reasons that may explain this toxicity: (1) Neurons are more sensitive to the environmental stimuli than cancer cells. Although lentivirus transduction is controlled to minimize the cytotoxicity to the cells, medium environment changes may also contribute to the cell death; (2) Protein accumulation that may cause autophagic or other types cell death. Proteins degradation by neurons may be slower and less efficient than tumour cells, which may turn on the autophagy process. With excessive proteins produced, neurons might turn to the autophagic cell death. (3) The toxicity of the proteins itself causes cell death. Yasuda et.al found that BNIP3 contains a BH3 domain similar to other pro-apoptotic Bcl-2 members; BNIP3 exhibits delayed cell-death activity that is partially

relieved by deletion of the BH3 domain in a rat kidney cell line (Yasuda et al. 1998). Therefore, BNIP3ΔTM or NIX ΔTM themselves can also cause cell death, which may not be easily observed in the cell lines due to their fast and active growing. However, in a stable post-mitotic cell, the neuron, the toxic effects are observed.

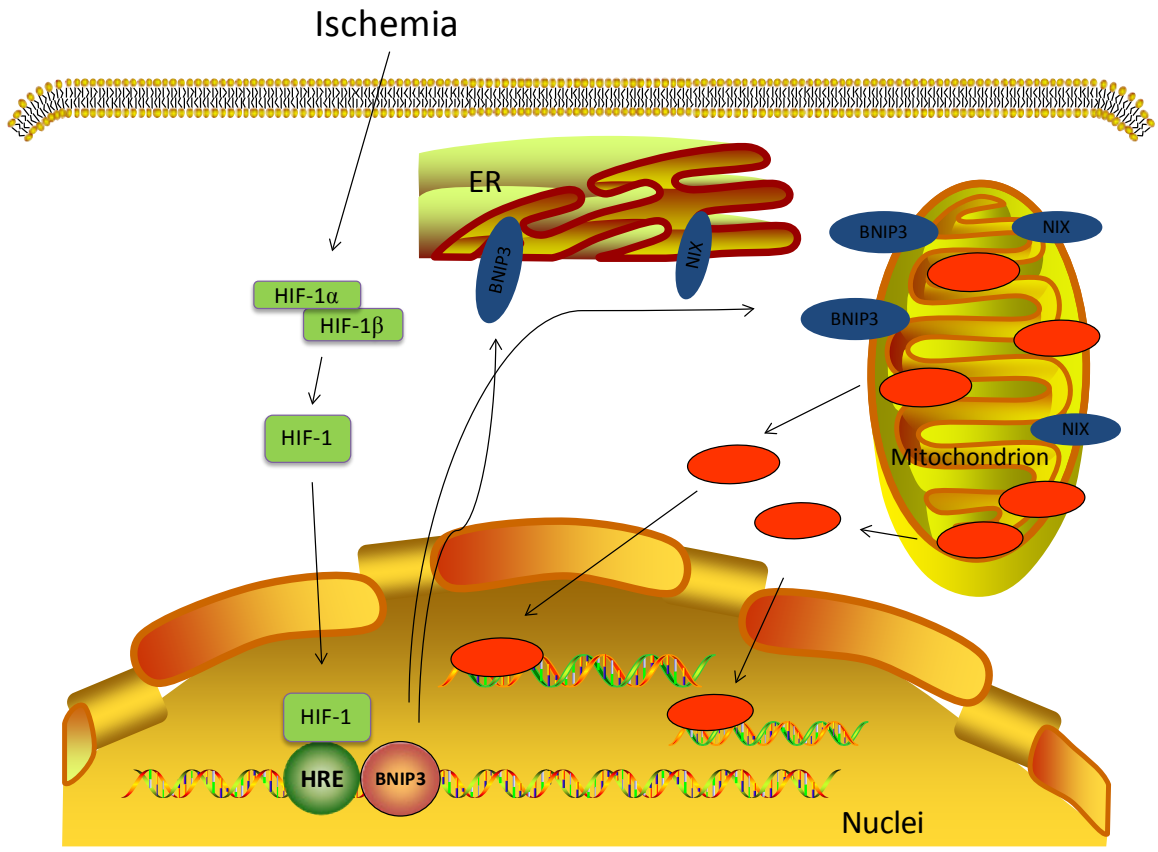

Figure 7.1 BNIP3 and/NIX mediated neuronal death during stroke.

BNIP3 is a pro-apoptotic member of the Bcl-2 family of proteins. It is not expressed in neurons except during ischemia. Under hypoxic conditions, HIF-1α becomes stabilized and binds to HIF-1β subunit to form the active HIF-1 complex. HIF-1 then translocates to the nucleus and binds to hypoxia responsive elements (HRE) to initiate BNIP3 expression. Upregulated BNIP3 becomes integrated in the outer membrane and leads to mitochondrial dysfunction. NIX is minimally expressed in cytosol in neurons in normal condition, but it integrates into the mitochondria and results in mitochondrial dysfunction during ischemia. Then, AIF and EndoG are translocated

from mitochondria into nuclei to cause DNA fragmentation and caspase-independent cell death. BNIP3 and NIX may also act on ER and cause autophagic cell death or programmed necrosis.

7.3 Caspase-independent cell death in neurons after ischemia

Although there are a lot of transcription factors identified to upregulate BNIP3 and NIX (Sowter et al. 2001; Fei et al. 2004), not a lot of researches have been done to figure out the downstream effectors of BNIP3 or NIX. Because both proteins are involved in caspase-independent death pathway, we paid more attention to the EndoG and AIF. EndoG has been linked to BNIP3-mediated ischemic cell death (Zhang, Yang, et al. 2007; Zhao et al. 2009) in neurons and cardiomyocytes (Zhang et al. 2011), so we used EndoG as a positive control to identify other downstream effectors under BNIP3 in ischemic neuronal death. Our data is consistent with previous reports (Zhao et al. 2009) that EndoG is translocated from mitochondria into the nuclei under OGD/reoxygenation injury and can be blocked by BNIP3 inhibition in cultured neurons. Significant amount of AIF translocation was found in cultured neurons after OGD injury, while cytochrome c release from mitochondria was not observed. Recent biochemical and genetic studies have revealed that AIF is an important mitochondrial protein after the ischemia-like condition *in vitro* (Cao et al. 2003) and cerebral ischemia *in vivo* (Plesnila et al. 2004; Zhu, Wang, Huang, et al. 2007). AIF emanates from mitochondria to facilitate degradation of nuclear chromatin, which results in a large-scale DNA fragmentation (Zhang et al. 2002). According to the report by Cao et.al, AIF is released from mitochondria 6 hours after OGD and reaches a very low level at 16 hours after OGD (Cao et al. 2003). However, they did not test the long-term release of AIF *in vitro*. Plesnila also found that AIF is released from mitochondria as early as 4 hours after a mild

OGD injury (Plesnila et al. 2004). Our data indicate that AIF starts to release from mitochondria within 24 hours after OGD, but due to the limited time points of the experiment, we cannot tell when and how AIF starts to release from mitochondria. Interestingly, we found that, once released from mitochondrion, AIF level in mitochondria is quite low and consistent till 72 hours after OGD. This suggests that AIF release by other protein is not dose- or time-dependent. The translocation of AIF and EndoG, but not cytochrome c, in this OGD/reoxygenation model suggests that the caspase-independent pathway plays a dominant role in determining neuronal death.

Our data, for the first time, strongly suggest that AIF is a mediator of BNIP3 and NIX-induced neuronal death in an OGD/reoxygenation condition: (1) BNIP3 and NIX upregulation, and AIF translocation were found after OGD, while the former occurred before or at the same time as the latter; (2) BNIP3, NIX and AIF have all been illustrated as playing roles in caspase-independent cell death and mediating necrotic programmed cell death (Webster, Graham, and Bishopric 2005; Chen et al.; Delavallee et al.); (3) knockdown of BNIP3 or NIX reduced AIF translocation, while BNIP3 or NIX over-expressed cells increase AIF translocation and DNA fragmentation. Besides, that double knockdown of BNIP3 and NIX did not provide additional AIF release suggests that BNIP3 and NIX may share the same interacting site with AIF. However, further research is needed to clarify how BNIP3 and NIX causes AIF release from mitochondria. Due to the similarities between AIF and EndoG, we suspect that they may share similar mechanisms.

7.4 Role of BNIP3-AIF/EndoG pathway in neuronal death

Due to the increased survival rates of infants from neonatal stroke, there is consequently an increased rate of children with developmental neurological disorders resulting from neonatal stroke. Understanding the pathogenesis of neonatal stroke is crucial to development of novel therapeutics for halting neurodegeneration after hypoxia-ischemia. Previous research in our lab has identified the primary role of BNIP3 in neonatal stroke, and AIF is also recognized as a major contributor to the neuronal loss induced by neonatal cerebral hypoxia-ischemia (Zhu, Wang, Huang, et al. 2007). Thus, we chose the neonatal stroke model for *in vivo* research to further test the role of AIF in BNIP3 mediated neuronal death. The model we used is more consistent and more cost-effective comparing with the MCAO model. Our data showed that ischemia-hypoxia injury caused an extensive damage to the neonatal brain, including cortex, hippocampus and striatum, with dramatic increase of BNIP3 upregulation, EndoG and AIF translocation. We also found that the lateral ventricle in ipsilateral brain was significantly enlarged after neonatal stroke compared with contralateral side. This change may result from the atrophy of the brain tissues caused by cell death: AIF and EndoG translocation may contribute to this brain damage, while the protection of BNIP3 knockdown may be through attenuating AIF and EnoG release. The enlarged lateral ventricle may also result from the inhibition of neurogenesis of cells originating from subventricular zone. Sandau and Handa found that BNIP3 mRNA was detected in neonatal cortices and hippocampi, and its level increases to 6.5 postnatal days (Sandau and Handa 2006). So BNIP3 may be a mediator of developmental cell death in the rat brain. BNIP3 knockout mice which have about 20% more cells in the central nerve system than WT mice also support this

explanation. AIF has been found to be involved in cell-type-specific neurogenesis; loss of AIF results in cell cycle abnormalities in a neuron-specific manner (Ishimura, Martin, and Ackerman 2008). Thus, BNIP3-AIF/EndoG-mediated caspase-independent cell death may be the key regulator in determining neuronal death or survival, as well as proliferation or differentiation.

7.5 Nec-1 attenuates hypoxia-induced caspase-independent neuronal death

Hypoxia is known to induce neuronal death during stroke in both *in vivo* and *in vitro* models. Here, our data showed that Nec-1 protects against prolonged hypoxia-induced cell death using several cell-death measurement methods. Although each method provided different numbers of cell death rate after Nec-1 treatment, most of them were between 26% and 36%. Among all these methods, we consider NeuN staining and trypan blue the most reliable ones, because they indicate the number of neurons that survived or died. Crystal violet staining is the most convenient and economical, but is also the most inaccurate. MTT assay measures the enzyme in the mitochondria, so it can also represent the function of mitochondria. LDH assay tells us about the overall cellular damage, but it cannot be directly used to represent the cell-death ratio. In spite of the sensitivity and specificity of each method, all results demonstrated that Nec-1 does protect neurons against hypoxia-caused damage.

The neuronal protection of Nec-1 was much greater in the *in vivo* model than the *in vitro* one, which is opposite to the effect of most drugs. This difference of the *in vivo* versus *in vitro* results may be because Nec-1 needs to be modified in an *in vivo* environment to

reach the maximal protection. This modification may come from the extracellular space, such as glial cells, or from the neurons but with environmental influence. In a different *in vitro* model (OGD/reoxygenation), the protective effect of Nec-1 is stronger than hypoxia, suggesting that OGD/reoxygenation is closer to the *in vivo* ischemia model. In addition, reoxygenation, which mimics the "reperfusion injury," results in a burst of ROS production (Chan 2004) and mitochondrial permeability transition (Crompton 1999), and these two factors are considered to be two triggers that induce programmed necrosis (Zhang et al. 2009; Baines 2011). This also explains why the programmed necrosis inhibitor, Nec-1, reduced more cellular damage in OGD model than it in prolonged hypoxia model. In the future, it would be interesting to explore the effects and the mechanisms of Nec-1 under OGD/reoxygenation condition in neurons.

Compared to Nec-1, Nec-1i did not show protection on neurons after hypoxia. In all cell-death and viability assays, it was found that the dissolvent DMSO has a certain toxic effect, although I tried to use the lowest concentration possible. This result is not consistent with Xu's report that DMSO has no toxic effect on glutamate-induced HT22 cell death (Xu et al. 2007). This inconsistency may partially be due to the sensitivity of neurons, since the same concentration of DMSO also has no effect on cell lines such as HEK 293 or CHO cells in this study. In test of the protection of Nec-1 on cardiomyocytes, Christopher found that Nec-1i can also reduce infarct size in an isolated and perfused heart, and both Nec-1 and Nec-1i fail to influence MPTP opening (Smith et al. 2007), suggesting that the protective mechanism of Nec-1 on cardiomyocytes may be different from neurons.

7.6 Nec-1 protects against caspase-independent neuronal death after ischemia

Most of the reports about Nec-1 mentioned that Nec-1 only protects necroptosis or programmed necrosis. If this is the case in all the cells and if Nec-1 protects all the neurons from necroptosis, these neurons, around 30% *in vitro* and around 60% *in vivo*, are going to die in this atypical way (necroptosis), in hypoxia or ischemia. The contribution of necroptosis to ischemic neuronal death was confirmed by Degterev (Degterev et al. 2005) *in vivo* and by Chen (Chen et al. 2011) *in vitro*, who incubated cultured neurons with OGD in the presence of a caspase inhibitor. This novel form of cell death is also implicated in neuronal damage in retinal ischemia-reperfusion injury model in rats (Rosenbaum et al.). In spite of different models or cell death stimuli, in all the reports about necroptosis, none of them is involved with the caspase family. In our ischemia model, I found that zVAD-fmk failed to rescue neurons from the prolonged hypoxia and was unable to provide further protection against hypoxia compared to Nec-1, suggesting that the caspase-independent cell-death pathway plays the major role in hypoxia-induced delayed neuronal death. This result also confirms that Nec-1 only protects against caspase-independent cell death in neurons. However, the question of how to define necroptosis in neurons arises. The current description of necroptosis is that it is a form of programmed cell death with the features of necrosis and that can be specifically inhibited by necrostatins (Christofferson and Yuan 2010). However, technically, there are no specific and well-defined morphological changes or markers available to distinguish necroptosis from other types of cell death.

7.7 Nec-1 blocks BNIP3 from integration into mitochondria

After Nec-1 was identified as a specific and potent inhibitor of necroptosis, a unique signalling pathway that requires the involvement of RIP1 and RIP3 was established to decide whether or not cells are dying by necroptosis (Galluzzi and Kroemer 2008). It has been demonstrated that a molecular switch to necrotic cell death facilitates the necrotic complex formation between RIP1 and RIP3 and following mutual phosphorylation within the complex (Cho et al. 2010). Furthermore, Cho et.al recently reported that, besides RIP1, Nec-1 also targets other factors crucial for necrosis induction in L929 cells (Cho et al. 2011). Thus, it still remains elusive whether necrosis is unmasked when essential effectors of apoptosis are impaired or whether or not necrosis is manifested by newly synthesized proteins and subsequent induction of protein-protein complex formation. We found that Nec-1 reduces the activity of BNIP3, and BNIP3-mediated cell death is necrotic-like, thus, we hypothesis that BNIP3 is one of the key regulator in necroptosis.

Previously, our lab has reported that BNIP3 mediates the delayed neuronal death process without cytochrome c release and caspase activation (Zhang, Yang, et al. 2007). In this study, I found that Nec-1 reduces BNIP3 integration into mitochondria in a dose-dependent manner without caspases involvement. This result is consistent with previous reports that Nec-1 only protects neurons from caspase-independent cell death (Degterev et al. 2005) and also explains why caspase inhibiters cannot reduce hypoxia-induced neuronal death. Our results are also support by Xu, who found that Nec-1 prevents glutamate-induced BNIP3 activation in HT-22 cells (Xu et al. 2007). However, in our *in vitro* model, Nec-1 reduced more than 60% of BNIP3 mitochondrial integration, while

Nec-1 only protected around 30% of cells from hypoxia. There are several reasons that may account for this difference: (1) BNIP3 is one of pro-apoptotic proteins that are involved in neuronal death. Once the function of BNIP3 is blocked, other proteins, like NIX, may be turned on and lead to cell death. (2) Although Nec-1 blocked the integration of BNIP3 into mitochondria, the interaction between BNIP3 and ER or other cellular organelle may not be influenced. BNIP3-induced autophagic cell death may take over the mitochondria-mediated cell death. (3) Other mechanisms that have been reported may function as parallel pathways that cause cell death, such as RIP1 (Degterev et al. 2008) and anti-inflammation effect (You et al. 2008). Since Nec-1 affects both BNIP3 and RIP1, we suspect that RIP1/RIP3 may act as an upstream protein of BNIP3. But more research is needed to investigate whether or not there is any connection between BNIP3 and RIP1/RIP3. Moreover, another BH3-only Bcl-2 family member Bmf is required for necroptosis-induced by either zVAD-fmk or TNF-α (Hitomi et al. 2008), so it would be interesting to find out whether Bmf plays the similar role in ischemic neuronal death and whether BNIP3 acts in a similar way as Bmf in necroptosis.

7.8 Nec-1 blocks AIF translocation after hypoxia or ischemia

Another protein that is corroborated by the discovery of the existence of necroptotic forms of cell death is mitochondrial protein AIF (Delavallee et al.). In mouse embryonic fibroblast cell line, MNNG-induced DNA damage leads to PARP-1 to calpain activation. Calpain in turn activates Bax, which facilitates the release of AIF from the mitochondrial intermembrane space to the cytosol. The activated calpain also regulates AIF release by cleaving the membrane-anchored AIF to the soluble form tAIF. Once liberated in the

cytosol, tAIF translocates to the nucleus, where it generates 3'-OH DNA breaks and stage I of chromatin condensation (Moubarak et al. 2007). Although alkylating-DNA-damage-induced programmed necrosis in neurons has not been reported yet, the role of AIF is well-documented in ischemia-induced cell death in neurons (Zhu, Wang, Huang, et al. 2007; Zhao et al. 2004). Based on our findings that Nec-1 can reduce AIF translocation in hypoxia- and ischemia-induced neuronal death *in vitro* and *in vivo*, we believe that AIF is also involved in the ischemia-induced programmed necrosis in neurons. Here, we also found that AIF may act as a downstream protein in BNIP3-mediated cell death. Together, our data suggest that BNIP3- and AIF-mediated neuronal death is a form of programmed necrosis after ischemia. Xu et.al found that Nec-1 reduced PARP activity in glutamate-induced necroptosis in HT-22 cells (Xu, Chua, et al. 2010), so the effect of Nec-1 on ischemic neuronal death may also involve PARP-1, a protein that has been implicated in AIF-mediated programmed necrosis. Nevertheless, further research is needed to identify ischemia-induced programmed necrosis in neurons, and the detailed roles these proteins in this specific cell death.

7.9 Nec-1 attenuates ischemia induced mitochondrial dysfunction

Necroptosis that Nec-1 works on specifically is linked to mitochondrial dysfunction (Cho et al. 2010), which is also found in hypoxia- or ischemia-induced neuronal death. Nec-1 is able to block hypoxia-induced BNIP3 and BNIP3-GST protein integration into mitochondria, and attenuates hypoxia and forced BNIP3 overexpression induced mitochondrial dysfunction, suggesting that mitochondria are the major target for Nec-1.

ROS potentially leads to cell death by directly oxidizing or triggering various downstream pathways (Morgan, Kim, and Liu 2007). Zhang et.al reported that the accumulation of mitochondrial ROS is RIP3-dependent programmed necrosis (Zhang et al. 2009). In our *in vitro* neuronal cell culture, Nec-1 reduced ROS production induced by hypoxia, which is consistent with Zhang's findings. However, the reduction of ROS production in neurons by Nec-1 is only around 5%, which is much weaker than its reduction in HT-22 cells in response to glutamate (Xu et al. 2007). Reduction of ROS production is much lower than the neuronal protection Nec-1 offers, which indicates that Nec-1's protective mechanism is not solely mediated by a reduction in ROS and that RIP1/RIP3 may not be the only target in Nec-1-protected neurons.

Mitochondrial membrane potential reflects performance of the electron transport chain. The change of mitochondrial membrane potential can indicate mitochondrial functions and a pathological disorder of this system (Iijima 2006). Mitochondrial membrane potential decreases during hypoxia or OGD, causes release of apoptogenic factors and loss of oxidative phosphorylation, and, subsequently, cell death (Ly, Grubb, and Lawen 2003). Thus, dissipation of mitochondrial membrane potential seems to be a consequence of severe energy deficiency, which leads to necrosis (Iijima et al. 2006). Chan et.al showed that programmed necrosis initiated by interaction between RIP1 and RIP3 are mediated through mitochondria (Cho et al. 2010). In my study, mitochondrial membrane potential was dramatically decreased after hypoxia but significantly retained by Nec-1. Therefore, Nec-1 has the ability to maintain mitochondrial physiological properties and, ultimately, rescue dying neurons. However, the expression level of RIP1 was quite low

and its expression change is minimal in neurons, we believe that blocking BNIP3 integration into mitochondria is the major reason why Nec-1 can reduce mitochondrial membrane potential loss. Our *in vitro* data that Nec-1 can reduce mitochondrial membrane potential loss in isolated mitochondria also confirms our hypothesis. Although Nec-1 can rescue mitochondrial function, reduction of mitochondria membrane potential loss is close to the percent of cell rescued. This indicates that mitochondrial function preservation is the major reason for these survival cells. Our data is consistent with Hsu', who found that Nec-1 counteracted the reduction in mitochondrial membrane potential in cadmium-induced necrotic model in Chinese hamster ovary (CHO) cells (Hsu et al. 2009). In summary, the effect of Nec-1on both ROS and mitochondrial membrane potential suggests that mitochondria are major Nec-1 acting sites.

Since the mechanism of how Nec-1 works on BNIP3 function is still unknown, we suspect that Nec-1 may modify the BNIP3 binding site on mitochondria. The failure of Nec-1 to impact BNIP3 integration while pre-incubating Nec-1 with isolated mitochondria suggests that the site is located on mitochondria, but not on the BNIP3 protein. We also found that Nec-1 can block MPTP opening caused by hypoxia or BNIP3, suggesting that Nec-1 interacts with MPTP and changes the opening of the pore. Our result is supported by Smith's report that, at the concentration of 100μM, Nec-1 delays the time it takes for MPTP to open by 91% (Smith et al. 2007). Furthermore, we found that the amount of MPTP opening reduction is similar to using the MPTP inhibitor cyclosporin A (CsA); combining Nec-1 and CsA failed to further decrease MPTP opening. CsA inhibits MPTP by targeting cyclophilin D, the intermembrane component

of MPTP (Halestrap et al. 1997). Therefore, Nec-1 may also act with CypD , like on CsA. This conclusion is consistent with Galluzzi and Kroemer's, who found that BNIP3 and CypD-dependent mitochondrial membrane potential represents the decision step of the regulated necrosis in shigella-infected nonmyeloid cells (Galluzzi and Kroemer 2009). Vanlangenakker proposed that RIP1 directly or indirectly targets the mitochondria and reduces the interaction between ANT and CypD, resulting in ATP depletion and induction of necrosis (Vandenabeele, Vanden Berghe, and Festjens 2006). If both of interactions are confirmed in neurons, Nec-1 may act on a different pathway from RIP1 in the upstream, but join in a common downstream pathway upon mitochondria to induce cell death. Thus, further study needs to focus on how Nec-1 acts on MPTP and whether or not blocking BNIP3 integration has something to do with RIP1/RIP3.

7.10 Nec-1 blocked AIF translocation, but not EndoG after hypoxia/ischemia in neurons

In our study, we have identified AIF and EndoG as downstream proteins of BNIP3. Here, we show that Nec-1 can reduce AIF translocation but has no effect on EndoG release. This difference indicates that AIF and EndoG release from mitochondria through different mechanisms, or that mitochondrial BNIP3 has more impact on AIF release than on EndoG release. That BNIP3 knockdown reduced more AIF translocation compared to EndoG in neonatal stroke supports that hypothesis: BNIP3 is the major regulator of AIF release and that EndoG may be influenced more by other factors. Another possibility is that Nec-1, besides acting on mitochondria, has direct or indirect interaction with AIF, causing significant AIF release. Although evidence suggests that AIF and EndoG

translocate in the same cell and that they may interact with each other in the nuclei, more research is needed to identify how AIF and EndoG selectively release from mitochondria.

7.11 Conclusion and future directions

In summary, the present study demonstrates that the BNIP3 death-gene family is one of the regulators of caspase-independent neuronal death in ischemic stroke. We showed that ischemia causes significant upregulation of the BNIP3 subfamily (BNIP3 and NIX), which integrates into mitochondria, releases AIF and EndoG from mitochondria with concomitant mitochondrial dysfunction, and finally causes cell death. This newly identified caspase-independent pathway will provide insights into mechanisms of delayed neuronal death and can be a new target to rescue neurons from ischemia. Nec-1 has proven to offer protection to neurons after ischemia and is recognized as a specific inhibitor of programmed necrosis. Our data suggested that Nec-1 is also an inhibitor of BNIP3. This small molecule will provide us with a useful tool to identify more a detailed pathway in programmed necrosis and new strategies for neuroprotection that can be potentially translocated to bedside care of stroke patients.

Despite the recent discovery of proteins in the caspase-independent cell-death pathway, there are a lot questions that still need to be answered. Future direction of research may include identifying upstream factors of BNIP3 or NIX, exposing the mechanism of how the BNIP3 family induces AIF and/or EndoG release, as well as discovering new therapeutic methods targeting the BNIP3 and NIX pathways.

References

Abe, K., M. Aoki, J. Kawagoe, T. Yoshida, A. Hattori, K. Kogure, and Y. Itoyama. 1995. Ischemic delayed neuronal death. A mitochondrial hypothesis. *Stroke* 26 (8):1478-1489.

Abe, T., N. Takagi, M. Nakano, and S. Takeo. 2004. The effects of monobromobimane on neuronal cell death in the hippocampus after transient global cerebral ischemia in rats. *Neurosci Lett* 357 (3):227-31.

Adachi, M., O. Sohma, S. Tsuneishi, S. Takada, and H. Nakamura. 2001. Combination effect of systemic hypothermia and caspase inhibitor administration against hypoxic-ischemic brain damage in neonatal rats. *Pediatr.Res.* 50 (5):590-595.

Alkayed, N. J., S. Goto, N. Sugo, H. D. Joh, J. Klaus, B. J. Crain, O. Bernard, R. J. Traystman, and P. D. Hurn. 2001. Estrogen and Bcl-2: gene induction and effect of transgene in experimental stroke. *J Neurosci* 21 (19):7543-50.

Althaus, J., M. Bernaudin, E. Petit, J. Toutain, O. Touzani, and A. Rami. 2006. Expression of the gene encoding the pro-apoptotic BNIP3 protein and stimulation of hypoxia-inducible factor-1alpha (HIF-1alpha) protein following focal cerebral ischemia in rats. *Neurochem.Int.* 48 (8):687-695.

An, S. J., T. C. Kang, S. K. Park, I. K. Hwang, S. S. Cho, M. H. Chung, and M. H. Won. 2002. Oxidative DNA damage and alteration of glutamate transporter expressions in the hippocampal Ca1 area immediately after ischemic insult. *Mol.Cells* 13 (3):476-480.

Antonawich, F. J. 1999. Translocation of cytochrome c following transient global ischemia in the gerbil. *Neurosci.Lett.* 274 (2):123-126.

Antonsson, B., S. Montessuit, S. Lauper, R. Eskes, and J. C. Martinou. 2000. Bax oligomerization is required for channel-forming activity in liposomes and to trigger cytochrome c release from mitochondria. *Biochem J* 345 Pt 2:271-8.

Arai, H., J. V. Passonneau, and W. D. Lust. 1986. Energy metabolism in delayed neuronal death of CA1 neurons of the hippocampus following transient ischemia in the gerbil. *Metab Brain Dis.* 1 (4):263-278.

Ardehali, M. R., and G. Rondouin. 2003. Microsurgical intraluminal middle cerebral artery occlusion model in rodents. *Acta Neurol Scand* 107 (4):267-75.

Arnoult, D., B. Gaume, M. Karbowski, J. C. Sharpe, F. Cecconi, and R. J. Youle. 2003. Mitochondrial release of AIF and EndoG requires caspase activation downstream of Bax/Bak-mediated permeabilization. *EMBO J* 22 (17):4385-99.

Arnoult, D., P. Parone, J. C. Martinou, B. Antonsson, J. Estaquier, and J. C. Ameisen. 2002. Mitochondrial release of apoptosis-inducing factor occurs downstream of cytochrome c release in response to several proapoptotic stimuli. *J Cell Biol* 159 (6):923-9.

Artus, C., H. Boujrad, A. Bouharrour, M. N. Brunelle, S. Hoos, V. J. Yuste, P. Lenormand, J. C. Rousselle, A. Namane, P. England, H. K. Lorenzo, and S. A. Susin. 2010. AIF promotes chromatinolysis and caspase-independent programmed necrosis by interacting with histone H2AX. *EMBO J* 29 (9):1585-99.

Ashwal, S., D. J. Cole, S. Osborne, T. N. Osborne, and W. J. Pearce. 1995. L-NAME reduces infarct volume in a filament model of transient middle cerebral artery occlusion in the rat pup. *Pediatr Res* 38 (5):652-6.

Ashwal, S., and W. J. Pearce. 2001. Animal models of neonatal stroke. *Curr Opin Pediatr* 13 (6):506-16.

Asoh, S., I. Ohsawa, T. Mori, K. Katsura, T. Hiraide, Y. Katayama, M. Kimura, D. Ozaki, K. Yamagata, and S. Ohta. 2002. Protection against ischemic brain injury by protein therapeutics. *Proc.Natl.Acad.Sci.U.S.A* 99 (26):17107-17112.

Aspey, B. S., S. Cohen, Y. Patel, M. Terruli, and M. J. Harrison. 1998. Middle cerebral artery occlusion in the rat: consistent protocol for a model of stroke. *Neuropathol Appl Neurobiol* 24 (6):487-97.

Ay, H. 2010. Advances in the diagnosis of etiologic subtypes of ischemic stroke. *Curr Neurol Neurosci Rep* 10 (1):14-20.

Azad, M. B., Y. Chen, E. S. Henson, J. Cizeau, E. McMillan-Ward, S. J. Israels, and S. B. Gibson. 2008. Hypoxia induces autophagic cell death in apoptosis-competent cells through a mechanism involving BNIP3. *Autophagy* 4 (2):195-204.

Azad, M. B., and S. B. Gibson. 2010. Role of BNIP3 in proliferation and hypoxia-induced autophagy: implications for personalized cancer therapies. *Ann N Y Acad Sci* 1210:8-16.

Baetz, D., K. M. Regula, K. Ens, J. Shaw, S. Kothari, N. Yurkova, and L. A. Kirshenbaum. 2005. Nuclear factor-kappaB-mediated cell survival involves transcriptional silencing of the mitochondrial death gene BNIP3 in ventricular myocytes. *Circulation* 112 (24):3777-85.

Bahi, N., J. Zhang, M. Llovera, M. Ballester, J. X. Comella, and D. Sanchis. 2006. Switch from caspase-dependent to caspase-independent death during heart development: essential role of endonuclease G in ischemia-induced DNA processing of differentiated cardiomyocytes. *J.Biol.Chem.* 281 (32):22943-22952.

Baines, C. P. 2011. The mitochondrial permeability transition pore and the cardiac necrotic program. *Pediatr Cardiol* 32 (3):258-62.

Balduini, W., V. De Angelis, E. Mazzoni, and M. Cimino. 2001. Simvastatin protects against long-lasting behavioral and morphological consequences of neonatal hypoxic/ischemic brain injury. *Stroke* 32 (9):2185-91.

Bali, B., Z. Nagy, and K. J. Kovacs. 2007. Oxygen-glucose deprivation-induced changes in organotypic cultures of the rat hippocampus. *Ideggyogy Sz* 60 (3-4):140-3.

Banerjee, J., and S. Ghosh. 2004. Bax increases the pore size of rat brain mitochondrial voltage-dependent anion channel in the presence of tBid. *Biochem Biophys Res Commun* 323 (1):310-4.

Bederson, J. B., L. H. Pitts, M. Tsuji, M. C. Nishimura, R. L. Davis, and H. Bartkowski. 1986. Rat middle cerebral artery occlusion: evaluation of the model and development of a neurologic examination. *Stroke* 17 (3):472-6.

Beech, J. S., S. C. Williams, C. A. Campbell, P. M. Bath, A. A. Parsons, A. J. Hunter, and D. K. Menon. 2001. Further characterisation of a thromboembolic model of stroke in the rat. *Brain Res* 895 (1-2):18-24.

Belayev, L., O. F. Alonso, R. Busto, W. Zhao, and M. D. Ginsberg. 1996. Middle cerebral artery occlusion in the rat by intraluminal suture. Neurological and pathological evaluation of an improved model. *Stroke* 27 (9):1616-22; discussion 1623.

Belizario, J. E., J. Alves, J. M. Occhiucci, M. Garay-Malpartida, and A. Sesso. 2007. A mechanistic view of mitochondrial death decision pores. *Braz J Med Biol Res* 40 (8):1011-24.

Bellot, G., R. Garcia-Medina, P. Gounon, J. Chiche, D. Roux, J. Pouyssegur, and N. M. Mazure. 2009. Hypoxia-induced autophagy is mediated through hypoxia-inducible factor induction of BNIP3 and BNIP3L via their BH3 domains. *Mol Cell Biol* 29 (10):2570-81.

Benchoua, A., C. Guegan, C. Couriaud, H. Hosseini, N. Sampaio, D. Morin, and B. Onteniente. 2001. Specific caspase pathways are activated in the two stages of cerebral infarction. *J Neurosci* 21 (18):7127-34.

Bernardi, P., and M. Forte. 2007. The mitochondrial permeability transition pore. *Novartis Found Symp* 287:157-64; discussion 164-9.

Betz, A. L., X. D. Ren, S. R. Ennis, and D. E. Hultquist. 1994. Riboflavin reduces edema in focal cerebral ischemia. *Acta Neurochir Suppl (Wien)* 60:314-7.

Bidere, N., H. K. Lorenzo, S. Carmona, M. Laforge, F. Harper, C. Dumont, and A. Senik. 2003. Cathepsin D triggers Bax activation, resulting in selective apoptosis-inducing factor (AIF) relocation in T lymphocytes entering the early commitment phase to apoptosis. *J Biol Chem* 278 (33):31401-11.

Birse-Archbold, J. L., L. E. Kerr, P. A. Jones, J. McCulloch, and J. Sharkey. 2005. Differential profile of Nix upregulation and translocation during hypoxia/ischaemia in vivo versus in vitro. *J Cereb Blood Flow Metab* 25 (10):1356-65.

Borlongan, C. V., S. J. Skinner, M. Geaney, A. V. Vasconcellos, R. B. Elliott, and D. F. Emerich. 2004. Intracerebral transplantation of porcine choroid plexus provides structural and functional neuroprotection in a rodent model of stroke. *Stroke* 35 (9):2206-10.

Bouchard, V. J., M. Rouleau, and G. G. Poirier. 2003. PARP-1, a determinant of cell survival in response to DNA damage. *Exp Hematol* 31 (6):446-54.

Boujrad, H., O. Gubkina, N. Robert, S. Krantic, and S. A. Susin. 2007. AIF-mediated programmed necrosis: a highly regulated way to die. *Cell Cycle* 6 (21):2612-9.

Brachmann, I., and K. L. Tucker. 2011. Organotypic slice culture of GFP-expressing mouse embryos for real-time imaging of peripheral nerve outgrowth. *J Vis Exp* (49).

Brewer, G. J. 1995. Serum-free B27/neurobasal medium supports differentiated growth of neurons from the striatum, substantia nigra, septum, cerebral cortex, cerebellum, and dentate gyrus. *J Neurosci Res* 42 (5):674-83.

Broker, L. E., F. A. Kruyt, and G. Giaccone. 2005. Cell death independent of caspases: a review. *Clin Cancer Res* 11 (9):3155-62.

Bruick, R. K. 2000. Expression of the gene encoding the proapoptotic Nip3 protein is induced by hypoxia. *Proc Natl Acad Sci U S A* 97 (16):9082-7.

Burton, T. R., D. D. Eisenstat, and S. B. Gibson. 2009. BNIP3 (Bcl-2 19 kDa interacting protein) acts as transcriptional repressor of apoptosis-inducing factor expression preventing cell death in human malignant gliomas. *J Neurosci* 29 (13):4189-99.

Burton, T. R., E. S. Henson, P. Baijal, D. D. Eisenstat, and S. B. Gibson. 2006. The pro-cell death Bcl-2 family member, BNIP3, is localized to the nucleus of human glial cells: Implications for glioblastoma multiforme tumor cell survival under hypoxia. *Int J Cancer* 118 (7):1660-9.

Calloni, R. L., B. C. Winkler, G. Ricci, M. G. Poletto, W. M. Homero, E. P. Serafini, and O. C. Corleta. 2010. Transient middle cerebral artery occlusion in rats as an experimental model of brain ischemia. *Acta Cir Bras* 25 (5):428-33.

Cande, C., I. Cohen, E. Daugas, L. Ravagnan, N. Larochette, N. Zamzami, and G. Kroemer. 2002. Apoptosis-inducing factor (AIF): a novel caspase-independent death effector released from mitochondria. *Biochimie* 84 (2-3):215-22.

Cande, C., N. Vahsen, I. Kouranti, E. Schmitt, E. Daugas, C. Spahr, J. Luban, R. T. Kroemer, F. Giordanetto, C. Garrido, J. M. Penninger, and G. Kroemer. 2004. AIF and cyclophilin A cooperate in apoptosis-associated chromatinolysis. *Oncogene* 23 (8):1514-21.

CANSIM Table 102-0529: Deaths, by cause. 2010. In *Statistics Canada*.

Cao, G., R. S. Clark, W. Pei, W. Yin, F. Zhang, F. Y. Sun, S. H. Graham, and J. Chen. 2003. Translocation of apoptosis-inducing factor in vulnerable neurons after transient cerebral ischemia and in neuronal cultures after oxygen-glucose deprivation. *J.Cereb.Blood Flow Metab* 23 (10):1137-1150.

Cao, G., Y. Luo, T. Nagayama, W. Pei, R. A. Stetler, S. H. Graham, and J. Chen. 2002. Cloning and characterization of rat caspase-9: implications for a role in mediating caspase-3 activation and hippocampal cell death after transient cerebral ischemia. *J Cereb Blood Flow Metab* 22 (5):534-46.

Cao, G., M. Minami, W. Pei, C. Yan, D. Chen, C. O'Horo, S. H. Graham, and J. Chen. 2001. Intracellular Bax translocation after transient cerebral ischemia: implications for a role of the mitochondrial apoptotic signaling pathway in ischemic neuronal death. *J Cereb Blood Flow Metab* 21 (4):321-33.

Cao, G., M. Xiao, F. Sun, X. Xiao, W. Pei, J. Li, S. H. Graham, R. P. Simon, and J. Chen. 2004. Cloning of a novel Apaf-1-interacting protein: a potent suppressor of apoptosis and ischemic neuronal cell death. *J Neurosci* 24 (27):6189-201.

Cao, G., J. Xing, X. Xiao, A. K. Liou, Y. Gao, X. M. Yin, R. S. Clark, S. H. Graham, and J. Chen. 2007. Critical role of calpain I in mitochondrial release of apoptosis-inducing factor in ischemic neuronal injury. *J Neurosci* 27 (35):9278-93.

Carloni, S., A. Carnevali, M. Cimino, and W. Balduini. 2007. Extended role of necrotic cell death after hypoxia-ischemia-induced neurodegeneration in the neonatal rat. *Neurobiol Dis* 27 (3):354-61.

Carmichael, S. T. 2005. Rodent models of focal stroke: size, mechanism, and purpose. *NeuroRx* 2 (3):396-409.

Chaitanya, G. V., and P. P. Babu. 2008. Activation of calpain, cathepsin-b and caspase-3 during transient focal cerebral ischemia in rat model. *Neurochem Res* 33 (11):2178-86.

Chan, P. H. 2004. Mitochondria and neuronal death/survival signaling pathways in cerebral ischemia. *Neurochem Res* 29 (11):1943-9.

Chang, Y. S., D. Mu, M. Wendland, R. A. Sheldon, Z. S. Vexler, P. S. McQuillen, and D. M. Ferriero. 2005. Erythropoietin improves functional and histological outcome in neonatal stroke. *Pediatr Res* 58 (1):106-11.

Chen, G., J. Cizeau, C. Vande Velde, J. H. Park, G. Bozek, J. Bolton, L. Shi, D. Dubik, and A. Greenberg. 1999. Nix and Nip3 form a subfamily of pro-apoptotic mitochondrial proteins. *J Biol Chem* 274 (1):7-10.

Chen, J., T. Nagayama, K. Jin, R. A. Stetler, R. L. Zhu, S. H. Graham, and R. P. Simon. 1998. Induction of caspase-3-like protease may mediate delayed neuronal death in the hippocampus after transient cerebral ischemia. *J.Neurosci.* 18 (13):4914-4928.

Chen, J., R. L. Zhu, M. Nakayama, K. Kawaguchi, K. Jin, R. A. Stetler, R. P. Simon, and S. H. Graham. 1996. Expression of the apoptosis-effector gene, Bax, is up-regulated in vulnerable hippocampal CA1 neurons following global ischemia. *J.Neurochem.* 67 (1):64-71.

Chen, M., and J. Wang. 2002. Initiator caspases in apoptosis signaling pathways. *Apoptosis* 7 (4):313-9.

Chen, W. W., H. Yu, H. B. Fan, C. C. Zhang, M. Zhang, C. Zhang, Y. Cheng, J. Kong, C. F. Liu, D. Geng, and X. Xu. 2011. RIP1 mediates the protection of geldanamycin on neuronal injury induced by oxygen-glucose deprivation combined with zVAD in primary cortical neurons. *J Neurochem*.

Chen, Y., W. Lewis, A. Diwan, E. H. Cheng, S. J. Matkovich, and G. W. Dorn, 2nd. Dual autonomous mitochondrial cell death pathways are activated by Nix/BNip3L and induce cardiomyopathy. *Proc Natl Acad Sci U S A* 107 (20):9035-42.

Chen, Y., W. Lewis, A. Diwan, E. H. Cheng, S. J. Matkovich, and G. W. Dorn, 2nd. 2010. Dual autonomous mitochondrial cell death pathways are activated by Nix/BNip3L and induce cardiomyopathy. *Proc Natl Acad Sci U S A* 107 (20):9035-42.

Chiang, T., R. O. Messing, and W. H. Chou. 2011. Mouse model of middle cerebral artery occlusion. *J Vis Exp* (48).

Chiarugi, A., E. Meli, M. Calvani, R. Picca, R. Baronti, E. Camaioni, G. Costantino, M. Marinozzi, D. E. Pellegrini-Giampietro, R. Pellicciari, and F. Moroni. 2003. Novel isoquinolinone-derived inhibitors of poly(ADP-ribose) polymerase-1: pharmacological characterization and neuroprotective effects in an in vitro model of cerebral ischemia. *J Pharmacol Exp Ther* 305 (3):943-9.

Chinnadurai, G., S. Vijayalingam, and S. B. Gibson. 2008. BNIP3 subfamily BH3-only proteins: mitochondrial stress sensors in normal and pathological functions. *Oncogene* 27 Suppl 1:S114-27.

Cho, B. B., and L. H. Toledo-Pereyra. 2008. Caspase-independent programmed cell death following ischemic stroke. *J Invest Surg* 21 (3):141-7.

Cho, Y., T. McQuade, H. Zhang, J. Zhang, and F. K. Chan. 2011. RIP1-dependent and independent effects of necrostatin-1 in necrosis and T cell activation. *PLoS One* 6 (8):e23209.

Cho, Y. S., S. Y. Park, H. S. Shin, and F. K. Chan. 2010. Physiological consequences of programmed necrosis, an alternative form of cell demise. *Mol Cells* 29 (4):327-32.

Choi, D. W. 1990. Limitations of in vitro models of ischemia. *Prog Clin Biol Res* 361:291-9.

Choi, D. W. 1996. Ischemia-induced neuronal apoptosis. *Curr.Opin.Neurobiol.* 6 (5):667-672.

Choudhury, S., S. Bae, Q. Ke, J. Y. Lee, J. Kim, and P. M. Kang. 2011. Mitochondria to nucleus translocation of AIF in mice lacking Hsp70 during ischemia/reperfusion. *Basic Res Cardiol* 106 (3):397-407.

Christofferson, D. E., and J. Yuan. 2010. Necroptosis as an alternative form of programmed cell death. *Curr Opin Cell Biol* 22 (2):263-8.

Cizeau, J., R. Ray, G. Chen, R. D. Gietz, and A. H. Greenberg. 2000. The C. elegans orthologue ceBNIP3 interacts with CED-9 and CED-3 but kills through a BH3- and caspase-independent mechanism. *Oncogene* 19 (48):5453-5463.

Cregan, S. P., V. L. Dawson, and R. S. Slack. 2004. Role of AIF in caspase-dependent and caspase-independent cell death. *Oncogene* 23 (16):2785-2796.

Cregan, S. P., A. Fortin, J. G. MacLaurin, S. M. Callaghan, F. Cecconi, S. W. Yu, T. M. Dawson, V. L. Dawson, D. S. Park, G. Kroemer, and R. S. Slack. 2002. Apoptosis-inducing factor is involved in the regulation of caspase-independent neuronal cell death. *J.Cell Biol.* 158 (3):507-517.

Crompton, M. 1999. The mitochondrial permeability transition pore and its role in cell death. *Biochem.J.* 341 (Pt 2):233-249.

Crumrine, R. C., A. L. Thomas, and P. F. Morgan. 1994. Attenuation of p53 expression protects against focal ischemic damage in transgenic mice. *J.Cereb.Blood Flow Metab* 14 (6):887-891.

Culmsee, C., and N. Plesnila. 2006. Targeting Bid to prevent programmed cell death in neurons. *Biochem.Soc.Trans.* 34 (Pt 6):1334-1340.

Culmsee, C., C. Zhu, S. Landshamer, B. Becattini, E. Wagner, M. Pellecchia, K. Blomgren, and N. Plesnila. 2005. Apoptosis-inducing factor triggered by poly(ADP-ribose) polymerase and Bid mediates neuronal cell death after oxygen-glucose deprivation and focal cerebral ischemia. *J.Neurosci.* 25 (44):10262-10272.

D'Amours, D., M. Germain, K. Orth, V. M. Dixit, and G. G. Poirier. 1998. Proteolysis of poly(ADP-ribose) polymerase by caspase 3: kinetics of cleavage of mono(ADP-ribosyl)ated and DNA-bound substrates. *Radiat Res* 150 (1):3-10.

Danial, N. N., A. Gimenez-Cassina, and D. Tondera. 2010. Homeostatic functions of BCL-2 proteins beyond apoptosis. *Adv Exp Med Biol* 687:1-32.

Daugas, E., S. A. Susin, N. Zamzami, K. F. Ferri, T. Irinopoulou, N. Larochette, M. C. Prevost, B. Leber, D. Andrews, J. Penninger, and G. Kroemer. 2000. Mitochondrio-nuclear translocation of AIF in apoptosis and necrosis. *FASEB J.* 14 (5):729-739.

David, K. K., M. Sasaki, S. W. Yu, T. M. Dawson, and V. L. Dawson. 2006. EndoG is dispensable in embryogenesis and apoptosis. *Cell Death Differ* 13 (7):1147-55.

De Simoni, A., and L. M. Yu. 2006. Preparation of organotypic hippocampal slice cultures: interface method. *Nat Protoc* 1 (3):1439-45.

Degterev, A., J. Hitomi, M. Germscheid, I. L. Ch'en, O. Korkina, X. Teng, D. Abbott, G. D. Cuny, C. Yuan, G. Wagner, S. M. Hedrick, S. A. Gerber, A. Lugovskoy, and J. Yuan. 2008. Identification of RIP1 kinase as a specific cellular target of necrostatins. *Nat Chem Biol* 4 (5):313-21.

Degterev, A., Z. Huang, M. Boyce, Y. Li, P. Jagtap, N. Mizushima, G. D. Cuny, T. J. Mitchison, M. A. Moskowitz, and J. Yuan. 2005. Chemical inhibitor of nonapoptotic cell death with therapeutic potential for ischemic brain injury. *Nat Chem Biol* 1 (2):112-9.

Delavallee, L., L. Cabon, P. Galan-Malo, H. K. Lorenzo, and S. A. Susin. AIF-mediated caspase-independent necroptosis: A new chance for targeted therapeutics. *IUBMB Life*.

Derugin, N., M. Wendland, K. Muramatsu, T. P. Roberts, G. Gregory, D. M. Ferriero, and Z. S. Vexler. 2000. Evolution of brain injury after transient middle cerebral artery occlusion in neonatal rats. *Stroke* 31 (7):1752-61.

Deshpande, J., K. Bergstedt, T. Linden, H. Kalimo, and T. Wieloch. 1992. Ultrastructural changes in the hippocampal CA1 region following transient cerebral ischemia: evidence against programmed cell death. *Exp.Brain Res.* 88 (1):91-105.

Dewson, G., and R. M. Kluck. 2009. Mechanisms by which Bak and Bax permeabilise mitochondria during apoptosis. *J Cell Sci* 122 (Pt 16):2801-8.

Didenko, V. V., H. Ngo, C. L. Minchew, D. J. Boudreaux, M. A. Widmayer, and D. S. Baskin. 2002. Caspase-3-dependent and -independent apoptosis in focal brain ischemia. *Mol.Med.* 8 (7):347-352.

Dijkhuizen, R. M., S. Knollema, H. B. van der Worp, G. J. Ter Horst, D. J. De Wildt, J. W. Berkelbach van der Sprenkel, K. A. Tulleken, and K. Nicolay. 1998. Dynamics of cerebral tissue injury and perfusion after temporary hypoxia-ischemia in the rat: evidence for region-specific sensitivity and delayed damage. *Stroke* 29 (3):695-704.

Dinapoli, V. A., C. L. Rosen, T. Nagamine, and T. Crocco. 2006. Selective MCA occlusion: a precise embolic stroke model. *J Neurosci Methods* 154 (1-2):233-8.

Ding, W. X., H. M. Ni, M. Li, Y. Liao, X. Chen, D. B. Stolz, G. W. Dorn, 2nd, and X. M. Yin. Nix is critical to two distinct phases of mitophagy, reactive oxygen species-mediated autophagy induction and Parkin-ubiquitin-p62-mediated mitochondrial priming. *J Biol Chem* 285 (36):27879-90.

Diwan, A., A. G. Koesters, A. M. Odley, S. Pushkaran, C. P. Baines, B. T. Spike, D. Daria, A. G. Jegga, H. Geiger, B. J. Aronow, J. D. Molkentin, K. F. Macleod, T. A. Kalfa, and G. W.

Dorn, 2nd. 2007. Unrestrained erythroblast development in Nix-/- mice reveals a mechanism for apoptotic modulation of erythropoiesis. *Proc Natl Acad Sci U S A* 104 (16):6794-9.

Diwan, A., M. Krenz, F. M. Syed, J. Wansapura, X. Ren, A. G. Koesters, H. Li, L. A. Kirshenbaum, H. S. Hahn, J. Robbins, W. K. Jones, and G. W. Dorn. 2007. Inhibition of ischemic cardiomyocyte apoptosis through targeted ablation of Bnip3 restrains postinfarction remodeling in mice. *J Clin Invest* 117 (10):2825-33.

Diwan, A., S. J. Matkovich, Q. Yuan, W. Zhao, A. Yatani, J. H. Brown, J. D. Molkentin, E. G. Kranias, and G. W. Dorn, 2nd. 2009. Endoplasmic reticulum-mitochondria crosstalk in NIX-mediated murine cell death. *J Clin Invest* 119 (1):203-12.

Dorn, G. W., 2nd. 2010. Mitochondrial pruning by Nix and BNip3: an essential function for cardiac-expressed death factors. *J Cardiovasc Transl Res* 3 (4):374-83.

Dorn, G. W., 2nd, and L. A. Kirshenbaum. 2008. Cardiac reanimation: targeting cardiomyocyte death by BNIP3 and NIX/BNIP3L. *Oncogene* 27 Suppl 1:S158-67.

Duan, Y., R. A. Gross, and S. S. Sheu. 2007. Ca2+-dependent generation of mitochondrial reactive oxygen species serves as a signal for poly(ADP-ribose) polymerase-1 activation during glutamate excitotoxicity. *J Physiol* 585 (Pt 3):741-58.

Duff, K., W. Noble, K. Gaynor, and Y. Matsuoka. 2002. Organotypic slice cultures from transgenic mice as disease model systems. *J Mol Neurosci* 19 (3):317-20.

Elliott, E. M., A. T. Malouf, and W. A. Catterall. 1995. Role of calcium channel subtypes in calcium transients in hippocampal CA3 neurons. *J Neurosci* 15 (10):6433-44.

Enari, M., H. Sakahira, H. Yokoyama, K. Okawa, A. Iwamatsu, and S. Nagata. 1998. A caspase-activated DNase that degrades DNA during apoptosis, and its inhibitor ICAD. *Nature* 391 (6662):43-50.

Endres, M., Z. Q. Wang, S. Namura, C. Waeber, and M. A. Moskowitz. 1997. Ischemic brain injury is mediated by the activation of poly(ADP-ribose)polymerase. *J Cereb Blood Flow Metab* 17 (11):1143-51.

Engel, O., S. Kolodziej, U. Dirnagl, and V. Prinz. 2011. Modeling stroke in mice - middle cerebral artery occlusion with the filament model. *J Vis Exp* (47).

Farooq, M., Y. Kim, S. Im, E. Chung, S. Hwang, M. Sohn, M. Kim, and J. Kim. 2001. Cloning of BNIP3h, a member of proapoptotic BNIP3 family genes. *Exp Mol Med* 33 (3):169-73.

Fei, P., W. Wang, S. H. Kim, S. Wang, T. F. Burns, J. K. Sax, M. Buzzai, D. T. Dicker, W. G. McKenna, E. J. Bernhard, and W. S. El-Deiry. 2004. Bnip3L is induced by p53 under hypoxia, and its knockdown promotes tumor growth. *Cancer Cell* 6 (6):597-609.

Ferrer, I., E. Lopez, R. Blanco, R. Rivera, J. Ballabriga, E. Pozas, and E. Marti. 1998. Bcl-2, Bax, and Bcl-x expression in the CA1 area of the hippocampus following transient forebrain ischemia in the adult gerbil. *Exp.Brain Res.* 121 (2):167-173.

Ferrer, I., and A. M. Planas. 2003. Signaling of cell death and cell survival following focal cerebral ischemia: life and death struggle in the penumbra. *J Neuropathol Exp Neurol* 62 (4):329-39.

Festjens, N., M. van Gurp, G. van Loo, X. Saelens, and P. Vandenabeele. 2004. Bcl-2 family members as sentinels of cellular integrity and role of mitochondrial intermembrane space proteins in apoptotic cell death. *Acta Haematol* 111 (1-2):7-27.

Fisher, M., and T. Tatlisumak. 2005. Use of animal models has not contributed to development of acute stroke therapies: con. *Stroke* 36 (10):2324-5.

Frazier, D. P., A. Wilson, R. M. Graham, J. W. Thompson, N. H. Bishopric, and K. A. Webster. 2006. Acidosis regulates the stability, hydrophobicity, and activity of the BH3-only protein Bnip3. *Antioxid Redox Signal* 8 (9-10):1625-34.

Friedlander, R. M., V. Gagliardini, H. Hara, K. B. Fink, W. Li, G. MacDonald, M. C. Fishman, A. H. Greenberg, M. A. Moskowitz, and J. Yuan. 1997. Expression of a dominant negative mutant of interleukin-1 beta converting enzyme in transgenic mice prevents neuronal cell death induced by trophic factor withdrawal and ischemic brain injury. *J Exp Med* 185 (5):933-40.

Frost, S. B., S. Barbay, M. L. Mumert, A. M. Stowe, and R. J. Nudo. 2006. An animal model of capsular infarct: endothelin-1 injections in the rat. *Behav Brain Res* 169 (2):206-11.

Fujiki, M., T. Hikawa, T. Abe, S. Uchida, M. Morishige, K. Sugita, and H. Kobayashi. 2006. Role of protein kinase C in neuroprotective effect of geranylgeranylacetone, a noninvasive inducing agent of heat shock protein, on delayed neuronal death caused by transient ischemia in rats. *J.Neurotrauma* 23 (7):1164-1178.

Fujita, K., T. Kato, K. Shibayama, H. Imada, M. Yamauchi, N. Yoshimoto, E. Miyachi, and Y. Nagata. 2006. Protective effect against 17beta-estradiol on neuronal apoptosis in hippocampus tissue following transient ischemia/recirculation in mongolian gerbils via down-regulation of tissue transglutaminase activity. *Neurochem.Res.* 31 (8):1059-1068.

Fukuda, T., H. Wang, H. Nakanishi, K. Yamamoto, and T. Kosaka. 1999. Novel non-apoptotic morphological changes in neurons of the mouse hippocampus following transient hypoxic-ischemia. *Neurosci Res* 33 (1):49-55.

Fuxe, K., B. Bjelke, B. Andbjer, H. Grahn, R. Rimondini, and L. F. Agnati. 1997. Endothelin-1 induced lesions of the frontoparietal cortex of the rat. A possible model of focal cortical ischemia. *Neuroreport* 8 (11):2623-9.

Gahwiler, B. H., S. M. Thompson, and D. Muller. 2001. Preparation and maintenance of organotypic slice cultures of CNS tissue. *Curr Protoc Neurosci* Chapter 6:Unit 6 11.

Galluzzi, L., O. Kepp, and G. Kroemer. 2009. RIP kinases initiate programmed necrosis. *J Mol Cell Biol* 1 (1):8-10.

Galluzzi, L., and G. Kroemer. 2008. Necroptosis: a specialized pathway of programmed necrosis. *Cell* 135 (7):1161-3.

Galluzzi, L., and G. Kroemer. 2009. Shigella targets the mitochondrial checkpoint of programmed necrosis. *Cell Host Microbe* 5 (2):107-9.

Gerriets, T., E. Stolz, M. Walberer, C. Muller, C. Rottger, A. Kluge, M. Kaps, M. Fisher, and G. Bachmann. 2004. Complications and pitfalls in rat stroke models for middle cerebral artery occlusion: a comparison between the suture and the macrosphere model using magnetic resonance angiography. *Stroke* 35 (10):2372-7.

Gibson, M. E., B. H. Han, J. Choi, C. M. Knudson, S. J. Korsmeyer, M. Parsadanian, and D. M. Holtzman. 2001. BAX contributes to apoptotic-like death following neonatal hypoxia-ischemia: evidence for distinct apoptosis pathways. *Mol Med* 7 (9):644-55.

Gillardon, F., I. Kiprianova, J. Sandkuhler, K. A. Hossmann, and M. Spranger. 1999. Inhibition of caspases prevents cell death of hippocampal CA1 neurons, but not impairment of hippocampal long-term potentiation following global ischemia. *Neuroscience* 93 (4):1219-1222.

Gillardon, F., C. Lenz, K. F. Waschke, S. Krajewski, J. C. Reed, M. Zimmermann, and W. Kuschinsky. 1996. Altered expression of Bcl-2, Bcl-X, Bax, and c-Fos colocalizes with DNA fragmentation and ischemic cell damage following middle cerebral artery occlusion in rats. *Brain Res Mol Brain Res* 40 (2):254-60.

Ginsberg, M. D., and R. Busto. 1989. Rodent models of cerebral ischemia. *Stroke* 20 (12):1627-42.

Gobeil, S., C. C. Boucher, D. Nadeau, and G. G. Poirier. 2001. Characterization of the necrotic cleavage of poly(ADP-ribose) polymerase (PARP-1): implication of lysosomal proteases. *Cell Death Differ* 8 (6):588-94.

Gogvadze, V., S. Orrenius, and B. Zhivotovsky. 2006. Multiple pathways of cytochrome c release from mitochondria in apoptosis. *Biochim Biophys Acta* 1757 (5-6):639-47.

Gorman, A. M., S. Orrenius, and S. Ceccatelli. 1998. Apoptosis in neuronal cells: role of caspases. *Neuroreport* 9 (10):R49-55.

Gotow, T., M. Shibata, S. Kanamori, O. Tokuno, Y. Ohsawa, N. Sato, K. Isahara, Y. Yayoi, T. Watanabe, J. F. Leterrier, M. Linden, E. Kominami, and Y. Uchiyama. 2000. Selective localization of Bcl-2 to the inner mitochondrial and smooth endoplasmic reticulum membranes in mammalian cells. *Cell Death Differ* 7 (7):666-74.

Graham, R. M., D. P. Frazier, J. W. Thompson, S. Haliko, H. Li, B. J. Wasserlauf, M. G. Spiga, N. H. Bishopric, and K. A. Webster. 2004. A unique pathway of cardiac myocyte death caused by hypoxia-acidosis. *J Exp Biol* 207 (Pt 18):3189-200.

Graham, S. H., and J. Chen. 2001. Programmed cell death in cerebral ischemia. *J Cereb Blood Flow Metab* 21 (2):99-109.

Greijer, A. E., Groep P. van der, D. Kemming, A. Shvarts, G. L. Semenza, G. A. Meijer, M. A. van de Wiel, J. A. Belien, P. J. van Diest, and Wall E. van der. 2005. Up-regulation of gene expression by hypoxia is mediated predominantly by hypoxia-inducible factor 1 (HIF-1). *J.Pathol.* 206 (3):291-304.

Greijer, A. E., and Wall E. van der. 2004. The role of hypoxia inducible factor 1 (HIF-1) in hypoxia induced apoptosis. *J.Clin.Pathol.* 57 (10):1009-1014.

Guicciardi, M. E., and G. J. Gores. 2009. Life and death by death receptors. *FASEB J* 23 (6):1625-37.

Gupta, Y. K., K. Sinha, and G. Chaudhary. 2002. Transient focal ischemia induces motor deficit but does not impair the cognitive function in middle cerebral artery occlusion model of stroke in rats. *J Neurol Sci* 203-204:267-71.

Guzzetta, F., F. Deodato, and T. Rando. 2000. Brain ischemic lesions of the newborn. *Childs Nerv Syst* 16 (10-11):633-7.

Ha, S. D., D. Ng, J. Lamothe, M. A. Valvano, J. Han, and S. O. Kim. 2007. Mitochondrial proteins Bnip3 and Bnip3L are involved in anthrax lethal toxin-induced macrophage cell death. *J Biol Chem* 282 (36):26275-83.

Halestrap, A. P., C. P. Connern, E. J. Griffiths, and P. M. Kerr. 1997. Cyclosporin A binding to mitochondrial cyclophilin inhibits the permeability transition pore and protects hearts from ischaemia/reperfusion injury. *Mol Cell Biochem* 174 (1-2):167-72.

Halterman, M. W., C. C. Miller, and H. J. Federoff. 1999. Hypoxia-inducible factor-1alpha mediates hypoxia-induced delayed neuronal death that involves p53. *J.Neurosci.* 19 (16):6818-6824.

Han, W., J. Xie, L. Li, Z. Liu, and X. Hu. 2009. Necrostatin-1 reverts shikonin-induced necroptosis to apoptosis. *Apoptosis* 14 (5):674-86.

Hara, A., H. Mori, and M. Niwa. 2000. Novel apoptotic evidence for delayed neuronal death in the hippocampal CA1 pyramidal cells after transient ischemia. *Stroke* 31 (1):236-238.

Haraldseth, O., T. Gronas, and G. Unsgard. 1991. Quicker metabolic recovery after forebrain ischemia in rats treated with the antioxidant U74006F. *Stroke* 22 (9):1188-92.

Hata, R., F. Gillardon, T. M. Michaelidis, and K. A. Hossmann. 1999. Targeted disruption of the bcl-2 gene in mice exacerbates focal ischemic brain injury. *Metab Brain Dis* 14 (2):117-24.

Hata, R., G. Mies, C. Wiessner, K. Fritze, D. Hesselbarth, G. Brinker, and K. A. Hossmann. 1998. A reproducible model of middle cerebral artery occlusion in mice: hemodynamic, biochemical, and magnetic resonance imaging. *J Cereb Blood Flow Metab* 18 (4):367-75.

Hayashi, K., R. Morishita, H. Nakagami, S. Yoshimura, A. Hara, K. Matsumoto, T. Nakamura, T. Ogihara, Y. Kaneda, and N. Sakai. 2001. Gene therapy for preventing neuronal death using hepatocyte growth factor: in vivo gene transfer of HGF to subarachnoid space prevents delayed neuronal death in gerbil hippocampal CA1 neurons. *Gene Ther.* 8 (15):1167-1173.

Hayashi, Y., I. Jikihara, T. Yagi, M. Fukumura, Y. Ohashi, Y. Ohta, H. Takagi, and M. Maeda. 2001. Immunohistochemical investigation of caspase-1 and effect of caspase-1 inhibitor in delayed neuronal death after transient cerebral ischemia. *Brain Res.* 893 (1-2):113-120.

Helton, R., J. Cui, J. R. Scheel, J. A. Ellison, C. Ames, C. Gibson, B. Blouw, L. Ouyang, I. Dragatsis, S. Zeitlin, R. S. Johnson, S. A. Lipton, and C. Barlow. 2005. Brain-specific knock-out of hypoxia-inducible factor-1alpha reduces rather than increases hypoxic-ischemic damage. *J Neurosci* 25 (16):4099-107.

Herceg, Z., and Z. Q. Wang. 1999. Failure of poly(ADP-ribose) polymerase cleavage by caspases leads to induction of necrosis and enhanced apoptosis. *Mol Cell Biol* 19 (7):5124-33.

Hetz, C., P. A. Vitte, A. Bombrun, T. K. Rostovtseva, S. Montessuit, A. Hiver, M. K. Schwarz, D. J. Church, S. J. Korsmeyer, J. C. Martinou, and B. Antonsson. 2005. Bax channel inhibitors prevent mitochondrion-mediated apoptosis and protect neurons in a model of global brain ischemia. *J.Biol.Chem.* 280 (52):42960-42970.

Higgins, G. C., P. M. Beart, and P. Nagley. 2009. Oxidative stress triggers neuronal caspase-independent death: endonuclease G involvement in programmed cell death-type III. *Cell Mol Life Sci* 66 (16):2773-87.

Hilger, T., J. A. Blunk, M. Hoehn, G. Mies, and P. Wester. 2004. Characterization of a novel chronic photothrombotic ring stroke model in rats by magnetic resonance imaging, biochemical imaging, and histology. *J Cereb Blood Flow Metab* 24 (7):789-97.

Himi, T., Y. Ishizaki, and S. Murota. 1998. A caspase inhibitor blocks ischaemia-induced delayed neuronal death in the gerbil. *Eur.J.Neurosci.* 10 (2):777-781.

Hitomi, J., D. E. Christofferson, A. Ng, J. Yao, A. Degterev, R. J. Xavier, and J. Yuan. 2008. Identification of a molecular signaling network that regulates a cellular necrotic cell death pathway. *Cell* 135 (7):1311-23.

Hocsak, E., B. Racz, A. Szabo, E. Pozsgai, A. Szigeti, E. Szigeti, F. Gallyas, Jr., B. Sumegi, S. Javor, and S. Bellyei. 2010. TIP47 confers resistance to taxol-induced cell death by

preventing the nuclear translocation of AIF and Endonuclease G. *Eur J Cell Biol* 89 (11):853-61.

Hoff, E. I., M. G. oude Egbrink, V. V. Heijnen, H. W. Steinbusch, and R. J. van Oostenbrugge. 2005. In vivo visualization of vascular leakage in photochemically induced cortical infarction. *J Neurosci Methods* 141 (1):135-41.

Holopainen, I. E. 2005. Organotypic hippocampal slice cultures: a model system to study basic cellular and molecular mechanisms of neuronal cell death, neuroprotection, and synaptic plasticity. *Neurochem Res* 30 (12):1521-8.

Hong, K. W., K. Y. Kim, J. H. Lee, H. K. Shin, Y. G. Kwak, S. O. Kim, H. Lim, and S. E. Yoo. 2002. Neuroprotective effect of (2S,3S,4R)-N''-cyano-N-(6-amino-3, 4-dihydro-3-hydroxy-2-methyl-2-dimethoxymethyl-2H-benzopyran-4-yl)-N'-benzylguani dine (KR-31378), a benzopyran analog, against focal ischemic brain damage in rats. *J Pharmacol Exp Ther* 301 (1):210-6.

Hong, S. J., T. M. Dawson, and V. L. Dawson. 2004. Nuclear and mitochondrial conversations in cell death: PARP-1 and AIF signaling. *Trends Pharmacol Sci* 25 (5):259-64.

Hong, S. S., H. Qian, P. Zhao, A. Bazzy-Asaad, and Y. Xia. 2007. Anisomycin protects cortical neurons from prolonged hypoxia with differential regulation of p38 and ERK. *Brain Res* 1149:76-86.

Hossmann, K. A. 2008. Cerebral ischemia: models, methods and outcomes. *Neuropharmacology* 55 (3):257-70.

Howells, D. W., M. J. Porritt, S. S. Rewell, V. O'Collins, E. S. Sena, H. B. van der Worp, R. J. Traystman, and M. R. Macleod. 2010. Different strokes for different folks: the rich diversity of animal models of focal cerebral ischemia. *J Cereb Blood Flow Metab* 30 (8):1412-31.

Hsu, T. S., P. M. Yang, J. S. Tsai, and L. Y. Lin. 2009. Attenuation of cadmium-induced necrotic cell death by necrostatin-1: potential necrostatin-1 acting sites. *Toxicol Appl Pharmacol* 235 (2):153-62.

Hu, Y., M. A. Benedict, D. Wu, N. Inohara, and G. Nunez. 1998. Bcl-XL interacts with Apaf-1 and inhibits Apaf-1-dependent caspase-9 activation. *Proc Natl Acad Sci U S A* 95 (8):4386-91.

Hua, R., and W. Walz. 2006. Minocycline treatment prevents cavitation in rats after a cortical devascularizing lesion. *Brain Res* 1090 (1):172-81.

Hui, L., D. S. Pei, Q. G. Zhang, Q. H. Guan, and G. Y. Zhang. 2005. The neuroprotection of insulin on ischemic brain injury in rat hippocampus through negative regulation of JNK signaling pathway by PI3K/Akt activation. *Brain Res* 1052 (1):1-9.

Hunt, R. W., and T. E. Inder. 2006. Perinatal and neonatal ischaemic stroke: a review. *Thromb Res* 118 (1):39-48.

Iijima, T. 2006. Mitochondrial membrane potential and ischemic neuronal death. *Neurosci Res* 55 (3):234-43.

Iijima, T., T. Mishima, K. Akagawa, and Y. Iwao. 2006. Neuroprotective effect of propofol on necrosis and apoptosis following oxygen-glucose deprivation--relationship between mitochondrial membrane potential and mode of death. *Brain Res* 1099 (1):25-32.

Imai, H., T. Koumura, R. Nakajima, K. Nomura, and Y. Nakagawa. 2003. Protection from inactivation of the adenine nucleotide translocator during hypoglycaemia-induced apoptosis by mitochondrial phospholipid hydroperoxide glutathione peroxidase. *Biochem J* 371 (Pt 3):799-809.

Imazu, T., S. Shimizu, S. Tagami, M. Matsushima, Y. Nakamura, T. Miki, A. Okuyama, and Y. Tsujimoto. 1999. Bcl-2/E1B 19 kDa-interacting protein 3-like protein (Bnip3L) interacts with bcl-2/Bcl-xL and induces apoptosis by altering mitochondrial membrane permeability. *Oncogene* 18 (32):4523-9.

Inoue, S., J. C. Drummond, D. P. Davis, D. J. Cole, and P. M. Patel. 2004. Combination of isoflurane and caspase inhibition reduces cerebral injury in rats subjected to focal cerebral ischemia. *Anesthesiology* 101 (1):75-81.

Irvine, R. A., N. Adachi, D. K. Shibata, G. D. Cassell, K. Yu, Z. E. Karanjawala, C. L. Hsieh, and M. R. Lieber. 2005. Generation and characterization of endonuclease G null mice. *Mol.Cell Biol.* 25 (1):294-302.

Ishimura, R., G. R. Martin, and S. L. Ackerman. 2008. Loss of apoptosis-inducing factor results in cell-type-specific neurogenesis defects. *J Neurosci* 28 (19):4938-48.

Iwashita, A., N. Tojo, S. Matsuura, S. Yamazaki, K. Kamijo, J. Ishida, H. Yamamoto, K. Hattori, N. Matsuoka, and S. Mutoh. 2004. A novel and potent poly(ADP-ribose) polymerase-1 inhibitor, FR247304 (5-chloro-2-[3-(4-phenyl-3,6-dihydro-1(2H)-pyridinyl)propyl]-4(3H)-quinazolinone) , attenuates neuronal damage in in vitro and in vivo models of cerebral ischemia. *J Pharmacol Exp Ther* 310 (2):425-36.

James, D., P. A. Parone, O. Terradillos, S. Lucken-Ardjomande, S. Montessuit, and J. C. Martinou. 2007. Mechanisms of mitochondrial outer membrane permeabilization. *Novartis Found Symp* 287:170-6; discussion 176-82.

Jones, S. M., A. E. Novak, and J. P. Elliott. 2011. Primary culture of cellular subtypes from postnatal mouse for in vitro studies of oxygen glucose deprivation. *J Neurosci Methods*.

Jordan, J., P. W. de Groot, and M. F. Galindo. 2011. Mitochondria: The Headquarters in Ischemia-Induced Neuronal Death. *Cent Nerv Syst Agents Med Chem*.

Joza, N., S. A. Susin, E. Daugas, W. L. Stanford, S. K. Cho, C. Y. Li, T. Sasaki, A. J. Elia, H. Y. Cheng, L. Ravagnan, K. F. Ferri, N. Zamzami, A. Wakeham, R. Hakem, H. Yoshida, Y. Y. Kong, T. W. Mak, J. C. Zuniga-Pflucker, G. Kroemer, and J. M. Penninger. 2001. Essential role of the mitochondrial apoptosis-inducing factor in programmed cell death. *Nature* 410 (6828):549-54.

Kalinowska, M., W. Garncarz, M. Pietrowska, W. T. Garrard, and P. Widlak. 2005. Regulation of the human apoptotic DNase/RNase endonuclease G: involvement of Hsp70 and ATP. *Apoptosis* 10 (4):821-30.

Kammouni, W., K. Wong, G. Ma, G. S. Firestein, S. B. Gibson, and H. S. El-Gabalawy. 2007. Regulation of apoptosis in fibroblast-like synoviocytes by the hypoxia-induced Bcl-2 family member Bcl-2/adenovirus E1B 19-kd protein-interacting protein 3. *Arthritis Rheum* 56 (9):2854-63.

Kanthasamy, A. G., V. Anantharam, D. Zhang, C. Latchoumycandane, H. Jin, S. Kaul, and A. Kanthasamy. 2006. A novel peptide inhibitor targeted to caspase-3 cleavage site of a proapoptotic kinase protein kinase C delta (PKCdelta) protects against dopaminergic neuronal degeneration in Parkinson's disease models. *Free Radic Biol Med* 41 (10):1578-89.

Kaste, M. 2005. Use of animal models has not contributed to development of acute stroke therapies: pro. *Stroke* 36 (10):2323-4.

Kawahara, N., Y. Wang, A. Mukasa, K. Furuya, T. Shimizu, T. Hamakubo, H. Aburatani, T. Kodama, and T. Kirino. 2004. Genome-wide gene expression analysis for induced ischemic tolerance and delayed neuronal death following transient global ischemia in rats. *J.Cereb.Blood Flow Metab* 24 (2):212-223.

Kelekar, A., and C. B. Thompson. 1998. Bcl-2-family proteins: the role of the BH3 domain in apoptosis. *Trends Cell Biol* 8 (8):324-30.

Kim, J. Y., J. J. Cho, J. Ha, and J. H. Park. 2002. The carboxy terminal C-tail of BNip3 is crucial in induction of mitochondrial permeability transition in isolated mitochondria. *Arch Biochem Biophys* 398 (2):147-52.

Kim, J. Y., Y. J. Kim, S. Lee, and J. H. Park. 2011. BNip3 is a mediator of TNF-induced necrotic cell death. *Apoptosis* 16 (2):114-26.

Kim, R., M. Emi, and K. Tanabe. 2005. Caspase-dependent and -independent cell death pathways after DNA damage (Review). *Oncol.Rep.* 14 (3):595-599.

Kirino, T. 2000. Delayed neuronal death. *Neuropathology.* 20 Suppl:S95-S97.

Klein, J. A., C. M. Longo-Guess, M. P. Rossmann, K. L. Seburn, R. E. Hurd, W. N. Frankel, R. T. Bronson, and S. L. Ackerman. 2002. The harlequin mouse mutation downregulates apoptosis-inducing factor. *Nature* 419 (6905):367-74.

Kobayashi, T., T. Kawamata, T. Mitsuyama, and T. Hori. 2007. Modified permanent middle cerebral artery occlusion rat model aiming to reduce variability in infarct size. *Neurol Res* 29 (8):884-7.

Koh, D. W., T. M. Dawson, and V. L. Dawson. 2005. Mediation of cell death by poly(ADP-ribose) polymerase-1. *Pharmacol Res* 52 (1):5-14.

Kothari, S., J. Cizeau, E. McMillan-Ward, S. J. Israels, M. Bailes, K. Ens, L. A. Kirshenbaum, and S. B. Gibson. 2003. BNIP3 plays a role in hypoxic cell death in human epithelial cells that is inhibited by growth factors EGF and IGF. *Oncogene* 22 (30):4734-44.

Krantic, S., N. Mechawar, S. Reix, and R. Quirion. 2007. Apoptosis-inducing factor: A matter of neuron life and death. *Prog.Neurobiol.* 81 (3):179-196.

Krassioukov, A. V., A. Ackery, G. Schwartz, Y. Adamchik, Y. Liu, and M. G. Fehlings. 2002. An in vitro model of neurotrauma in organotypic spinal cord cultures from adult mice. *Brain Res Brain Res Protoc* 10 (2):60-8.

Kristensen, B. W., J. Noraberg, and J. Zimmer. 2001. Comparison of excitotoxic profiles of ATPA, AMPA, KA and NMDA in organotypic hippocampal slice cultures. *Brain Res* 917 (1):21-44.

Kroemer, G., L. Galluzzi, P. Vandenabeele, J. Abrams, E. S. Alnemri, E. H. Baehrecke, M. V. Blagosklonny, W. S. El-Deiry, P. Golstein, D. R. Green, M. Hengartner, R. A. Knight, S. Kumar, S. A. Lipton, W. Malorni, G. Nunez, M. E. Peter, J. Tschopp, J. Yuan, M. Piacentini, B. Zhivotovsky, and G. Melino. 2009. Classification of cell death: recommendations of the Nomenclature Committee on Cell Death 2009. *Cell Death Differ* 16 (1):3-11.

Kroemer, G., and S. J. Martin. 2005. Caspase-independent cell death. *Nat.Med.* 11 (7):725-730.

Kruidering, M., and G. I. Evan. 2000. Caspase-8 in apoptosis: the beginning of "the end"? *IUBMB Life* 50 (2):85-90.

Kubasiak, L. A., O. M. Hernandez, N. H. Bishopric, and K. A. Webster. 2002. Hypoxia and acidosis activate cardiac myocyte death through the Bcl-2 family protein BNIP3. *Proc Natl Acad Sci U S A* 99 (20):12825-30.

Kubli, D. A., M. N. Quinsay, C. Huang, Y. Lee, and A. B. Gustafsson. 2008. Bnip3 functions as a mitochondrial sensor of oxidative stress during myocardial ischemia and reperfusion. *Am J Physiol Heart Circ Physiol* 295 (5):H2025-31.

Kuroiwa, T., G. Xi, Y. Hua, T. N. Nagaraja, J. D. Fenstermacher, and R. F. Keep. 2009. Development of a rat model of photothrombotic ischemia and infarction within the caudoputamen. *Stroke* 40 (1):248-53.

Kuschinsky, W., and F. Gillardon. 2000. Apoptosis and cerebral ischemia. *Cerebrovasc.Dis.* 10 (3):165-169.

Kuwana, T., and D. D. Newmeyer. 2003. Bcl-2-family proteins and the role of mitochondria in apoptosis. *Curr Opin Cell Biol* 15 (6):691-9.

Laake, J. H., F. M. Haug, T. Wieloch, and O. P. Ottersen. 1999. A simple in vitro model of ischemia based on hippocampal slice cultures and propidium iodide fluorescence. *Brain Res Brain Res Protoc* 4 (2):173-84.

Landshamer, S., M. Hoehn, N. Barth, S. Duvezin-Caubet, G. Schwake, S. Tobaben, I. Kazhdan, B. Becattini, S. Zahler, A. Vollmar, M. Pellecchia, A. Reichert, N. Plesnila, E. Wagner, and C. Culmsee. 2008. Bid-induced release of AIF from mitochondria causes immediate neuronal cell death. *Cell Death Differ* 15 (10):1553-63.

Lang-Rollin, I. C., H. J. Rideout, M. Noticewala, and L. Stefanis. 2003. Mechanisms of caspase-independent neuronal death: energy depletion and free radical generation. *J.Neurosci.* 23 (35):11015-11025.

Lang-Rollin, I., M. Maniati, O. Jabado, K. Vekrellis, S. Papantonis, H. J. Rideout, and L. Stefanis. 2005. Apoptosis and the conformational change of Bax induced by proteasomal inhibition of PC12 cells are inhibited by bcl-xL and bcl-2. *Apoptosis* 10 (4):809-20.

Le, D. A., Y. Wu, Z. Huang, K. Matsushita, N. Plesnila, J. C. Augustinack, B. T. Hyman, J. Yuan, K. Kuida, R. A. Flavell, and M. A. Moskowitz. 2002. Caspase activation and neuroprotection in caspase-3- deficient mice after in vivo cerebral ischemia and in vitro oxygen glucose deprivation. *Proc.Natl.Acad.Sci.U.S.A* 99 (23):15188-15193.

Lee, B. I., D. J. Lee, K. J. Cho, and G. W. Kim. 2005. Early nuclear translocation of endonuclease G and subsequent DNA fragmentation after transient focal cerebral ischemia in mice. *Neurosci.Lett.* 386 (1):23-27.

Lee, H., and S. G. Paik. 2006. Regulation of BNIP3 in normal and cancer cells. *Mol.Cells* 21 (1):1-6.

Lei, Z., Y. Ruan, A. N. Yang, and Z. C. Xu. 2006. NMDA receptor mediated dendritic plasticity in cortical cultures after oxygen-glucose deprivation. *Neurosci Lett* 407 (3):224-9.

Leo, C., L. C. Horn, and M. Hockel. 2006. Hypoxia and expression of the proapoptotic regulator BNIP3 in cervical cancer. *Int.J.Gynecol.Cancer* 16 (3):1314-1320.

Lesuisse, C., and L. J. Martin. 2002. Long-term culture of mouse cortical neurons as a model for neuronal development, aging, and death. *J Neurobiol* 51 (1):9-23.

Lewerenz, J., S. Thomsen, J. A. Steinbeck, and A. Methner. 2003. Short-term serum supplementation improves glucose-oxygen deprivation in primary cortical cultures grown under serum-free conditions. *Methods Cell Sci* 25 (3-4):227-36.

Li, D., Z. Shao, T. L. Vanden Hoek, and J. R. Brorson. 2007. Reperfusion accelerates acute neuronal death induced by simulated ischemia. *Exp Neurol* 206 (2):280-7.

Li, H., F. Colbourne, P. Sun, Z. Zhao, A. M. Buchan, and C. Iadecola. 2000. Caspase inhibitors reduce neuronal injury after focal but not global cerebral ischemia in rats. *Stroke* 31 (1):176-82.

Li, J., and J. Yuan. 2008. Caspases in apoptosis and beyond. *Oncogene* 27 (48):6194-206.

Li, J., J. Zhou, Y. Li, D. Qin, and P. Li. 2010. Mitochondrial fission controls DNA fragmentation by regulating endonuclease G. *Free Radic Biol Med* 49 (4):622-31.

Li, L. Y., X. Luo, and X. Wang. 2001. Endonuclease G is an apoptotic DNase when released from mitochondria. *Nature* 412 (6842):95-99.

Li, X., J. A. Klaus, J. Zhang, Z. Xu, K. K. Kibler, S. A. Andrabi, K. Rao, Z. J. Yang, T. M. Dawson, V. L. Dawson, and R. C. Koehler. 2010. Contributions of poly(ADP-ribose) polymerase-1 and -2 to nuclear translocation of apoptosis-inducing factor and injury from focal cerebral ischemia. *J Neurochem* 113 (4):1012-22.

Li, X., M. Nemoto, Z. Xu, S. W. Yu, M. Shimoji, S. A. Andrabi, J. F. Haince, G. G. Poirier, T. M. Dawson, V. L. Dawson, and R. C. Koehler. 2007. Influence of duration of focal cerebral ischemia and neuronal nitric oxide synthase on translocation of apoptosis-inducing factor to the nucleus. *Neuroscience* 144 (1):56-65.

Li, Y., V. G. Sharov, N. Jiang, C. Zaloga, H. N. Sabbah, and M. Chopp. 1995. Ultrastructural and light microscopic evidence of apoptosis after middle cerebral artery occlusion in the rat. *Am J Pathol* 146 (5):1045-51.

Lindsay, J., M. D. Esposti, and A. P. Gilmore. 2011. Bcl-2 proteins and mitochondria--specificity in membrane targeting for death. *Biochim Biophys Acta* 1813 (4):532-9.

Lipton, P. 1999. Ischemic cell death in brain neurons. *Physiol Rev* 79 (4):1431-568.

Liu, C. L., B. K. Siesjo, and B. R. Hu. 2004. Pathogenesis of hippocampal neuronal death after hypoxia-ischemia changes during brain development. *Neuroscience* 127 (1):113-123.

Lo, E. H. 2008. Experimental models, neurovascular mechanisms and translational issues in stroke research. *Br J Pharmacol* 153 Suppl 1:S396-405.

Low, R. L. 2003. Mitochondrial Endonuclease G function in apoptosis and mtDNA metabolism: a historical perspective. *Mitochondrion.* 2 (4):225-236.

Ludwig, R. L., S. Bates, and K. H. Vousden. 1996. Differential activation of target cellular promoters by p53 mutants with impaired apoptotic function. *Mol.Cell Biol.* 16 (9):4952-4960.

Ly, J. D., D. R. Grubb, and A. Lawen. 2003. The mitochondrial membrane potential (deltapsi(m)) in apoptosis; an update. *Apoptosis* 8 (2):115-28.

MacManus, J. P., I. Rasquinha, U. Tuor, and E. Preston. 1997. Detection of higher-order 50- and 10-kbp DNA fragments before apoptotic internucleosomal cleavage after transient cerebral ischemia. *J.Cereb.Blood Flow Metab* 17 (4):376-387.

Marsh, J. D., and S. G. Keyrouz. 2010. Stroke prevention and treatment. *J Am Coll Cardiol* 56 (9):683-91.

Matsumori, Y., S. M. Hong, K. Aoyama, Y. Fan, T. Kayama, R. A. Sheldon, Z. S. Vexler, D. M. Ferriero, P. R. Weinstein, and J. Liu. 2005. Hsp70 overexpression sequesters AIF and reduces neonatal hypoxic/ischemic brain injury. *J Cereb Blood Flow Metab* 25 (7):899-910.

McAuley, M. A. 1995. Rodent models of focal ischemia. *Cerebrovasc Brain Metab Rev* 7 (2):153-80.

McBean, D. E., and P. A. Kelly. 1998. Rodent models of global cerebral ischemia: a comparison of two-vessel occlusion and four-vessel occlusion. *Gen Pharmacol* 30 (4):431-4.

McBean, D. E., V. Winters, A. D. Wilson, C. B. Oswald, B. J. Alps, and J. M. Armstrong. 1995. Neuroprotective efficacy of lifarizine (RS-87476) in a simplified rat survival model of 2 vessel occlusion. *Br J Pharmacol* 116 (8):3093-8.

Meberg, P. J., and M. W. Miller. 2003. Culturing hippocampal and cortical neurons. *Methods Cell Biol* 71:111-27.

Meloni, B. P., A. J. Meade, D. Kitikomolsuk, and N. W. Knuckey. 2011. Characterisation of neuronal cell death in acute and delayed in vitro ischemia (oxygen-glucose deprivation) models. *J Neurosci Methods* 195 (1):67-74.

Memezawa, H., H. Minamisawa, M. L. Smith, and B. K. Siesjo. 1992. Ischemic penumbra in a model of reversible middle cerebral artery occlusion in the rat. *Exp Brain Res* 89 (1):67-78.

Merz, F., M. Muller, G. Taucher-Scholz, F. Rodel, H. Stocker, K. Schopow, L. Laprell, F. Dehghani, M. Durante, and I. Bechmann. 2010. Tissue slice cultures from humans or rodents: a new tool to evaluate biological effects of heavy ions. *Radiat Environ Biophys* 49 (3):457-62.

Mink, J., and J. Miller. 2011. Opening the window of opportunity for treating acute ischemic stroke. *Nursing* 41 (1):24-32.

Mohamad, N., A. Gutierrez, M. Nunez, C. Cocca, G. Martin, G. Cricco, V. Medina, E. Rivera, and R. Bergoc. 2005. Mitochondrial apoptotic pathways. *Biocell* 29 (2):149-161.

Molina, C. A. 2011. Reperfusion therapies for acute ischemic stroke: current pharmacological and mechanical approaches. *Stroke* 42 (1 Suppl):S16-9.

Montague, J. W., F. M. Hughes, Jr., and J. A. Cidlowski. 1997. Native recombinant cyclophilins A, B, and C degrade DNA independently of peptidylprolyl cis-trans-isomerase activity. Potential roles of cyclophilins in apoptosis. *J Biol Chem* 272 (10):6677-84.

Moreau, C., P. F. Cartron, A. Hunt, K. Meflah, D. R. Green, G. Evan, F. M. Vallette, and P. Juin. 2003. Minimal BH3 peptides promote cell death by antagonizing anti-apoptotic proteins. *J Biol Chem* 278 (21):19426-35.

Morgan, M. J., Y. S. Kim, and Z. Liu. 2007. Lipid rafts and oxidative stress-induced cell death. *Antioxid Redox Signal* 9 (9):1471-83.

Moroni, F., E. Meli, F. Peruginelli, A. Chiarugi, A. Cozzi, R. Picca, P. Romagnoli, R. Pellicciari, and D. E. Pellegrini-Giampietro. 2001. Poly(ADP-ribose) polymerase inhibitors attenuate necrotic but not apoptotic neuronal death in experimental models of cerebral ischemia. *Cell Death Differ* 8 (9):921-32.

Moubarak, R. S., V. J. Yuste, C. Artus, A. Bouharrour, P. A. Greer, J. Menissier-de Murcia, and S. A. Susin. 2007. Sequential activation of poly(ADP-ribose) polymerase 1, calpains, and Bax is essential in apoptosis-inducing factor-mediated programmed necrosis. *Mol Cell Biol* 27 (13):4844-62.

Mouw, G., J. L. Zechel, Y. Zhou, W. D. Lust, W. R. Selman, and R. A. Ratcheson. 2002. Caspase-9 inhibition after focal cerebral ischemia improves outcome following reversible focal ischemia. *Metab Brain Dis* 17 (3):143-51.

Muiras, M. L., and A. Burkle. 2000. Defending genomic stability over life span: a proposed role for PARP-1. *Exp Gerontol* 35 (6-7):703-9.

Nagasawa, H., and K. Kogure. 1989. Correlation between cerebral blood flow and histologic changes in a new rat model of middle cerebral artery occlusion. *Stroke* 20 (8):1037-43.

Nakayama, H., W. D. Dietrich, B. D. Watson, R. Busto, and M. D. Ginsberg. 1988. Photothrombotic occlusion of rat middle cerebral artery: histopathological and hemodynamic sequelae of acute recanalization. *J Cereb Blood Flow Metab* 8 (3):357-66.

Nemoto, E. M., G. K. Shiu, J. Nemmer, and A. L. Bleyaert. 1982. Attenuation of brain free fatty acid liberation during global ischemia: a model for screening potential therapies for efficacy? *J Cereb Blood Flow Metab* 2 (4):475-80.

Ness, J. M., C. A. Harvey, A. Strasser, P. Bouillet, B. J. Klocke, and K. A. Roth. 2006. Selective involvement of BH3-only Bcl-2 family members Bim and Bad in neonatal hypoxia-ischemia. *Brain Res* 1099 (1):150-9.

Nielsen, M., K. L. Lambertsen, B. H. Clausen, M. Meldgaard, N. H. Diemer, J. Zimmer, and B. Finsen. 2009. Nuclear translocation of endonuclease G in degenerating neurons after permanent middle cerebral artery occlusion in mice. *Exp Brain Res* 194 (1):17-27.

Niimura, M., N. Takagi, K. Takagi, R. Mizutani, N. Ishihara, K. Matsumoto, H. Funakoshi, T. Nakamura, and S. Takeo. 2006. Prevention of apoptosis-inducing factor translocation is a possible mechanism for protective effects of hepatocyte growth factor against neuronal cell death in the hippocampus after transient forebrain ischemia. *J.Cereb.Blood Flow Metab* 26 (11):1354-1365.

Nikolova, S., S. Moyanova, S. Hughes, M. Bellyou-Camilleri, T. Y. Lee, and R. Bartha. 2009. Endothelin-1 induced MCAO: dose dependency of cerebral blood flow. *J Neurosci Methods* 179 (1):22-8.

Ning, M., X. Wang, and E. H. Lo. 2009. Reperfusion injury after stroke: neurovascular proteases and the blood-brain barrier. *Handb Clin Neurol* 92:117-36.

Nitatori, T., N. Sato, S. Waguri, Y. Karasawa, H. Araki, K. Shibanai, E. Kominami, and Y. Uchiyama. 1995. Delayed neuronal death in the CA1 pyramidal cell layer of the gerbil hippocampus following transient ischemia is apoptosis. *J.Neurosci.* 15 (2):1001-1011.

Noda, T., S. Iwai, M. Hamada, Y. Fujita, and Y. Yura. 2009. Induction of apoptosis of detached oral squamous cell carcinoma cells by safingol. Possible role of Bim, focal adhesion kinase and endonuclease G. *Apoptosis* 14 (3):287-97.

Noraberg, J. 2004. Organotypic brain slice cultures: an efficient and reliable method for neurotoxicological screening and mechanistic studies. *Altern Lab Anim* 32 (4):329-37.

Noraberg, J., F. R. Poulsen, M. Blaabjerg, B. W. Kristensen, C. Bonde, M. Montero, M. Meyer, J. B. Gramsbergen, and J. Zimmer. 2005. Organotypic hippocampal slice cultures for studies of brain damage, neuroprotection and neurorepair. *Curr Drug Targets CNS Neurol Disord* 4 (4):435-52.

Northington, F. J. 2006. Brief update on animal models of hypoxic-ischemic encephalopathy and neonatal stroke. *ILAR J* 47 (1):32-8.

Northington, F. J., D. M. Ferriero, E. M. Graham, R. J. Traystman, and L. J. Martin. 2001. Early Neurodegeneration after Hypoxia-Ischemia in Neonatal Rat Is Necrosis while Delayed Neuronal Death Is Apoptosis. *Neurobiol.Dis.* 8 (2):207-219.

Nyormoi, O., Z. Wang, and M. Bar-Eli. 2003. Sequence-based discovery of a synthetic peptide inhibitor of caspase 6. *Apoptosis* 8 (4):371-6.

Oorschot, D. E. 1996. Total number of neurons in the neostriatal, pallidal, subthalamic, and substantia nigral nuclei of the rat basal ganglia: a stereological study using the cavalieri and optical disector methods. *J Comp Neurol* 366 (4):580-99.

Opitz-Araya, X., and A. Barria. 2011. Organotypic hippocampal slice cultures. *J Vis Exp* (48).

Padosch, S. A., and B. W. Bottiger. 2003. Neuronal apoptosis following cerebral ischaemia: pathophysiology and possible therapeutic implications. *Curr.Opin.Anaesthesiol.* 16 (5):439-445.

Padosch, S. A., P. Vogel, and B. W. Bottiger. 2001. [Neuronal apoptosis following cerebral ischemia. Basis, physiopathology and treatment strategies]. *Anaesthesist* 50 (12):905-20.

Pan, J., Q. G. Zhang, and G. Y. Zhang. 2005. The neuroprotective effects of K252a through inhibiting MLK3/MKK7/JNK3 signaling pathway on ischemic brain injury in rat hippocampal CA1 region. *Neuroscience* 131 (1):147-159.

Park, Y. C., J. H. Jeong, K. J. Park, H. J. Choi, Y. M. Park, B. K. Jeong, Y. Higuchi, and Y. H. Yoo. 2005. Sulindac activates nuclear translocation of AIF, DFF40 and endonuclease G but not induces oligonucleosomal DNA fragmentation in HT-29 cells. *Life Sci* 77 (16):2059-70.

Parrish, J., L. Li, K. Klotz, D. Ledwich, X. Wang, and D. Xue. 2001. Mitochondrial endonuclease G is important for apoptosis in C. elegans. *Nature* 412 (6842):90-94.

Pastorino, J. G., S. T. Chen, M. Tafani, J. W. Snyder, and J. L. Farber. 1998. The overexpression of Bax produces cell death upon induction of the mitochondrial permeability transition. *J Biol Chem* 273 (13):7770-5.

Paterson, I. A., A. J. Barber, D. L. Gelowitz, and C. Voll. 1997. (-)Deprenyl reduces delayed neuronal death of hippocampal pyramidal cells. *Neurosci.Biobehav.Rev.* 21 (2):181-186.

Petito, C. K., J. Torres-Munoz, B. Roberts, J. P. Olarte, T. S. Nowak, Jr., and W. A. Pulsinelli. 1997. DNA fragmentation follows delayed neuronal death in CA1 neurons exposed to transient global ischemia in the rat. *J.Cereb.Blood Flow Metab* 17 (9):967-976.

Pevsner, P. H., J. W. Eichenbaum, D. C. Miller, G. Pivawer, K. D. Eichenbaum, A. Stern, K. L. Zakian, and J. A. Koutcher. 2001. A photothrombotic model of small early ischemic infarcts in the rat brain with histologic and MRI correlation. *J Pharmacol Toxicol Methods* 45 (3):227-33.

Piccini, A., and R. Malinow. 2001. Transient oxygen-glucose deprivation induces rapid morphological changes in rat hippocampal dendrites. *Neuropharmacology* 41 (6):724-9.

Pieper, A. A., A. Verma, J. Zhang, and S. H. Snyder. 1999. Poly (ADP-ribose) polymerase, nitric oxide and cell death. *Trends Pharmacol Sci* 20 (4):171-81.

Plesnila, N. 2004. Role of mitochondrial proteins for neuronal cell death after focal cerebral ischemia. *Acta Neurochir.Suppl* 89:15-19.

Plesnila, N., C. Zhu, C. Culmsee, M. Groger, M. A. Moskowitz, and K. Blomgren. 2004. Nuclear translocation of apoptosis-inducing factor after focal cerebral ischemia. *J.Cereb.Blood Flow Metab* 24 (4):458-466.

Plesnila, N., S. Zinkel, D. A. Le, S. min-Hanjani, Y. Wu, J. Qiu, A. Chiarugi, S. S. Thomas, D. S. Kohane, S. J. Korsmeyer, and M. A. Moskowitz. 2001. BID mediates neuronal cell death after oxygen/ glucose deprivation and focal cerebral ischemia. *Proc.Natl.Acad.Sci.U.S.A* 98 (26):15318-15323.

Polster, B. M., G. Basanez, A. Etxebarria, J. M. Hardwick, and D. G. Nicholls. 2005. Calpain I induces cleavage and release of apoptosis-inducing factor from isolated mitochondria. *J Biol Chem* 280 (8):6447-54.

Prats, E., M. Noel, J. Letourneau, V. Tiranti, J. Vaque, R. Debon, M. Zeviani, L. Cornudella, and A. Ruiz-Carrillo. 1997. Characterization and expression of the mouse endonuclease G gene. *DNA Cell Biol.* 16 (9):1111-1122.

Prunell, G. F., V. A. Arboleda, and C. M. Troy. 2005. Caspase function in neuronal death: delineation of the role of caspases in ischemia. *Curr Drug Targets CNS Neurol Disord* 4 (1):51-61.

Puka-Sundvall, M., U. Hallin, C. Zhu, X. Wang, J. O. Karlsson, K. Blomgren, and H. Hagberg. 2000. NMDA blockade attenuates caspase-3 activation and DNA fragmentation after neonatal hypoxia-ischemia. *Neuroreport* 11 (13):2833-6.

Pulsinelli, W. A., J. B. Brierley, and F. Plum. 1982. Temporal profile of neuronal damage in a model of transient forebrain ischemia. *Ann Neurol* 11 (5):491-8.

Pulsinelli, W. A., D. E. Levy, and T. E. Duffy. 1983. Cerebral blood flow in the four-vessel occlusion rat model. *Stroke* 14 (5):832-4.

Puyal, J., A. Vaslin, V. Mottier, and P. G. Clarke. 2009. Postischemic treatment of neonatal cerebral ischemia should target autophagy. *Ann Neurol* 66 (3):378-89.

Ramenghi, L. A., L. Bassi, M. Fumagalli, A. Ometto, M. Groppo, A. De Carli, S. Pisoni, F. Dessimone, P. Fare, and F. Mosca. 2010. Neonatal stroke. *Minerva Pediatr* 62 (3 Suppl 1):177-9.

Rami, A. 2008. Upregulation of Beclin 1 in the ischemic penumbra. *Autophagy* 4 (2):227-9.

Rami, A., S. Jansen, I. Giesser, and J. Winckler. 2003. Post-ischemic activation of caspase-3 in the rat hippocampus: evidence of an axonal and dendritic localisation. *Neurochem.Int.* 43 (3):211-223.

Ray, R., G. Chen, C. Vande Velde, J. Cizeau, J. H. Park, J. C. Reed, R. D. Gietz, and A. H. Greenberg. 2000. BNIP3 heterodimerizes with Bcl-2/Bcl-X(L) and induces cell death independent of a Bcl-2 homology 3 (BH3) domain at both mitochondrial and nonmitochondrial sites. *J Biol Chem* 275 (2):1439-48.

Regula, K. M., K. Ens, and L. A. Kirshenbaum. 2002. Inducible expression of BNIP3 provokes mitochondrial defects and hypoxia-mediated cell death of ventricular myocytes. *Circ Res* 91 (3):226-31.

Reiner, P. B., A. G. Laycock, and C. J. Doll. 1990. A pharmacological model of ischemia in the hippocampal slice. *Neurosci Lett* 119 (2):175-8.

Rice, J. E., 3rd, R. C. Vannucci, and J. B. Brierley. 1981. The influence of immaturity on hypoxic-ischemic brain damage in the rat. *Ann Neurol* 9 (2):131-41.

Richard, M. J., T. M. Saleh, B. El Bahh, and J. A. Zidichouski. 2010. A novel method for inducing focal ischemia in vitro. *J Neurosci Methods* 190 (1):20-7.

Rickels, E. 1993. Middle cerebral artery occlusion in rats: a neurological and pathological evaluation of a reproducible model. *Neurosurgery* 32 (3):479.

Ripple, M. O., M. Abajian, and R. Springett. 2010. Cytochrome c is rapidly reduced in the cytosol after mitochondrial outer membrane permeabilization. *Apoptosis* 15 (5):563-73.

Romijn, H. J., M. A. Hofman, and A. Gramsbergen. 1991. At what age is the developing cerebral cortex of the rat comparable to that of the full-term newborn human baby? *Early Hum Dev* 26 (1):61-7.

Rosenbaum, D. M., A. Degterev, J. David, P. S. Rosenbaum, S. Roth, J. C. Grotta, G. D. Cuny, J. Yuan, and S. I. Savitz. Necroptosis, a novel form of caspase-independent cell death, contributes to neuronal damage in a retinal ischemia-reperfusion injury model. *J Neurosci Res* 88 (7):1569-76.

Saavedra, R. A., M. Murray, Lacalle S. de, and A. Tessler. 2000. In vivo neuroprotection of injured CNS neurons by a single injection of a DNA plasmid encoding the Bcl-2 gene. *Prog.Brain Res.* 128:365-372.

Saelens, X., N. Festjens, L. Vande Walle, M. van Gurp, G. van Loo, and P. Vandenabeele. 2004. Toxic proteins released from mitochondria in cell death. *Oncogene* 23 (16):2861-74.

Sairanen, T., R. Szepesi, M. L. Karjalainen-Lindsberg, J. Saksi, A. Paetau, and P. J. Lindsberg. 2009. Neuronal caspase-3 and PARP-1 correlate differentially with apoptosis and necrosis in ischemic human stroke. *Acta Neuropathol* 118 (4):541-52.

Sakahira, H., M. Enari, and S. Nagata. 1998. Cleavage of CAD inhibitor in CAD activation and DNA degradation during apoptosis. *Nature* 391 (6662):96-9.

Sandau, U. S., and R. J. Handa. 2006. Localization and developmental ontogeny of the pro-apoptotic Bnip3 mRNA in the postnatal rat cortex and hippocampus. *Brain Res.* 1100 (1):55-63.

Savas, A., P. C. Warnke, T. Ginap, T. J. Feuerstein, and C. B. Ostertag. 2001. The effects of continuous and single-dose radiation on choline uptake in organotypic tissue slice cultures of rabbit hippocampus. *Neurol Res* 23 (6):669-75.

Schielke, G. P., G. Y. Yang, B. D. Shivers, and A. L. Betz. 1998. Reduced ischemic brain injury in interleukin-1 beta converting enzyme-deficient mice. *J Cereb Blood Flow Metab* 18 (2):180-5.

Schneiders, U. M., L. Schyschka, A. Rudy, and A. M. Vollmar. 2009. BH3-only proteins Mcl-1 and Bim as well as endonuclease G are targeted in spongistatin 1-induced apoptosis in breast cancer cells. *Mol Cancer Ther* 8 (10):2914-25.

Sedelnikova, O. A., D. R. Pilch, C. Redon, and W. M. Bonner. 2003. Histone H2AX in DNA damage and repair. *Cancer Biol Ther* 2 (3):233-5.

Seth, R., C. Yang, V. Kaushal, S. V. Shah, and G. P. Kaushal. 2005. p53-dependent caspase-2 activation in mitochondrial release of apoptosis-inducing factor and its role in renal tubular epithelial cell injury. *J Biol Chem* 280 (35):31230-9.

Sharkey, J., and S. P. Butcher. 1995. Characterisation of an experimental model of stroke produced by intracerebral microinjection of endothelin-1 adjacent to the rat middle cerebral artery. *J Neurosci Methods* 60 (1-2):125-31.

Sheldon, R. A., J. Chuai, and D. M. Ferriero. 1996. A rat model for hypoxic-ischemic brain damage in very premature infants. *Biol Neonate* 69 (5):327-41.

Sheng, H., D. T. Laskowitz, R. D. Pearlstein, and D. S. Warner. 1999. Characterization of a recovery global cerebral ischemia model in the mouse. *J Neurosci Methods* 88 (1):103-9.

Shimizu, S., M. Narita, and Y. Tsujimoto. 1999. Bcl-2 family proteins regulate the release of apoptogenic cytochrome c by the mitochondrial channel VDAC. *Nature* 399 (6735):483-7.

Siegelin, M. D., L. S. Kossatz, J. Winckler, and A. Rami. 2005. Regulation of XIAP and Smac/DIABLO in the rat hippocampus following transient forebrain ischemia. *Neurochem.Int.* 46 (1):41-51.

Siesjo, B. K., and K. Katsura. 1992. Ischemic brain damage: focus on lipids and lipid mediators. *Adv.Exp.Med.Biol.* 318:41-56.

Sims, N. R., and M. F. Anderson. 2008. Isolation of mitochondria from rat brain using Percoll density gradient centrifugation. *Nat Protoc* 3 (7):1228-39.

Singh, M. H., S. M. Brooke, I. Zemlyak, and R. M. Sapolsky. 2010. Evidence for caspase effects on release of cytochrome c and AIF in a model of ischemia in cortical neurons. *Neurosci Lett* 469 (2):179-83.

Slemmer, J. E., C. Zhu, S. Landshamer, R. Trabold, J. Grohm, A. Ardeshiri, E. Wagner, M. I. Sweeney, K. Blomgren, C. Culmsee, J. T. Weber, and N. Plesnila. 2008. Causal role of apoptosis-inducing factor for neuronal cell death following traumatic brain injury. *Am J Pathol* 173 (6):1795-805.

Smith, C. C., S. M. Davidson, S. Y. Lim, J. C. Simpkin, J. S. Hothersall, and D. M. Yellon. 2007. Necrostatin: a potentially novel cardioprotective agent? *Cardiovasc Drugs Ther* 21 (4):227-33.

Smith, C. M., Y. Chen, M. L. Sullivan, P. M. Kochanek, and R. S. Clark. 2011. Autophagy in acute brain injury: feast, famine, or folly? *Neurobiol Dis* 43 (1):52-9.

Sola, A., H. Peng, M. Rogido, and T. C. Wen. 2008. Animal models of neonatal stroke and response to erythropoietin and cardiotrophin-1. *Int J Dev Neurosci* 26 (1):27-35.

Soldani, C., and A. I. Scovassi. 2002. Poly(ADP-ribose) polymerase-1 cleavage during apoptosis: an update. *Apoptosis* 7 (4):321-8.

Sowter, H. M., P. J. Ratcliffe, P. Watson, A. H. Greenberg, and A. L. Harris. 2001. HIF-1-dependent regulation of hypoxic induction of the cell death factors BNIP3 and NIX in human tumors. *Cancer Res.* 61 (18):6669-6673.

Stefanis, L. 2005. Caspase-dependent and -independent neuronal death: two distinct pathways to neuronal injury. *Neuroscientist* 11 (1):50-62.

Stegh, A. H., B. C. Barnhart, J. Volkland, A. Algeciras-Schimnich, N. Ke, J. C. Reed, and M. E. Peter. 2002. Inactivation of caspase-8 on mitochondria of Bcl-xL-expressing MCF7-Fas cells: role for the bifunctional apoptosis regulator protein. *J Biol Chem* 277 (6):4351-60.

Strosznajder, R., and B. Gajkowska. 2006. Effect of 3-aminobenzamide on Bcl-2, Bax and AIF localization in hippocampal neurons altered by ischemia-reperfusion injury. the immunocytochemical study. *Acta Neurobiol.Exp.(Wars.)* 66 (1):15-22.

Stutzmann, J. M., V. Mary, F. Wahl, O. Grosjean-Piot, A. Uzan, and J. Pratt. 2002. Neuroprotective profile of enoxaparin, a low molecular weight heparin, in in vivo models of cerebral ischemia or traumatic brain injury in rats: a review. *CNS Drug Rev* 8 (1):1-30.

Sun, H. S., T. A. Doucette, Y. Liu, Y. Fang, L. Teves, M. Aarts, C. L. Ryan, P. B. Bernard, A. Lau, J. P. Forder, M. W. Salter, Y. T. Wang, R. A. Tasker, and M. Tymianski. 2008. Effectiveness of PSD95 inhibitors in permanent and transient focal ischemia in the rat. *Stroke* 39 (9):2544-53.

Suzuki, M., R. J. Youle, and N. Tjandra. 2000. Structure of Bax: coregulation of dimer formation and intracellular localization. *Cell* 103 (4):645-54.

Tamura, A., D. I. Graham, J. McCulloch, and G. M. Teasdale. 1981. Focal cerebral ischaemia in the rat: 1. Description of technique and early neuropathological consequences following middle cerebral artery occlusion. *J Cereb Blood Flow Metab* 1 (1):53-60.

Tanaka, S., M. Takehashi, S. Iida, T. Kitajima, Y. Kamanaka, T. Stedeford, M. Banasik, and K. Ueda. 2005. Mitochondrial impairment induced by poly(ADP-ribose) polymerase-1 activation in cortical neurons after oxygen and glucose deprivation. *J.Neurochem.* 95 (1):179-190.

Thal, S. E., C. Zhu, S. C. Thal, K. Blomgren, and N. Plesnila. 2011. Role of apoptosis inducing factor (AIF) for hippocampal neuronal cell death following global cerebral ischemia in mice. *Neurosci Lett* 499 (1):1-3.

Thilmann, R., Y. Xie, P. Kleihues, and M. Kiessling. 1986. Persistent inhibition of protein synthesis precedes delayed neuronal death in postischemic gerbil hippocampus. *Acta Neuropathol.(Berl)* 71 (1-2):88-93.

Thomas, M. P., W. W. Webster, R. B. Norgren, Jr., D. T. Monaghan, and R. A. Morrisett. 1998. Survival and functional demonstration of interregional pathways in fore/midbrain slice explant cultures. *Neuroscience* 85 (2):615-26.

Thorburn, A. 2004. Death receptor-induced cell killing. *Cell Signal* 16 (2):139-44.

Tian, F., K. Deguchi, T. Yamashita, Y. Ohta, N. Morimoto, J. Shang, X. Zhang, N. Liu, Y. Ikeda, T. Matsuura, and K. Abe. 2010. In vivo imaging of autophagy in a mouse stroke model. *Autophagy* 6 (8):1107-14.

Tracking Heart Disease and Stroke in Canada. June 2009.

Tracy, K., and K. F. Macleod. 2007. Regulation of mitochondrial integrity, autophagy and cell survival by BNIP3. *Autophagy* 3 (6):616-9.

Trichonas, G., Y. Murakami, A. Thanos, Y. Morizane, M. Kayama, C. M. Debouck, T. Hisatomi, J. W. Miller, and D. G. Vavvas. 2010. Receptor interacting protein kinases mediate retinal detachment-induced photoreceptor necrosis and compensate for inhibition of apoptosis. *Proc Natl Acad Sci U S A* 107 (50):21695-700.

Tsubokawa, T., M. Yamaguchi-Okada, J. W. Calvert, I. Solaroglu, N. Shimamura, K. Yata, and J. H. Zhang. 2006. Neurovascular and neuronal protection by E64d after focal cerebral ischemia in rats. *J Neurosci Res* 84 (4):832-40.

Tsujimoto, Y. 1998. Role of Bcl-2 family proteins in apoptosis: apoptosomes or mitochondria? *Genes Cells* 3 (11):697-707.

Tuor, U. I., M. R. Del Bigio, and P. D. Chumas. 1996. Brain damage due to cerebral hypoxia/ischemia in the neonate: pathology and pharmacological modification. *Cerebrovasc Brain Metab Rev* 8 (2):159-93.

Tureyen, K., R. Vemuganti, K. A. Sailor, and R. J. Dempsey. 2004. Infarct volume quantification in mouse focal cerebral ischemia: a comparison of triphenyltetrazolium chloride and cresyl violet staining techniques. *J Neurosci Methods* 139 (2):203-7.

Tureyen, K., R. Vemuganti, K. A. Sailor, and R. J. Dempsey. 2005. Ideal suture diameter is critical for consistent middle cerebral artery occlusion in mice. *Neurosurgery* 56 (1 Suppl):196-200; discussion 196-200.

Uchiyama, Y., M. Koike, and M. Shibata. 2008. Autophagic neuron death in neonatal brain ischemia/hypoxia. *Autophagy* 4 (4):404-8.

Unal-Cevik, I., M. Kilinc, A. Can, Y. Gursoy-Ozdemir, and T. Dalkara. 2004. Apoptotic and necrotic death mechanisms are concomitantly activated in the same cell after cerebral ischemia. *Stroke* 35 (9):2189-94.

Uren, R. T., G. Dewson, C. Bonzon, T. Lithgow, D. D. Newmeyer, and R. M. Kluck. 2005. Mitochondrial release of pro-apoptotic proteins: electrostatic interactions can hold cytochrome c but not Smac/DIABLO to mitochondrial membranes. *J Biol Chem* 280 (3):2266-74.

van, Loo G., P. Schotte, Gurp M. van, H. Demol, B. Hoorelbeke, K. Gevaert, I. Rodriguez, A. Ruiz-Carrillo, J. Vandekerckhove, W. Declercq, R. Beyaert, and P. Vandenabeele. 2001. Endonuclease G: a mitochondrial protein released in apoptosis and involved in caspase-independent DNA degradation. *Cell Death.Differ.* 8 (12):1136-1142.

van Wijk, S. J., and G. J. Hageman. 2005. Poly(ADP-ribose) polymerase-1 mediated caspase-independent cell death after ischemia/reperfusion. *Free Radic Biol Med* 39 (1):81-90.

Vande, Velde C., J. Cizeau, D. Dubik, J. Alimonti, T. Brown, S. Israels, R. Hakem, and A. H. Greenberg. 2000. BNIP3 and genetic control of necrosis-like cell death through the mitochondrial permeability transition pore. *Mol.Cell Biol.* 20 (15):5454-5468.

Vandenabeele, P., T. Vanden Berghe, and N. Festjens. 2006. Caspase inhibitors promote alternative cell death pathways. *Sci STKE* 2006 (358):pe44.

Vannucci, R. C., and S. J. Vannucci. 1997. A model of perinatal hypoxic-ischemic brain damage. *Ann N Y Acad Sci* 835:234-49.

Varecha, M., J. Amrichova, M. Zimmermann, V. Ulman, E. Lukasova, and M. Kozubek. 2007. Bioinformatic and image analyses of the cellular localization of the apoptotic proteins endonuclease G, AIF, and AMID during apoptosis in human cells. *Apoptosis* 12 (7):1155-71.

Virag, L. 2005. Structure and function of poly(ADP-ribose) polymerase-1: role in oxidative stress-related pathologies. *Curr Vasc Pharmacol* 3 (3):209-14.

Vosler, P. S., D. Sun, S. Wang, Y. Gao, D. B. Kintner, A. P. Signore, G. Cao, and J. Chen. 2009. Calcium dysregulation induces apoptosis-inducing factor release: cross-talk between PARP-1- and calpain-signaling pathways. *Exp Neurol* 218 (2):213-20.

Vyssokikh, M., L. Zorova, D. Zorov, G. Heimlich, J. Jurgensmeier, D. Schreiner, and D. Brdiczka. 2004. The intra-mitochondrial cytochrome c distribution varies correlated to the formation of a complex between VDAC and the adenine nucleotide translocase: this affects Bax-dependent cytochrome c release. *Biochim Biophys Acta* 1644 (1):27-36.

Walden, J., E. J. Speckmann, D. Bingmann, and H. Straub. 1990. Augmentation of N-methyl-D-aspartate induced depolarizations by GABA in neocortical and archicortical neurons. *Brain Res* 510 (1):127-9.

Walls, K. C., A. P. Ghosh, M. E. Ballestas, B. J. Klocke, and K. A. Roth. 2009. bcl-2/Adenovirus E1B 19-kd interacting protein 3 (BNIP3) regulates hypoxia-induced neural precursor cell death. *J Neuropathol Exp Neurol* 68 (12):1326-38.

Wang, C. X., T. Yang, and A. Shuaib. 2001. An improved version of embolic model of brain ischemic injury in the rat. *J Neurosci Methods* 109 (2):147-51.

Wang, C. X., Y. Yang, T. Yang, and A. Shuaib. 2001. A focal embolic model of cerebral ischemia in rats: introduction and evaluation. *Brain Res Brain Res Protoc* 7 (2):115-20.

Wang, G. L., and G. L. Semenza. 1993. Characterization of hypoxia-inducible factor 1 and regulation of DNA binding activity by hypoxia. *J Biol Chem* 268 (29):21513-8.

Wang, H. H., H. L. Hsieh, and C. M. Yang. 2011. Nitric oxide production by endothelin-1 enhances astrocytic migration via the tyrosine nitration of matrix metalloproteinase-9. *J Cell Physiol* 226 (9):2244-56.

Wang, J. Y., Q. Xia, K. T. Chu, J. Pan, L. N. Sun, B. Zeng, Y. J. Zhu, Q. Wang, K. Wang, and B. Y. Luo. 2011. Severe global cerebral ischemia-induced programmed necrosis of hippocampal CA1 neurons in rat is prevented by 3-methyladenine: a widely used inhibitor of autophagy. *J Neuropathol Exp Neurol* 70 (4):314-22.

Wang, W., C. Redecker, H. J. Bidmon, and O. W. Witte. 2004. Delayed neuronal death and damage of GDNF family receptors in CA1 following focal cerebral ischemia. *Brain Res.* 1023 (1):92-101.

Wang, X., C. Yang, J. Chai, Y. Shi, and D. Xue. 2002. Mechanisms of AIF-mediated apoptotic DNA degradation in Caenorhabditis elegans. *Science* 298 (5598):1587-92.

Wang, Y., N. S. Kim, J. F. Haince, H. C. Kang, K. K. David, S. A. Andrabi, G. G. Poirier, V. L. Dawson, and T. M. Dawson. 2011. Poly(ADP-ribose) (PAR) binding to apoptosis-inducing factor is critical for PAR polymerase-1-dependent cell death (parthanatos). *Sci Signal* 4 (167):ra20.

Wang, Y., T. Ma, M. Li, X. Sun, and S. Gu. 2011. Regulated hypoxia/reperfusion-dependent modulation of ERK1/2, cPLA2, and Bcl-2/Bax: a potential mechanism of neuroprotective effect of penehyclidine hydrochloride. *Int J Neurosci* 121 (8):442-9.

Wang, Y. Z., and T. L. Xu. 2011. Acidosis, Acid-Sensing Ion Channels, and Neuronal Cell Death. *Mol Neurobiol*.

Webster, K. A., R. M. Graham, and N. H. Bishopric. 2005. BNip3 and signal-specific programmed death in the heart. *J Mol Cell Cardiol* 38 (1):35-45.

Wei, L., D. J. Ying, L. Cui, J. Langsdorf, and S. P. Yu. 2004. Necrosis, apoptosis and hybrid death in the cortex and thalamus after barrel cortex ischemia in rats. *Brain Res.* 1022 (1-2):54-61.

Wen, T. C., M. Rogido, P. Gressens, and A. Sola. 2004. A reproducible experimental model of focal cerebral ischemia in the neonatal rat. *Brain Res Brain Res Protoc* 13 (2):76-83.

Wen, Y. D., R. Sheng, L. S. Zhang, R. Han, X. Zhang, X. D. Zhang, F. Han, K. Fukunaga, and Z. H. Qin. 2008. Neuronal injury in rat model of permanent focal cerebral ischemia is associated with activation of autophagic and lysosomal pathways. *Autophagy* 4 (6):762-9.

Widlak, P., L. Y. Li, X. Wang, and W. T. Garrard. 2001. Action of recombinant human apoptotic endonuclease G on naked DNA and chromatin substrates: cooperation with exonuclease and DNase I. *J Biol Chem* 276 (51):48404-9.

Wiebers, D. O., H. P. Adams, Jr., and J. P. Whisnant. 1990. Animal models of stroke: are they relevant to human disease? *Stroke* 21 (1):1-3.

Wood, N. I., B. V. Sopesen, J. C. Roberts, P. Pambakian, A. L. Rothaul, A. J. Hunter, and T. C. Hamilton. 1996. Motor dysfunction in a photothrombotic focal ischaemia model. *Behav Brain Res* 78 (2):113-20.

Wu, Y., M. Dong, N. J. Toepfer, Y. Fan, M. Xu, and J. Zhang. 2004. Role of endonuclease G in neuronal excitotoxicity in mice. *Neurosci Lett* 364 (3):203-7.

Xie, C., W. R. Markesbery, and M. A. Lovell. 2000. Survival of hippocampal and cortical neurons in a mixture of MEM+ and B27-supplemented neurobasal medium. *Free Radic Biol Med* 28 (5):665-72.

Xu, D., Y. Bureau, D. C. McIntyre, D. W. Nicholson, P. Liston, Y. Zhu, W. G. Fong, S. J. Crocker, R. G. Korneluk, and G. S. Robertson. 1999. Attenuation of ischemia-induced cellular and behavioral deficits by X chromosome-linked inhibitor of apoptosis protein overexpression in the rat hippocampus. *J.Neurosci.* 19 (12):5026-5033.

Xu, X., C. C. Chua, J. Kong, R. M. Kostrzewa, U. Kumaraguru, R. C. Hamdy, and B. H. Chua. 2007. Necrostatin-1 protects against glutamate-induced glutathione depletion and caspase-independent cell death in HT-22 cells. *J Neurochem* 103 (5):2004-14.

Xu, X., C. C. Chua, M. Zhang, D. Geng, C. F. Liu, R. C. Hamdy, and B. H. Chua. 2010. The role of PARP activation in glutamate-induced necroptosis in HT-22 cells. *Brain Res* 1343:206-12.

Xu, X. H., S. M. Zhang, W. M. Yan, X. R. Li, H. Y. Zhang, and X. X. Zheng. 2006. Development of cerebral infarction, apoptotic cell death and expression of X-chromosome-linked inhibitor of apoptosis protein following focal cerebral ischemia in rats. *Life Sci* 78 (7):704-12.

Xu, Y., S. Huang, Z. G. Liu, and J. Han. 2006. Poly(ADP-ribose) polymerase-1 signaling to mitochondria in necrotic cell death requires RIP1/TRAF2-mediated JNK1 activation. *J Biol Chem* 281 (13):8788-95.

Xu, Z., J. Zhang, K. K. David, Z. J. Yang, X. Li, T. M. Dawson, V. L. Dawson, and R. C. Koehler. 2010. Endonuclease G does not play an obligatory role in poly(ADP-ribose) polymerase-dependent cell death after transient focal cerebral ischemia. *Am J Physiol Regul Integr Comp Physiol* 299 (1):R215-21.

Yamashima, T., Y. Kohda, K. Tsuchiya, T. Ueno, J. Yamashita, T. Yoshioka, and E. Kominami. 1998. Inhibition of ischaemic hippocampal neuronal death in primates with cathepsin B inhibitor CA-074: a novel strategy for neuroprotection based on 'calpain-cathepsin hypothesis'. *Eur.J.Neurosci.* 10 (5):1723-1733.

Yanamoto, H., I. Nagata, N. Hashimoto, and H. Kikuchi. 1998. Three-vessel occlusion using a micro-clip for the proximal left middle cerebral artery produces a reliable neocortical infarct in rats. *Brain Res Brain Res Protoc* 3 (2):209-20.

Yasuda, M., P. Theodorakis, T. Subramanian, and G. Chinnadurai. 1998. Adenovirus E1B-19K/BCL-2 interacting protein BNIP3 contains a BH3 domain and a mitochondrial targeting sequence. *J.Biol.Chem.* 273 (20):12415-12421.

Yin, W., G. Cao, M. J. Johnnides, A. P. Signore, Y. Luo, R. W. Hickey, and J. Chen. 2006. TAT-mediated delivery of Bcl-xL protein is neuroprotective against neonatal hypoxic-ischemic brain injury via inhibition of caspases and AIF. *Neurobiol Dis* 21 (2):358-71.

Yonekura, I., N. Kawahara, H. Nakatomi, K. Furuya, and T. Kirino. 2004. A model of global cerebral ischemia in C57 BL/6 mice. *J Cereb Blood Flow Metab* 24 (2):151-8.

You, Z., S. I. Savitz, J. Yang, A. Degterev, J. Yuan, G. D. Cuny, M. A. Moskowitz, and M. J. Whalen. 2008. Necrostatin-1 reduces histopathology and improves functional outcome after controlled cortical impact in mice. *J Cereb Blood Flow Metab* 28 (9):1564-73.

Youle, R. J., and A. Strasser. 2008. The BCL-2 protein family: opposing activities that mediate cell death. *Nat Rev Mol Cell Biol* 9 (1):47-59.

Yu, S. W., H. Wang, T. M. Dawson, and V. L. Dawson. 2003. Poly(ADP-ribose) polymerase-1 and apoptosis inducing factor in neurotoxicity. *Neurobiol Dis* 14 (3):303-17.

Yu, S. W., H. Wang, M. F. Poitras, C. Coombs, W. J. Bowers, H. J. Federoff, G. G. Poirier, T. M. Dawson, and V. L. Dawson. 2002. Mediation of poly(ADP-ribose) polymerase-1-dependent cell death by apoptosis-inducing factor. *Science* 297 (5579):259-63.

Yuan, J., M. Lipinski, and A. Degterev. 2003. Diversity in the mechanisms of neuronal cell death. *Neuron* 40 (2):401-413.

Yurkova, N., J. Shaw, K. Blackie, D. Weidman, R. Jayas, B. Flynn, and L. A. Kirshenbaum. 2008. The cell cycle factor E2F-1 activates Bnip3 and the intrinsic death pathway in ventricular myocytes. *Circ Res* 102 (4):472-9.

Yussman, M. G., T. Toyokawa, A. Odley, R. A. Lynch, G. Wu, M. C. Colbert, B. J. Aronow, J. N. Lorenz, and G. W. Dorn, 2nd. 2002. Mitochondrial death protein Nix is induced in cardiac hypertrophy and triggers apoptotic cardiomyopathy. *Nat Med* 8 (7):725-30.

Zamzami, N., S. A. Susin, P. Marchetti, T. Hirsch, I. Gomez-Monterrey, M. Castedo, and G. Kroemer. 1996. Mitochondrial control of nuclear apoptosis. *J Exp Med* 183 (4):1533-44.

Zha, H., C. Aime-Sempe, T. Sato, and J. C. Reed. 1996. Proapoptotic protein Bax heterodimerizes with Bcl-2 and homodimerizes with Bax via a novel domain (BH3) distinct from BH1 and BH2. *J Biol Chem* 271 (13):7440-4.

Zhang, D. W., J. Shao, J. Lin, N. Zhang, B. J. Lu, S. C. Lin, M. Q. Dong, and J. Han. 2009. RIP3, an energy metabolism regulator that switches TNF-induced cell death from apoptosis to necrosis. *Science* 325 (5938):332-6.

Zhang, F., W. Yin, and J. Chen. 2004. Apoptosis in cerebral ischemia: executional and regulatory signaling mechanisms. *Neurol.Res.* 26 (8):835-845.

Zhang, H. M., P. Cheung, B. Yanagawa, B. M. McManus, and D. C. Yang. 2003. BNips: a group of pro-apoptotic proteins in the Bcl-2 family. *Apoptosis* 8 (3):229-36.

Zhang, J., M. Dong, L. Li, Y. Fan, P. Pathre, J. Dong, D. Lou, J. M. Wells, D. Olivares-Villagomez, Kaer L. Van, X. Wang, and M. Xu. 2003. Endonuclease G is required for early embryogenesis and normal apoptosis in mice. *Proc.Natl.Acad.Sci.U.S.A* 100 (26):15782-15787.

Zhang, J., and P. A. Ney. 2009. Role of BNIP3 and NIX in cell death, autophagy, and mitophagy. *Cell Death Differ* 16 (7):939-46.

Zhang, J., J. Ye, A. Altafaj, M. Cardona, N. Bahi, M. Llovera, X. Canas, S. A. Cook, J. X. Comella, and D. Sanchis. 2011. EndoG links Bnip3-induced mitochondrial damage and caspase-independent DNA fragmentation in ischemic cardiomyocytes. *PLoS One* 6 (3):e17998.

Zhang, R. L., M. Chopp, Z. G. Zhang, Q. Jiang, and J. R. Ewing. 1997. A rat model of focal embolic cerebral ischemia. *Brain Res* 766 (1-2):83-92.

Zhang, S., and W. Wang. 1999. Altered expression of bcl-2 mRNA and Bax in hippocampus with focal cerebral ischemia model in rats. *Chin Med J (Engl)* 112 (7):608-11.

Zhang, S., Z. Zhang, G. Sandhu, X. Ma, X. Yang, J. D. Geiger, and J. Kong. 2007. Evidence of oxidative stress-induced BNIP3 expression in amyloid beta neurotoxicity. *Brain Res* 1138:221-30.

Zhang, X., J. Chen, S. H. Graham, L. Du, P. M. Kochanek, R. Draviam, F. Guo, P. D. Nathaniel, C. Szabo, S. C. Watkins, and R. S. Clark. 2002. Intranuclear localization of apoptosis-inducing factor (AIF) and large scale DNA fragmentation after traumatic brain injury in rats and in neuronal cultures exposed to peroxynitrite. *J Neurochem* 82 (1):181-91.

Zhang, Y., B. Fortune, L. O. Atchaneeyasakul, T. McFarland, K. Mose, P. Wallace, J. Main, D. Wilson, B. Appukuttan, and J. T. Stout. 2008. Natural history and histology in a rat model of laser-induced photothrombotic retinal vein occlusion. *Curr Eye Res* 33 (4):365-76.

Zhang, Z., X. Yang, S. Zhang, X. Ma, and J. Kong. 2007. BNIP3 Upregulation and EndoG Translocation in Delayed Neuronal Death in Stroke and in Hypoxia. *Stroke*.

Zhao, H., M. A. Yenari, D. Cheng, O. L. Barreto-Chang, R. M. Sapolsky, and G. K. Steinberg. 2004. Bcl-2 transfection via herpes simplex virus blocks apoptosis-inducing factor translocation after focal ischemia in the rat. *J.Cereb.Blood Flow Metab* 24 (6):681-692.

Zhao, H., M. A. Yenari, D. Cheng, R. M. Sapolsky, and G. K. Steinberg. 2003. Bcl-2 overexpression protects against neuron loss within the ischemic margin following experimental stroke and inhibits cytochrome c translocation and caspase-3 activity. *J Neurochem* 85 (4):1026-36.

Zhao, S. T., M. Chen, S. J. Li, M. H. Zhang, B. X. Li, M. Das, J. C. Bean, J. M. Kong, X. H. Zhu, and T. M. Gao. 2009. Mitochondrial BNIP3 upregulation precedes endonuclease G translocation in hippocampal neuronal death following oxygen-glucose deprivation. *BMC Neurosci* 10:113.

Zheng, Y. Q., J. X. Liu, X. Z. Li, L. Xu, and Y. G. Xu. 2009. RNA interference-mediated downregulation of Beclin1 attenuates cerebral ischemic injury in rats. *Acta Pharmacol Sin* 30 (7):919-27.

Zhou, Q. L., G. Strichartz, and G. Davar. 2001. Endothelin-1 activates ET(A) receptors to increase intracellular calcium in model sensory neurons. *Neuroreport* 12 (17):3853-7.

Zhu, B., L. Y. Li, G. Y. Lu, Y. L. Xue, and T. H. Ye. 2010. [Effects of naloxone on the expression of stem cell factor and C-kit receptor in combined oxygen-glucose deprivation of primary cultured human embryonic neuron in vitro]. *Zhongguo Yi Xue Ke Xue Yuan Xue Bao* 32 (2):215-21.

Zhu, C., L. Qiu, X. Wang, U. Hallin, C. Cande, G. Kroemer, H. Hagberg, and K. Blomgren. 2003. Involvement of apoptosis-inducing factor in neuronal death after hypoxia-ischemia in the neonatal rat brain. *J Neurochem* 86 (2):306-17.

Zhu, C., X. Wang, J. Deinum, Z. Huang, J. Gao, N. Modjtahedi, M. R. Neagu, M. Nilsson, P. S. Eriksson, H. Hagberg, J. Luban, G. Kroemer, and K. Blomgren. 2007. Cyclophilin A participates in the nuclear translocation of apoptosis-inducing factor in neurons after cerebral hypoxia-ischemia. *J Exp Med* 204 (8):1741-8.

Zhu, C., X. Wang, Z. Huang, L. Qiu, F. Xu, N. Vahsen, M. Nilsson, P. S. Eriksson, H. Hagberg, C. Culmsee, N. Plesnila, G. Kroemer, and K. Blomgren. 2007. Apoptosis-inducing factor is a major contributor to neuronal loss induced by neonatal cerebral hypoxia-ischemia. *Cell Death Differ* 14 (4):775-84.

Zhu, S., Y. Zhang, G. Bai, and H. Li. 2011. Necrostatin-1 ameliorates symptoms in R6/2 transgenic mouse model of Huntington's disease. *Cell Death Dis* 2:e115.

Zimmer, J., B. W. Kristensen, B. Jakobsen, and J. Noraberg. 2000. Excitatory amino acid neurotoxicity and modulation of glutamate receptor expression in organotypic brain slice cultures. *Amino Acids* 19 (1):7-21.